Harnessing the genetic potential for arbuscular mycorrhizal symbiosis in rice

Emily Kate Servanté

Darwin College,
Department of Plant Sciences,
University of Cambridge

International Rice Research Institute
(IRRI), Philippines

This thesis is submitted for the degree of
Doctor of Philosophy, March 2023.

Declaration

This thesis is the result of my own work and includes nothing which is the outcome of work done in collaboration except as declared here and specified in the text. Blumenol analyses described in Chapter Three and Four were performed by myself, Dr. Rayko Halitschke and Catarina Rocha at Max Planck Institute of Chemical Ecology, Germany. Further apocarotenoid metabolic analyses described in Chapter Three were performed by myself and Dr. Laura Perez at Royal Holloway University of London, UK. In Chapter Four, ionomic analyses were performed by Dr. Paulina Flis at University of Nottingham, UK. In Chapter Five, analyses of AM and growth trait in field trials at International Rice Research Institute, Philippines, were performed by myself, Dr. Amelia Henry and the Drought Physiology Team. In Section 5.1, material was sampled from DSR Breeding Trials belonging to Dr. Shalabh Dixit and the DSR Breeding Team at IRRI.

The thesis is not substantially the same as any work that has already been submitted before for any degree or other qualification except as declared in the preface and specified in the text. It does not exceed the prescribed word limit for the Faculty of Biology Degree Committee (60,000 words).

Emily Kate Servanté

31st March 2023

Abstract

Harnessing the genetic potential for arbuscular mycorrhizal symbiosis in rice.

Emily Kate Servanté

Arbuscular mycorrhizal fungi (AMF) have long been recognised to form a mutually beneficial symbiosis with over 80% of land plants present today. The symbiosis provides an integral link to mineral nutrients in the soil (Bago et al., 2000; Jakobsen & Rosendahl, 1990; Smith & Read, 2008) and this has led to increasing interest in the potential for use of AMF as natural biofertilizers in sustainable agroecosystems (Berruti et al., 2015). Despite this, such potential is currently limited by the variable nature of plant host response, particularly mycorrhizal growth responsiveness (MGR) (Hetrick et al., 1992; Lehnert et al., 2018; Taylor et al., 2015; Thirkell et al., 2022; Xavier & Germida, 1998). Here, in collaboration with the International Rice Research Institute (IRRI), Philippines, we use a glasshouse and field approach to address the genetic potential for AM symbiosis in rice, *Oryza sativa,* a staple food crop for over half of the world's population (Childs & LeBeau, 2023).

First, use of foliar abundance of blumenol C glycosides (Mindt et al., 2019; M. Wang et al., 2018) as a novel, high throughput (HTP) marker of AM colonisation was newly evaluated in rice. I offer the first interrogation of blumenol phenotypes in rice mutants with aberrant AMF life cycle stages and report that extraradical colonisation is not sufficient to promote accumulation. In addition, I newly report that blumenol accumulation is independent to SL signalling, the phosphate starvation response network and downstream D14L/SMAX1 signalling, which are integral parts of AM symbiosis regulation, and provide further evidence for a model of blumenol biosynthesis in rice.

I further describe evidence supporting recommendation of abundance of 11-carboxyblumenol C glucosides as a foliar marker of AM colonisation in model and diverse cultivars of rice. The marker was successfully used to probe natural variation in AM colonisation and host response in a panel of *Indica* rice from the 3K-RG (Z. Li

et al., 2014; W. Wang et al., 2018), a germplasm containing large amounts of diversity which has not yet been interrogated for AM phenotypes. I described natural variation in AM colonisation and host responsiveness, identified exciting candidate genes and provided data for further interrogation of genetic determinants of MGR and host response. This will have exciting applications for future studies interrogating AM symbiosis in diverse rice cultivars.

Importantly, in addition to use of glasshouse experiments to probe phenotypes without interference of other factors, understanding of the potential of AMF as natural biofertilizers of rice requires placement of the interaction in a field context. First-look assessments in the field at IRRI, Philippines identified the potential for AMF in dry, direct seeded (DSR), sustainable agroecosystems of rice. Furthermore, a field experiment additionally identified natural variation in host response to AMF-inoculation compared to native AMF, corroborating glasshouse results and further evidencing genetic variation in host response to AM symbiosis in rice. The trial valuably defined field conditions for future, complementary analyses of genetic determinants of host responsiveness in the field at IRRI.

Overall, the project advocates for use of blumenols as a novel tool for large scale studies of natural variation in AM colonisation and response in rice. I successfully identified candidate genetic determinants of blumenol abundance and colonisation, providing further evidence for the genetic potential for AM symbiosis in rice. In addition, the collaborative study with IRRI, Philippines offers groundwork and recommendations for further studies assessing the potential for AMF as biofertilizers driving beneficial host response in the rice field.

Acknowledgements

A huge thank you to my supervisor, Prof Uta Paszkowski, for her unwavering support and enthusiasm over the years. Without Uta, I would never have found myself in the exciting world of arbuscular mycorrhizal symbiosis and it's been an amazing journey together ever since. To the whole Cereal Symbiosis lab- you have never failed to provide help, advice and laughs and I have loved being surrounded by such a fun, collaborative, and supportive group.

The PhD was supported by a DTP Targeted Studentship (ref: 2118594), and I thank the BBSRC for funding. I would also like to thank my second supervisor, Dr. Amelia Henry at the International Rice Research Institute, Philippines. Although our communications began in the chaos of the Covid pandemic and Zoom calls, your support was constant. Thank you for welcoming me to IRRI and for teaching me about rice in the field. A special thank you to the IRRI community and to Dr. Dmytro Chebotarov for help with the GWAS analyses. Further, I thank Prof Ian Baldwin, Dr. Rayko Halitschke and Catarina Rocha at MPI CE, Jena for blumenol analyses.

The Department of Plant Sciences is an amazing home for a PhD, and I thank all the people who provided research and postgraduate support. To Fon, Brett, Nat, Jake, Sam, Ben, Satish and Farah- thank you for teatime. Thank you, Annie, for the countless coffees and smiles to support us through. I am also grateful to the amazing senior scientists who have supported me, especially Dr. Jeongmin Choi and Dr. Leonie Luginbuehl, and the whole of the Endosymbiosis and Crop Science Centre communities for invaluable advice and discussions.

Outside of the Plants Department, Holly, Anna, Rebecca, Orla, Rachel, Elizabeth, Sam G: you have been there since day one and I have loved being on the PhD journey with you all. A special thank you to the 'GWAS harvesters'; the Cereal Symbiosis lab, my housemates and friends who all joined the effort- it was a long week, and I may never eat Domino's pizza again, but I couldn't have done it without you! To Alice, Kate, Fiona, Ali P, and Vicky, you first made Cambridge a home and have been there ever since.

Finally, I have an amazing group of friends and family outside of Cambridge. Thank you especially to Grassie, Grandpa, Grandad, my amazing parents and two lovely sisters, Jules and Charl, for your constant love and support. Thanks for always being at the end of the phone to spur me on. Lastly, to George, for making me laugh when I'd forgotten to and for sharing these PhD years together.

Table of Contents

1 CHAPTER ONE- INTRODUCTION 11

1.1 Arbuscular mycorrhizal (AM) symbiosis 11
1.1.1 Pre-symbiotic communication 13
1.1.2 Extraradical contact and initial penetration..... 17
1.1.3 Formation of AM intraradical structures 18
1.1.4 Bi-directional nutrient exchange and hormonal changes 20

1.2 Blumenols and apocarotenoids associated to AM colonisation..... 24
1.2.1 Apocarotenoids implicated in AM symbiosis 24
1.2.2 Crosstalk between apocarotenoids implicated in AM symbiosis..... 31

1.3 Genetic diversity in AM symbiotic establishment and benefit 33
1.3.1 Natural variation in AM colonization 33
1.3.2 Genetic mapping of AM traits..... 35
1.3.3 Genetic diversity of rice 38
1.3.4 AMF in rice cultivation systems..... 40
1.3.5 Assessing AM colonisation in rice..... 42

1.4 Research Objectives 43

2 CHAPTER TWO- MATERIALS AND METHODS 45

2.1 Plant growth and inoculation..... 45
2.1.1 Oryza sativa material 45
2.1.2 Seed sterilisation and germination 45
2.1.3 Fungal subculture 45
2.1.4 Fungal spore extraction 46
2.1.5 Seedling planting and inoculation- cone experiments 46
2.1.6 Plant cultivation 46

2.2 Microscopic quantification of AM colonisation..... 47
2.2.1 Root harvest - trypan blue staining 47
2.2.2 Microscopic quantification of AM colonisation 48

2.3 Molecular techniques- DNA & RNA 48
2.3.1 Genomic DNA (gDNA) extraction..... 48
2.3.2 Genotyping - polymerase chain reaction (PCR) 49
2.3.3 Root harvest – RNA extraction 49
2.3.4 cDNA synthesis 50
2.3.5 qRT-PCR expression analysis 50

2.4 Blumenol metabolite analysis 51
2.4.1 Sample preparation- extraction..... 51
2.4.2 Targeted blumenol analysis 51

2.5 Strigolactone (SL) and apocarotenoid metabolome analysis 52
2.5.1 Sample preparation- extraction..... 52
2.5.2 Analysis of SLs and apocarotenoids in LC-MS. 53
2.5.3 Data analysis of LC-MS files. 54

2.6 Ionomics analysis 54
2.6.1 Sample preparation- extraction 54
2.6.2 ICP-MS 54

2.7 Genome wide association study (GWAS) of AM traits 55
2.7.1 Selection of diverse panel of *Indica* rice 55
2.7.2 Glasshouse conditions and block design of the *Indica* rice panel 55
2.7.3 Seed sterilisation and planting of GWAS glasshouse experiment 56
2.7.4 Growth and inoculation of GWAS glasshouse experiment 56
2.7.5 Trait phenotyping of the *Indica* panel 57
2.7.6 Genome Wide Association Mapping and candidate gene analysis 58

2.8 Field experiments at IRRI, Philippines 60
2.8.1 Seedling planting and inoculation- AMF field experiment 61
2.8.2 Harvest and phenotyping- AMF field experiment 63
2.8.3 Growth conditions- DSR AM trial 64
2.8.4 Harvest and AM phenotyping- DSR AM trial 64

2.9 Statistics 64
2.9.1 Statistical analysis of data 64
2.9.2 Correlation analysis of data 65

2.10 Genotype and Chemical Tables 65

3 CHAPTER THREE- EXPLORING BLUMENOL ACCUMULATION DURING AM SYMBIOSIS IN RICE 82

3.1 Investigating blumenol as a foliar marker of AM colonisation in rice 82
3.1.1 Introduction 82
3.1.2 Results 83
3.1.3 Discussion 94

3.2 Investigating the role of AM signalling pathways and phosphate suppression in blumenol accumulation during AM symbiosis 97
3.2.1 Introduction 97
3.2.2 Results 100
3.2.3 Discussion 107

3.3 Investigating the role of SL biosynthesis and signalling genes in blumenol accumulation during AM symbiosis 109
3.3.1 Introduction 109
3.3.2 Results 111
3.3.3 Discussion 121

3.4 Investigating the requirement for SL and blumenol biosynthesis genes for efficient AM colonisation in rice 123
3.4.1 Introduction 123
3.4.2 Results 125
3.4.3 Discussion 132

3.5 Conclusions 133

4 CHAPTER FOUR– GENETIC ANALYSIS OF AM SYMBIOSIS ESTABLISHMENT AND BENEFIT IN A DIVERSE PANEL OF RICE 135

4.1 Selection of a diverse *Indica* rice panel from the 3K-RG 135
4.1.1 Introduction 135
4.1.2 Results 136
4.1.3 Discussion 142

4.2 Analysis of natural variation in AM colonisation and response in a diverse panel of rice 143
4.2.1 Introduction 143
4.2.2 Results 147
4.2.3 Discussion 171

4.3 A Genome Wide Association Study (GWAS) interrogating genetic variation in establishment of AM symbiosis in rice 173
4.3.1 Introduction 173
4.3.2 Results 175
4.3.3 Discussion and a comment on future analyses 191

4.4 Conclusions 192

4.5 Supplementary Figures 193

5 CHAPTER FIVE- AM SYMBIOSIS IN THE RICE FIELD 198

5.1 Investigating the potential for AM colonisation in direct-seeded rice cultivation at IRRI, Philippines 198
5.1.1 Introduction 198
5.1.2 Results 201
5.1.3 Discussion 204

5.2 Investigating the impact of AMF inoculation on diverse *Indica* cultivars in the field 206
5.2.1 Introduction 206
5.2.2 Results 208
5.2.3 Discussion 225

5.3 Conclusions 228

6 CHAPTER SIX– GENERAL DISCUSSION 230

6.1 Blumenol is recommended as a high throughput marker of AM colonisation in rice 230

6.2 A model for blumenol accumulation during AM symbiosis in rice; independent to phosphate and D14L/SMAX1 mediated signalling 232

6.3 (Re)defining the requirement for SLs and apocarotenoids during AM symbiosis in rice 233

6.4 Natural variation in AM colonisation and responsiveness in diverse rice cultivars 235

6.5 Genetic mapping of AM colonisation in rice 236

6.6 The potential for AMF in sustainable rice agroecosystems 238

6.7 Final Conclusions..... 239

7 REFERENCES 240

1 Chapter One- Introduction

1.1 Arbuscular mycorrhizal (AM) symbiosis

Arbuscular mycorrhizal fungi (AMF), *Glomeromycotina*, form intimate associations with >80% land plants present today (Soudzilovskaia et al., 2020); colonizing their roots to act as natural biofertilizers. Extraradical mycelium of AMF can extend past root nutrient depletion zones and provide an essential supply of nutrients such as inorganic phosphorous (P_i) and nitrogen to the plant. In return, plants transfer up to 20% of their photosynthetic carbon (Bago et al., 2000; I. Jakobsen & Rosendahl, 1990; S. E. Smith & Read, 2008). Collectively, the symbiosis has important implications for global nutrient cycling and ecosystem function (Van Der Heijden et al., 1998). At a socioeconomic scale, it has potential to be harnessed into sustainable agriculture (Berruti et al., 2015). In typical farming systems, P_i and nitrogen supplies are achieved by applying artificial fertilizers to the soil. As rock phosphorous and nitrogen sources become increasingly implicated in loss of ecosystem diversity, are limiting to mine (both economically and in resource) and global food demand increases, focus has turned to the potential to use AM symbiosis as a method to improve soil structure and reduce the mass application of fertilizer in crop farming (Berruti et al., 2015; Cordell et al., 2009).

AM symbiosis first evolved ~400-450 million years ago, when early diverging land plants emerged; likely aiding the movement of plants from aquatic to terrestrial lifestyles (Remy et al., 1994). Interaction with AMF is thought to have occurred by a transition of dominance from the more basal *Mucuromycotina* phylum to *Glomeromycotina*, allowing a resultant widespread and prevalent association with vascular plants (Field et al., 2015). Today, most plant species can engage and loss in the ability to do so, including in the model plant *Arabidopsis thaliana,* is associated with an absence of a suite of mycorrhizal genes, such as those required for a common symbiosis pathway (CSP) that co-evolved with intracellular endosymbioses (Radhakrishnan et al., 2020). Notably, reverse genetic approaches suggest that these mycorrhizal genes play crucial roles in establishment and maintenance of the ancestral AM interaction (Bravo et al., 2016; Delaux et al., 2014).

Remarkably, AMF structures found in fossil records of rhizomes of early land plants show a high degree of morphological similarity to those found in roots of modern plants today (Remy et al., 1994). Canonical structures are formed during the ancient symbiosis (Figure 1.1 & Figure 1.2). Briefly, during the pre-symbiotic phase, AMF spores (SP) germinate and form extraradical hyphae (EH) (Figure 1.1; Figure 1.2a). Initial recognition between fungus and plant is built upon an exchange of signals that can regulate the other's metabolism and development, sign-posting presence of the partners. After recognition, EH of the fungus differentiate into hyphopodial (HP) structures that contact the plant root surface and penetrate epidermal cells (Figure 1.1; Figure 1.2b). This triggers construction of a pre-penetration apparatus, through which the fungus can pass via intra- and intercellular hyphae (IH) from epidermal to cortical cells (Figure 1.1; Figure 1.2c-f). Arbuscules (A), highly branched hyphal structures, are then formed within inner cortical cells of the plant root (Figure 1.1; Figure 1.2d-f), and surrounded by a special membrane, the periarbuscular membrane (PAM), made by the plant (S. E. Smith & Read, 2008). This interface is the site of nutrient transfer; as described in a comprehensive review (Luginbuehl & Oldroyd, 2017). Successful carbon transfer by the plant to AMF results in the formation of vesicles and daughter spores (Figure 1.1; Figure 1.2e-f), which store fatty acids and carbon for future AMF survival and spore germination.

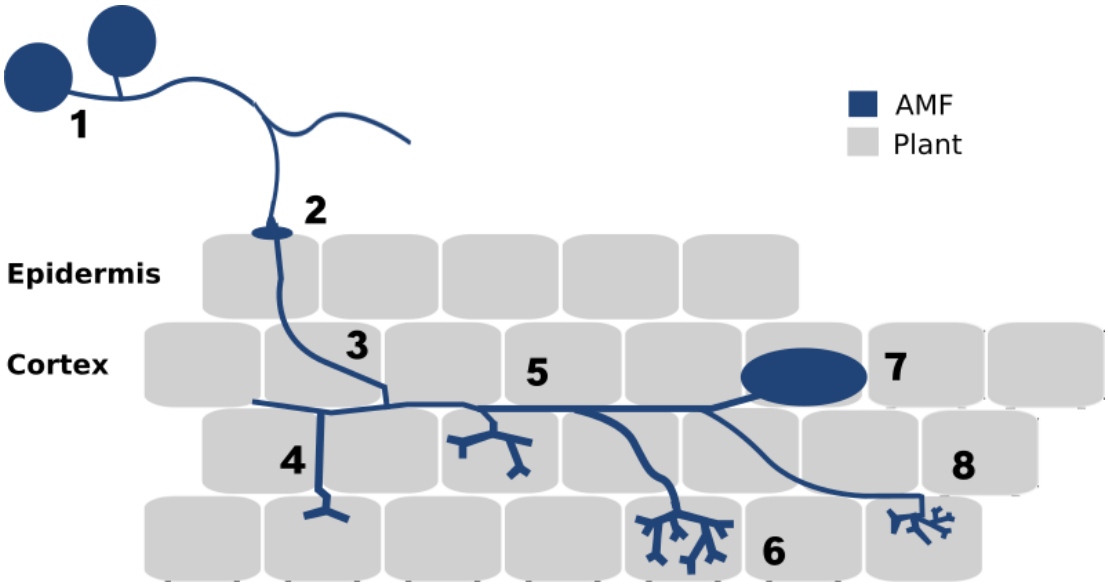

***Figure 1.1 Stages of AM colonisation**. Initial perception and recognition of AMF and plant root relies on a pre-symbiotic dialogue involving diffusible signals such as oligosaccharides and plant hormones like SLs (Stage 1). During this first stage, perception of fungal oligosaccharides stimulates calcium spiking in plant nuclei, which triggers downstream components of the common symbiosis signalling pathway (CSP). Downstream signalling of*

the CSP facilitates rhizodermal penetration through formation of hyphopodia that attach to the plant root surface (Stage 2). Fungal root-like structures, hyphae, then grow inter- and intra-cellularly towards the inner cortex (Stage 3). This cortical invasion results in formation of intraradical fungal structures that are essential to the establishment and maintenance of AM symbiosis. Arbuscules are highly branched structures that are the site of nutrient-carbon transfer in the plant. Their formation is facilitated by the plant root cell by nuclear movement and formation of a pre-penetration apparatus, which allows formation of an initial arbuscular 'trunk' (Stage 4). The arbuscule then develops through increased branching and formation of fine-branches (Stages 5-6). It is enveloped by a plant-derived peri-arbuscular membrane, which forms the site of nutrient transfer. Successful carbon transfer by the plant to AMF results in the formation of vesicles and daughter spores (Stage 7), which store fatty acids and carbon for future AMF survival and spore germination. Arbuscules are dynamic structures, collapsing after ~10 days (Stage 8).

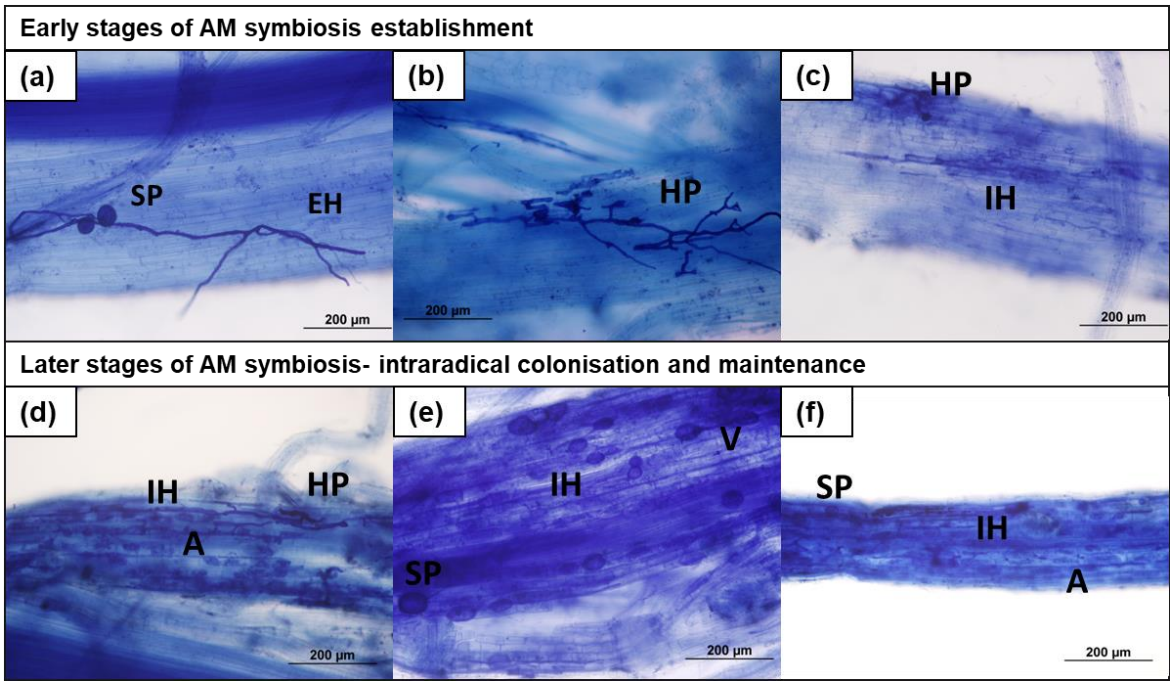

Figure 1.2 Representative images of canonical AMF structures formed within the plant root during AM symbiosis establishment and maintenance. *Scale bar represents 200um. Canonical AMF structures observed by trypan blue staining are denoted. Extraradical Hyphae (EH), Hyphopodia (HP), Intraradical Hyphae (IH), Arbuscules (A), Vesicles (V) and Spores (S) are indicated.*

1.1.1 Pre-symbiotic communication

The interaction between AMF and plant is initiated by a suite of diffusible signals (Stage 1, Figure 1.1). Plants roots exudate molecules into the rhizosphere, the external zone around the root, to sign-post AMF to their colonisable roots. In parallel, AMF release molecules that, upon recognition, prime the root for colonisation. Together, the bouquet of signals released into the rhizosphere initiate signalling that

is essential to establishing physical contact for effective colonisation between the partners.

Plant root exudates have been studied for many years and their effect on AMF identified function as chemical communication molecules. Strigolactones (SLs) were initially characterised as plant development hormones (Soundappan et al., 2015; L. Wang et al., 2015; Zhou et al., 2013) but also have an important role in the rhizospheric communication with AMF, inducing spore germination, hyphal branching, mitosis, respiration and growth to prime the fungus for interaction with the root (Akiyama et al., 2005; Besserer et al., 2008, 2006). It is suggested that SL function evolved in the last common ancestor of mosses and seed plants, potentially originating as signals enhancing environmental adaptability (Decker et al., 2017). Recent evidence suggests all core biosynthetic enzymes originated at or before the base of land plants (Delaux et al., 2012; Kodama et al., 2022; Walker et al., 2019), consistent with the idea that SLs evolved as rhizospheric signals that aided the transition of plants from aquatic to terrestrial environments (Walker et al., 2019).

Additional plant exudate signals involved in pre-symbiotic communication have been elucidated. Flavonoids are known to induce hyphal elongation in AMF and accumulate in plant host roots according to symbiotic status (Larose et al., 2002; Singla & Garg, 2017). Distinct fatty acids have additionally recently been found to stimulate hyphal branching and AMF metabolism (Kameoka et al., 2019). In addition, aberrant AM colonisation in the rice mutant of the GlcNAc transporter, NO PERCEPTION 1 (NOPE1) suggests that signals related to N-acetylglucosamines (GlcNAcs) are required (Nadal et al., 2017). Notably, SL and flavonoid biosynthetic mutants are still partially to fully colonised (Becard et al., 1995; C. Gutjahr et al., 2012; Kobae et al., 2018), whilst colonisation is severely reduced in *nope1* (Nadal et al., 2017), suggesting GlcNAc perception or associated signalling is pertinent for efficient root colonisation.

AMF reciprocally signal the plant host root through release of oligosaccharide molecules, built with a β-1-4-linked GlcNAc backbone. Mycorrhizal-lipochitooligosaccharides (Myc-LCOs) and short-chain chitooligosaccharides (COs), such as chitotetraose (CO_4) and chitopentaose (CO_5) have been identified in

germinating AMF spore exudates (GSEs) and are collectively known as 'Myc' factors. These molecules trigger responses such as gene transcriptional activation and intracellular calcium (Ca^{2+}) oscillations, which facilitate downstream CSP signalling for root colonisation (Genre et al., 2013). In addition, the first example of a proteinaceous signal exuded by AMF has been described. SL-INDUCED PUTATIVE SECRETED PROTEIN 1 (SIS1) is released by *R. irregularis* in response to SLs and knockdown resulted in significant suppression of colonization and stunted arbuscules, suggesting that the protein positively regulates pre-symbiotic and symbiotic stages of AM colonisation (Tsuzuki et al., 2016). Since GSEs contain a mix of GlcNAc signals, the relative proportions of these and other molecules and proteins may allow specific identification of AMF by the plant amongst other microbes simultaneously signalling in the rhizosphere (Genre et al., 2013).

Upon perception of such Myc factor signals, plant hosts initiate a rapid root response that enhances ability to accommodate AMF. Oligosaccharides are perceived by receptor-like kinases (RLKs) present on the root cell surface, which have lysin motifs (LysM) that can bind GlcNAc molecules. AM-associated RLKs include NOD FACTOR RECEPTOR 1 (NFR1) in legumes (Antolín-Llovera et al., 2014), named rice CHITIN ELICITOR RECEPTOR KINASE 1 (CERK1) (Carotenuto et al., 2017; Chiu et al., 2018; X. Zhang et al., 2015) and NFR5. Perception of oligosaccharides leads to activation of the common symbiosis pathway (CSP), responsible for initiation of both AM symbiosis and root nodule symbiosis with nitrogen-fixing bacteria (RNS). Mutants of the receptor complexes have diverse effects, likely due to redundancy. For example, *cerk1* mutants, homologous to NFR1, have significantly reduced AM colonization in rice (Chiu et al., 2018; Feng et al., 2019; Gibelin-Viala et al., 2019; Leppyanen et al., 2018; Liao et al., 2018; Miyata et al., 2014; L. Zhang et al., 2019; X. Zhang et al., 2015) whilst NFR5 mutants are redundant with no AM phenotype (Feng et al., 2019; Maillet et al., 2011; X. Zhang et al., 2015). Additional LCO receptors have been identified in solanaceous species, such as *Phylk10* and *Sllyk10* (Girardin et al., 2019). Overall, this suggests that recognition of AMF involves complex combinations of different LysM-RLKs and suites of signals in different plant species (Chiu & Paszkowski, 2020).

Many of the host mechanisms involved in the CSP molecular programme were initially found by study of mutants of legume hosts defective in RNS, which is thought to have evolved from the more ancient AM symbiosis (Gutjahr & Parniske, 2013; Van Rhijn et al., 1997). Ca^{2+} spiking downstream to oligosaccharide perception triggers developmental changes in the plant required to facilitate the signalling programme (Genre et al., 2013). SYMBIOSIS RECEPTOR KINASE (SYMRK) activates perinuclear Ca^{2+} oscillations (Charpentier et al., 2016) via nuclear ATP-powered Ca^{2+} pump MCA8, nuclear porins NENA, NUCLEAR PORE NUP85 and NUP133 and Ca^{2+} channels encoded by *CASTOR/POLLUX* genes. Ca^{2+} oscillations are believed to activate nuclear CALCIUM/CALMODULIN-DEPENDENT KINASE (CCaMK) (Groth et al., 2010; C. Gutjahr et al., 2008; S. Kim et al., 2019; Shimoda et al., 2012; Yano et al., 2008), which phosphorylates the transcriptional regulator CYCLOPS (Genre & Russo, 2016). CYCLOPS interacts with DELLA to activate symbiotic genes such as *RAM1*, a major GRAS transcription factor implicated in lipid biosynthesis, fine branching of the arbuscule and nutrient exchange (Luginbuehl et al., 2017). Compared to strong nodulation defects, mutants of the CSP are defective in AM colonization but can establish intraradical structures in some cases (C. Gutjahr et al., 2008). The specificity of the oscillations for AM colonization is debated, as spiking in response to GSEs is lost in *Oscerk1,* which can still establish a delayed AM colonization with normal intracellular structures (Carotenuto et al., 2017).

In contrast, AM symbiosis is fully abolished in rice upon mutation of *DWARF-14-LIKE (D14L),* an α/β-fold hydrolase receptor involved in regulated plant response to AMF (C. Gutjahr et al., 2015). D14L is a homolog of *A. thaliana* KARRIKIN INSENSITIVE 2 (KAI2), which binds karrikin (KAR), a smoke-derived compound responsible for vegetation restoration post-wildfire. KAI2 has previously been implicated in drought resistance, photomorphogenesis, seed germination and seedling establishment (Flematti et al., 2004; X. D. Sun & Ni, 2011; Waters et al., 2012; Waters & Smith, 2013). Although D14L can directly bind KAR, the ligand required for AM symbiosis remains unknown (Choi et al., 2020). Recently, D14L-mediated signalling components have been elucidated in rice. Binding of D14L to the F-box E3 ligase DWARF3 targets degradation of SMAX1, a negative regulator. Such regulation facilitates downstream AMF-induced transcription of symbiotic genes, such as the

transcription factors *CYCLOPS* and *NSP2*, vital for CSP symbiosis establishment and SL biosynthesis respectively. Interestingly, SMAX1 additionally regulates genes across the entire SL biosynthesis pathway, acting as a crosstalk between hormonal and pre-symbiotic signalling. The SL receptor D14 is evolutionarily younger than D14L and evolved through gradual neofunctionalization of KAI2 paralogs (Bythell-Douglas et al., 2017). An ancestral SL, bryosymbiol (BSB) is present in diverse bryophytes and vascular plants. In *Marcantia paleacea,* BSB is secreted, and required for AM symbiosis, but not perceived due to lack of perception by KAI2 and the absence of cognate SL receptors. This work further suggested that SLs were first rhizospheric signals and the evolution of SLs as endogenous hormones occurred only after the evolution of a cognate receptor from KAI2 (Kodama et al., 2022).

1.1.2 Extraradical contact and initial penetration

Initial physical contact between AMF and plants occurs when AMF hyphae differentiate into foot-like structures, named hyphopodia, that attach to the root epidermal surface (Figure 1.1; Figure 1.2b-c). Hyphopodial differentiation has long been recognised as being dependent on contact recognition with the root epidermal surface, although the particular rhizodermal cell wall properties governing this remain to be elucidated (Nagahashi & Douds, 1997). SL biosynthetic genes *CCD8/D10* and *CCD7*/*D17* are thought to be required for efficient hyphopodia formation (Kobae et al., 2018), although they are not essential as normal hyphopodia have also been reported in the mutants (C Gutjahr et al., 2012; Kobae et al., 2018). In contrast, other pre-communication receptor mutants such as *nope1* in maize and rice and *d14l* in rice show deficient or absent hyphopodia, respectively (Choi et al., 2020; C. Gutjahr et al., 2015; Nadal et al., 2017), suggesting that early signalling by these pathways is indispensable to the initial contact stage.

After hyphopodial engagement, host plants accommodate AMF through concurrent modification of cellular organisation and symbiotic-specific gene expression. A pre-penetration apparatus (PPA) forms as an invagination of the plasma membrane, supported by a novel network of cytoskeleton and endoplasmic reticulum (Genre et al., 2008). This tube-like infection structure facilitates movement of hyphae through cells, allowing invasion of AMF through the epidermal tissue to the cortex (Figure

1.1; Figure 1.2). The CSP and associated symbiotic gene expression is thought to be essential for PPA formation (Genre et al., 2008, 2005). Accordingly, mutants defective in CSP, such as *castor, pollux* and *ccamk*, form initial contact structures on the root surface but intracortical invasion is abolished (Banba et al., 2008; Genre et al., 2005; C. Gutjahr et al., 2008; Wegel et al., 1998). Furthermore, ectopic expression of *SYMRK* and *CCaMK* induces expression of symbiosis-specific genes in absence of AMF and leads to the formation of PPA-like structures (Ried et al., 2014; Takeda et al., 2012). This suggests a direct role of the CSP in orchestrating signalling programmes facilitating plant intracellular accommodation of AMF. The spatiotemporal specifics of this, however, remain unclear (Choi et al., 2018).

1.1.3 Formation of AM intraradical structures

The resultant hallmark of intraradical invasion is the development of highly branched tree-like structures named arbuscules (Figure 1.1; Figure 1.2d-f). Arbuscule formation is associated with reorganisation of the plant cortical host cellular structures to create space and avoid rupture (Balestrini et al., 1992; Genre et al., 2008, 2005). An arbuscule develops first from a single hyphal trunk that enters the cell. Hypha continually bifurcate and dichotomously branch, forming a tree-like arbuscule which fills plant cortical cells. A novel symbiosis-specific plant-derived membrane, the peri-arbuscular membrane (PAM), forms continuous with the plasma membrane and envelopes the developing structure. The spatiotemporal dynamics of arbuscule and PAM formation facilitate the mutually beneficial share of resources between plant and AMF, although the processes orchestrating this remain unclear (Pumplin et al., 2012). Recent ultrastructure analysis of periarbuscular and fungal membrane surfaces identified that invasive hyphal growth is associated to fungal membrane tubules (memtubs) and periarbuscular evagination. In addition, extracellular vesicles continually form in the peri-arbuscular interface but their origin and function remain unknown (Roth et al., 2019).

Once established within roots, the arbuscule forms the site of reciprocal nutrient and carbon exchange. Host symbiotic-specific phosphate transporters, such as MtPT4 and OsPT11 are located on the PAM domain covering the fine branches of the arbuscule (Genre et al., 2008; Kobae & Hata, 2010; Pumplin & Harrison, 2009).

Mutants of the transporters themselves or that are defective in polar localisation are unable to form fine branches, resulting in premature arbuscule degeneration, stunted arbuscule structures and loss of maintenance of symbiosis (Javot et al., 2007; Paszkowski et al., 2002; Yang et al., 2012; X. Zhang et al., 2015). Similarly, half-size ATP binding cassette (ABC) transporter heterodimers, STR1/STR2 are likely required for the export of long-chain fatty acids into peri-arbuscular space. Mutants in the genes involved in FA synthesis and transport have severely reduced AM colonisation, aberrant arbuscule form and function, and are crucial for maintenance of the symbiosis (Bravo et al., 2017; C Gutjahr et al., 2012; Jiang et al., 2017; Luginbuehl et al., 2017; Q. Zhang et al., 2010).

Gain of fatty acids from plants allows AMF to produce lipid storage vesicles that are found intra-radically within or between host cells (Figure 1.1; Figure 1.2e). AMF are fatty acid auxotrophs (Tisserant et al., 2013) yet use triacylglycerol as their main carbon source, meaning fatty acid transfer from the plant host is integral to their life cycle (Jiang et al., 2017; Luginbuehl et al., 2017). Well-nourished AMF produce asexual spores that contain both nuclei from parental migration and mitotic division. Importantly, these spores also host storage lipids that can support further spore germination and asymbiotic germ-tube proliferation (Marleau et al., 2011). It remains unclear how vesicle and spore formation are regulated, although their successful development is frequently correlated to lipid transfer from the plant host (Keymer et al., 2017).

Arbuscules typically have a life span within plant cells of about two to eight days, after which they shrink and degenerate (Alexander et al., 1989; Toth & Miller, 1984) (Figure 1.1; Figure 1.2d-f). Microscopic observation suggests that collapse begins at fine-branches and progresses back towards the trunk. At the base, distinct fungal septa develop that separate the degenerative, metabolically inactive hypha from the living hypha (Kobae et al., 2014). Hyphal shrink is followed by degeneration of the PAM and associated proteins; forming distinctive signs of degenerative arbuscules or ‘arbuscule collapse’ (Kobae & Hata, 2010). In *Medicago truncatula,* such collapse is associated with transcriptional regulation of plant hydrolytic enzymes by MYB-like transcription factor MYB1, the expression of which is enhanced by *DELLA* and *NSP1* transcription factors which contribute to expression of genes required for symbiosis

development. Combinatorial use of transcription factors likely enables sequential activation of the transcriptional programmes facilitating degeneration, although the signalling that activates these remain unknown (Floss et al., 2017). Overall, evidence suggests an active role of the plant host in orchestrating arbuscule degeneration during root colonisation. The root is continuously recolonised during the AMF life cycle, sometimes in cells that have previously accommodated arbuscules. The plant regulates such simultaneous arbuscule formation and degradation by cell via transcriptional changes, some of which remain to be elucidated (Luginbuehl & Oldroyd, 2017).

1.1.4 Bi-directional nutrient exchange and hormonal changes

The hallmark benefit of AM colonisation to plant hosts is the gain of nutrients that are otherwise limited in the rhizosphere. Plants are sessile in nature, meaning that they can only mine the area surrounding their roots, the rhizosphere, for resources. Some of the most essential minerals, such as inorganic phosphorous (P_i) and nitrogen, are often limited due to their chemical properties. P_i, the only form of phosphorous that can be taken up by plants, is limited due to binding of orthophosphate to calcium or aluminium ions. This immobilises the P_i source, meaning a depletion zone forms around the root once all available resource has been mined. Nitrogen, in comparison, is often present in forms that are very mobile in the soil, such as nitrate (NO_3^-) and ammonium (NH_4^+). This means the N source is easily leached away and crop plants only can utilise 30-40% of the applied N fertilization (Raun & Johnson, 1999). It is well acknowledged that mycorrhizal uptake pathways of P_i and N can contribute significantly to host acquisition (S. E. Smith, 2003; S. E. Smith & Read, 2008; S. E. Smith et al., 2004; S. Wang et al., 2020). In addition, AMF can improve plant biomass and grain content of micronutrients such as zinc (Zn) (Ma et al., 2019; Pellegrino et al., 2015).

Soil nutrient composition induces modest changes in microbial community composition but can be a big influencer in the placement of microbial interactions on the mutualism-pathogenicity continuum and in facilitating symbiotic interaction (Fabiańska et al., 2019; Hiruma et al., 2016; Leff et al., 2015). AMF, for example,

preferentially colonise plant roots in P_i limited conditions; symbiosis is suppressed by the host if supply is otherwise abundant (Kobae et al., 2016; Mosse, 1973; Yang et al., 2012). Nutrients can be absorbed by two pathways in mycorrhizal roots- directly through the root epidermis or indirectly via transfer from AMF hyphae. A 'switch' from a direct P_i uptake pathway to the symbiotic pathway occurs in low P_i conditions (Paszkowski et al., 2002; S. E. Smith, 2003; S. E. Smith et al., 2004; Yang et al., 2012). Such nutrient-driven regulation has recently been elucidated further and PHR transcription factors involved in the P_i starvation response were identified as master regulators of AM signalling and associated symbiotic transporter expression, ensuring symbiotic uptake occurs only upon P_i starvation in the plant host (Das et al., 2022; Shi et al., 2021; Z. Wang et al., 2014). In the symbiotic P_i pathway, fungal transporters of Pht1 family likely facilitate P_i uptake, which is then transported in the form of polyphosphate granules along extraradical hyphae to the intraradical mycelium network (Benedetto et al., 2005; Harrison & Van Buuren, 1995; Maldonado-Mendoza et al., 2001; Yang et al., 2012). Polyphosphate is then hydrolysed and released as orthophosphate into the peri-arbuscular space (Ezawa et al., 2004). AM-induced transporters, such as PT11, localise on the fine branches of the PAM and facilitate orthophosphate uptake by the plant (Ezawa et al., 2004; Harrison et al., 2002; Javot et al., 2007; Karandashov et al., 2004; Nagy et al., 2005; Paszkowski et al., 2002). 70-100% of Pi can be supplied by symbiotic uptake, although the fate of Pi after uptake from the arbuscule remains unresolved (S. E. Smith, 2003; Yang et al., 2012).

Nitrogen transfer in AM symbiosis is less well understood. Primary N sources for rice include nitrate (NO_3^-) in aerobic upland and ammonium (NH_4^+) in flooded soil and it is suggested that AMF can uptake both, as well as organic N forms. After uptake, nitrogen is transported in the form of arginine to arbuscules, where it is released into the periarbuscular space for uptake by the plant (Cruz et al., 2007; Govindarajulu et al., 2005; Javot et al., 2007; Tanaka & Yano, 2005). Active transport of nutrients across the plant membrane requires energy provided by proton transport generating an electrochemical gradient (Sze et al., 1999). Accordingly, symbiosis-induced proton ATPases have been identified, several with specific expression in arbusculated cells (Gianinazzi-Pearson et al., 2000; F. Krajinski et al., 2002; F. Krajinski et al., 2014; E. Wang et al., 2014). Labelling studies have previously

suggested that N is transported in the form of NH_4^+ from AMF (Cruz et al., 2007; Govindarajulu et al., 2005; Leigh et al., 2009) and transporters such as *GmAMT4.1* and *SbAMT3.1,* localised on the PAM and transcriptionally induced under mycorrhizal conditions, have been described (Breuillin-Sessoms et al., 2015; Gomez et al., 2009; Guether et al., 2009; Kobae et al., 2010; Koegel et al., 2013; S. Wang et al., 2020). More recently, mycorrhizal NO_3^- acquisition via host nitrate transporters such as *OsNPF4.5* have also been identified; likely forming an additional symbiotic N uptake route conserved in gramineous species. Overall, the symbiotic N uptake route can contribute up to 40% of N acquisition in plants (S. Wang et al., 2020).

In return for nutrient benefit, plants supply up to 20% of their photosynthetic carbon to AMF (I. Jakobsen & Rosendahl, 1990; S. E. Smith & Read, 2008). AMF are fatty acid auxotrophs and, since lipids comprise up to 95% of spore dry weight and up to 53% of vesicle dry weight (Jabaji-Hare, 1988; Jabaji-Hare et al., 1984), plant hosts provide the lipid source required for AMF to complete their asexual lifecycle; maintaining colonisation of their roots in the process. Previous ^{13}C radioisotope labelling provided evidence for glucose transfer to AMF, which is taken up by high-affinity monosaccharide transporters and converted to glycogen and trehalose for fungal metabolism (Helber et al., 2011; Schüßler et al., 2006; Shachar-Hill et al., 1995). Notably, transcriptomic data revealed that AMF lack eukaryotic fatty acid synthase (FAS) genes required for de novo long-chain fatty acid synthesis (Tisserant et al., 2013). It was subsequently discovered that a regulated export pathway supplies plant fatty acids to the AMF host, dependent on RAM1 and RAM-dependent WRINKLED transcription factors (Jiang et al., 2017; Luginbuehl et al., 2017). STR1/STR2 ABCG transporters are likely required for the export of long-chain fatty acids into peri-arbuscular space (Bravo et al., 2017; C Gutjahr et al., 2012; Jiang et al., 2017; Luginbuehl et al., 2017; Q. Zhang et al., 2010).

Importantly, AMF fall on the mutualism-pathogenicity continuum and can become parasitic to host plants when costs outweigh relative benefit of the interaction (Johnson et al., 1997). Bi-directional exchange in AM symbiosis is described to follow a “free-market” model in which both partners exert control over supply and demand. On the fungal side, a recent study identified genetic diversity in AMF-driven regulation of the fatty acid pathway in cassava (Savary et al., 2020). On the plant

side, reactive responses to nutrient status maintain the reciprocal reward (Kiers et al., 2011). Transporters function both in sensing of nutrient conditions and in facilitating AM symbiosis for plant control of the bi-directional exchange. Mutants of the *MtPT4* P_i-transporter show premature degeneration of arbuscules and early abortion of symbiosis (Javot et al., 2007). The AMMONIUM TRANSPORTER 2 family protein AMT2-3 cannot transport ammonium but is required for aborted symbiosis in *Mtpt4*. The phenotype can be rescued in low nitrogen conditions, suggesting that host nitrogen requirement additionally has an important role in maintenance of symbiosis (Breuillin-Sessoms et al., 2015). In addition, the plant sucrose transporter/sensor SUT2 negatively regulates AM colonisation, exerting control of sugar flux to AMF (Bitterlich et al., 2014) and expression of the fatty acid exporters *STR* and *STR2* is repressed by high P_i (W. Wang et al., 2017).

Systemic response to nutrient status can also regulate root colonisation. Response to P_i-starvation in rice is facilitated by the transcription factor PHOSPHATE STARVATION RESPONSE 1 (PHR1), which regulates P_i transporters in the root via shoot-derived microRNA399 and miR827 (Aung et al., 2006; Chiou et al., 2006; X. L. Hou et al., 2005; Hsieh et al., 2009; C. Wang et al., 2009; Z. Wang et al., 2014). Recent evidence eluded that this starvation response integrates nutrient cues to regulate AM symbiosis. PHR transcription factors, including PHR2 in rice, regulate AM colonisation in response to host phosphate starvation status by targeting genes required for pre-symbiotic signalling and root colonisation (Das et al., 2022; Shi et al., 2021). It is reported that this regulation occurs through the symbiotic GRAS-type transcription factors NSP1 and NSP2, which induce expression of AM-associated genes and regulate many enzymes involved in apocarotenoid biosynthesis, including the SL biosynthesis pathway. NSP-induced regulation of symbiotic perception through components of these pathways likely promotes AM colonisation through D14L/SMAX1 signalling (X.-R. Li et al., 2022; W. Liu et al., 2011). Such control allows the plant host to ensure that the high energetic carbon cost of hosting AMF is compensated by nutrient gain, particularly in environments in which it would otherwise fail to do so. The mechanisms of this are only recently being elucidated but are essential to understanding the plant host benefit of symbiosis.

1.2 Blumenols and apocarotenoids associated to AM colonisation

Plants use hormones and small molecules for coordinated responses to environmental cues, including the interaction with AM fungi. Apocarotenoids are a subclass of such molecules, derived from plant isoprenoids and carotenoids by cleavage using carotenoid cleavage dioxygenase (CCD) enzymes or reactive oxygen species (Fiorilli et al., 2019). CCDs are an evolutionarily conserved family of enzymes (X. Hou et al., 2016; J. Y. Wang et al., 2019) and most cleave at certain double bond(s) in their respective carotenoid/apocarotenoid substrate (Walter & Strack, 2011), although more general substrate and site specificity can occur (Ilg et al., 2014). CCD1 enzymes can cleave several carotenoid and apocarotenoids; acting on linear and cyclic substrates (Ilg et al., 2014). CCD4 cleaves at specific carbon positions in molecules such as zeaxanthin or bicyclic carotenoids (Bruno et al., 2015, 2016). CDD7 and CCD8 are implicated in SL biosynthesis. CCD7 is stereospecific enzyme, whilst CCD8 is unusual in its ability to sequentially cleave specific isomers of the subsequent substrate products (Alder et al., 2012; Bruno et al., 2016, 2017). Recently, a survey of 69 plant species identified an overlooked subfamily of CCDs, represented by ZAXINONE SYNTHASE (ZAS) and ZAS2 in rice (Ablazov et al., 2022; Alder et al., 2008, 2012; J. Y. Wang et al., 2019). Respective apocarotenoids produced by the CCDs have diverse functions in plant development and response to environmental stimuli, with some being implicated in AM symbiosis.

1.2.1 Apocarotenoids implicated in AM symbiosis

1.2.1.1 Strigolactones

Initially characterized as compounds exuded from roots that induce germination in root parasitic *Striga* (Butler, 1994; C. E et al., 1966), SLs are now described as plant apocarotenoid hormones with a methylbutenolide ring (D-ring) linked in *R* configuration to a structurally variable second moiety (Al-Babili & Bouwmeester, 2015). The finding that branching/high tillering mutants in different plant species were SL deficient aided in breakthrough discovery of SL biosynthetic enzyme candidates. Genetic studies in rice identified four main enzymatic reactions. First, reversible isomerisation of β-carotene to 9-cis-β-carotene (9-cis-C_{40}) occurs via iron-

binding β-carotene isomerase, DWARF 27 (D27) (Abuauf et al., 2018; Alder et al., 2012). This product is cleaved to 9-cis-β-apo-10'-carotenal (9-cis-C_{27}) by the stereospecific CCD7/D17 (Alder et al., 2012; Bruno et al., 2014). This is further cleaved by CCD8/D10 to form carlactone (CL) (Alder et al., 2012; Bruno et al., 2017). CL is transported from the plastid to the cytosol, where cytochrome P450 MAX1 CYP711A enzymes facilitate subsequent structural diversification into canonical and non-canonical SLs (Y. Zhang et al., 2014). Rice contains five MAX1 homologs and transient expression in *Nicotiana bethamiana* suggests that all functional enzymes can convert CL into carlactonic acid, which is synthesized to the canonical SLs 4-deoxyorobanchol (4DO) and orobanchol by sequential action of OsMAX-900 and OsMAX-1400 (Ito et al., 2022; Yoneyama et al., 2018).

SL signalling occurs through binding of SL to the α/β hydrolase receptor D14, which forms a complex with the F-box protein D3 (Arite et al., 2009; Hamiaux et al., 2012; Ishikawa et al., 2005). This complex facilitates ubiquitination and degradation of D53, a SMAX1-LIKE (SMXL) protein that represses SL signalling. Mutation of the genes involved in the SL signalling pathway results in insensitivity to SLs and aberrant AM colonisation phenotypes. *d3* mutants are severely in defected AM colonisation, with reduced frequencies of arbuscule and vesicle formation. In contrast, *d14* have increased AM colonisation rates (Yoshida et al., 2012). This suggests that *D3* but not *D14* is essential to AM colonisation, likely due to the additional role in of *D3* in AM signalling by *D14L/D3*-mediated suppression of *SMAX1,* which is vital for AM symbiosis establishment (Choi et al., 2020). In addition, *d14* mutants show significantly increased numbers of hypodermal passage cells, which AMF can move through. This indicates a role for SLs in shaping exodermal morphology, which may additionally facilitate accommodation of AMF in root tissue (G. Liu et al., 2019).

As previously noted, SLs trigger a range of responses in AMF; including spore germination, hyphal branching, mitosis, respiration and growth (Akiyama et al., 2005; Besserer et al., 2008, 2006). In addition, mutants of SL biosynthesis genes *D10/CCD8* and *D17/CCD7* have reduced AM colonisation of roots but form canonical AMF structures, suggesting SLs are required but not essential to colonisation (C Gutjahr et al., 2012; Kobae et al., 2018; Yoshida et al., 2012). No AM

phenotype has been studied in *D27* mutants to date. SLs are exuded by the plant root in a mechanism including the ABC-transporter, PLEIOTROPHIC DRUG RESISTANCE 1 (PDR1), identified in petunia but conserved between plant species (Banasiak et al., 2020; Kretzschmar et al., 2012). Transcription of *PDR1* is upregulated in low-Pi conditions, linking nutritional status of the plant with need for beneficial colonisation. Localisation of PDR1 in plasma membrane of cortical cells in root tip and hypodermal cells suggests that it facilitates guidance of AMF hyphae to the appropriate root surfaces for interaction. Notably, the identity of fungal SL perception machinery remains unknown (Kretzschmar et al., 2012).

SLs are diverse in structure and function, with over 30 SLs isolated from root exudates of different species to date (Xie, 2016). Canonical SLs have tricyclic lactones (ABC rings) as their second moiety while non-canonical SLs contain a moiety other than the ABC ring (Jia et al., 2018; Yoneyama et al., 2018). The identification of an ancestral SL, BSB, that is essential for symbiosis but not endogenous hormone function in *M. paleacea* suggests that SLS first evolved to facilitate communication with AMF. Notably, composition of SLs exuded from roots is diverse in vascular species and the essentiality of such for establishment of AM colonisation remains unclear (Taulera et al., 2020). Recent reports indicate that only certain SLs are important for AM symbiosis establishment in rice (Ito et al., 2022). *MAX1 Os900-KO* mutants lacking canonical SLs 4DO and orobanchol and non-canonical MeO-5-DS is1 but that still produce a novel non-canonical SL derivative (CL+30) don’t show tillering and reduced shoot height but exhibit a delay in AM symbiosis (Ito et al., 2022). In species such as black oat and sunflower, no known canonical SLs have been detected despite occurrence of AM colonisation (H. Il Kim et al., 2014; Ueno et al., 2014). These species do accumulate the non-canonical SL precursor CL, which has previously been reported to promote hyphal branching and could additionally act as a rhizospheric symbiotic signal (Mori et al., 2016). Non-canonical SLs such as lotuslactone in *L. japonicus,* heliolactone in sunflower and zealactone in maize are weak to moderate inducers of hyphal branching (Xie et al., 2019). Overall, there is diversity in SL identity and requirement of specific derivatives for promotion of AM symbiosis requires further investigation.

Production of SLs can be influenced by the environment and biosynthesis and export is upregulated in conditions that favour AM colonisation, such as in P_i and nitrogen deficiency (López-Ráez et al., 2008; H. Sun et al., 2014). Under P_i starvation, expression of AM-associated genes, *NSP1, NSP2* and apocarotenoid biosynthesis genes, including SLs, are promoted by the phosphate starvation responsive transcription factor, PHR2 (Das et al., 2022; Shi et al., 2021). Similarly, a novel feedback mechanism regulating SL content through root-to-shoot mobile CLE-peptides was recently identified. Perception of CLE peptides by the receptor-like kinase SUNN mechanistically modulates expression of SL biosynthetic genes; regulating SL content and AM colonisation level (Müller et al., 2019). Since the root-to-shoot mobile CLE-peptide *CLE53* is repressed in low P_i conditions, it is suggested that this pathway may represent an additional means for autoregulation of colonisation in response to nutrient availability through SL production (Karlo et al., 2020).

Overall, diverse SLs are positive regulators of AM colonisation; promoting pre-symbiotic dialogue between AMF and plant via enhancement of fungal ability to colonise roots. Crosstalk to other plant hormone and signalling pathways likely facilitates this nutrient-mediated response, although the spatiotemporal mechanisms and SL derivatives required remain to be elucidated.

1.2.1.2 Abscisic Acid

Abscisic acid (ABA) is an apocarotenoid with essential function as a key plant hormone in abiotic stress response, plant growth and development, seed maturation and promotion of pathogen defence (Dodd, 2013; Merilo et al., 2015; Tuan et al., 2018). Work in ABA defective mutants in tomato suggested that ABA has a direct effect on arbuscule formation as well as an indirect effect on ethylene levels, which inhibits symbiosis (Herrera-Medina et al., 2007; J. Á. Martín-Rodríguez et al., 2011). More recently, components of the ABA signalling pathway were found to be required for AM colonisation, independent of ethylene signalling (Charpentier et al., 2014). ABA accumulates in mycorrhizal roots (Danneberg et al., 1993; Ludwig-Müller, 2010; Meixner et al., 2005) and such accumulation may be required for regulated

promotion of symbiosis by ABA signalling components, the expression of which are induced by ABA (Charpentier et al., 2014).

In addition, ABA regulates production of other phytohormones, and this may cause direct or indirect effects on AM symbiosis. For example, ABA is a positive regulator of SLs, which promote symbiosis (López-Ráez et al., 2010). In addition, levels of gibberellic acid (GA) increase in mycorrhizal roots. GA negatively regulates arbuscule formation and ABA synthesis. Since ABA has been implicated in attenuated GA biosynthesis, it has been suggested that ABA could act to modify bioactive GA level to regulate symbiosis (J. A. Martín-Rodríguez et al., 2016). Overall, these data suggest that ABA can regulate AM colonisation by inhibition of ethylene production and promotion of phytohormone signalling.

1.2.1.3 Zaxinone

Recently, ZAXINONE SYNTHASE (ZAS) and ZAS2 were identified as a part of a novel subfamily of CCDs common across the plant kingdom. In rice, ZAS enzymes catalyse 3-OH-all-*trans*- *β*-apo-10'-carotenal (apo-10'-zeaxanthinal) into 3-OH-all-*trans*-apo-13-carotene (zaxinone) apocarotenoids. Mutant analysis demonstrated the importance of zaxinone in growth promotion and SL content, with aberrant shoot and root growth and increased SL content in *zas* mutants restored by exogenous application (J. Y. Wang et al., 2019). More recent analysis suggests that zaxinone additionally promotes sugar metabolism, root cell division and hormone regulation in rice, acting as a novel hormone regulating plant growth and metabolism in response to environmental stimuli (J. Y. Wang et al., 2021).

Zaxinone has been implicated in AM symbiosis and *ZAS* orthologs are absent in the genomes of non-AMF host species (Ablazov et al., 2022; J. Y. Wang et al., 2019). *OsZAS* expression is upregulated at early and late states of colonisation (J. Y. Wang et al., 2019), whilst *OsZAS2* is only upregulated at later time points, localised in arbusculated cells and uncoupled to SL (Ablazov et al., 2022). Root colonisation is reduced in *zas* and *zas2* mutants despite increased root expression of SL biosynthesis genes and increased SLs in root exudates. The reduced colonisation could be due to a strict requirement for zaxinone in AM symbiosis, although this

remains to be determined in mutants where zaxinone is completely abolished. It is suggested that regulation of SL biosynthesis upon AMF presence and P_i-limitation is dependent on *ZAS* enzymes and is essential for efficient colonisation (Ablazov et al., 2022; Votta et al., 2022; J. Y. Wang et al., 2019).

1.2.1.4 Blumenols and Mycorradicin

Both mycorradicin and blumenols are apocarotenoids that have long been associated to AM colonisation - root accumulation is considered as a 'signature of AM symbiosis' (Fiorilli et al., 2019; Hill et al., 2018; Walter et al., 2007; M. Wang et al., 2018). A "yellow pigment" identified to accumulate in roots colonised by AMF was first described in 1924 (Jones, 1924). This was later identified as a C_{14} polyenic acid chromophore termed mycorradicin (Klingner et al., 1995). It was found that C_{14} mycorradicin was formed by oxidative cleavage resulting in two additional C_{13} cylohexanone derivatives from a C_{40} apocarotenoid precursor (Klingner et al., 1995). Such C_{13} cyclohexanone derivatives, named blumenins and blumenols (the aglycon part of blumenin) were later identified in mycorrhizal roots of cereals, with the abundance of compound directly related to the degree of root length colonisation (Fester et al., 1999; W. Maier et al., 1995). Mycorradicin and blumenols were first reported to be derived from carotenoids (Maier et al., 1998) and that biosynthesis occurs by oxidative cleavage of a common carotenoid precursor of the plastidial MEP pathway was later identified by evidence that AMF induce MEP pathway genes; expression correlating spatially and temporally with accumulation of the two apocarotenoids (Walter et al., 2000; Walter et al., 2007).

Current models for the biosynthetic pathway assume that the common C_{40} precursor is cleaved by a CCD (CCD4 or CCD7) to form a C_{27} intermediate and C_{13} cyclohexanone. The intermediate is subsequently cleaved by CCD1 to the mycorradicin precursor, rosafluene-dialdehyde $C_{14,}$ and a C_{13} cyclohexanone, blumenol (Floß et al., 2008; X. Hou et al., 2016; Z. Sun et al., 2008; Vogel et al., 2010). Knockdown of *MtCCD1* resulted in reduction of C_{14} mycorradicin but only ~50% reduction in C_{13} cyclohexanone accumulation during AM colonisation. The resultant product included a C_{27} apocarotenoic carboxylic acid, suggesting that a second CCD is involved in the cleavage of the elusive C_{40} carotenoid precursor in

mycorrhizal roots, with CCD1 likely cleaving the resultant C_{27} intermediate (Floss et al., 2008). CCD7 has been identified as a candidate for such C_{40} cleavage (Alder et al., 2008) and blumenol and mycorradicin are reduced in tomato *ccd7* mutants (Vogel et al., 2010). Notably, this would require a subsequent isomerization of the intermediates for substrate specificity of CCD7 (Bruno & Al-Babili, 2016). It has been suggested that D27 may facilitate this, although no direct evidence has been reported (Fiorilli et al., 2019; M. Wang et al., 2018).

Notably, some blumenol derivatives, namely blumenol C glycosides, accumulate specifically in roots after AMF-inoculation and are not induced by other environmental stimuli such as pathogens or abiotic stress (Maier et al., 1997; M. Wang et al., 2018). In addition, the correlation to root colonisation is widespread across different plant and AMF species (Strack & Fester, 2006; M. Wang et al., 2018). Despite this, the function of blumenols and mycorradicin in AM symbiosis remains unknown. The finding that AM colonisation is maintained in *MtCCD1* mutants, despite near abolished mycorradicin accumulation, suggested that mycorradicin is not essential for AM symbiosis. (Floss et al., 2008). Blumenols have been suggested to be involved in maintenance of AM symbiosis once the interaction has formed; supported by an increase in blumenol concentration as the symbiosis progresses, particularly in root cells hosting AMF structures (Fester et al., 2002). In addition, mutants with reduced blumenol production are associated with increased amount of dead and degenerating arbuscules or reduced colonisation sites (Floß et al., 2008; Floss et al., 2008; Kobae et al., 2018). Exogeneous application of blumenin, which blumenol forms the aglycone part of, inhibited colonisation and arbuscule development in early stages of barley AM colonisation, suggesting the role is not in pre-symbiotic rhizosphere communication (Fester et al., 1999).

Colorimetric and chromatographic assays characterising mycorradicin and blumenol during root colonisation has been reported for over a century (Fester et al., 1999; Fyson & Oaks, 1992; Jones, 1924; W.N. & J.W., 1977). Some cereal crops and species of the Liliaceae and Fabaceae naturally produce enough yellow pigment to visually screen roots for colonisation (Klingner et al., 1995), as used successfully in maize to identify mutants with impaired colonisation (Paszkowski et al., 2006). Notably, not all plants produce enough pigments for visual decolouration of roots

upon AM colonisation, meaning the method cannot be used for all plant species. Importantly, in 2018, abundance of five blumenol C glycosides were identified that quantitatively accumulated in AM-colonised roots of multiple crop and model species, including *Solanum lycopersicum, Solanum tuberosum, Medicago truncatula, Hordeum vulgare, Triticum aestivum* and *Nicotiana attenuata* (Hill et al., 2018; Schliemann et al., 2008; M. Wang et al., 2018). Blumenol could be detected in foliar material and correlated to AM colonisation rates measured in roots. The nature of shoot accumulation provided a sensitive, non-destructive high-throughput (HTP) alternative for detection of AM colonization in the plant roots. Novel use of blumenol in a HTP screen in AM inoculated *N. attenuata* identified an AM-associated gene important for root colonisation level (M. Wang et al., 2018). Such a finding has exciting implications for the ability to screen large populations for quantitative root colonisation traits using accumulation of these apocarotenoids.

1.2.2 Crosstalk between apocarotenoids implicated in AM symbiosis

A model for current understanding of AM-associated apocarotenoid biosynthesis is given in Figure 1.3. Crosstalk between mycorrhizal-associated apocarotenoid biosynthesis pathways is evident and has been described previously. For example, SL production is dependent on interaction with ABA and zaxinone (Abuauf et al., 2018; J. Y. Wang et al., 2019). In addition, CCD7 and potentially D27 have been implicated in both SL and blumenol and mycorradicin biosynthesis (Vogel et al., 2010; M. Wang et al., 2018), indicating potential for cross-talk between these pathways. Notably, unlike *CCD7, CCD8* and SL signalling genes, the SL biosynthesis gene *D27* is highly conserved and present in some cyanobacteria (Ruyter-Spira & Bouwmeester, 2012), suggesting this enzyme may have an ancestral role in apocarotenoid pathways. Whether D27 is integral to coordinating regulated crosstalk between such pathways, remains unknown.

The implication of such crosstalk in AM symbiosis establishment and maintenance remains unclear. Mutants of zaxinone production have reduced AM colonisation, which could be due to loss of SL regulation, zaxinone production or requirement for *ZAS* enzymes (Ablazov et al., 2022; J. Y. Wang et al., 2019). Similarly, AM colonisation is reduced in mutants of CCD enzymes implicated in SL biosynthesis (C

Gutjahr et al., 2012; Kobae et al., 2018) and this could be due to requirement for certain SL derivatives, blumenol and mycorradicin production or downstream effects. Apocarotenoid biosynthesis requires an isoprenoid substrate derived from the MEP pathway and subsequent carotenoid biosynthesis. Recent studies of DXS2 mutants of the upstream isoprenoid MEP pathway and PSY mutants of the upstream carotenoid pathway identified reduced AM colonisation and AMF marker gene expression in addition to reduced SL, blumenol and mycorradicin apocarotenoids. Whether the impaired AM phenotypes are due to lack of either of the mycorrhizal apocarotenoids or additional effects from absence of other DXS2-dependent isoprenoids or PSY-dependent (apo)carotenoids remains unknown (Floß et al., 2008; Stauder et al., 2018). Overall, promotion of AM colonisation in permissive conditions could occur through unknown regulatory networks or AM-associated apocarotenoids and the implication of crosstalk between associated apocarotenoids remains to be further investigated (X.-R. Li et al., 2022; W. Liu et al., 2011).

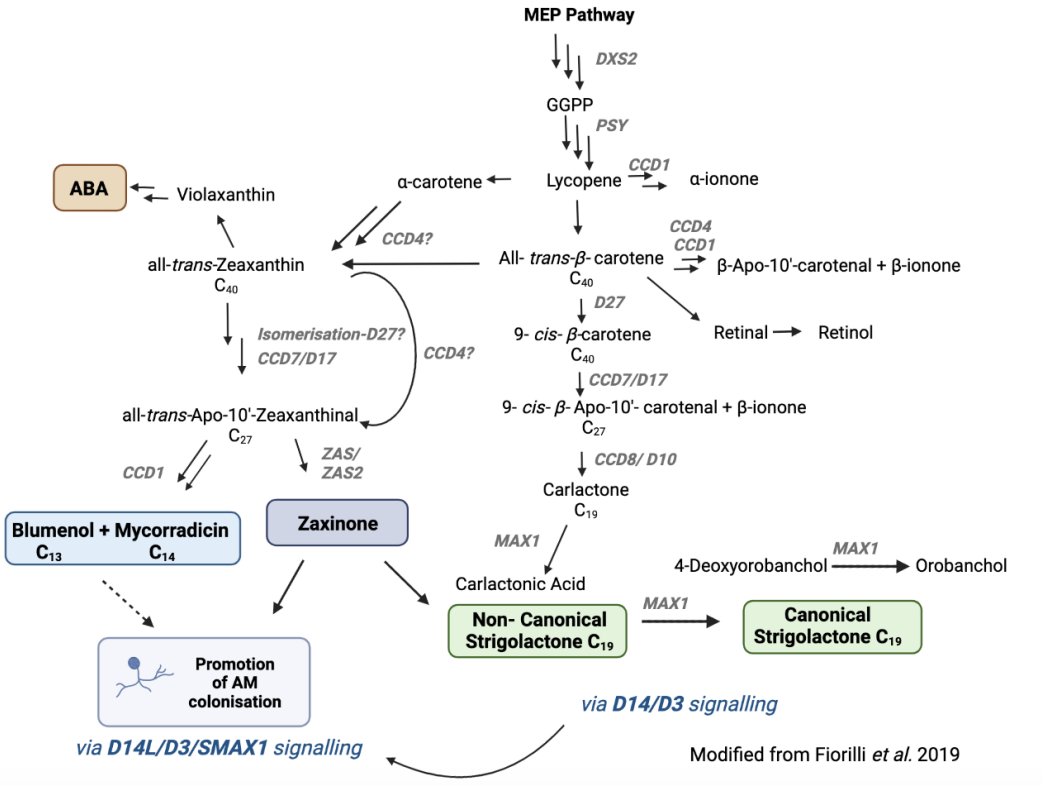

Figure 1.3 Summary of the current model of biosynthesis of AM-associated apocarotenoids, including SLs, ABA, zaxinones, blumenol and mycorradicin.

1.3 Genetic diversity in AM symbiotic establishment and benefit

1.3.1 Natural variation in AM colonization

Establishment of AM colonisation can be dependent on several factors acting in scales of impact. On a community level, environmental factors such as light, shading, soil composition, pH, flooding and carbon cycling can affect AM colonisation levels (Goldmann et al., 2020; W. Liu et al., 2016; Shenton et al., 2016; Staddon et al., 2003; Y. Wang et al., 2021). In addition, biotic factors including plant and microbial community, host specificity and interaction to pathogens/parasites impact the interaction (Bever, 2002; Bever et al., 2012; Bidartondo et al., 2002; Graham & Abbott, 2000; Iver Jakobsen & Hammer, 2015; Šmilauer et al., 2020).

Zooming into individual organisms, both plant and AMF derived factors affect the ability to establish colonisation. AMF factors such as fungal capacity for nutrient mobilisation and extra- and intraradical mycelial networks can affect symbiotic performance and colonisation rate (Avio et al., 2006; Thonar et al., 2011). In addition, inter and intra-specific genetic variation in AMF affects the interaction (Koch et al., 2017; Mensah et al., 2015; Sanders & Rodriguez, 2016; Savary et al., 2020). On a plant level, species ability to fix carbon and uptake nutrients without AMF i.e. non-mycorrhizal response to the external environment, affects the need and functional ability to interact with AMF. Cellular factors influencing signalling, morphological changes and nutrient status drive the symbiosis. This genetic drive is demonstrated in the abolishment of AM colonisation in mutants of genes required for AM symbiosis (C. Gutjahr et al., 2008; C. Gutjahr et al., 2015; Nadal et al., 2017) and the existence of non-host plant species which have independently lost the ability to establish symbiosis (Cosme et al., 2018; B. Wang & Qiu, 2006).

Intra-specific differences in root colonisation has been identified in crops such as wheat, maize, barley, chickpea and rice (Anneberg & Segraves, 2019; Bazghaleh et al., 2018; Gao et al., 2007; Jeong et al., 2015; H. Li et al., 2016; Taylor et al., 2015; Thirkell et al., 2022). For example, a study in maize found AM colonisation varied between cultivars depending on germplasm, origin, and year of release. Compared

to inbred lines and older landraces, modern hybrids were found to have greater colonisation, suggesting that modern cultivation doesn't necessarily lead to suppressed colonisation, as has previously been suggested (G. H. An et al., 2010). Similarly, genetic variation in AM colonisation level and phosphate transporter expression among both irrigated and upland rice accessions was identified across diverse rice cultivars (Jeong et al., 2015). Importantly, this large extent of genetic variation in AM symbiosis within a species is not consistent across all plants. Genetic diversity in AM colonisation in *M. truncatula*, for example, is debated, with low and inconsistent variation in AM colonisation compared to genetic diversity in pathogen infection between 32 lines (Dreher et al., 2017).

AM symbiosis has been reported to beneficially affect plant hosts through enhanced pathogen defence (Cameron et al., 2013; Cordier et al., 1998), and tolerance to salt (Al-Karaki & Hammad, 2001), heat (Gavito et al., 2005; Maya & Matsubara, 2013) and drought stress (Augé, 2001; Ruiz-Lozano et al., 2001, 2012; Ruiz-Sánchez et al., 2010). The most studied benefit, however, is that establishment of AM colonisation can supply up to 100% of Pi for the plant and, facilitated by a switch from the direct uptake pathway to an AM-specific route (S. E. Smith et al., 2004; Yang et al., 2012). The induction of other mineral transporters, particularly in N exchange, and increased amounts of mineral elements such as sulphur, copper and zinc in mycorrhizal plants suggest that AMF may provide additional macro- and micro-nutrient services, although the associated AM-induced transporter and signalling pathways remain to be further elucidated (Javot et al., 2011; M. Li et al., 2022; Ma et al., 2019; S. Wang et al., 2020; Watts-Williams et al., 2019). The resultant impact on the plant - 'AM outcome' - is dependent on both successful establishment of the plant-fungal association and the interaction of this with requirements and limitations imposed by environmental factors, which is driven by host and AMF genetic factors.

Such outcome forms the 'mycorrhizal responsiveness' and can be beneficial, detrimental or neutral when compared to the best response under non-mycorrhizal conditions. This is most often measured as relative difference between performance without and without AMF, mycorrhizal growth response (MGR). It will be the ability to consistently provide beneficial plant response to root colonisation which will

determine the agronomic viability of AMF as natural biofertilizers, measured as traits such as growth, stature, dry weight and grain number and quality (Fester et al., 2011; Sawers et al., 2008; Taylor et al., 2015).

Intra-specific differences in AM outcome have been reported across multiple crop species in the field; different field conditions and fungal species give variable degrees of growth or yield increase in AM colonised plants (Hong et al., 2012; H. Y. Li et al., 2005; Ortas, 2012; M.H. Ryan & Angus, 2003; Walder et al., 2012). Such differences are environmentally and genetically driven, as evidenced in meta-analysis, where Lehmann et al. found mycorrhizal responsiveness reported in 39 papers and over 320 crop genotypes was overall effected by factors such as soil density, pH, seed pre-germination, experiment duration and plant and AMF species (Lehmann et al., 2012). In rice, cultivar- and ecotype-specific responses to AMF in terms of yield, growth promotion and pathogen defence have been reported in the field; independent of root colonisation level (Campo et al., 2020; Diedhiou et al., 2016; Sisaphaithong et al., 2017; Y. Wang et al., 2021). Varietal differences in MGR are additionally reported in diverse cultivars grown in glasshouse conditions in multiple plant species (Davidson et al., 2019; B. A. D. Hetrick et al., 1996; Lehnert et al., 2017; Sawers et al., 2010; Thirkell et al., 2022; Watts-Williams et al., 2019) and were similarly environmentally and genetically driven. In a meta-analysis of 639 studies reporting AM colonisation and responsive observations in pot experiments, Qin et al. report that factors such as plant host, colonisation level, experiment duration, pot-size, substrate and soil pH affected biomass outcomes (Qin et al., 2022). In maize, shoot phosphate content, expression of phosphate transporters and abundance of fungal structures was found to vary and link to superior growth response in specific cultivars, despite similar levels of colonisation (Sawers et al., 2017). This further indicates involvement of plant genetic factors in driving mycorrhizal responsiveness, in some cases independent to colonisation. The mechanistic basis of such, however, remains largely unknown.

1.3.2 Genetic mapping of AM traits

Many transcriptomic studies report a suite of genes required for establishment of AM symbiosis. A phylogenetic study in *M. truncatula* identified a core collection of 138

mycorrhizal genes that are conserved in all plant species able to form AM symbiosis (Bravo et al., 2016). Additional transcriptomic studies have identified conserved sets of genes differentially expressed during AM symbiosis, showing a broad range of host genes that are important for the interaction (J. An et al., 2018; Das et al., 2022; Tromas et al., 2012; S. Wang et al., 2020). Crucially, only a few of these candidate genes have been associated to genomic regions or QTLs previously associated to AM traits (Davidson et al., 2019; R. Huang et al., 2020; Ortiz-Berrocal et al., 2017; M. Wang et al., 2018).

Genetic mapping aims to disentangle genotype-phenotype associations and identify genetic sources of phenotypic variation. Traditional linkage mapping in plants includes a diversity of experimental populations including F_2 populations from variable parents, multi-parent advanced generation inter-cross (MAGIC) lines and recombinant inbred lines (RILs). Genetic mapping of variation in AM colonisation has been studied for many years, with early work in bread wheat identifying six chromosomal regions that may be associated to mycorrhizal responsive genes (B. A. Hetrick et al., 1995). More recently, quantitative trait loci (QTL) mapping of *N. attenuata* RILs from parental lines that differ in AM colonisation level identified a homologue of a known gene required for pre-communication in AM symbiosis, *NOPE1* (Nadal et al., 2017; M. Wang et al., 2018). In tomato, QTL mapping of 130 RILs identified 8 QTLs associated to colonisation, and candidate genes included AM-associated *SlCCaMK* and *SlLYK3* (Plouznikoff et al., 2019). In addition, QTLs corresponding to mycorrhizal responsiveness have been identified in 197 RILs in maize (Kaeppler et al., 2000), and a study of a trihybrid population of *Allium* (Galván et al., 2011).

Traditional linkage mapping studies require less genetic markers for identification but diversity is limited to parental lines of the segregating populations and markers give a low genetic resolution of 10-30cM, meaning pleiotropic and physically close genes cannot be distinguished (Bartoli & Roux, 2017; C. Zhu et al., 2008). Notably, genome mapping has advanced in recent years to overcome these limitations, with genome wide association studies (GWAS) providing a powerful tool for identifying QTLs and single nucleotide polymorphisms (SNPs) associated to a given traits. In this case, QTLs are identified by examining the strength of linkage disequilibrium (LD), the

degree of non-random association between alleles at different loci, between markers and functional polymorphisms across a set of diverse germplasm. GWAS based on LD to identify QTLs was first established in human genetics (Lander & Schork, 1994), but is now used widely in plant breeding. Typically, GWAS in crop species are performed using a panel of lines, with multiple replicates of each line and an average of these phenotypes used as the response variable. GWAS has been increasingly fostered in plant genetics due to the advent of increasingly available genomic sequence data and improved statistical methods that consider population structure and kinship relationships in the association model (J. Yu et al., 2006; C. Zhu et al., 2008).

In recent years, genome-wide mapping of AM traits has resulted in reports of QTLs in multiple species, including wheat (De Vita et al., 2018; Ganugi et al., 2021; Lehnert et al., 2018), soybean (Pawlowski et al., 2020), cultivated sunflower (Stahlhut et al., 2021) and maize (M. Li et al., 2022; Ramírez-Flores et al., 2020). In the first report in rice, Davidson et al., interrogated the Rice Diversity Panel 1 and found 23 putative QTLs mapping to hyphal colonisation rates. Candidate genes include a calcium/calmodulin serine/threonine protein kinase and two ammonium transporter genes (Davidson et al., 2019). Such GWAS studies show the great potential for determining genomic regions driving AM colonisation and plant responsiveness. The application is in its infancy, and it will be exciting in future years to see putative candidates further validated for function in AM symbiosis.

Recently, an elegant strategy used mapping to identify QTLs associated to host responsiveness. Ramírez-Florez et al. incorporated AMF-resistance into a genetic mapping population to allow for evaluation of maize response to AMF in the field. AMF could account for ~30% of grain production in susceptible lines, indicating the ‘mycorrhizal benefit’ that plants can derive from efficient symbiosis. Genetic variation in genotype performance with AMF was identified, with several QTLs mapping to host benefit (Ramírez-Flores et al., 2020). In the same year, chromosome single-segment substitution lines comparing variants of the *OsCERK1* CSP gene present in wild Dongxiang rice compared to elite *Indica* lines linked natural variation in the gene to greater AM colonisation and host response in the field (R. Huang et al., 2020). Together, this advocates twofold for the potential for natural allelic variation in

symbiotic genes to (1) modulate AM colonisation and (2) improve crop performance, (in)dependent of AM colonisation level. Identification of genetic determinants for such benefit could improve the capacity of plants to profit from AMF in future sustainable breeding programmes.

1.3.3 Genetic diversity of rice

Rice is a staple food crop for more than half of the world's population. The USDA estimates that world rice production in 2022/23 reached 503.0 million tonnes, 2% below the year-earlier record and the first decline in supply since 2004/5. Notably, 2022/23 consumption was 516.1 million metric tonnes (Childs & LeBeau, 2023) and it is estimated that production should increase by 25% by 2030 to keep up with predicted global population growth. In the face of climate change and limited resources, this needs to be achieved using sustainable practices for land, water, and fertiliser- all whilst withstanding potentially severe environmental stresses. Genetic improvement will be integral to achieving such a goal (Z. Li et al., 2014).

The two major sub-species of cultivated rice are *Oryza sativa,* Asian rice and *Oryza glaberrima,* African rice. Most of global rice production is of the *O. sativa* species, which for over 2000 years has been described as two major groups- Xian, tropics adapted and referred to as 籼 or *Indica* and Geng, temperate and tropical adapted, referred to as 粳 or *Japonica.* More recently, five genetically distinct subpopulations- *indica, aus/boro, temperate japonica, aromatic (basmati/sadri)* and *tropical japonica* have been identified (Garris et al., 2005; Glaszmann, 1987; Kato et al., 1928). Such ecological diversification of rice was enhanced by natural and human selection: diversity of climate, soils, water availability and resultant cultivation practices have facilitated the huge genetic diversity of rice cultivars observed today (J. L. Maclean et al., 2002).

Rice has long been produced in a wide range of climates – from wet deep-waters to dry deserts- and the four main ecosystems (J. L. Maclean et al., 2002) are summarised in Figure 1.4. Broadly, lowland rice includes rice grown in fields that are flooded for all or part of the growing season, including rain-fed lowland, irrigated lowland, deep-water and mangrove swamps. Submerging lowland rice paddy fields

limits pest spread, competition from weeds and increases the availability of nutrients in the soil. Despite this, the practice relies of use of huge amounts of water and requires large amounts of labour for land preparation, transplanting of seedlings into soil, cultivation, and harvest. Low input systems include rice produced in rainfed lowlands and upland rice. Such rice is often directly seeded and requires comparatively less water and labour for growth. Upland rice is lower yielding; often grown in crop rotation systems in subsistence farming. Recent statistics of rice growth in the tropics suggests that lowland and upland rice account for 92 and 8% of total rice cultivation area, respectively (Saito et al., 2018).

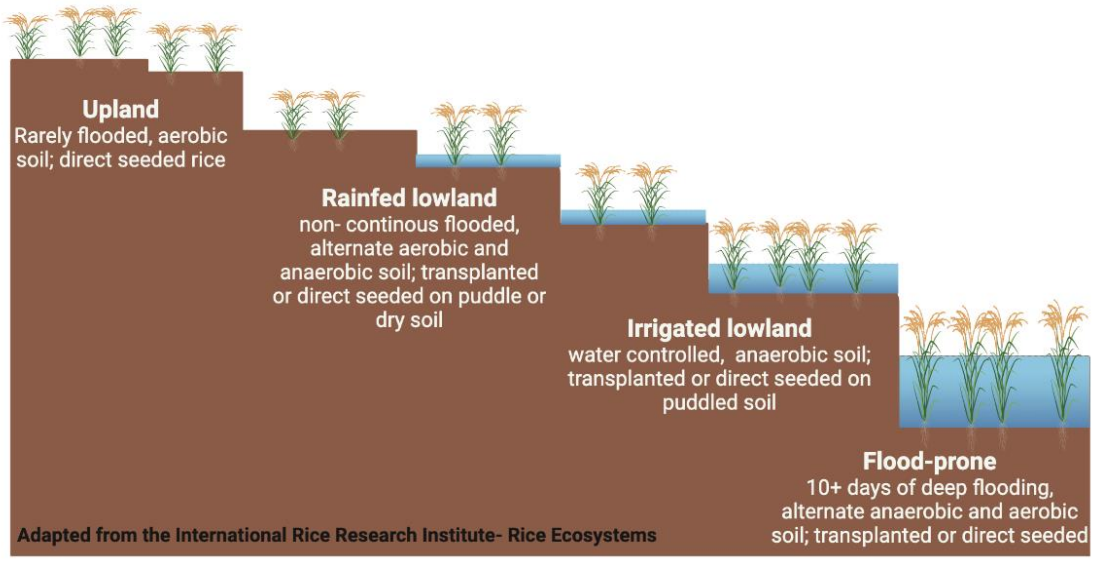

Figure 1.4 Diagram depicting four broad rice ecosystems, adapted from IRRI-Rice Ecosystems. *Upland rice is grown at upper, un-bunded level or sloped fields. It is rarely flooded and often planted through direct seeding. Rainfed lowland is grown in non-continuous flooded systems, meaning the soil alternates between aerobic and anaerobic conditions. Rice is planted either through transplanting or seeding into wet soil or dry direct seeding. Irrigated lowland rice is grown in water-controlled, flooded systems that are anaerobic. It is planted through transplanting or direct seeding into puddled soil. Flood-prone or deepwater rice is grown with over ten days of deep flooding. Rice is planted either through transplanting or direct seeding.*

Rice has a large amount of within- species and within- subpopulation diversity and over 230,000 germplasms are maintained in international and national genebanks worldwide (J. Y. Li et al., 2014; Z. Li et al., 2014). Many diversity panels representing these have been developed, such as the Rice Diversity Panels 1 and 2 (RDP1, RDP2), which include ~1500 accessions of landrace and elite *O. sativa* rice genotyped using genome-wide high density rice array (HDRA) (McCouch et al., 2016) and the novel Bengal and Assam Aus panel of 226 *aus* accessions (Norton et al., 2018). In addition, the 3,000 Rice Genomes Project (3K-RG), produced a giga-

dataset of publicly available genome sequences, derived from 3,024 rice accessions with global representation of both genetic and functional diversity. The rice genome sequences produced have an average of 14X depth of coverage; meaning high-quality genomes representing variable rice accessions are now available for genetic mapping studies (J. Y. Li et al., 2014). The accessions map to nine subpopulations, most of which connect by geographical origin and genetic variation is captured in the 29 million SNPs, 2.4 million small indels and over 90,000 structural variants that are reported in 3,010 of the accessions (W. Wang et al., 2018). Overall, these panels provide extensive genomic annotation to aid in GWAS studies and the potential to identify candidate genes in rice.

1.3.4 AMF in rice cultivation systems

Common problems constraining global rice production include low nutrient status, low pH and high P fixation of soils (Haefele et al., 2014). Intensive farming including high chemical input, flooding and mechanical techniques can overcome such limitation but many farmers in developing countries still rely on limited resources or economic investment, meaning natural soil quality remains a major factor for global crop yields. In addition, fertilisers including rock phosphorous and nitrogen sources are becoming increasingly limiting to mine (both economically and in resource). The process of re-establishing a natural AMF community for biofertilisation in rice grown in reduced water systems could provide a promising alternative to conventional, high input agriculture systems in rice faming.

Currently, over 75% of global rice production is from rice cultivated under flooded, submerged conditions in lowland fields (J. L. Maclean et al., 2002). Traditional rice cultivation involves transplanting of rice seedling from nursery into puddled soils (Sandhu et al., 2021). Submerging lowland rice paddy fields limits pest spread, competition from weeds and increases the availability of nutrients in the soil. Despite this, the practice requires large amounts of labour for land preparation, cultivation and harvest and relies of use of huge amounts of water. In addition, waterlogging land contributes to emission of large amounts of greenhouse gases, particularly methane, for which rice cultivation currently contributes ~12% of global emissions (Haefele et al., 2009). As these become increasingly limiting issues in rice

production, cultivation methods in many countries are moving towards more sustainable practices.

Numerous alternative, more sustainable cultivation strategies have been developed in the last decades. Alternate wetting and drying (AWD) irrigation involves intermittent irrigation of the field, with cycles of flooding and drying to reduce water use. Similarly, direct seeded rice (DSR) is a low-input demand method involving sowing pre-germinated seed into a puddled soil surface (wet seeding), standing water (water seeding) or dry seeding into a seedbed/directly onto the field (dry seeding). DSR is then grown wet or dry, with irrigation ranging from fully flooded to rainfed conditions. A shift to practices such as AWD or DSR could substantially reduce crop water and labour requirements for rice production (Rahman, 2019).

Such a shift provides an exciting opportunity for consideration of AMF in modern rice cultivation systems. AMF respire aerobically and thus it was previously thought that anoxic, waterlogged paddy conditions were non-mycorrhizal. More recently, it has been recognized that AMF are present in waterlogged systems, potentially due to aerenchyma in roots providing a supply of atmospheric oxygen (Wang et al., 2015). Reports of the benefit of AMF in paddy cultivation are varied, but root colonisation is often severely suppressed (Bernaola et al., 2018; M. Vallino et al., 2009; Y. Wang et al., 2015).

As cultivation methods move towards practices with reduced puddling and aerobic condition, there is an opportunity to newly consider the potential for AM symbiosis in providing natural biofertilization in rice cultivation. Previous studies assessing AWD in Italy suggested that AMF are present in wetland and dried soils and, although initially suppressed in wetland conditions, functional symbiosis establishment could plastically adapt to soil drying (Vallino et al., 2009). Similarly, root colonisation has been observed glasshouse experiments assessing native colonisation of rice grown aerobically in soil collected from rice paddy fields that were previously waterlogged (Jeong et al., 2015; Das et al., 2022). Such data suggests that AMF survive in flooded soil and can plastically adapt to sustain functional root colonisation once aerobic conditions are established. Further work is required to understand the abundance and plant host benefit of colonization by such recovered AMF

communities, but the findings advocate for the new potential of AMF fertilisation in future sustainable cultivation systems.

1.3.5 Assessing AM colonisation in rice

Much of the insights in genetic and physiological factors facilitating symbiosis has been discovered in glasshouse or controlled environments to limit interference of additional environmental or genetic factors (Smith and Read, 2008; Ryan and Graham, 2018). Plants are inoculated with or without known species of AMF for trait comparison against noncolonised controls. *Rhizophagus irregularis* (formerly *Glomus intraradices*) has been the most extensively studied 'model' AMF due to the ability for large-scale production of sterile spores in vitro. In addition, genome assemblies of multiple isolates of *R. irregularis* are available (Tisserant el al., 2013), including a recent, highly contiguous assembly and high-quality annotation (Manley et al.,2023). The discovery of functionally relevant genes driving symbiosis has been facilitated by controlled documentation of root colonisation in plant hosts with altered genes inoculated with a single model AMF species (Montero et al., 2018).

Despite this, in order to assess the viability of AMF as biofertilizers in rice cultivation, we additionally need to understand the extent of colonisation and host benefit in the field. In a meta-analysis, Lehmann et al. found mycorrhizal responsiveness reported in 39 papers and over 320 crop genotypes was overall effected by factors such as soil density, pH, seed pre-germination, experiment duration and plant and AMF species (Lehmann et al., 2012). Rice in the field is subject to environmental variation such as extreme night and day temperatures or fluctuations in water availability, particularly during rainy seasons. In addition, substrate, soil compaction, plant root architecture constraint in pot systems and native microbe community composition could affect the outcome of symbiosis (as reviewed by (Ryan and Graham., 2018)). Throughout this PhD project, genetic, molecular, and physiological analyses were used to assess the genetic potential for establishment and benefit of AM symbiosis in aerobic rice cultivation. Glasshouse and field experiments were conducted to assess the impact of AMF on diverse *Indica* rice lines, and subsequent genetic mapping identified candidate regions associated to AM colonisation. Such work

provides further understanding towards the potential for future breeding programmes focused on rice production including AMF communities.

Figure.5 Genetic diversity of rice observed in a subset of cultivars growing in diversity assessments at IRRI, Philippines

1.4 Research Objectives

The broad aim of the PhD was to harness the genetic potential for establishment and response to arbuscular mycorrhizal (AM) symbiosis in rice. Establishment of the high coverage, 3K-RG *Oryza sativa* genome sequence dataset (Z. Li et al., 2014) provided opportunity to further investigate genetic diversity in rice. In addition, identification of a novel shoot metabolite marker for AM fungal root colonisation, blumenols, allowed for development of a HTP screening method to interrogate variation in AM outcome between accessions (Mindt et al., 2019; M. Wang et al., 2018). This provided a strong basis for a Genome Wide Association Study (GWAS) aiming to identify genetic regions required for AM colonisation and beneficial response in rice.

The objectives of the PhD were to:

1. Evaluate the use of blumenols as a HTP marker of AM colonisation in rice

2. Determine genetic variation in:
    a) levels of colonisation by *R. irregularis* and
    b) mycorrhizal responsiveness and AM benefit in glasshouse and field conditions.

The results of such will be explored in the thesis as follows:

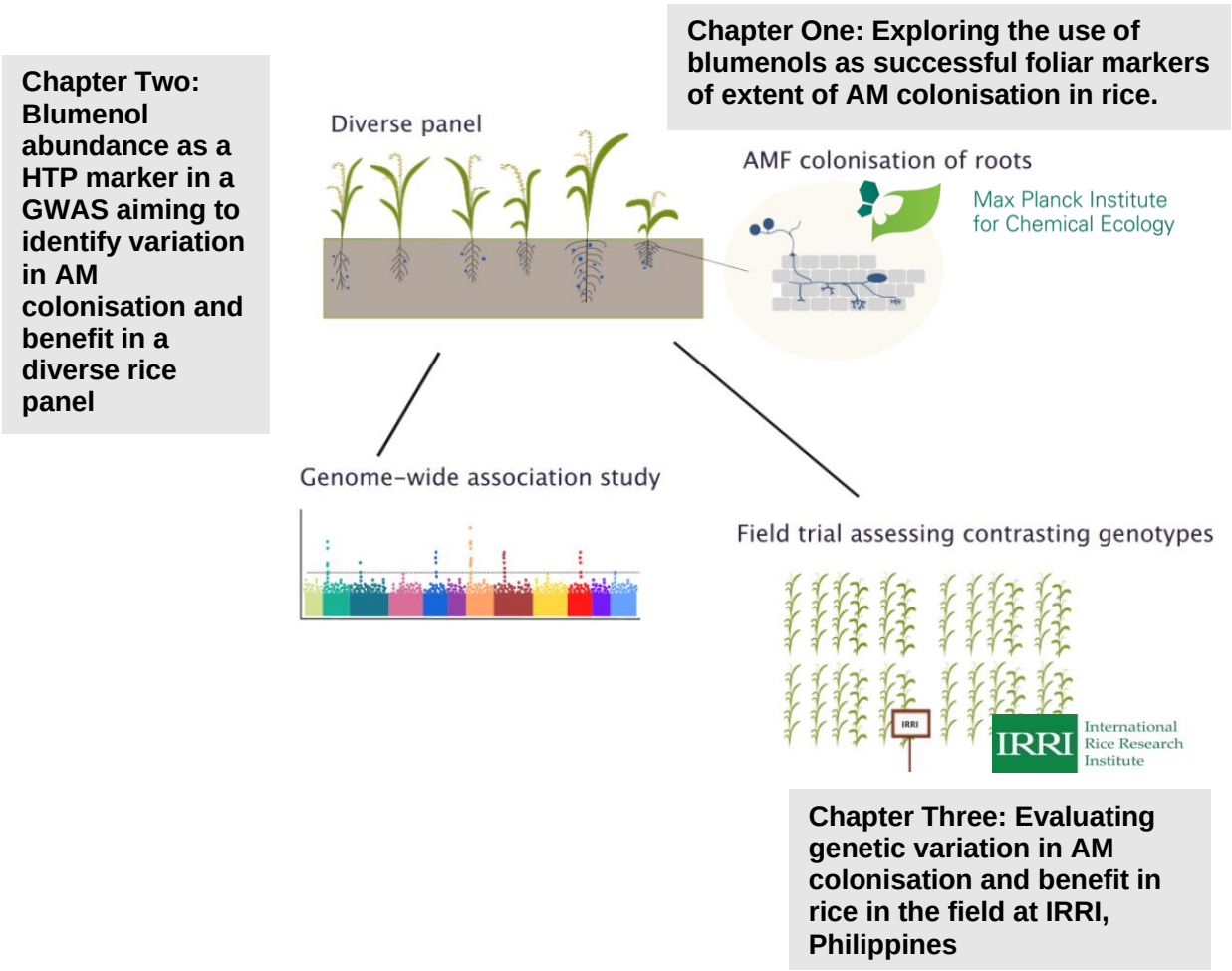

Figure 1.6 Graphical abstract of PhD objectives and Chapters in this thesis.

2 Chapter Two- Materials and Methods

2.1 Plant growth and inoculation

2.1.1 Oryza sativa material

Oryza sativa, Asian rice, genotypes used in cone experiments interrogating AM phenotypes included wild-type (WT) cv. *Nipponbare* and corresponding mutants in this cultivar, namely *ccamk-1, pollux-2,* and *str1-2;* WT cv. *Shiokari* and corresponding *d10-1, d17-1, d27-1, d14-1* and *d3-1* mutants and WT cv. *Dongjin* and *smax1-1* mutant. Mutant information is described in Table 2.1. In addition, diverse seeds of *Indica* cultivar were obtained from the International Rice Research Institute, Philippines (IRRI), (https://gringlobal.irri.org/gringlobal) and used in initial blumenol correlation analyses (Table 2.2) and the *Indica* panel selection and GWAS experiments (Table 2.18).

2.1.2 Seed sterilisation and germination

Rice seeds were de-husked and surface sterilized using brief treatment in 70% (v/v) ethanol. They were then shaken for 20 minutes in 3% (w/v) sodium hypochlorite using a Polymax 1040 platform shaker (Heidolph, Schwabach, Germany). The sodium hypochlorite was removed, and seeds washed in autoclaved de-ionised water (diH_2O) three times. Sterile seeds were then placed on 0.6% (w/v) bacto-agar plates, sealed with micropore tape and kept in a 30°C incubator for four to six days, dependent on germination rate. Seedlings were planted once they developed at least a seminal root and coleoptile.

2.1.3 Fungal subculture

Rhizophagus irregularis spores were propagated on 1% (w/v) agarose plates containing hairy carrot roots (*Daucus carota* L.) (Bécard & Fortin, 1988). Plate media was composed of the solutions noted in Table 2.3. A section of media containing hairy carrot roots of up to one month old (and propagated hyphae and spores) was plated onto fresh square plates using a sterile scalpel. Plates were covered in 3M micropore tape and parafilm and stored in darkness at 25°C. Plates were suitable for spore/hyphal extraction at a minimum of 3 months post subculture.

2.1.4 Fungal spore extraction

For inoculation assays, spores were extracted from plates. Citrate buffer (Table 2.4). was added to agar medium containing propagated spores and hairy carrot roots. Roots were cut and agitated with a sterile scalpel and the solution was left stirring for one hour. Spores were then sieved from the solution, first through a 500μm mesh (for removal of cut roots) and then through a 0.045μm mesh for collection. Spores were washed and suspended in diH_2O. To calculate concentration of the spore suspension, 10μl was pipetted onto a microscope slide with an etched grid. The slide was viewed under a light microscope (Nikon, Minato, Japan) and the number of spores within the grid counted. This was repeated and an average of the number of spores per 10μl used to calculate the concentration of spores in the extraction volume. The spore suspension was diluted to required concentration (100, 300, 500 and 700 spores per ml- experiment dependent) using diH_2O.

2.1.5 Seedling planting and inoculation- cone experiments

Seedlings were grown in cones of 2.5cm diameter and 12cm length, which contained sterile quartz- sand. The growth medium was inoculated with 1ml diH_2O (mock treatment) or 1ml spores suspended in diH_2O (inoculated treatment) at a layer of sterile quartz- sand filling ~ three-quarters of the cone. A small layer of sand was added on top of the inoculated layer, allowing plant roots to grow into established hyphal networks. Seedlings were planted using sterile forceps. A layer of sand was added, and all plants were watered with diH_2O. Once planted, the cones were transferred to the growth chamber for plant cultivation. A representative image of cone experiment setup is given in Figure 2.1. Cone position was randomized to negate the effect of biotic and abiotic variation in the growth chamber. Plants were covered with a plastic lid for the first two weeks of growth whilst seedlings established.

2.1.6 Plant cultivation

Unless noted, plants were kept in walk-in chambers with the following conditions: 12h:12h light:dark cycle at 28:20°C and 60% relative humidity. All plants were watered three times a week up to two weeks post inoculation (wpi) with diH_2O, after

which they are fertilized twice weekly using half Hoagland solution (Table 2.5 & 2.6) and once weekly with diH_2O only. All plants were fertilized with half Hoaglands of an AM permissive, 25μm P_i concentration (Table 2.5) unless otherwise stated, in which a solution with modified P_i concentration was used (Table 2.6). Plants were harvested at six wpi for all experiments unless otherwise stated (Figure 2.1).

Figure 2.1 Rice seedlings in a cone-experiment setup in mock- and AMF- inoculated sand substrate. *Plants are representative of typical plant growth from a cone experiment at 6 weeks post inoculation.*

2.2 Microscopic quantification of AM colonisation

2.2.1 Root harvest - trypan blue staining

Plants were removed from sterile-quartz sand and washed in diH_2O. Roots were cut into 2cm pieces, mixed using sterile forceps and a representative sample of all root types transferred into 2ml Eppendorf tubes containing 10% (v/v) KOH. Samples were incubated at 95^oC for 30 minutes in KOH and then washed three times in diH_2O. Root samples were then incubated in 1.5ml of 0.3M HCl for 20 minutes. HCl was removed and 1ml of 0.1% (w/v) Trypan Blue (Sigma-Aldrich, St Louis, USA) staining solution (Table 2.7) was added. Samples were incubated for 5 minutes at 95^oC. Roots were then stored in trypan blue or immediately transferred onto slides. To make microscope slides, roots were first washed in 50% (w/v) acidic glycerol. Ten representative roots were transferred onto glass microscope slides using forceps. A drop of 50% (w/v) acidic glycerol was pipetted onto the slide before adding a cover slip. Slides were sealed with varnish to prevent drying.

2.2.2 Microscopic quantification of AM colonisation

Percent root length colonization (% RLC) was determined by analysis of ten root pieces per plant, representative of total root length colonisation. Fungal structures were scored according to a modified gridline intersect method (Paszkowski et al., 2006), based on the protocol of Brundrett et al., 1984 in which the number of fungal structures are counted using a gridline intersect (Giovanetti and Mosse, 1980). Structures are marked as present or absent in the field of vision at 10 equal intervals along each root piece. 10 root pieces per plant were sampled and collated to overall give 100 root sites measured per plant. This was used to calculate both percent of total root length colonization (% RLC) and % of each fungal structure. Fungal structures scored include extraradical hyphae (EH), intraradical hyphae (IH), hyphopodia (H), arbuscules (A), vesicles (V) and spores (SP). Representative images of fungal structures were taken with GX Microscope and GXCAM-U3PRO-6.3 (GT Vision LTD, Suffolk, UK) at 20X magnification. A scale bar was included in images for reference.

2.3 Molecular techniques- DNA & RNA

2.3.1 Genomic DNA (gDNA) extraction

Tissue samples were added to 2ml Eppendorf tubes, shock frozen in liquid nitrogen and stored at -80°C. Three glass beads (3mm ⌀) were added to foliar samples or 2 metal beads (4mm ⌀) to root samples. Material was then lysed using Qiagen Tissue Lyser II (Qiagen, Hilden, Germany) at 30 Hz for 1-minute intervals. Genomic DNA (gDNA) was extracted using gDNA extraction buffer (Table 2.8). 300μl of extraction buffer was added and the sample then vortexed. Samples were incubated for 10 minutes at 98°C before centrifuging (13,000rpm) for 2 minutes at room temperature. 300μl of 100% (w/v) isopropanol was added to the supernatant and samples were centrifuged (13,000 rpm) for 15 minutes at room temperature. The supernatant was poured off and the pellet washed in 70% (w/v) EtOH. Samples were centrifuged (13,000 rpm) for 10 minutes at room temperature. The supernatant was poured off and tubes centrifuged (13,000 rpm) for 10 seconds to remove residual EtOH. The pellet was air-dried for 10 minutes and dissolved in 100μl of diH_2O. gDNA was

quantified using NanoDrop spectrophotometer (Thermofisher Scientific, Massachusetts, USA) and stored at -20ºC.

2.3.2 Genotyping - polymerase chain reaction (PCR)

For genotyping, a PCR reaction mix (Table 2.9) and GoTaq2 Flexi polymerase (Promega) was added to gDNA sample. PCR reaction was carried out by a PTC-225 Gradient Thermal Cycler (MJ Research, Florida, USA) with annealing temperature adjusted to be optimal for the genotyping primer pair used (Table 2.10). On completion of PCR, the products were pipetted into wells of 0.8% (w/v) agarose gels containing 1μg/ml ethidium bromide. A DNA ladder was added for reference. The gel was electrophoresed at 120mV until the PCR product has moved down the lane and DNA bands have separated by size. The gel was then viewed under UV light to confirm the presence/absence of the expected product band size and to establish the sample genotype.

2.3.3 Root harvest – RNA extraction

Plants were harvested as in Section 2.2.1 and a representative sample of all root types transferred into 2ml Eppendorf tubes containing two steel balls (4 mm ⌀). Samples were shock frozen in liquid nitrogen and lysed using Qiagen Tissue Lyser II (Qiagen, Hilden, Germany) at 30 Hz for 1-minute intervals until material was a fine powder. 1ml of Trizol (Table 2.11) was added and the sample incubated at room temperature for 5 minutes. 0.2ml of 100% (w/v) chloroform was added and tubes shaken vigorously for 15 seconds. The samples were incubated for 2-3 minutes at room temperature, before centrifuging (13,000rpm) for 15 minutes at 4ºC. 600μl of the colourless upper aqueous phase was added to a fresh 1.5ml Eppendorf tube and mixed with 0.5ml of 100% (w/v) isopropanol. The sample was centrifuged (13,000 rpm) for 10 minutes at 4ºC and supernatant removed. The remaining pellet was washed in ice-cold 75% (w/v) EtOH and centrifuged again for 10 minutes at 4ºC. The supernatant was removed, and pellet dissolved in 60μl of diH_2O. The sample was incubated in 60μl of 4M LiCl for 1 hour at -20ºC. The supernatant was removed, and pellet washed twice in ice-cold 75% (w/v) EtOH. EtOH was then removed, and pellet dried for 5-10 minutes. 25μl of ice-cold diH_2O was added to dissolve the RNA. Extracted RNA samples concentration and integrity was assessed on NanoDrop

spectrophotometer (Thermofisher Scientific, Massachusetts, USA). To check for RNA degradation, samples were run on 1.5% (w/v) agarose gel with loading dye added. The gel was electrophoresed at 120mV for approximately 40 minutes, until the RNA has moved down the lane and bands had separated by size into clear rRNA bands of 28S and 18S, with the 28S band approximately twice the intensity.

2.3.4 cDNA synthesis

1μg of RNA was treated with DNaseI (Sigma-Aldrich, St Louis, USA), following manufacturer's guidelines, to ensure no gDNA contamination. DNA-free RNA was then used for First Strand complementary DNA (cDNA) synthesis using SuperScript II Reverse Transcriptase (Invitrogen, Massachusetts, USA), following manufacturer's guidelines. cDNA produced was quantified by spectrophotometry using a NanoDrop (Thermofisher Scientific, Massachusetts, USA) and stored at -20°C.

2.3.5 qRT-PCR expression analysis

Primers for Quantitative Reverse Transcriptase PCR (qRT-PCR) were designed using NCBI Primer-BLAST tool. Primer efficiency was tested using two-fold serial dilutions of DNA. For gene expression analysis, cDNA was diluted at 1:12 ratio with ice-cold diH_2O. qRT-PCR reaction mix (Table 2.12) with primers of tested efficiency (Table 2.13) was added to DNA in 96 and 384-well plates. All reactions used standard PCR cycling programme (Table 2.14) with CFX96 Touch Real-Time PCR detection system (Bio-Rad, California, USA). All samples were tested in plates alongside diH_2O negative control and three housekeeping genes: Cyclophilin (CP2, LOC_Os02g02890), Ubiquitin (UbiQ, LOC_Os02g02890) and GAPDH (LOC_Os02g02890). The Ct value per gene of interest was quantified against the Ct values for the three housekeeping genes using a Geometric Mean calculation. Geometric mean Ct values were recorded as Ct normalised to CP2 and $\log_{10}(x+1000)$ transformed for scaling. Where Ct values and melting point were equivalent to diH_2O negative control, a value of 0 was recorded, which corresponds to $\log_{10}$(Expression) = - 6 and zero expression. This method was as used previously (Choi et al., 2020; Guimil et al., 2005).

2.4 Blumenol metabolite analysis

All ICP-MS analysis was conducted by myself, Dr Rayko Halitschke, Catarina Rocha and Prof. Ian Baldwin at Max Planck Institute for Chemical Ecology, Jena, Germany.

2.4.1 Sample preparation- extraction

Plants were harvested as in Section 2.2.1, and shoots were additionally cut into 2cm pieces and mixed using forceps. A representative sample of ~100-200mg fresh weight of root and shoot pieces were weighed and collected in 2ml Eppendorf tubes containing two steel balls (4mm ⌀). Samples were then shock frozen in liquid nitrogen before grinding to a powder in a GenoGrinder 2000 (SPEX SamplePrep, New Jersey, USA) for 1-minute intervals at 1000 strokes/min. Fresh weight measurements were used for normalisation. Tissue powder shock frozen in liquid N_2 was extracted with 800-1000µl (experiment dependent) of MeOH extraction buffer (Table 2.15), containing 80% (v/v) MeOH and 10ng/µl PH-200 phytohormone mix (10ng/µl of phytohormones D6-JA, D-4-SA, D6-JA-Ile and 10ng/µl of internal standard D_6-ABA (ChemCruz, Santa Cruz Biotechnology, Texas USA) . Samples were shaken in a GenoGrinder 2000 (SPEX SamplePrep, New Jersey, USA) for 60 seconds at 1000 strokes/min. Samples were then centrifuged (2,000 x g) for 20 minutes at 4°C. Supernatant was transferred to a fresh 1.5ml Eppendorf tube and centrifuged again under the same conditions. Approximately 700μl of supernatant was transferred to 1.5ml screw neck vials and used in sensitive liquid chromatography mass spectrometry (LC-MS) analysis. The analysis used a Ultra High Performance Liquid Chromatography (UHPLC) triple quadrupole Mass Spectrometry (MS) instrument [Ultimate 3000 RSLC (Thermo Fisher Scientific, Massachusetts, USA); EVO-Q EliteTM (Bruker, Massachusetts, USA)].

2.4.2 Targeted blumenol analysis

100μl of MeOH-extracted sample was transferred to skirted 96-well microplates and sealed. A mixed quality control sample was prepared by combining 10μl aliquots of each sample in the plate into a 1.5 ml screw neck vial. Extraction buffer was used as a blank and for signal background calculations. The UHPLC method was as described previously (Mindt et al., 2019; M. Wang et al., 2018) and quantifier and

qualifier m/z fragments used to detect derivatives are described in Table 2.16. Peak area integration for targeted compounds and internal standard was found using the software MS Data Review Version 8.2.1 (MS Workstation, Bruker Daltonics). Analyte peak area (PA) for targeted compounds was normalized relative the internal standard D_6-ABA, meaning the overall blumenol derivative abundance was calculated as ng/g fresh mass of sample. This was calculated by the following equation:

$$Blumenol\ abundance, ng/g\ freshweight = \frac{\left(\frac{PA_{analyte}}{PA_{Internal\ standard}}\ x\ mass, ng_{\ internal\ standard}\right)}{mass, g_{\ sample}}$$

2.5 Strigolactone (SL) and apocarotenoid metabolome analysis

All ICP-MS analysis was conducted by myself, Dr Laura Perez and Prof. Paul Fraser at Royal Holloway University, UK.

2.5.1 Sample preparation- extraction

Samples were harvested as in Section 2.2.1 and a representative sample of all root types was collected in foil before shock freezing in liquid nitrogen. Samples were freeze-dried for 24 hours and ground in Qiagen Tissue Lyser II (Qiagen, Hilden, Germany) at room temperature for 30 second intervals until a powder. The extraction method was adapted from (Floková et al., 2020; J. Y. Wang et al., 2022) and optimised for low amounts of dried material. Approximately 10mg of tissue is extracted in 10ng/µl mix of internal standards D_6-ABA and GR24 (CaymanChem, Michigan, USA) in 0.5ml of 60% (v/v) Acetone (Table 2.17). Samples were shaken for 30 minutes at 4ºC in dark conditions. Samples were centrifuged (2,000 x g) for 5 minutes at 4ºC. Supernatant was transferred to a fresh 1.5ml Eppendorf tube and speed dried in GeneVac Concentrator EZ-2 Plus SpeedVacuum (GeneVac Ltd, Ipswich, UK) for 90 minutes using HPLC fraction method. The dried extract was then stored at -20ºC and later submitted to solid-phase extraction (SPE) fractionation to concentrate and desalt solutions, enriching strigolactones (SLs) and apocarotenoids based on interaction with long alkyl chains of C18 sorbents. This method is as described previously for SL analysis in complex samples (Floková et al., 2020).

Crude extracts were further concentrated using polymeric reverse phase-based Oasis® HLB columns (150 mg/3 ml, Waters, Milford, MA, USA). The sorbent was activated with 1ml of 100% acetonitrile, washed in MS grade H_2O and equilibrated with 0.5ml 10% (v/v) aqueous acetonitrile (v/v). Samples were passed through the activated column. Compounds not retained by the sorbent, such as salts and polar compounds, were washed out with additional 1ml of 10% aqueous acetonitrile (v/v). SL analytes were eluted from the column with 0.5ml of 100% aqueous acetone and speed dried in GeneVac Concentrator EZ-2 Plus SpeedVacuum (GeneVac Ltd, Ipswich, UK) for 90 minutes using low boiling point (BP) method. Dry samples were stored at -80°C until LC–MS analysis. On the day of LC-MS analysis, the dried extracts were dissolved in 50µl of 20% acetonitrile, centrifuged to clean-up any possible particulates and injected into the LC-MS. An injection volume of 5µl was used. An empty tube and a tube containing the ISTD mix only were used as negative and positive controls of extraction, respectively.

2.5.2 Analysis of SLs and apocarotenoids in LC-MS.

The extracts enriched with strigolactones and apocarotenoids were analysed in an UHPLC-Q-TOF system using an electrospray ion source in positive mode. The equipment used was a 1290 Infinity UHPLC and a 6560Ion Mobility Q-TOF (Agilent Technologies, California, USA), and compounds were separated using a reverse phase C18 column Zorbax Eclipse Plus RRHD 2.1x50 mm 1.8µm (Agilent Technologies, California, USA). The chromatographic method consisted in binary linear gradient of 2.5% acetonitrile (vol.) (solvent A) and acetonitrile (solvent B) both with 0.1% (vol.) formic acid as additive. Separation started off at 2% B isocratic for 1 min and increase to 98% B over 5 min; then, after 4 min washing step at 98% B, conditions return to 2% B in 3 min followed by 5 min of column re-equilibration. The flow rate was set at 0.3ml/min and column temperature was 35°C. The outlet of the column was connected to a photodiode array detector (PDA) in line with the mass spectrometer. The PDA scan absorption spectra from 190 to 500nm. The settings of the electrospray ionisation source were as follow: gas temperature, 325°C; dry gas flow, 5L/min; nebulizer, 35psi; sheat gas temperature, 275 °C; sheat gas flow, 12L/min; VCap, 4000V; nozzle voltage, 500V and fragmentor at 400V. The mass range was 100-1700m/z recorded in centroid mode at a rate of 0.9 spectra/sec. A

reference mass solution (purine 5 mM, HP-0921 2.5mM) was constantly infused to enable mass calibration throughout the chromatographic run.

2.5.3 Data analysis of LC-MS files.

A library of compounds of interest was created in Agilent's PCDL Manager software (Agilent Technologies, California, USA) and used for "peak-picking" in samples and peak's area integration. Compounds of interest (strigolactones and apocarotenoids) were identified based on mass accuracy and chemical formula generated, retention time and fragmentation pattern when sufficient intensity threshold triggered the MS/MS event, using Mass Hunter Qual Analysis software (Agilent Technologies, California, USA). The spectral and chromatographic data was compared to literature data and then incorporated into in-house library. All compounds were detected as sodium adducts, as previously reported (Floková et al., 2020).

2.6 Ionomics analysis

2.6.1 Sample preparation- extraction

Shoot material was cut from roots and rinsed twice in pure 18 MΩ H_2O to reduce surface mineral contamination. Shoot was cut into 2-3cm pieces and mixed to ensure a representative sample was collected. Ceramic scalpels and plastic forceps were used to minimize metal contamination. All biological replicates per genotype were pooled into 5ml Eppendorf tubes and transferred into an oven at 90°C overnight. Dried samples were then sent to University of Nottingham Ionomics Facility, UK for analysis.

2.6.2 ICP-MS

All ICP-MS analysis was conducted by Dr Paulina Flis and Prof. David Salt at University of Nottingham Ionomics Facility, UK. The method was as previously published (X. Y. Huang et al., 2019), with the modification that a PerkinElmer NexION 2000 ICP-MS (PerkinElmer, Massachusetts, USA) equipped with an Elemental Scientific Inc. autosampler (Elemental Scientific, Nebraska, USA) was used. The foliar elemental concentrations (ppm) of the following was determined:

lithium (Li 7), sodium (Na 23), magnesium (Mg 24), phosphorous (P 31), sulphur (S 34), potassium (K 39), calcium (Ca 43), manganese (Mn 55), iron (Fe 56), cobalt (Co 59), nickel (Ni 60), copper (Cu 63), zinc (Zn 66), rubidium (Rb 85), strontium (Sr 88) and molybdenum (Mo 98).

2.7 Genome wide association study (GWAS) of AM traits

2.7.1 Selection of diverse panel of *Indica* rice

A panel of 218 *Indica* rice accessions (Table 2.18) was selected from the 3,000 rice genomes project (3K-RG), which recently re-sequenced a core collection of 3,024 rice genomes from 89 countries to advance global breeding programs (Z. Li et al., 2014). The panel was chosen due to diversity and representation of the *Indica* subpopulation, as described in Chapter 4. Seed of the 218 cultivars was obtained in collaboration with Dr Amelia Henry, IRRI from the International Rice Genebank, IRRI, Philippines (https://www.irri.org/international-rice-genebank).

2.7.2 Glasshouse conditions and block design of the *Indica* rice panel

The GWAS experiment was grown in Zone 5 Glasshouse of the University of Cambridge Botanic Gardens, UK. The daytime temperature was set to approx. 28^0C and night to approx. 23^0C. Plants received ambient light plus supplementary 12-hour daylight of 390-410 w/m^2. Five biological replicates of mock-inoculated and five biological replicates of AMF-inoculated plants per genotype were grown, with a total of ~2000 plants in the experimental study (~200 genotypes x 10 replicates). The panel was grown in a randomized block design in which genotype pairs (1 mock and 1 AMF-inoculated plant) per replicate were randomly assigned to sub-blocks, each of which contained ~ 22 plants across two trays. The experiment was further split such that the sub-blocks were split into five blocks and planted and harvested over five days in a staggered manner. Each ‘day’ contained one replicate of each genotype pair. The blocks were used in order to estimate and account for spatial variation in the glasshouse (Montgomery, 1984).

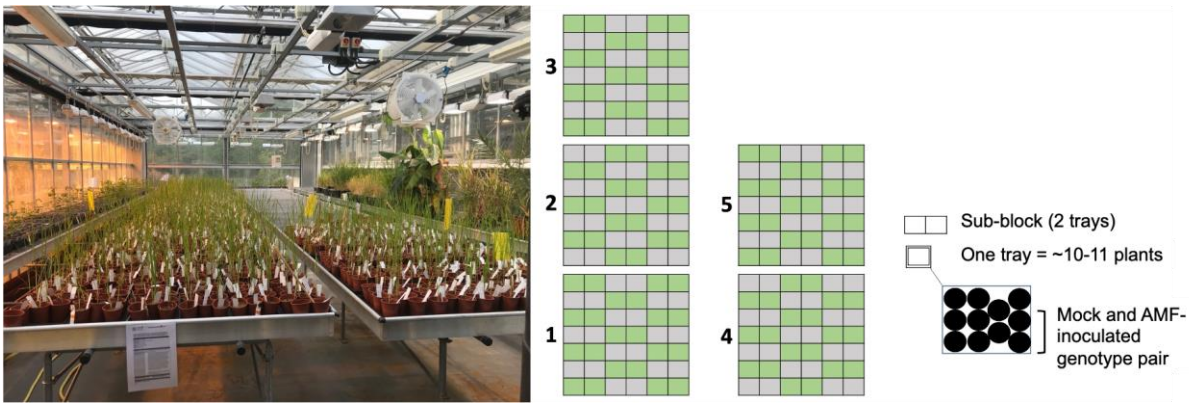

Figure 2.2 Randomized block design of GWAS glasshouse experiment at University of Cambridge Botanic Garden Experimental Glasshouses, UK.

2.7.3 Seed sterilisation and planting of GWAS glasshouse experiment

Rice husks arrived coated in fungicide, which required further cleaning than described in Section 1.1.1. Rice seeds were de-husked, washed in autoclaved diH_2O and surface sterilized using 2-minute treatment in 70% (*v/v)* ethanol. They were then shaken for 40 minutes in 5% (*w/v)* sodium hypochlorite using a Heidolph Polymax 1040 platform shaker (Heidolph, Schwabach, Germany). The sodium hypochlorite was then removed, and seeds washed in autoclaved diH_2O three times. Seeds were then germinated as previously described.

2.7.4 Growth and inoculation of GWAS glasshouse experiment

All plants were grown in 0.5ml capacity, 9cm x 8cm 'Lily of the Valley' pots, obtained from Dejex Horticulture, UK. In mock-inoculated plants, pots were three-quarter filled with sterile quartz-sand mixed with diH_2O. In AMF-inoculated plants, pots were three-quarter filled with sand mixed with spores of *R. irregularis* at a concentration of 800 spores/pot. Aseptic spore solution inoculum was obtained from PremierTech, Canada (PTB297-L-ASP-A). After diluting appropriately in diH_2O, spores were mixed into sand at a ratio of 10ml per 100g sand using a soil mixer. Seedlings were added to the pots using forceps and covered with appropriate sand. All pots were watered with diH_2O to settle the seedlings (Figure 2.3A). Pots were covered with mesh for the

first 2 weeks of growth to create a humid environment. Plants watered 3 times a week up to 2 wpi with diH_2O, after which they are fertilized twice weekly using half Hoagland solution (Table 2.5) and once weekly with diH_2O only. Plants were harvested at eight wpi whilst at vegetative stage (Figure 2.3B).

A **B**

Figure 2.3 Representative images of the glasshouse experiment. *(A) Representative image of rice seedlings after being transferred to mock- and AMF-inoculated sand in randomized block design. (B) Representative image of growth of the rice plants in the glasshouse after seven weeks post inoculation.*

2.7.5 Trait phenotyping of the *Indica* panel

Existing phenotypic data for the selected lines was assessed for agronomic traits. Phenotypic data was retrieved from the qualitative morpho-agronomic data available for the 3K-RG (https://snp-seek.irri.org/). Four agronomic traits were selected for analysis including seed coat colour, seedling height (cm), spikelet fertility and panicle length at post-harvest stage. In addition, several phenotypes were measured in the GWAS glasshouse experiment for both mock and AMF-inoculated plants. Plant height was measured at seedling stage (4wpi). At harvest (8wpi), foliar blumenol (Section 2.4), foliar ionome (Section 2.6), plant height and shoot and root biomass were measured. For all traits except blumenol abundance, mock and AMF-inoculated plants were analysed and compared. Blumenol abundance was only analysed in AMF-inoculated plants since previous studies found a strict association of blumenol abundance to AM colonised plants (Chapter Three). Plant height was measured in the glasshouse before harvest, using a ruler to assess the height (cm) of the tallest leaf. On harvest, after separating root and shoot using a scalpel,

washing in diH_2O and drying, shoot and root fresh weight were measured. Samples were then dried overnight in an oven set at 90^oC and dry weight of root and shoot measured. Where foliar material was taken for blumenol and ionome analysis, the fresh weight of this was multiplied by the average water content of the rice leaves found after drying and used as an estimate for missing material. All phenotype data was visualized in R 4.2.1 (R Core Team 2022).

2.7.6 Genome Wide Association Mapping and candidate gene analysis

Genome wide association mapping was performed in R 4.2.1 (R Core Team 2022). Phenotype data was pre-processed in R. Data was $\log_{10}$ transformed to fit assumptions of normality, assessed using a Shapiro-wilk test for normality. A normal distribution was obtained after a $\log_{10}(X + 100)$ transformation for 11-hydroxyblumenol-C-Glc and a square root (X + 1000) transformation for 11-carboxyblumenol-C-Glc. Best linear unbiased predictors (BLUPs) were calculated for transformed blumenol abundance using the lme4 package in R with the following model: $Y \sim 1 + (1|Taxa) + (1|sub.block)$. Broad-sense heritability was estimated based on the model results using the bwardr package, Cullis_H2 function (Cullis et al., 2006).

For genotypic data, the panel of 196 genotypes used in GWAS was extracted from the 2M SNP database available for the 3K-RG panel (W. Wang et al., 2018). SNP variants with minor allele frequency (MAF) >5%, missing data < 10% and minor allele count > 8 were first filtered from the ‘3KRG Filtered SNP Set’. This gave ~ 2,088,720 SNPs. These were then pruned to reduce highly correlative SNPs (R2 = 0.95, $p < 0.05$), creating a "non-redundant" subset that would be computationally efficient whilst representing variation across the whole genome. A total of 386,173 SNPs in the non-redundant set were mapped to Nipponbare reference sequence and used for population structure analysis and GWAS. The GAPIT package was used to implement BLINK and MLM models. Principal component and kinship analyses were performed in Tassel v5.0, with a Centered IBS model to estimate kinship (Bradbury et al., 2007). A scree plot of eigenvalue variance against PCs was used to select the number of PC required to sufficiently describe variance. PC=4, the

point of ‘elbow’ on the plot was selected (Figure 2.4). PC and kinship were included in the MLM model and PC was included in BLINK. A Bonferroni-correction of 1/N, with N independent markers of 386,173 SNPs and $\alpha = 0.05$, was used to determine a stringent genome-wide P-value significance threshold of $1.3e^{-7}$, ($-\log_{10}(P) = 6.88$). SNPs within 200kb (based on linkage disequilibrium decay reported in rice previously (Davidson et al., 2019; K. Zhao et al., 2011) of the candidate SNP loci were considered to represent clusters, analysed using the MLM model. Single SNPs with no other SNPs ($p < 0.001$) within 200kb were not considered QTLs. In addition, since the Bonferroni correction is considered a conservative significance threshold, SNPs in MLM model above $P < 0.0001$, $-\log_{10}(P) > 4$ were considered ‘suggestive’ of association. This ‘suggestive’ threshold is as described previously for detection of QTLs associated to AM traits in rice (Davidson et al., 2019).

Genes within 200kb of candidate SNPs were annotated with MSU7 or RAP-DB ID using Rice Gene Hub tool (https://rice-genome-hub.southgreen.fr/find/genes) and considered as potential candidates. Their potential to be related to AM traits was assessed by comparison of gene ID with (a) a list of 205 genes with a genetically determined or putative function in AM symbiosis (Das et al., 2022) and (b) transcriptomic data of genes differentially expressed in rice inoculated with *R. irregularis* and grown similarly to this GWAS experiment (S. Wang et al., 2020). SNPEff using SNP SEEK tool (https://snp-seek.irri.org), which incorporates SnpEff program to categorise variants within the ‘3KRG Filtered SNP’ set based on their predicted effects on coding regions (Cingolani et al., 2012), was used to determine variants, namely SNPs and insertion or deletions (INDELs) in the genes. A candidate gene list was then produced and assessed for potential to be associated to variation blumenol abundance and AM symbiosis.

In addition, functional SNP annotation of lead SNPs was performed using SNPEff analysis in SNP SEEK tool (https://snp-seek.irri.org) using cultivars within the selected panel. Haplotype analysis of blumenol abundance in causal SNPs was performed in R 4.2.1 (R Core Team 2022) using dplyr and ggplot2 package. In addition, non-coding effects of causal SNPs were interrogated using RiceVarMap2. RiceVarMap2 includes chromatin accessibility profiles from six tissues of *Zhenshan97* cultivar measured using Assay for Tranposase-Accessible Chromatin

with sequencing (ATAC-seq assay) and gives a score from -2 to 2 for predicted change in accessibility using a logarithmic ratio of the predicted accessibility of the alternative genotype to the value of the reference genotype. The more extreme the score the more likely the variant affects chromatin (H. Zhao et al., 2015b). Overall, the pipeline should facilitate comprehensive analysis of the potential effects of variants on proximal genes.

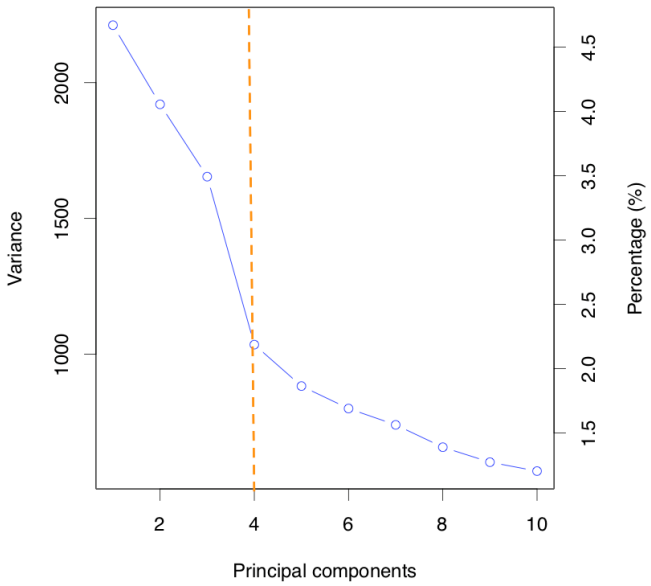

Figure 2.4 Scree plot of eigenvalue variance. *Scree plot depicts variance described by principal components. The 'elbow' of the plot, the point after which additional PCs would add relatively little information, is noted with a yellow dashed line. PC=4 was selected.*

2.8 Field experiments at IRRI, Philippines

The AMF field experiment was conducted in collaboration with Dr Amelia Henry and the Drought Physiology Group, IRRI. Field experiments and harvest was conducted mainly by her group.

The DSR field experiment was sampled from ongoing DSR breeding trials by Dr Shalabh Dixit and his group. Sampling of the material was conducted in collaboration with his group, DSR Breeding Trials Team, Dr Amelia Henry and the Drought Physiology Group.

2.8.1 Seedling planting and inoculation- AMF field experiment

Twelve genotypes were selected for the AMF field experiment (Table 2.19). The field experiment was conducted in a previously low phosphate, fallow field in upland farm plots at IRRI, Philippines. The plots had optional covers, which were used during heavy rain to prevent puddling and keep irrigated condition. The experiment was conducted during the wet season, with seeds planted on 27 June 2022 (Table 2.20). The experiment was planted in a randomized design, with two plots – one non-inoculated (containing native AMF only) and the other inoculated with Mykovam® AMF Inoculum (native AMF + AMF inoculum). Each plot had 3 rows per genotype, with a total of 36 linear meters of row (Figure 2.5). Rows were dug as 1-inch-deep lines of 1m length. AMF inoculum, Mykovam®, a soil-based fertiliser, was obtained from National Institute of Molecular Biology and Biotechnology at University of Philippines, Los Baños. It contains spore propagules and root fragments of plants infected with 12 species of AMF, which were grown in glasshouse conditions (agora.uplb.edu.ph/food-security-and-sovereignty/mykovam/), (Figure 2.6). AMF inoculum was added to the AMF-inoculated plot only by hand-application into rows at a rate of 50g per linear meter. Seeds were then sown directly onto dry soil by hand-sowing into the rows. Soil was added back into the rows. The plots were irrigated to soil capacity with no stagnant flooding. Limited fertiliser was added to the plots to promote AM colonisation, with two topdressing applications of urea at 50kg N per hectare to ensure plant growth (Table 2.20). A net was used to cover plots, preventing birds from eating seed or early seedling damage from pests. Plots were manually weeded throughout the growing season. The growth calendar and fertiliser application regime is summarized in Table 2.20.

A

B

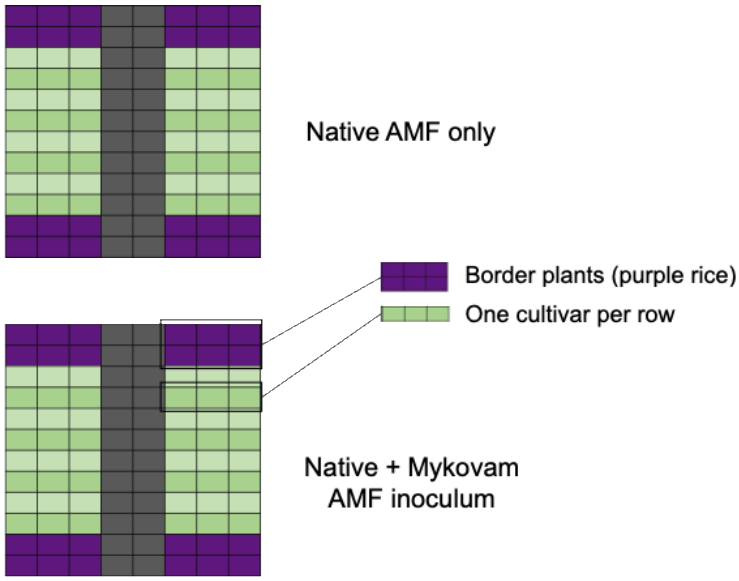

Figure 2.5 AMF field experiment and randomized design in upland farm, IRRI. *(A) Representative image of the field trial plots and cultivar rows at IRRI, Philippines. (B) Diagram of randomised design of the trial. Plots were either native or native + AMF-inoculated with Mykovam® 12 AMF species mix inoculum. Each genotype was planted in three replicate rows per plot, with 36 total rows per plot. Borders of purple rice were included.*

Figure 2.6 Mykovam® Inoculum. *Inoculum was obtained from obtained from National Institute of Molecular Biology and Biotechnology at University of Philippines, Los Baños. It contains spore propagules and root*

fragments of plants infected with 12 species of AMF, which were grown in glasshouse conditions (agora.uplb.edu.ph/food-security-and-sovereignty/mykovam/).

2.8.2 Harvest and phenotyping- AMF field experiment

Two time points were selected for phenotyping, with three plants per genotype row harvested as biological replicates. All plants were harvested from soil and washed before analysis. Firstly, a sample of plants were harvested at six weeks post planting, at vegetative stage. Total crown root number, plant height (height of tallest leaf in cm) and shoot dry weight (weight of shoot material after drying overnight in oven at 90°C) was assessed by the Drought Physiology Group, IRRI. In addition, soil samples were taken for uniformity testing. Soil pH measured in water and $CaCl_2$, soil nitrate (mg exch NO3-N/kg soil) and ammonium (mg exch NH4-N/kg soil) was assessed by the IRRI team using standard protocols. During growing, days to flowering (DTF) was noted per plot for all genotypes. After flowering, plants were harvested and the following growth yield traits were assessed by the Drought Physiology Team, IRRI: plant height, straw dry weight, grain dry weight, grain yield, straw biomass and harvest index. Grain yield was measured as grams of grain per m^2 and straw biomass as grams of straw dry weight per m^2. Harvest index was calculated as previously (Hühn, 1990) as the ratio of grain to straw biomass:

$$Harvest\ Index = \frac{Grain\ Yield\ (g\ m^{-2})}{Grain\ Yield\ (g\ m^{-2})\ +\ Straw\ Biomass\ \ (g\ m^{-2})}$$

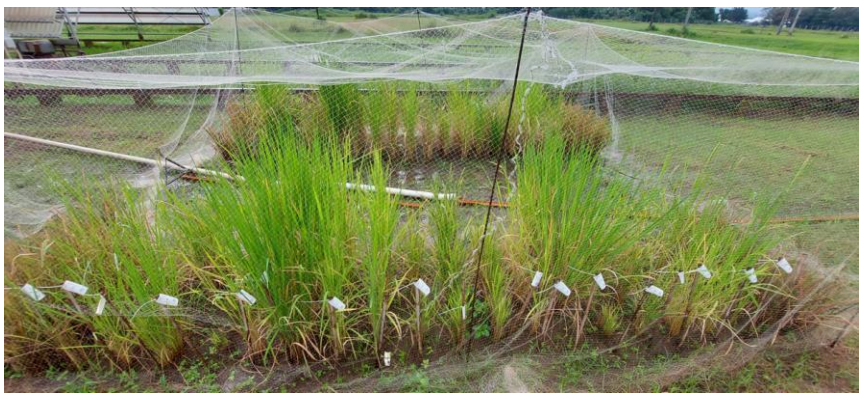

Figure 2.7 Rice cultivars in AMF field trial plot before harvest, with nets used to prevent loss of seed from birds and other pests.

2.8.3 Growth conditions- DSR AM trial

The DSR experiment was sampled from a breeding trial, which included four plots of different irrigation and planting methods. The breeding trial was conducted during the wet season 2022 at IRRI, Philippines under the lead of Dr Shalabh Dixit, Head of DSR Breeding at IRRI. The trials included selected mid to early flowering lines grown to yield in different DSR and transplanted conditions. The four trial conditions, planting method, data and irrigation are summarised in Table 2.21. Each plot contained a randomized block design, with 10 replicate blocks of $2m^2$ per cultivar. The trials were fertilised at the recommended rate as in Table 2.22B.

2.8.4 Harvest and AM phenotyping- DSR AM trial

The rice cultivar *NSIC Rc222 (IRRI 154)* was selected for analysis of AM phenotypes between the plots. Plants were harvested at late vegetative stage. Three biological replicate plants of *NSIC Rc222* per each of the 10 replicate blocks per plot were harvested and pooled for analysis. Plants were washed in H_2O and dried before root sampling. Trypan blue staining and AM quantification was conducted as described in Section 1.2.1 and 1.2.2, except the experiment was conducted using equivalent reagents from the Drought Physiology Group, IRRI and an Olympus BX51 fluorescence microscope (Olympus, Tokyo, Japan) from the Crop Physiology Group, IRRI for quantification and images.

2.9 Statistics

2.9.1 Statistical analysis of data

All statistical analysis was done using RSTUDIO (http://www.Rproject.org/) using R version 4.2.1. Graphs were made using ggplot2 (Wickham, H., 2016) package. Mean values and standard deviations were calculated per genotype, per condition. Assumptions of normality and equal variance were analysed using histograms and QQ plots of data and Shapiro Wilk test. Statistical differences between non-normally distributed data were analysed using the non-parametric Kruskal–Wallis and post hoc testing using Fischer's least significant difference at 5% significance level. Pairwise comparisons between genotypes identified statistically different groups, denoted by different letters or asterisks on graphs. This was performed using base R

and agricolae (v1.3-5; de Mendiburu, 2021) package. This protocol was as adapted from that previously described (Pimprikar et al., 2016). For analysis of difference between mean values according to two categorical variables, a two-way ANOVA was performed with Tukey's Honest Significant Difference post-hoc test at standard threshold of p=0.05. Data was $\log_{10}$-transformed where required to allow homogeneity of variance for this test. This was analysed using base R.

2.9.2 Correlation analysis of data

Blumenol correlation analyses used linear regression of blumenol abundance against % colonisation, as described previously (M. Wang et al., 2018). This was analysed using base R and stats (R Core Team, 2013) package. Correlation matrices with Pearson's correlation coefficient quoted at $p < 0.05$ were produced to model correlation between multiple traits. All correlation analysis was done using base R and corrplot (v0.92; Wei and Simko, 2021) package.

2.10 Genotype and Chemical Tables

Table 2.1 Rice material used in AM cone studies. *Genotype, cultivar ecotype, mutant information and reference per mutant is denoted.*

Genotype	Cultivar	Mutant information	Reference
Nipponbare (WT)	*Nipponbare*	WT	-
Shiokari (WT)	*Shiokari*	WT	-
Dongjin (WT)	*Dongjin*	WT	-
ccamk-1	*Nipponbare*	Tos17 insertion mutant line	(C. Gutjahr et al., 2008; Miyao et al., 2003)
pollux-2	*Nipponbare*	Tos17 insertion mutant line	(C. Gutjahr et al., 2008; Miyao et al., 2003)
cerk1	*Nipponbare*	Knock-out mutant line	(Miyata et al., 2014; X. Zhang et al., 2015)
str1-2	*Nipponbare*	T-DNA insertion line	(C Gutjahr et al., 2012; Sallaud et al., 2004)
smax1-1	*Dongjin*	CRISPR mutation	(Choi et al., 2020)
d3-1	*Shiokari*	Tillering dwarf mutant line	(Ishikawa et al., 2005; Yoshida et al., 2012)

d14-1	*Shiokari*	Tillering dwarf mutant line	(Arite et al., 2009; Ishikawa et al., 2005)
d10-1	*Shiokari*	Tillering dwarf mutant line	(Arite et al., 2007; Ishikawa et al., 2005)
d17-1	*Shiokari*	Tillering dwarf mutant line	(Ishikawa et al., 2005; Umehara et al., 2008)
d27-1	*Shiokari*	Tillering dwarf mutant line	(Hao et al., 2009; Ishikawa et al., 2005)

Table 2.2 Lines from the International Rice Research Institute used in blumenol analyses. *IRRI IRGC number, name, ecotype, country of origin and cultivation is denoted per cultivar. All information was obtained from accession information available on IRRI SNP Seek (https://snp-seek.irri.org/).*

IRRI Code	Accession Name	Cultivar	Country	Cultivation
IRGC 128059	IR 1813-694-2::IRGC 32656-2	*Aus/boro*	Bangladesh	Upland
IRGC 121119	SICAN::IRGC 117029-1	*Indica*	Peru	Lowland
IRGC 127212	BARKHE TAULI::IRGC 16116-1	*Indica*	Nepal	-
IRGC 127444	ITA 117::IRGC 75235-1	*Indica*	Nigeria	Upland
IRGC 122272	UPL RI 7::IRTP 9897-C1	*Intermediate*	Philippines	Upland
IRGC 128023	DADKHANI::IRGC 45454-2	*Indica*	India	Paddy
IRGC 132361	O. SATIVA::IRGC 10164-2	*Indica*	India	Upland
IRGC 128015	CHITRAJ 14-134::IRGC 37837-2	*Indica*	Bangladesh	Lowland
IRGC 128304	GUANG XUAN LIU HAO::IRGC 77341-1	*Indica*	China	Paddy
Model	Nipponbare	*japonica*	Japan	
Model	Shiokari	*japonica*	Japan	
IRGC 125658	ASU::IRGC 62154-1	*Indica*	Bhutan	Traditional
IRGC 125958	CHAMA (DWARF)::IRGC 69487-1	*Indica*	Zambia	Traditional
IRGC 127278	CHING CH'UNG::IRGC 65002-1	*Indica*	Taiwan	Traditional
IRGC 127361	ESCONDE CACHO::IRGC 74305-1	*Indica*	Brazil	
IRGC 127404	HEGAR MANAH::IRGC 17733-1	*Indica*	Indonesia	Traditional
IRGC 125836	MEI FENG 9::IRGC 63735-1	*Indica*	China	
IRGC 125842	MIN ZAO 6::IRGC 63772-1	*Indica*	China	
IRGC 127772	RUS RUSSEI::IRGC 94341-1	*Indica*	Cambodia	

Table 2.3 Fungal subculture media recipe

Solution	Chemical	g in 100X stock (g/L)	ml in final solution used (1L)
A	KNO_3	8.00	10
	KCl	6.50	
	$MgSO_4.7H_2O$	73.10	
	KH_2PO_4	0.48	
B	$Ca(NO_3)_2.4H_2O$	28.80	10
C	Na Fe EDTA	0.80	10
D (Microelements)	$MnCl_2.4H_2O$	0.60	1
	H_3BO_3	0.15	
	$ZnSO_4.7H_2O$	0.26	
	$CuSO_4.5H_2O$	0.01	
E	$Na_2MoO_4.2H_2O$	0.24	1
F	KCl	0.08	1
G (Vitamins)	Glycine	0.30	1
	Thiamine hydrochloride	0.01	
	Pyidoxine hydrochloride	0.01	
	Nicotinic acid	0.05	
	Myo Inositol	5.00	
H	Sucrose	-	15
I	Gellum Gum	-	3.5

Table 2.4 Fungal spore extraction buffer

Solution	Chemical	ml
A	0.1M citrate buffer	1.7
B	0.1M sodium citrate	8.3
C	di H_2O	90
Buffer set to pH 6.0 using small volumes of HCl or NaOH		

Table 2.5 Hoaglands solution for normal, AM-permissive conditions (25 µm Pi)

Solution	Chemical	M.W	g in 20X stock (g/L)	ml in final ½ Hoagland used (1L)
A	KNO_3	101.11	10	25
	$Ca(NO_3)_2.4H_2O$	236.15	2.36	

	$MgSO_4.7H_2O$	246.48	9.86	
B (25 μm Pi)	KH_2PO_4	136.09	0.68	5
	KCl	74.56	6.9	
C	Fe Citrate	-	0.5	5
D	$MnSO_4.H_2O$	169.02	0.137	0.5
	$ZnSO_4.7H_2O$	287.54	0.02	
	$CuSO_4.5H_2O$	249.68	0.008	
E	$Na_2B_4O_7.10H_2O$	381.4	0.2	0.5
	$(NH_4)_6Mo_7O_{24}.4H_2O$	1235.86	0.01	

Table 2.6 Hoagland solution for increased Pi condition (250um Pi or 2500um Pi). *Chemical composition is as in Table 2.4 but B solution is altered depending on Pi condition.*

Solution	**Chemical**	**M.W**	**g in 20X stock (g/L)**	**ml in final ½ Hoagland used (1L)**
B (250 μm Pi)	KH_2PO_4	136.09	6.8	0.5
	KCl	74.56	3.73	
B (2500 μm Pi)	KH_2PO_4	136.09	68	0.05
	KCl	74.56	0	

Table 2.7 Trypan blue staining solution

Solution	**Chemical**	**Composition**
A	10% (w/v) KOH	10g/100ml
B	0.3M HCl	24.3ml HCL_{conc} /L
C	0.1% trypan blue	100mg in 50ml lactic acid, 25ml glycerol, 25ml di H_2O (for 100ml)
D	50% acidic glycerol	1:1 of glycerol: 0.3M HCl

Table 2.8 gDNA extraction buffer

Solution	**Chemical**	**M.W**	**Final**	**Stock**	**For 50 mL**
A	KCl	74.54	1M	N/A	3.727 g
B	TRIS (pH 7.5)	10X	100 mM	1 M	5 mL
C	EDTA	50X	10 mM	0.5 M	1 mL
D	MilliQ H_2O	-	-	-	36 mL

Table 2.9 PCR reaction mix

Solution	Chemical	μl per sample reaction
A	H_2O	6.15
B	$MgCl_2$ (25mM)	1.4
C	dNTP (10mM)	0.4
D	5X GoTaq green buffer	4
E	Betaine (5M)	5
F	F primer (10 μm)	1
G	R primer (10 μm)	1
H	GoTaq2 Flexi	0.002

Table 2.10 Genotyping primers

Primer	Background Cultivar	MSU ID	Sequence	Reference
ccamk-1	*Nipponbare*	LOC_05g41090	TGTTCTCTTCCACAAAAGACACAT	(C. Gutjahr et al., 2008)
			GAGGTTTTAGGCTGATCAAGTCAT	
pollux-2	*Nipponbare*	LOC_01g64980	WT F: GCAGCTAGCTATAGCAAACAAGAG	(C. Gutjahr et al., 2008)
			WT R: TTTCATCGGATGCTAAAACAATAA	
			mutant F: GCAGCTAGCTATAGCAAACAAGAG	
			mutant R: ATTGTTAGGTTGCAAGTTAGTTAAGA	
pt11	*Nipponbare*	LOC_01g46860	WT F: AAGGGACAAAACACACAGGC	(Yang et al., 2012)
			WT R: TCTGA TCACCAAACTGCTCG	
			mutant F: AAGGGACAAAACACACAGGC	
			mutant R: AGGTTGCAAGTTAGTTAAGA	
str1-2	*Nipponbare*	LOC_Os09g23640	CCCTGGATGAATCAATGACAG	(C Gutjahr
			GCCGTAATGAGTGACCGCATCG	

				et al., 2012)
cerk1	*Nipponbare*	LOC_Os08g42580	WT F: CACCAACATGGCGGATCTCT	(Chiu et al., 2018)
			WT R: AGCTGCCTGTACTGCACAAA	
			mutant F: TTAAGCTAAGCATCCGTAAGCAAAGA	
			mutant R: CCAAAACTGCTTCAAATAACCGCTCA	
smax1-1	*Dongjin*	LOC_Os08g15230	WT F: TTCCCCTGTCGAAATCTTGG	
			WT R: ATGACCGATTCAAATTTCGC	
			mutant F: TTGGGGTTTCTACAGGACGTAAC	
			mutant R: ATGACCGATTCAAATTTCGC	
d3-1	*Shiokari*	LOC_Os06g06050	GCTCTAAGTCCGATCCGTGA	(Yoshida et al., 2012)
			TGTGTGGTGCCATGGATGAA	
d14-1	*Shiokari*	LOC_Os03g10620	GTGCTGTCGCATGGCTTC	(Arite et al., 2009)
			CTTGAAGACGGTCTGGCAGA	
d10-1	*Shiokari*	LOC_Os01g54270	CTTCTGAGGTAAGCTCGTGGA	(Umehara et al., 2008)
			CCCTTGATGGTCTCCGTGAG	
d17-1	*Shiokari*	LOC_Os04g46470	GAGGCCAAGTCCAAAGATG	This study
			TCTCCACGAACCTGCATGC	
Primer	**Background Cultivar**	**MSU ID**	**Sequence**	**Reference**
ccamk-1	*Nipponbare*	LOC_05g41090	TGTTCTCTTCCACAAAAGACACAT	(C. Gutjahr et al., 2008)
			GAGGTTTTAGGCTGATCAAGTCAT	
pollux-2	*Nipponbare*	LOC_01g64980	WT F: GCAGCTAGCTATAGCAAACAAGAG	(C. Gutjahr et al., 2008)
			WT R: TTTCATCGGATGCTAAAACAATAA	
			mutant F: GCAGCTAGCTATAGCAAACAAGAG	

			mutant R: ATTGTTAGGTTGCAAGTTAGTTAAGA	
pt11	*Nipponbare*	LOC_01g46860	WT F: AAGGGACAAAACACACAGGC	(Yang et al., 2012)
			WT R: TCTGA TCACCAAACTGCTCG	
			mutant F: AAGGGACAAAACACACAGGC	
			mutant R: AGGTTGCAAGTTAGTTAAGA	
str1-2	*Nipponbare*	LOC_Os09g23640	CCCTGGATGAATCAATGACAG	(C Gutjahr et al., 2012)
			GCCGTAATGAGTGACCGCATCG	
cerk1	*Nipponbare*	LOC_Os08g42580	WT F: CACCAACATGGCGGATCTCT	(Chiu et al., 2018)
			WT R: AGCTGCCTGTACTGCACAAA	
			mutant F: TTAAGCTAAGCATCCGTAAGCAAAGA	
			mutant R: CCAAAACTGCTTCAAATAACCGCTCA	
smax1-1	*Dongjin*	LOC_Os08g15230	WT F: TTCCCCTGTCGAAATCTTGG	
			WT R: ATGACCGATTCAAATTTCGC	
			mutant F: TTGGGGTTTCTACAGGACGTAAC	
			mutant R: ATGACCGATTCAAATTTCGC	
d3-1	*Shiokari*	LOC_Os06g06050	GCTCTAAGTCCGATCCGTGA	(Yoshida et al., 2012)
			TGTGTGGTGCCATGGATGAA	
d14-1	*Shiokari*	LOC_Os03g10620	GTGCTGTCGCATGGCTTC	(Arite et al., 2009)
			CTTGAAGACGGTCTGGCAGA	
d10-1	*Shiokari*	LOC_Os01g54270	CTTCTGAGGTAAGCTCGTGGA	(Umehara et al., 2008)
			CCCTTGATGGTCTCCGTGAG	
d17-1	*Shiokari*	LOC_Os04g46470	GAGGCCAAGTCCAAAGATG	This study
			TCTCCACGAACCTGCATGC	

Table 2.11 Trizol solution

Solution	Chemical	Concentration in Trizol solution	Quantity for 1L Trizol
A	Guanidium Thiocyanate	0.8M	94.52g
B	Ammonium Thiocyanate	0.4M	30.45g
C	Sodium acetate (pH 5)	0.1M	33.33 mL of 3M NaAc (pH 5)
D	Glycerol	5% (v/v)	50mL
E	Phenol (pH 5)	38% (v/v)	380mL (pH 5)

Table 2.12 qRT-PCR reaction mix

Solution	Chemical	μl per sample reaction
A	H_2O	7.35
B	$MgCl_2$ (25mM)	3.2
C	dNTP (10mM)	0.4
D	5X GoTaq colourless buffer	4
E	Primer mix (F + R, 3 μm)	1
F	10X SYBR green	1
G	GoTaq2 Flexi	0.05
H	Sample cDNA template	3

Table 2.13 qRT-PCR primers

Primer	Gene	MSU ID	Sequence	Reference
Cyclophilin 2 (CP2)	rice housekeeping gene	LOC_Os02g02890	GTGGTGTTAGTCTTTTTATGAGTTCGT	(C. Gutjahr et al., 2008)
			ACCAAACCATGGGCGATCT	
Ubiquitin (UbiQ)	rice housekeeping gene	LOC_Os02g02890	CATGGAGCTGCTGCTGTTCTAG	(C. Gutjahr et al., 2008)
			CAGACAACCATAGCTCCATTGG	
GAPDH	rice housekeeping gene	LOC_Os02g02890	CTGATGATATGGACCTGAGTCTACTTTT	(C. Gutjahr et al., 2008)
			CAACTGCACTGGACGGCTTA	
		-	GCTATTTTGATCATTGCCGCC	

*Ri*EF1α	*R.irregularis* housekeeping gene		TCATTAAAACGTTCTTCCGACC	(Pérez-Tienda et al., 2014)
AM1	AM early marker gene	LOC_Os04g04750	ACCTCGCCAAAATATATGTATGCTATT TTTGCTTGCCACACGTTTTAA	(C. Gutjahr et al., 2008)
AM3	AM early marker gene	LOC_Os01g57400	CTGTTGTTACATCTACGAATAAGGAGAAG CAACTCTGGCCGGCAAGT	(C. Gutjahr et al., 2008)
AM14	AM late marker gene	LOC_Os01g46860	GAGAAGTTCCCTGCTTCAAGCA CATATCCCAGATGAGCGTATCATG	(C. Gutjahr et al., 2008)
PT11	AM late marker gene, AM-specific Pi transporter	LOC_Os11g26140	CCAACACCGTTGCAAGTACAATAC GCACTTTGAAATTGGACTGTAAGAAA	(C. Gutjahr et al., 2008)
IPS1	Pi starvation marker gene	LOC_Os03g05334	AAGGGCAGGGCACACTCCACATTATC ATTAGAGCAAGGACCGAAACACAAAC	(C. Wang et al., 2009)

Table 2.14 qPCR cycle programme

	Initial Denaturation	**Denaturation**	**Annealing**	**Extension**	**Final Extension**	**Hold**
Temp (^{0}C)	96	96	Primer specific (see table X)	72	72	16
Time	2 min	30 sec	30 sec	60 sec	10 min	N/A
		30 cycles				

Table 2.15 Blumenol extraction buffer

Solution	**Chemical**	**mL for 1L buffer**	**Final concentration per 800 μl buffer**
A	MilliQ H_2O	200	-
B	MeOH (gradient grade for LC)	800	-
C	D6-ABA (10 $ng\ \mu l^{-1}$)	1.25	10ng

Table 2.16 Quantifier and qualifier m/z fragments used to detect blumenol derivatives in rice. *Compound name gives compound name, mass/charge ratio (m/z) and ionization polarity. Transition in m/z is denoted and includes multiple reaction monitoring (MRM) value, which is a means of monitoring only specific m/z values on interest and was defined previously* (Mindt et al., 2019). *The 11-hydroxyblumenol-C-Glc and 11-carboxyblumenol-C-Glc derivatives have previously been confirmed by NMR. Fragmentation of 11-carboxyblumenol-C-Glc m/z 241.2 aglycon precursor [M+H-Glc]+ allows for a sensitive MRM detection in addition to the MRM of the m/z 403.2 molecular ion [M+H]+. The identity of 11-carboxyblumenol C-Glc-Glc and 11-carboxyblumenol C-Mal-Glc detected in rice has not been confirmed* (Mindt et al., 2019). *ABA and blumenol A-Glc were confirmed with internal standards. D_6-ABA is an internal standard included in the extraction buffer.*

R_T in min	Compound Name	Transition in m/z
2.811	11-hydroxyblumenol-Glc_389	MRM 209.2, (+) 389.2 > 209.2 [7.5V]
2.47	11-hydroxyblumenol-Glc-Glc_551	MRM 209.2, (+) 551.3 > 209.2 [10.0V]
4.014	D_6 ABA	MRM 159.0, (-) 269.2 > 159.0 [10.0V]
3.173	11-carboxyblumenol_241_pos	MRM 195.1, (+) 241.2 > 195.1 [10.0V]
3.18	11-carboxyblumenol-Glc_403_pos	MRM 195.1, (+) 403.2 > 195.1 [12.5V]
3	Blumenol A - Glc_387_pos	MRM 207.1, (+) 387.2 > 207.1 [8.0V]
3	Blumenol A - fragment 207_pos	MRM 95.2, (+) 207.1 > 95.2 [14.0V]
2.46	Blumenol A - Glc_385_neg	MRM 153.1, (-) 385.2 > 153.1 [14.0V]
4	ABA	MRM 153.0, (-) 263.1 > 153.0 [9.0V]
3.1	11-carboxyblumenol-Glc-Glc_565_pos	MRM 223.2, (+) 565.2 > 223.2 [10.0V]
3.6	11-carboxyblumenol-MalGlc_489_pos	MRM 195.1, (+) 489.2 > 195.1 [12.5V]

Table 2.17 SL and Apocarotenoid extraction buffer

Solution	Chemical	μl added per sample	Final concentration added to each sample
A	H_2O (HPLC grade)	200	-
B	Acetone (HPLC grade)	300	-
C	D6-ABA (1 $ng\ \mu l^{-1}$) and GR24 (1 $ng\ \mu l^{-1}$)	5	5ng

Table 2.18 GWAS panel of 218 genotypes in selected diverse Indica panel. *IRRI IRIS ID (3K_DNA_IRIS), IRGC genetic stock number (GS), accession name (Genotype.Name), country of origin (CO), subpopulation (K9 and K15 (W. Wang et al., 2018)), cultivation practice where available, T- traditional landrace. P- paddy cultivation, I- irrigated cultivation, and whether the line is included in the 196 accessions or 191 accessions after removing PC outliers for GWAS analysis.*

IRIS ID	Genetic Stock	Genotype	Country	K15	K9	CP	191 panel	196 panel
IRIS_313-12067	IRGC 127100	531::IRGC 82643-1	Philippines	ind1.2.1	indx	T	Y	Y
IRIS_313-12014	IRGC 127105	ADANKARU::IRGC 79842-1	Nigeria	ind2.1	ind2	T	Y	Y
IRIS_313-7636	IRGC 126992	ADNY 11::C1	Mali	ind1.2.2	ind1B		Y	Y
IRIS_313-12057	IRGC 127116	AI JIAO ZI::IRGC 82255-1	China	ind3.2.2	indx		Y	Y
IRIS_313-10610	IRGC 132315	ALAGUSAMBA::IRGC 8944-2	Sri Lanka	ind2.2	ind2	T	Y	Y
IRIS_313-10257	IRGC 127031	ALTAMIRA 9::IRGC 116953-1	Nicaragua	indx	indx	I	Y	Y
IRIS_313-12146	IRGC 127121	AM BEUS::IRGC 87189-1	Cambodia	indx	indx	T	Y	Y
IRIS_313-11624	IRGC 127122	ANADI WHITE::IRGC 61897-1	Nepal	ind1.1	ind1A	T	Y	Y
IRIS_313-8621	IRGC 126174	ARC 11663::IRGC 42695-1	India	indx	ind1B		Y	Y
IRIS_313-9560	IRGC 125643	ARC 11857::IRGC 40972-1	India	indx	indx		Y	Y
IRIS_313-8585	IRGC 127033	ARC 11901::IRGC 21727-1	India	indx	indx		Y	Y
IRIS_313-8603	IRGC 126042	ARC 12884::IRGC 22417-1	India	indx	indx		Y	Y
IRIS_313-8069	IRGC 121966	ARIANA::GERVEX 396-C1	Romania	ind3.1	indx		Y	Y
IRIS_313-12148	IRGC 127172	ARN'-SAR THNGORN'::IRGC 87205-1	Cambodia	ind3.2.1	ind3	T	Y	Y
IRIS_313-12147	IRGC 127171	ARNG'-KAR PHAR ONG::IRGC 87196-1	Cambodia	ind3.2.1	ind3	T	Y	Y
IRIS_313-11812	IRGC 127175	ASFALA::IRGC 70650-1	Kenya	ind3.2.1	ind3	T	Y	Y
IRIS_313-9572	IRGC 125658	ASU::IRGC 62154-1	Bhutan	indx	indx	T	Y	Y
IRIS_313-11160	IRGC 127195	B 38::IRGC 34409-1	Liberia	ind3.1	ind3		Y	Y
IRIS_313-10990	IRGC 127206	BALIBUD::IRGC 26871-1	Philippines	ind3.2.2	indx	T		Y
IRIS_313-10762	IRGC 127207	BANDI::IRGC 17214-1	Indonesia	ind3.1	ind3	T	Y	Y
IRIS_313-10045	IRGC 125673	BANTA TIMA::IRGC 69474-1	Gambia	indx	indx	T	Y	Y
IRIS_313-9384	IRGC 125674	BARIK KUDI::IRGC 52807-1	India	indx	ind2	T	Y	Y
IRIS_313-10731	IRGC 127212	BARKHE TAULI::IRGC 16116-1	Nepal	ind1.1	ind1A			
IRIS_313-8312	IRGC 131932	BATU::IRGC 71508-1	Malaysia	ind3.1	ind3	T	Y	Y
IRIS_313-9348	IRGC 125684	BK 26::IRGC 45197-1	India	ind2.1	ind2		Y	Y
IRIS_313-10016	IRGC 125954	BOHOTO BALOOCHESTAN::IRGC 66237-1	Iran	indx	indx	T	Y	Y
IRIS_313-10554	IRGC 127235	BONG SEN::IRGC 7011-1	Viet Nam	indx	ind3			
IRIS_313-11757	IRGC 131972	BORIZINA 640::IRGC 68382-1	Madagascar	ind3.2.1	ind3		Y	Y
IRIS_313-10340	IRGC 127040	BR 4973-34-6-6::IRGC 117317-1	Bangladesh	indx	indx			
IRIS_313-10325	IRGC 125956	CAMPONI::IRGC 116963-1	Surinam	indx	indx		Y	Y
IRIS_313-10260	IRGC 125957	CEA 3::IRGC 116965-1	Paraguay	indx	indx		Y	Y
IRIS_313-12187	IRGC 127255	CHAM LEK::IRGC 89387-1	Lao People's Democratic Republic	ind3.2.2	indx			Y
IRIS_313-10046	IRGC 125958	CHAMA (DWARF)::IRGC 69487-1	Zambia	indx	ind1B	T	Y	Y
IRIS_313-11714	IRGC 127256	CHAMPION::IRGC 66327-1	Guyana	indx	indx		Y	Y

IRIS_313-9917	IRGC 125699	CHANDINA::IRGC 36420-1	Sri Lanka	indx	ind1B	T	Y	Y
IRIS_313-12329	IRGC 128258	CHAO DO::IRGC 106666-1	Lao People's Democratic Republic	indx	indx	T	Y	Y
IRIS_313-12188	IRGC 127260	CHAO DO::IRGC 89430-1	Lao People's Democratic Republic	ind3.2.1	ind3		Y	Y
IRIS_313-11513	IRGC 127269	CHATO::IRGC 55825-1	Ecuador	ind1.2.2	ind1B		Y	Y
IRIS_313-12005	IRGC 132395	CHE MAH::IRGC 79480-1	Malaysia	ind3.1	ind3	T	Y	Y
IRIS_313-11692	IRGC 127273	CHIAYI WU-K'O::IRGC 64974-1	Taiwan	ind1.1	ind1A	T	Y	Y
IRIS_313-11693	IRGC 127278	CHING CH'UNG::IRGC 65002-1	Taiwan	ind3.2.2	indx	T	Y	Y
IRIS_313-11694	IRGC 127279	CHING LIU::IRGC 65018-1	Taiwan	ind3.2.2	indx	T	Y	Y
IRIS_313-9822	IRGC 125716	CRILLO LA FRIA::IRGC 10793-1	Venezuela	ind1.1	ind1A	P	Y	Y
IRIS_313-10300	IRGC 125960	CT 9506-18-7-1T-2::IRGC 116973-1	Colombia	indx	indx	I	Y	Y
IRIS_313-10352	IRGC 120922	CT 9737-6-1-1-2-2P-M::IRGC 117330-1	Colombia	indx	indx		Y	Y
IRIS_313-10263	IRGC 125961	CUYAMEL 3820::IRGC 116975-1	Mexico	indx	indx	I	Y	Y
IRIS_313-10177	IRGC 125719	DA GANG ZHAN::IRGC 67103-1	China	ind3.2.2	indx		Y	Y
IRIS_313-8514	IRGC 126196	DAA MANSA::IRGC 67559-1	Ghana	ind1.2.2	ind1B	T	Y	Y
IRIS_313-10103	IRGC 125721	DALSUNG 41::IRGC 79385-1	Korea, Republic of	indx	indx	P	Y	Y
IRIS_313-12151	IRGC 132279	DAMNOEUB KRACHAK SESS::IRGC 87380-1	Cambodia	ind3.2.1	ind3	T	Y	Y
IRIS_313-11177	IRGC 127309	DELI POCONG::IRGC 35265-1	Indonesia	ind3.1	indx	T	Y	Y
IRIS_313-11525	IRGC 127319	DIAMBARANG::IRGC 56726-1	Guinea-Bissau	ind3.2.1	ind3	T	Y	Y
IRIS_313-11196	IRGC 132333	DICULA::IRGC 36729-2	Philippines	ind3.2.2	ind3	T	Y	Y
IRIS_313-12325	IRGC 127321	DISSI::IRGC 101346-1	Cameroon	ind2.1	ind2	P	Y	Y
IRIS_313-11723	IRGC 127320	DISSIGBE::IRGC 66916-1	Guinea	ind2.1	ind2	T	Y	Y
IRIS_313-12334	IRGC 127334	DO KHAW::IRGC 106977-1	Lao People's Democratic Republic	ind3.2.1	ind3	T	Y	Y
IRIS_313-10544	IRGC 127340	DONGREM::IRGC 6688-1	India	ind2.2	ind2		Y	Y
IRIS_313-9533	IRGC 125729	DUD KUNING::IRGC 44-1	Indonesia	ind3.2.1	ind3		Y	Y
IRIS_313-10972	IRGC 128033	DUDA MONOR::IRGC 26335-2	Bangladesh	indx	ind2	T	Y	Y
IRIS_313-10984	IRGC 128034	DUDHSAR::IRGC 26609-2	Bangladesh	ind2.1	ind2	T	Y	Y
IRIS_313-8631	IRGC 125608	DUDRE::IRGC 52523-1	India	ind2.2	ind2		Y	Y
IRIS_313-9482	IRGC 125730	E 2024::IRGC 67958-1	China	ind1.2.1	ind1B		Y	Y
IRIS_313-10655	IRGC 128285	EA HOUM::IRGC 11783-1	Lao People's Democratic Republic	indx	indx		Y	Y
IRIS_313-10293	IRGC 125962	ECIA 24-107-1::IRGC 116978-1	Cuba	ind1.2.2	ind1B		Y	Y
IRIS_313-12286	IRGC 128038	EKAYIN SAW::IRGC 97468-2	Myanmar	ind3.2.1	ind3	T	Y	Y
IRIS_313-11912	IRGC 127361	ESCONDE CACHO::IRGC 74305-1	Brazil	ind3.1	ind3		Y	Y
IRIS_313-12016		EX AUBERGE::IRGC 79898-1	Egypt	ind3.2.2	indx	T	Y	Y
IRIS_313-10109	IRGC 125735	EX EBOKOZURU::IRGC 79912-1	Nigeria	ind3.1	ind3	T	Y	Y
IRIS_313-10113	IRGC 125736	EX FOILAEIN (NAPUTO)::IRGC 81675-1	Mozambique	indx	indx		Y	Y
IRIS_313-10047	IRGC 125737	EX MARABA GURUKU::IRGC 69582-1	Nigeria	ind1.1	ind1A	T	Y	Y
IRIS_313-12017	IRGC 127364	EX SANDEMA::IRGC 79964-1	Ghana	ind3.2.2	indx	T		Y
IRIS_313-10114	IRGC 125739	FACAGRO 64::IRGC 82059-1	Burundi	ind2.2	ind2	I	Y	Y

IRIS_313-15896	IRGC 126957	FEDEARROZ 50::G1	Colombia	ind1.2.1	ind1B		Y	Y
IRIS_313-11551		FELEGBASEH::IRGC 58443-1	Sierra Leone	indx	ind3	T	Y	Y
IRIS_313-11758	IRGC 131987	FOFFI::IRGC 68438-1	Cote d'Ivoire	ind2.1	ind2		Y	Y
IRIS_313-10768	IRGC 132423	GADABUNG (GUNDIL)::IRGC 17569-2	Indonesia	ind3.1	ind3	T	Y	Y
IRIS_313-10769	IRGC 127375	GAJA BARU::IRGC 17586-1	Indonesia	indx	indx	T	Y	Y
IRIS_313-11573	IRGC 127379	GAO LIANG ZAO::IRGC 59563-1	China	indx	indx		Y	Y
IRIS_313-9817	IRGC 121342	GEANT W 7::IRGC 9620-1	Netherlands	indx	ind2	P	Y	Y
IRIS_313-8212	IRGC 122060	GIZA 178::GERVEX 1681-C1	Egypt	indx	indx		Y	Y
IRIS_313-11388	IRGC 132250	GLAM::IRGC 47978-2	Thailand	ind3.2.1	ind3	T	Y	Y
IRIS_313-10985	IRGC 132424	GOBOL SAIL (BALAM)::IRGC 26624-2	Bangladesh	ind2.1	ind2	T	Y	Y
IRIS_313-10772	IRGC 127388	GOJOT::IRGC 17669-1	Indonesia	ind3.1	ind3	T	Y	Y
IRIS_313-7681	IRGC 122076	H 15-23-DA::C1	Mali	indx	indx		Y	Y
IRIS_313-10614	IRGC 128049	HAM MOON::IRGC 9135-2	Hong Kong	ind3.2.2	indx		Y	Y
IRIS_313-9795	IRGC 125759	HD 10::IRGC 6638-1	Australia	indx	ind2	P	Y	Y
IRIS_313-10774	IRGC 127404	HEGAR MANAH::IRGC 17733-1	Indonesia	indx	indx	T	Y	Y
IRIS_313-10824	IRGC 128053	HOING CANTEL::IRGC 19282-2	Indonesia	ind3.1	ind3	T	Y	Y
IRIS_313-10966	IRGC 127424	HURANG ARISO LUTA::IRGC 26055-1	Brazil	ind3.2.2	indx			Y
IRIS_313-10271	IRGC 125966	IA CUBA 17::IRGC 116990-1	Cuba	indx	indx		Y	Y
IRIS_313-11914	IRGC 132252	IB 11::IRGC 74420-2	Burundi	indx	ind2	T	Y	Y
IRIS_313-10275	IRGC 125968	ICTA MOTAGUA::IRGC 116995-1	Guatemala	indx	indx	I	Y	Y
IRIS_313-10968	IRGC 127428	IH PEN SHIM MING::IRGC 26067-1	Brazil	ind1.1	ind1A		Y	Y
IRIS_313-10775	IRGC 128056	INDEL::IRGC 17748-2	Indonesia	indx	indx	T	Y	Y
IRIS_313-10314	IRGC 125969	INIAP 10::IRGC 117000-1	Ecuador	indx	indx	I	Y	Y
IRIS_313-10307	IRGC 127050	INIAP 6::IRGC 117002-1	Ecuador	indx	indx		Y	Y
IRIS_313-11122	IRGC 128059	IR 1813-694-2::IRGC 32656-2	Philippines	indx	ind1B	P		
IRIS_313-10397	IRGC 120991	IRGA 318-11-6-9-2B::IRGC 117339-1	Colombia	indx	ind1B		Y	Y
IRIS_313-10399	IRGC 120992	IRGA 346-111-2-1F::IRGC 117341-1	Colombia	ind3.1	indx		Y	Y
IRIS_313-11930	IRGC 127444	ITA 117::IRGC 75235-1	Nigeria	indx	ind1B	P		
IRIS_313-11576	IRGC 127459	JIANG HUI DAO::IRGC 59688-1	China	ind3.2.2	indx		Y	Y
IRIS_313-10279	IRGC 126066	JUMA 62::IRGC 117011-1	Dominican Republic	indx	indx		Y	Y
IRIS_313-10654	IRGC 128335	KA SAEN::IRGC 11642-1	Lao People's Democratic Republic	ind3.2.1	ind3	P	Y	Y
IRIS_313-11131	IRGC 132254	KALAI::IRGC 33151-2	Myanmar	indx	indx	P		
IRIS_313-11939	IRGC 127484	KAMPTI::IRGC 75626-1	Burkina Faso	ind3.2.1	ind3	T	Y	Y
IRIS_313-9461	IRGC 125795	KARANTABA 1::IRGC 15924-1	Senegal	indx	ind3		Y	Y
IRIS_313-11779	IRGC 127500	KATUMANI::IRGC 69695-1	Tanzania	ind3.2.1	ind3	T	Y	Y
IRIS_313-12287	IRGC 127501	KAUK HNYINGWA::IRGC 97487-1	Myanmar	ind3.2.1	ind3	T		
IRIS_313-11205	IRGC 128075	KAZALSAIL::IRGC 37161-2	Bangladesh	ind2.1	ind2	T		
IRIS_313-8559	IRGC 125615	KEERIPALA CHILL PADDY::IRGC 49790-1	India	ind2.2	ind2			
IRIS_313-9329	IRGC 131941	KERITING TINGGI::IRGC 19972-1	Indonesia	ind3.1	ind3	T	Y	Y
IRIS_313-9590	IRGC 125799	KETAN SERANG::IRGC 14615-1	Indonesia	indx	ind3	T	Y	Y
IRIS_313-11780	IRGC 127524	KILOMBERO::IRGC 69698-1	Tanzania	ind3.2.1	ind3	T	Y	Y

IRIS_313-11098	IRGC 134993	KOLUBA::IRGC 30463-3	Sierra Leone	ind3.1	ind3		Y	Y
IRIS_313-11039	IRGC 128093	KWANG LU AI 4::IRGC 28480-2	China	ind1.1	ind1A	P	Y	Y
IRIS_313-10010	IRGC 125818	LALKA (LAL DHAN)::IRGC 64946-1	Fiji	indx	ind2	T	Y	Y
IRIS_313-11577	IRGC 127551	LANG QIAN CHE::IRGC 59730-1	China	indx	ind1A		Y	Y
IRIS_313-8568	IRGC 125619	LARHA MUGAD::IRGC 52339-1	India	ind2.2	ind2	T	Y	Y
IRIS_313-9791	IRGC 125821	LEAD::IRGC 5805-1	Malawi	indx	indx		Y	Y
IRIS_313-9342	IRGC 126236	LUA CHAN HUONG::IRGC 16800-1	Viet Nam	ind3.2.1	ind3	T		
IRIS_313-10748	IRGC 127578	LUA DUC::IRGC 16718-1	Viet Nam	ind3.2.2	indx	T	Y	Y
IRIS_313-10842	IRGC 128099	LUBUK LINGGAU::IRGC 20000-2	Indonesia	ind3.1	ind3	T	Y	Y
IRIS_313-10510	IRGC 127589	MAGSIING::IRGC 5211-1	Philippines	ind3.2.2	indx	T	Y	Y
IRIS_313-11782	IRGC 128376	MALAGASY::IRGC 69717-1	Zambia	indx	ind2	T	Y	Y
IRIS_313-11940	IRGC 127599	MALOBA (DISSI ROUGE)::IRGC 75700-1	Burkina Faso	indx	indx	T	Y	Y
IRIS_313-11977	IRGC 127601	MAMORIAKA::IRGC 77867-1	Madagascar	indx	indx	T	Y	Y
IRIS_313-11615	IRGC 132408	MANARE (PHOM)::IRGC 61437-1	Guinea	ind3.2.1	ind3	T	Y	Y
IRIS_313-12066	IRGC 127609	MARAMAY::IRGC 82628-1	Philippines	ind3.2.1	ind3	T	Y	Y
IRIS_313-10609	IRGC 127612	MATHOLUWA::IRGC 8901-1	Sri Lanka	indx	indx	T	Y	Y
IRIS_313-12082	IRGC 127614	MAVOLATSIKA::IRGC 83137-1	Madagascar	ind2.2	ind2	T	Y	Y
IRIS_313-10168	IRGC 125836	MEI FENG 9::IRGC 63735-1	China	indx	indx		Y	Y
IRIS_313-9935	IRGC 126167	MEKENZIE SMALL::IRGC 49895-1	Guyana	ind2.1	ind2		Y	Y
IRIS_313-11760	IRGC 127623	MENAHARA 505::IRGC 68709-1	Madagascar	indx	ind2		Y	Y
IRIS_313-8215	IRGC 122168	MERLE::GERVEX 1685-C1	France	indx	indx		Y	Y
IRIS_313-11339	IRGC 128109	MILAGROSA::IRGC 44634-2	Philippines	ind2.1	ind2	T	Y	Y
IRIS_313-10040	IRGC 125840	MILYANG 77::IRGC 69340-1	Korea, Republic of	ind1.2.2	ind1B	I	Y	Y
IRIS_313-10170	IRGC 125842	MIN ZAO 6::IRGC 63772-1	China	ind1.1	ind1A		Y	Y
IRIS_313-11341	IRGC 128110	MINDANAO::IRGC 44642-2	Philippines	ind3.2.1	ind3	T	Y	Y
IRIS_313-9862	IRGC 126139	MODDAI KARUPPAN::IRGC 15465-1	Sri Lanka	ind2.2	ind2	T	Y	Y
IRIS_313-11811	IRGC 127632	MOSHI::IRGC 70648-1	Kenya	indx	ind2	T	Y	Y
IRIS_313-11941	IRGC 128394	MOUI SAMBA::IRGC 75751-1	Burkina Faso	ind1.2.2	ind1B	T	Y	Y
IRIS_313-10048	IRGC 125996	MOVE (MOKOLE)::IRGC 69739-1	Benin	indx	indx	T	Y	Y
IRIS_313-9557	IRGC 125845	MULLIKURUVA::IRGC 77529-1	India	indx	ind2	T	Y	Y
IRIS_313-11889	IRGC 127639	MURGI BRINJ::IRGC 73109-1	Pakistan	indx	indx	T	Y	Y
IRIS_313-11158	IRGC 127644	NAN ERH AI 5::IRGC 34255-1	China	ind1.1	ind1A		Y	Y
IRIS_313-12354	IRGC 127649	NASAENG::IRGC 107818-1	Lao People's Democratic Republic	indx	indx	T	Y	Y
IRIS_313-11841	IRGC 127679	NIAW NARAI::IRGC 71353-1	Thailand	ind3.2.1	ind3	T	Y	Y
CX140-CX140		NIPPONBARE	Japan				Y	
IRIS_313-11762	IRGC 127682	NS 1515::IRGC 68947-1	Madagascar	ind2.1	ind2		Y	Y
IRIS_313-11761	IRGC 127683	NS 199::IRGC 68864-1	Cote d'Ivoire	ind2.2	ind2		Y	Y
IRIS_313-10628	IRGC 132361	O. SATIVA::IRGC 10164-2	India	indx	ind2	T	Y	Y
IRIS_313-8068	IRGC 122184	ORIONE::GERVEX 333-C1	Italy	indx	indx		Y	Y
IRIS_313-11764	IRGC 127697	P 41::IRGC 68987-1	Liberia	indx	ind3	I	Y	Y

IRIS_313-9402	IRGC 131944	PA FADAYA::IRGC 58524-1	Sierra Leone	indx	indx	T	Y	Y
IRIS_313-11554	IRGC 132291	PA RABICHINA::IRGC 58609-1	Sierra Leone	ind3.1	ind3	T	Y	Y
IRIS_313-11843	IRGC 132290	PAN DAWK MAHK::IRGC 71380-1	Thailand	ind3.2.1	ind3	T	Y	Y
IRIS_313-9351	IRGC 125868	PARA NELLU::IRGC 50009-1	India	ind2.2	ind2		Y	Y
IRIS_313-12135	IRGC 127726	PERUBAK LUEY::IRGC 86436-1	Malaysia	ind1.2.1	ind1B		Y	Y
IRIS_313-9623	IRGC 126001	PESAGRO 102::IRGC 78703-1	Brazil	ind1.2.1	indx		Y	Y
IRIS_313-10158	IRGC 126080	PICO NEGRO::IRGC 55849-1	Ecuador	indx	indx		Y	Y
IRIS_313-11763	IRGC 127734	PJ 110::IRGC 68981-1	Cameroon	indx	indx	I	Y	Y
IRIS_313-10234	IRGC 125873	PSBRC 50::IRGC 99706-1	Philippines	ind1.2.1	ind1B	I		
IRIS_313-11844	IRGC 127745	PUEY TAW::IRGC 71405-1	Thailand	ind3.2.1	ind3	T	Y	Y
IRIS_313-11849	IRGC 128439	PULUT SELEMYAM::IRGC 71820-1	Malaysia	indx	ind3	T	Y	Y
IRIS_313-9271	IRGC 125878	PURA BINNI::IRGC 26772-1	Bangladesh	ind2.1	ind2	T	Y	Y
IRIS_313-9898	IRGC 125880	QUERO ASSAN::IRGC 28860-1	Portugal	ind3.2.1	ind3		Y	Y
IRIS_313-11807	IRGC 127757	R 582::IRGC 70504-1	Colombia	indx	indx	P	Y	Y
IRIS_313-11808	IRGC 128444	R 762::IRGC 70531-1	Colombia	indx	indx	P	Y	Y
IRIS_313-8614	IRGC 126264	RAJHUSAI (ACR 12)::IRGC 53630-1	India	ind2.1	ind2		Y	Y
IRIS_313-10147		RD 19::IRGC 39174-1	Thailand	ind3.2.1	ind3	I		
IRIS_313-10034	IRGC 125886	RIZ INDETERMINE::IRGC 69014-1	Niger	ind3.2.2	indx		Y	Y
IRIS_313-11178	IRGC 128152	RUJAK DANAN::IRGC 35446-2	Indonesia	ind3.1	ind3	T	Y	Y
IRIS_313-12251	IRGC 127772	RUS RUSSEI::IRGC 94341-1	Cambodia	ind3.2.1	ind3			
IRIS_313-11162	IRGC 127775	SABRAN::IRGC 34630-1	Indonesia	ind1.2.1	ind1B	T	Y	Y
IRIS_313-9325	IRGC 125894	SADA RUPA::IRGC 77299-1	Bangladesh	indx	ind1B	T	Y	Y
IRIS_313-8737	IRGC 126270	SADAJIRA 19-287::IRGC 38320-1	Bangladesh	ind2.1	ind2	P		
IRIS_313-12308	IRGC 127782	SAM SI::IRGC 99020-1	Lao People's Democratic Republic	ind3.2.1	ind3	T	Y	Y
IRIS_313-10661	IRGC 127781	SAMBA::IRGC 11993-1	Sri Lanka	ind2.2	ind2	T	Y	Y
IRIS_313-11344	IRGC 128157	SAMON::IRGC 44735-2	Philippines	indx	ind3	T	Y	Y
IRIS_313-11953	IRGC 127783	SAN BAO GU::IRGC 76732-1	China	ind1.1	ind1A		Y	Y
IRIS_313-12309	IRGC 127785	SANPATONG NYAY::IRGC 99050-1	Lao People's Democratic Republic	ind3.2.1	ind3	T	Y	Y
IRIS_313-11568	IRGC 127789	SATHIYA::IRGC 59225-1	Nepal	ind1.1	ind1A	T	Y	Y
		SHIOKARI	Japan					
IRIS_313-11547		SHWE SABA::IRGC 58206-1	Myanmar	indx	indx			
IRIS_313-10285	IRGC 121119	SICAN::IRGC 117029-1	Peru	indx	indx		Y	Y
IRIS_313-9867	IRGC 126088	SIGARDIS::IRGC 15555-1	Sri Lanka	indx	ind1B	T	Y	Y
IRIS_313-9944	IRGC 126312	SOLOMON RED RICE::IRGC 50950-1	Solomon Islands	indx	indx		Y	Y
IRIS_313-10573	IRGC 128168	SOSSOKA OULE::IRGC 7850-2	Mali	ind2.1	ind2		Y	Y
IRIS_313-10640	IRGC 128169	SR 26 B::IRGC 10803-2	India	ind2.1	ind2	P	Y	Y
IRIS_313-12143	IRGC 132300	SRAU KHGNAERNG::IRGC 87073-1	Cambodia	ind3.2.1	ind3	T	Y	Y
IRIS_313-11088	IRGC 128170	SRAU KHSAI::IRGC 29896-2	Cambodia	ind3.2.1	ind3		Y	Y
IRIS_313-8996	IRGC 126169	SRAU SENG::IRGC 30290-1	Viet Nam	ind3.2.1	ind3	T	Y	Y
IRIS_313-11089	IRGC 127824	SRAU THMOR::IRGC 29904-1	Cambodia	indx	ind3		Y	Y

IRIS_313-10077	IRGC 125917	TAMASHIRO HIKARI::IRGC 74534-1	Japan	ind2.1	indx	T	Y	Y
IRIS_313-11989	IRGC 132416	TAMBAS JANGKOK::IRGC 78724-1	Brunei Darussalam	ind3.1	ind3	T	Y	Y
IRIS_313-11787	IRGC 127845	TANDAKAY FINGO::IRGC 69793-1	Gambia	ind2.1	ind2	T		
IRIS_313-12232	IRGC 127852	TE SAN AI 2::IRGC 93355-1	China	indx	indx		Y	Y
IRIS_313-10054	IRGC 125924	TOC 5430::IRGC 70487-1	Panama	ind1.2.1	indx	P	Y	Y
IRIS_313-10226	IRGC 125925	TONG GU HONG::IRGC 81026-1	China	ind3.2.2	indx			
IRIS_313-9926	IRGC 126162	TOURBE::IRGC 47066-1	Chad	indx	indx	T	Y	Y
IRIS_313-10750		TRANG LUA::IRGC 16781-1	Viet Nam	ind3.2.1	ind3	T	Y	Y
IRIS_313-9469	IRGC 125929	TSAO SHENG LI 1::IRGC 1309-1	China	ind1.1	ind1A	T	Y	Y
IRIS_313-11996	IRGC 127869	TUI (KIDAYAN)::IRGC 79058-1	Philippines	ind3.2.2	ind3	T	Y	Y
IRIS_313-7797	IRGC 122272	UPL RI 7::IRTP 9897-C1	Philippines	indx	indx			
IRIS_313-10823	IRGC 127880	UTRI DELI::IRGC 19182-1	Indonesia	ind3.1	ind3	T	Y	Y
IRIS_313-9317	IRGC 125933	VEN THAP::IRGC 56138-1	Viet Nam	ind3.2.2	indx	T	Y	Y
IRIS_313-11346	IRGC 132371	WAGWAG PUTI::IRGC 44804-2	Philippines	indx	ind1B	T	Y	Y
IRIS_313-11347	IRGC 127892	WAGWAG RAOIS::IRGC 44805-1	Philippines	ind3.2.2	indx	T		Y
IRIS_313-11345	IRGC 127891	WAGWAG::IRGC 44802-1	Philippines	ind3.2.2	indx	T		Y
IRIS_313-9187	IRGC 126991	WANGKOD::IRGC 71646-1	Malaysia	indx	ind2	T		
IRIS_313-9372	IRGC 125937	WI BIR SHUN::IRGC 4602-1	China	ind1.1	ind1A		Y	Y
IRIS_313-11954	IRGC 128504	XIA HONG GU::IRGC 76803-1	China	ind1.1	ind1A		Y	Y
IRIS_313-8622	IRGC 126294	XITTO::IRGC 6671-1	India	ind2.2	ind2		Y	Y
IRIS_313-10171	IRGC 125944	YA NONG ZAO 4::IRGC 63908-1	China	ind1.1	ind1A		Y	Y
IRIS_313-12138	IRGC 127896	YADU BARA::IRGC 86912-1	Bhutan	indx	indx	T	Y	Y
IRIS_313-10753	IRGC 128205	ZACATEPEC::IRGC 16901-2	United States of America	ind1.2.2	ind1B		Y	Y
IRIS_313-11453	IRGC 127916	ZINYA KOLAMBA::IRGC 52402-1	India	ind2.2	ind2	T		
IRIS_313-11528	IRGC 127917	ZO::IRGC 56914-1	Cote d'Ivoire	ind3.2.1	ind3	T	Y	Y

Table 2.19 IRRI AMF Field Experiment cultivar list*. Accession name, IRIS accession, country of origin and subpopulation (K=9, (W. Wang et al., 2018)) is denoted.*

Accession	IRIS	Country	Subpop.
CHAMA (DWARF)::IRGC 69487-1	IRIS_313-10046	Zambia	ind1B
CHING CH'UNG::IRGC 65002-1	IRIS_313-11693	Taiwan	indx
SICAN::IRGC 117029-1	IRIS_313-10285	Peru	indx
BONG SEN::IRGC 7011-1	IRIS_313-10077	Vietnam	ind3
LEAD::IRGC 5805-1	IRIS_313-9791	Malawi	indx
MODDAI KARUPPAN::IRGC 15465-1	IRIS_313-9862	Sri Lanka	ind2
PAN DAWK MAHK::IRGC 71380-1	IRIS_313-11843	Thailand	ind3
HAM MOON::IRGC 9135-2	IRIS_313-10614	Hong Kong	indx
KILOMBERO::IRGC 69698-1	IRIS_313-11780	Tanzania	ind3
MOSHI::IRGC 70648-1	IRIS_313-11811	Kenya	ind2
NIPPONBARE	CX140	Japan	temp
IR 64	CX230	Philippines	ind1B

Table 2.20 IRRI AMF Field Experiment growth calendar and fertilizer application regime. *Date of sowing, fertilizer application (50N urea topdressing) and sampling is denoted. No phosphate fertiliser was added to maintain low nutrient conditions whilst ensuring enough nitrogen was available to avoid death or yellowing of leaves in deficiency. Table obtained from the Drought Physiology Group, IRRI, who conducted the activities.*

Date	IRRI Field Experiment
27/06/2022	sow (with inoculum in inoc treatment)
02/07/2022	sow
28/07/2022	50N urea topdress
08/08/2022	sampling - roots into 10% KOH and shoots frozen in liquid N
10/08/2022	sampling - roots into 10% KOH and shoots frozen in liquid N
16/08/2022	soil sampling
25/08/2022	50N urea topdress
Nov-22	Harvest at yield

Table 2.21 DSR Field Experiment growth calendar and fertiliser application regime. *(A) DSR breeding trial code, title, planting date and irrigation method is denoted. (B) A normal regime of fertilser application as per IRRI wet season trials was added to trials. Tables were obtained from the DSR Breeding Trials Group, IRRI, who conducted the activities.*

A

Study Code	Study Title	Planting method	Direct Seeding/ Transplanting Date	Irrigation Method
DSR22WS-08	Yield trial of selected fixed lines mid-early under dry DSR	dry DSR (irrigated)	May 24, 2022	Soil is kept at field capacity. When the tensiometer reading is at -10 kPa, irrigation must be given. No stagnant water.
DSR22WS-09	Yield trial of selected fixed lines mid-early under puddled DSR	wet DSR (puddled)	May 18, 2022	Stagnant flooding
DSR22WS-11	Yield trial of selected fixed lines mid-early under drought	dry DSR (rainfed)	May 25, 2022	Irrigation is only done when the tensiometer reading is at -50 kPa.
DSR22WS-13	Yield trial of selected fixed lines mid-early under transplanted condition	transplanted	June 17, 2022	Flooded

B

WET SEASON

Fertilizer Element	Recommended Rate (kg/Ha)	Source	N-P2O5-K2O (%)	Time of Application**	Application Rate (kg/Ha)
P	30	Di-Ammonium Phosphate (DAP)	46	Basal before seeding	65.22
N*	11		18	Basal before seeding	
K	10	KCl (Muriate of Potash)	63	Basal before seeding	15.87
N	19	Urea	46	14 DAS	41.3
N	30	Urea	46	28 DAS	65.22
N	30	Urea	46	42 DAS	65.22
N	30	Urea	46	56 DAS	65.22
K	10	KCl (Muriate of Potash)	63	56 DAS	15.87

*added with P in DAP (Total N recommended rate: 120 kg/Ha)
Recommended fertilizer rates: 120:30:20 N:P2O5:K2O in kg/ha)

3 Chapter Three- Exploring blumenol accumulation during AM symbiosis in rice

3.1 Investigating blumenol as a foliar marker of AM colonisation in rice

3.1.1 Introduction

The extent of AM symbiosis development in host plants has historically been quantified using ink or trypan blue staining of fungal structures followed by microscopic inspection (Phillips & Hayman, 1970; Vierheilig et al., 1998). Since the structures that the fungus forms are relatively uniform amongst diverse plant-fungal interaction, canonical AMF structures are identified and scored in host roots (Giovannetti & Mosse, 1980). However, these protocols rely on time-consuming microscopic inspection to quantify fungal root colonisation. In addition, expression of AMF housekeeping genes are used as an indirect assessment of fungal biomass and, where available, temporal expression of host marker genes exclusively activated in AM symbiosis are used to define early and late stages of development of colonisation (Montero et al., 2018). In rice, these include early marker genes such as *AM1* and *AM3* activated prior to arbuscule development and late markers *PT11* and *AM14* activated during arbuscule formation (C. Gutjahr et al., 2008). Such detailed phenotyping of AM colonisation has uncovered complex spatiotemporal relationships and suites of genes governing AM symbiosis establishment and maintenance (Montero et al., 2018). Despite the utility, the protocol requires considerable time-investment from RNA isolation, cDNA synthesis and quantitative Reverse Transcription-PCR (qRT-PCR). Hence, neither microscopy nor gene expression-based methodologies appeared suitable for my large-scale genetic diversity screen, and an alternative procedure was sought.

Recently, a novel, non-destructive foliar metabolite marker of AM symbiosis was described (M. Wang et al., 2018). Blumenol-C glycosides show widespread root and shoot accumulation in correlation to percentage root length colonisation in multiple crop and fungal species. In addition, use of blumenol in a HTP screen in a recombinant inbred line population (RILs) of *Nicotiana attenuata* lines identified an

AM-associated gene important for root colonisation level (M. Wang et al., 2018). This suggested that analysis of AMF-indicative blumenol could be a HTP screening tool for AM phenotyping in forward genetic screens. Importantly, the blumenol-C glycosides derivatives differed between species, meaning their species-specific chemical nature must be determined before use in phenotyping of other plant species. Wang et al. characterised the AMF-indicative blumenol derivatives in multiple crop and model species including *N. attenuata, Solanum lycopersicum, Hordeum vulgare* and *Triticum aestivum* (M. Wang et al., 2018) but *Oryza sativa* (rice) had not been included. In addition, use in genetically diverse panels beyond biparental RILs in *N. attenuata* has not yet been described. Since genetic variation has previously been described for other AM-associated apocarotenoids (Yuexing Wang et al., 2020), the degree of variation in blumenol abundance observed in relation to root colonisation should first be assessed in diverse lines to define suitability as a HTP screening tool assessing AM symbiosis in diverse panels.

This study aimed to examine the suitability of the novel, foliar blumenol marker for determining the extent of AM fungal colonisation in rice roots. Firstly, the primary derivatives accumulating in foliar material over multiple time points post AMF-inoculation of wild-type plants were assessed to (a) establish the identity of the blumenol-C-glucoside derivative best correlating with AM colonisation in rice and (b) measure the correlation with abundance of fungal colonisation. In addition, success of the foliar AM marker in diverse rice cultivars, including model cv. *japonica* and panels of accessions from the diverse 3K-RG (Z. Li et al., 2014), was interrogated to further mark suitability as a HTP screening technique in subsequent large-scale genetic studies probing AM colonisation in rice.

3.1.2 Results

3.1.2.1 Are blumenol C glycosides good foliar markers of AM colonisation in rice?

To determine if foliar abundance of blumenol correlated with root AM colonisation level in rice, a time-course experiment of *Nipponbare* wild-type plants inoculated with the model AMF, *Rhizophagus irregularis* was conducted and foliar abundance of 11-carboxyblumenol C-Glc was directly compared to fungal root colonisation observed

at different time points. Root length colonisation increased over time post inoculation, with a significant difference after five wpi (Kruskal Wallis test, $p < 0.05$, Figure 3.1A). Similarly, foliar blumenol abundance increased over time post inoculation, again with a significant increase after five wpi (KW, $p < 0.05$, Figure 3.1B). No 11-carboxyblumenol C-Glc was identified in mock plants at any time point (Figure 3.1B).

Correlation was further assessed in the following blumenol C-glycoside derivatives identified in rice: 11-carboxyblumenol (m/z 403, molecular ion $[M^+H]^+$), its aglyconic precursor (m/z 241) and 11-hydroxyblumenol (m/z 389, molecular ion $[M^+H]^+$). In a linear model of blumenol accumulation against total intraradical colonisation, all derivatives showed a positive linear correlation to percentage intraradical colonisation ($R^2 > 0.47$, $p < 0.001$, Figure 3.1C-E). Correlation was evident in 11-hydroxyblumenol C-Glc, although some accumulation in mock-inoculated plants was observed ($R^2=0.58$, $p <0.001$, Figure 3.1E). 11-carboxyblumenol C-Glc was found to be the best indicator, with a strict accumulation in AMF-inoculated plants in both the glyconic derivative (m/z 403.2, molecular ion $[M^+H]^+$, $R^2=0.47$, $p = 0.001$, Figure 3.1C) and its aglyconic precursor (m/z 241, $R^2=0.48$, $p < 0.001$, Figure 3.1C). All reference to blumenol accumulation in experiments beyond this section will therefore refer to abundance of the 11-carboxyblumenol C-Glc derivative.

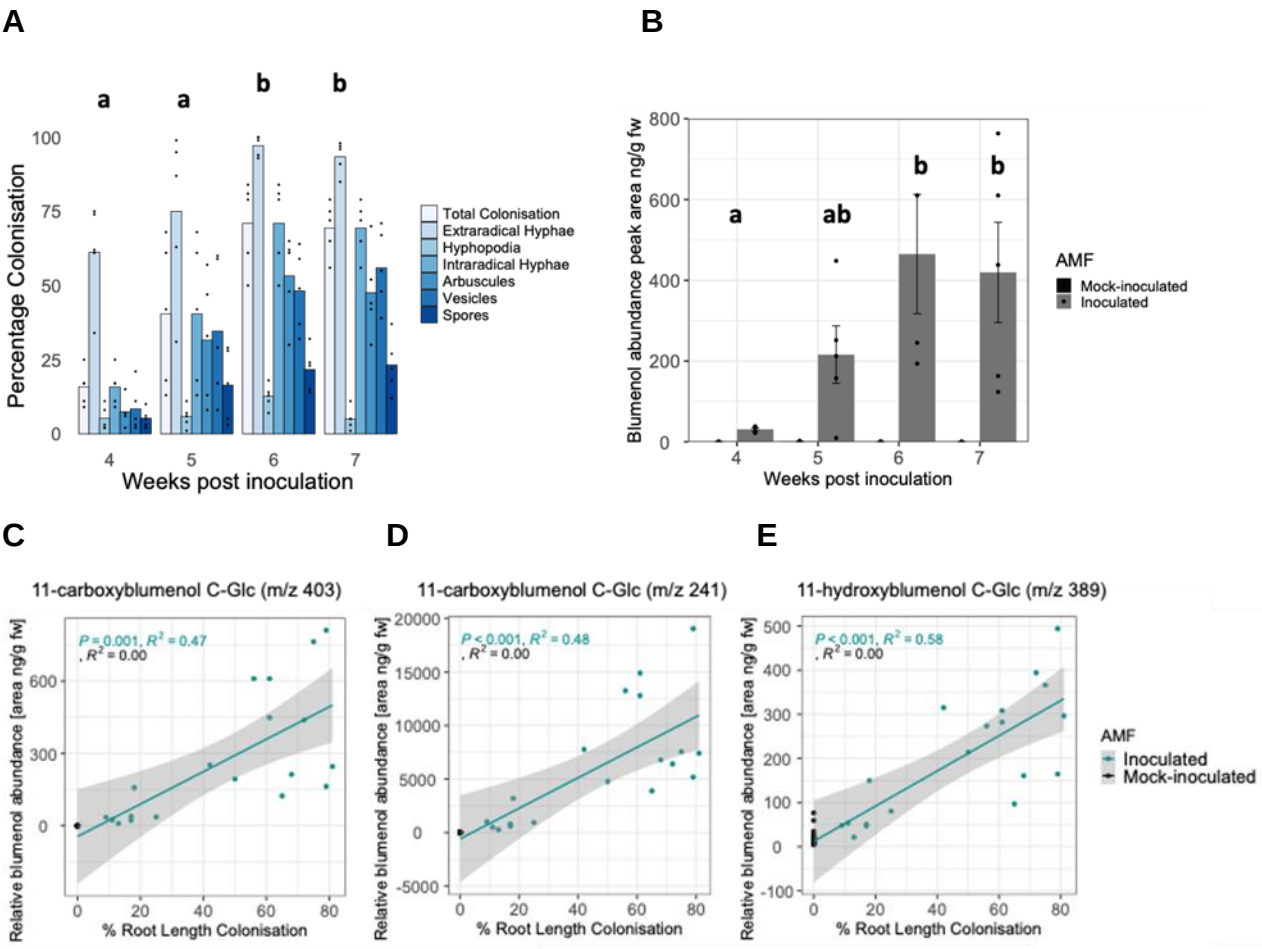

Figure 3.1.Correlation of foliar blumenol derivatives to AM colonisation in rice. *(A) Root colonization data analysed at 4, 5, 6 and 7 weeks post inoculation by microscopic analysis of the percentage of root length colonization (%RLC) and (B) relative blumenol accumulation in shoot material from the same samples. (C-E) Linear regression between abundance of % arbuscules (%A) and blumenol C-glycoside derivatives (C) 11-carboxyblumenol C-Glc (m/z 403, molecular ion $[M^{+}H]^{+}$), (D) its glyconic precursor (m/z 241) and (E) 11-hydroxyblumenol C-Glc (m/z 389, molecular ion $[M^{+}H]^{+}$). (A) Bar charts show root colonization data for Nipponbare wild-type. Percentage of Total Colonisation, Extraradical Colonisation (EH), Hyphopodia (H), Intraradical Hyphae (IH), Arbuscules (A), Vesicles (V) and Spores (S) is indicated per root length. Error bars represent mean ± standard error. Data points of 4-5 biological replicates of each genotype are shown, with 10 technical replicates used in root counting. (B) Bar charts show foliar blumenol accumulation (11-carboxyblumenol C-Glc) for the same plants. Data points of 4-5 biological replicates are shown. Black bars indicate mock-inoculated samples and grey indicate inoculated samples. Error bars represent mean ± standard error. A Kruskal-Wallis test was performed, followed by post-hoc pairwise comparison using the agricolae R package. Different letters represent significant difference (p-value <0.05) between time post inoculation. (C-E) Linear regression between abundance of % intraradical hyphae and blumenol C-glycoside derivatives (C) 11-carboxyblumenol C-Glc (m/z 403, molecular ion[M+H]+), (D) its glyconic precursor (m/z 241) and (E) 11-hydroxyblumenol (m/z 389, molecular ion [M+H]+). A linear regression model was fitted and R^2 and p-value of the regression are denoted. Black dots indicate mock-inoculated samples and teal indicate inoculated samples.*

To further determine the robustness of the correlation, inoculation gradient experiments with increasing *R. irregularis* inoculum concentrations were conducted in three model *Oryza sativa* subsp. *japonica* cultivars: *Nipponbare, Shiokari* and *Dongjin.* Notably, *Shiokari* was grown in an independent experiment and included an additional concentration of 500 spores/plant. In all model *japonica* cultivars, total intracellular colonisation increased with greater inoculum strength (KW, $p < 0.05$, Figure 3.2A). Accordingly, foliar blumenol colonisation increased with inoculum strength (KW, $p < 0.05$, Figure 3.2B). A linear model of blumenol accumulation against total intraradical colonisation confirmed that the correlation was maintained in all three model cultivars ($p < 0.001$, Figure 3.2C-E): *Dongjin* ($R^2 = 0.53$), *Nipponbare* ($R^2 = 0.59$) and *Shiokari* ($R^2=0.53$).

To further determine the maintenance of blumenol accumulation during AM colonisation progression, the correlation of blumenol to canonical AMF structures was analysed across the above-mentioned *japonica* cultivars. A significant correlation between 11-carboxyblumenol C-Glc and all AMF structures was observed. The greatest correlation was observed in intraradical structures, such as arbuscules ($R^2 = 0.57$, $p < 0.001$, Figure 3.3D), intraradical hyphae ($R^2 = 0.53$, $p < 0.001$, Figure 3.3C) and vesicles ($R^2 = 0.48$, $p < 0.001$, Figure 3.3E). In contrast, I found a weaker correlation to extracellular hyphae ($R^2 = 0.35$, $p < 0.001$, Figure 3.3A) and spores ($R^2 = 0.24$, $p < 0.001$, Figure 3.3B).

Overall, 11-carboxyblumenol C-Glc is reported as the blumenol C derivative in foliar material that robustly reflects degree of mycorrhizal intraradical colonisation in model rice cultivars.

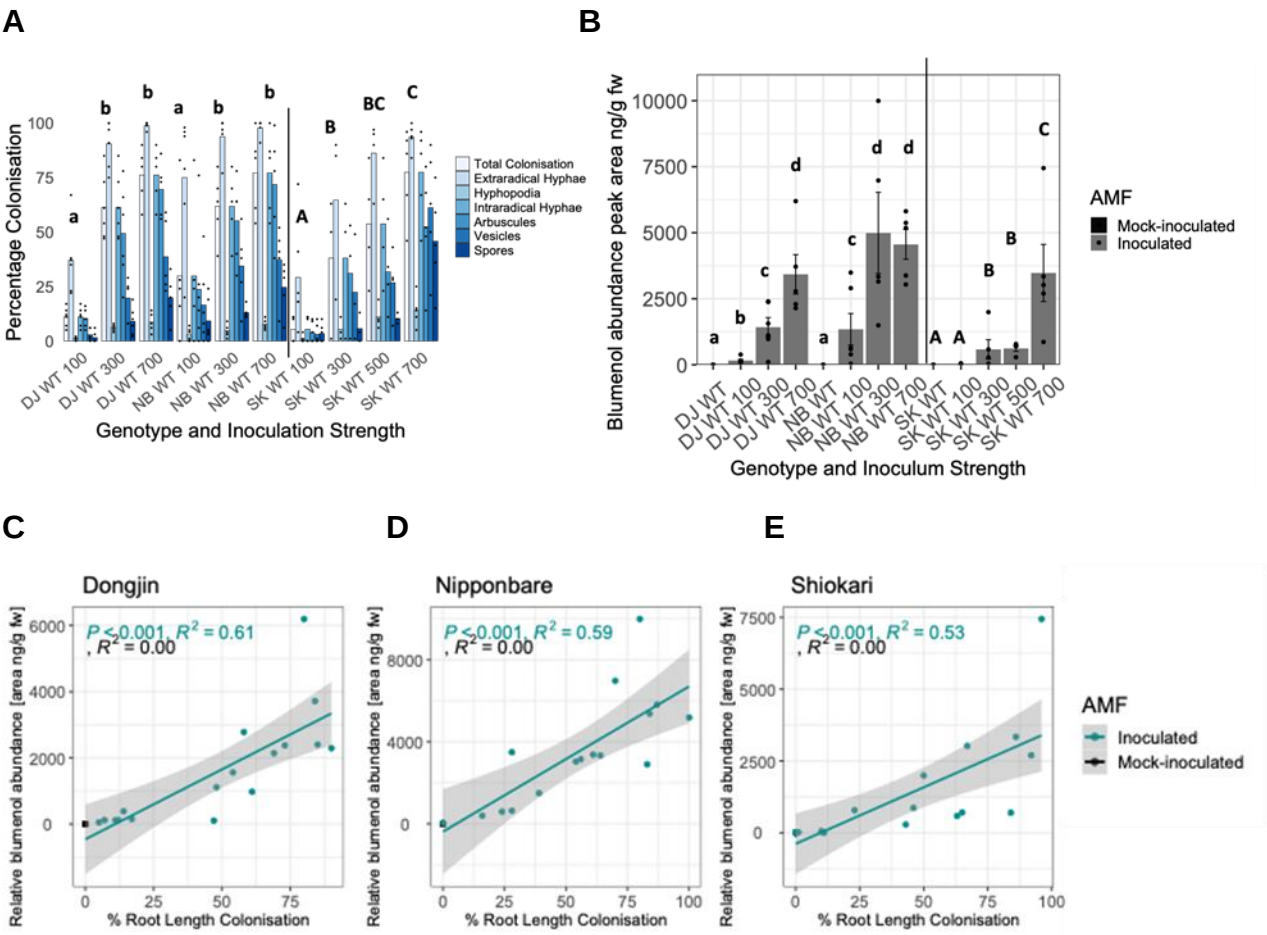

Figure 3.2. Correlation of AMF-indicative blumenol derivatives in different model cv. japonica cultivars of rice. *AM root colonization data analysed by (A) microscopic analysis of the percentage of root length colonization (%RLC) and (B) blumenol accumulation (11-carboxyblumenol C-Glc) in shoot material from the same samples. Data of separate experiments is indicated on graphs. Nippobare and Dongjin wild-type were grown in inoculum concentrations of 0, 100,300 & 700 spores per plant, analysed at 6 weeks post inoculation (wpi), Shiokari was grown in a separate experiment and additionally included 500 spores per plant, analysed at 9wpi. (A) Bar charts show root colonization data, Percentage of Total Colonisation, Extraradical Colonisation (EH), Hyphopodia (H), Intraradical Hyphae (IH), Arbuscules (A), Vesicles (V) and Spores (S) is indicated as percent total per root length. Error bars represent mean ± standard error. Data points of 4-5 biological replicates of each genotype are shown, with 10 technical replicates used in root counting. (B) Bar charts show foliar blumenol accumulation (11-carboxyblumenol C-Glc) of the same plants. Data points of 4-5 biological replicates are shown. Error bars represent mean ± standard error. A Kruskal-Wallis test was performed, followed by post-hoc pairwise comparison using the agricolae R package. Different letters represent significant difference (p-value <0.05) between genotype conditions. (C-E) Correlation analysis between % intraradical hyphae in root material and peak area of blumenol accumulation in foliar material of the same plants, inoculated with different inoculum concentrations. Correlation is noted in (C) Dongjin, (D) Nipponbare, and (E) Shiokari cultivars of rice. A linear regression model was fitted. R^2 and p value of the regression are denoted on the graph, with $p < 0.05$. Black dots indicate mock-inoculated samples and teal indicate inoculated samples.*

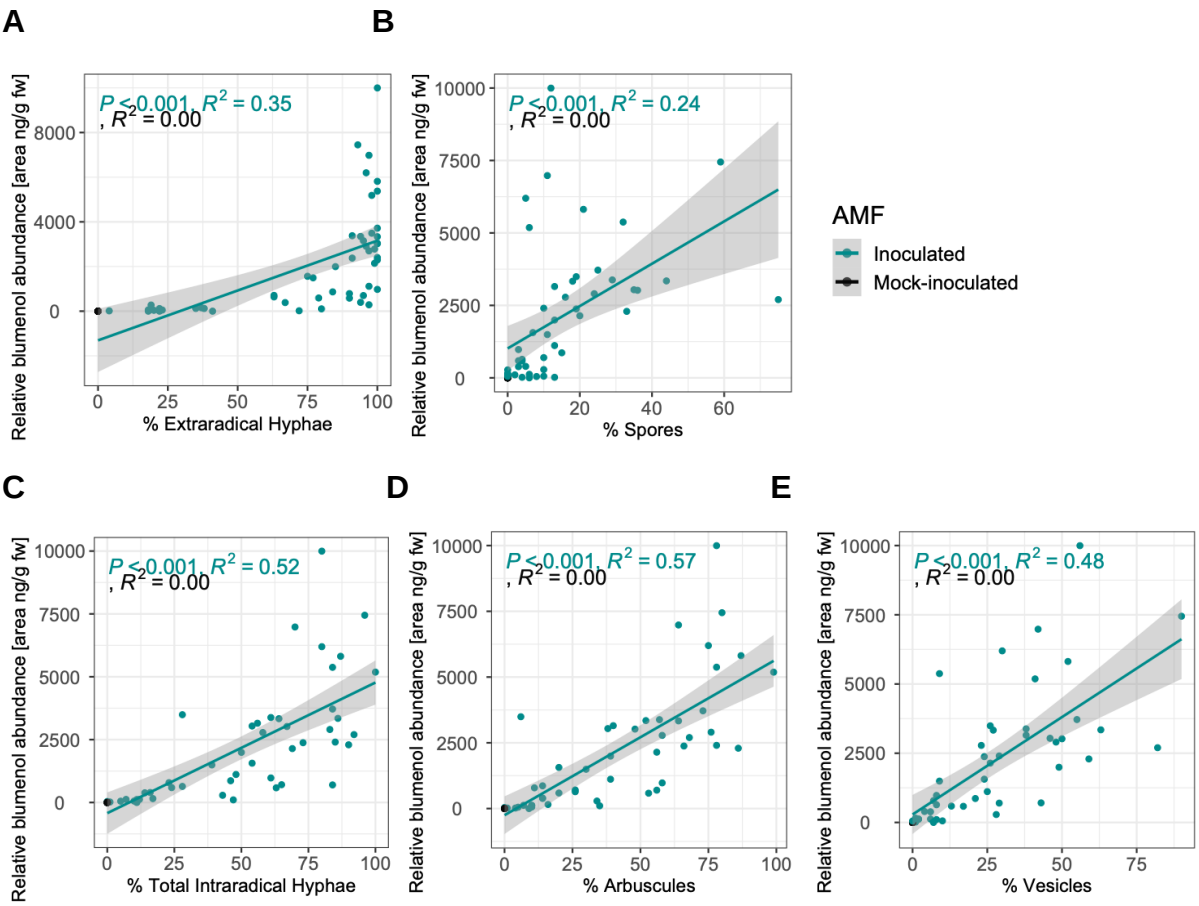

Figure 3.3. Correlation of aerial AMF-indicative blumenol derivatives to canonical AMF structures formed in host root. *Correlation analysis between foliar blumenol abundance (11-carboxyblumenol C-Glc) and root length colonisation for % (A) extraradical hyphae, (B) spores, (C) intraradical hyphae, (D) arbuscules and (E) vesicles. Data includes Nippobare and Dongjin wild-type grown in inoculum concentrations of 0,100,300 & 700 spores per plant, analysed at 6 weeks post inoculation (wpi) and Shiokari was grown in a separate experiment, which additionally includes 500 spores per plant, analysed at 9wpi. Data points of 4-5 biological replicates per genotype and inoculum concentration are included. A linear regression model was fitted.* R^2 *and p value of regression is denoted. Black dots indicate mock-inoculated samples and teal indicate inoculated samples.*

3.1.2.2 Are blumenol C glycosides good foliar AM markers in diverse rice cultivars?

To examine the use of blumenol as a foliar marker of AM colonisation in rice beyond *cv. japonica* models, the correlation was additionally assessed in genetically diverse rice accessions. Eight cultivars were selected from the diverse 3K-RG dataset (Z. Li et al., 2014) using the following criteria: variation in cultivation history, subpopulation, and country of origin (Figure 3.4C). The selected lines included diverse *O. sativa* subspecies of *indica, intermediate* and *aus/boro*, which are distinct genetic groups

(Z. Li et al., 2014). Total arbuscular AM colonisation varied significantly between the cultivars, from 46.3 ± 13.3% in *IRGC 127444* to 86.2 ± 7.5% in *IRGC 128059* (KW, $p < 0.05$, Figure 3.4A). Global mean total colonisation of all cultivars was 68.5%, calculated for relative comparisons (Figure 3.4A).

In all diverse cultivars, foliar blumenol accumulated strictly in AMF-inoculated plants (Figure 3.4B). Overall, a trend for positive correlation between foliar blumenol abundance and root colonisation was observed across the eight cultivars, but the correlation was weak and non-significant (R^2=0.05, $p = 0.168$, Figure 3.4D). Notably, comparison of blumenol and root colonisation abundance per cultivar relative to global mean identified six lines with correlative blumenol accumulation and two lines with uncoupled correlation, summarised in Figure 3.4C. Global mean foliar blumenol abundance of all cultivars was 3044.1 ng/g fw (Figure 3.4B). A positive correlation of blumenol abundance to root colonisation was observed in *IRGC 127444,* which had the lowest total root colonisation of 46.3 ± 13.3% below global mean value, and the lowest foliar blumenol abundance, additionally below the global blumenol mean. Similarly, high colonisation of 86.2 ± 7.5% and 83.7 ± 13.7%, greater than global mean, was observed in *IRGC 128059* and *IRGC 127212* respectively and foliar blumenol abundance was similarly greater than global mean. In *IRGC 128023,* both root colonisation and blumenol abundance were comparable to global means (Figure 3.4A-B).

In contrast, although *IRGC 128304* had foliar blumenol abundance above global mean, total arbuscular colonisation was comparatively lower and below global mean at 58.2 ± 4.7% (KW, $p < 0.05$, Figure 3.4A). In addition, the lowest foliar abundance of blumenol, below average, was observed in *IRGC 132361* but total root colonisation was comparatively higher and above global mean at 74.6 ± 16.9% (KW, $p < 0.05$, Figure 3.4A-B). Further regression analysis of the ‘non-correlative’ and ‘correlative’ cultivars separately confirmed such segregation, with no correlation in the two ‘non-correlative’ cultivars (R^2=0.06, p=0.507, Figure 3.4E) and a positive, significant correlation in the other six ‘correlative’ cultivars (R^2=0.20, $p = 0.013$, Figure 3.4F). Overall, in all diverse lines foliar blumenol accumulated strictly in AMF-inoculated lines and, although a positive correlation was observed, this was not

consistent across all cultivars measured. This could be due to natural variation in blumenol production and/or accumulation in the diverse cultivars.

A

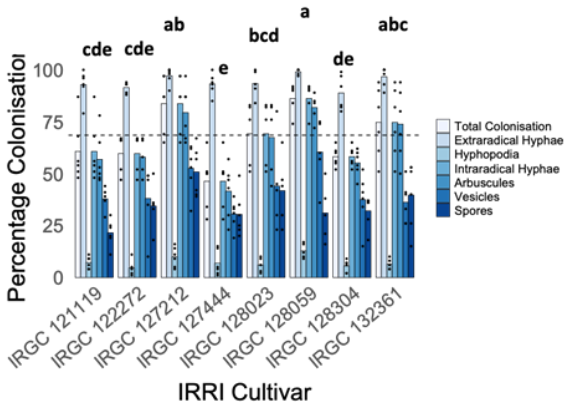

B

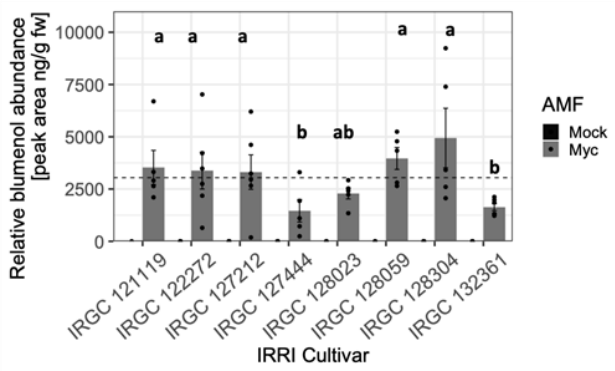

C

IRGC No.	Accession Name	Subpop.	Country	Cultivation	Correlation of blumenol to root colonisation?
IRGC 121119	SICAN::IRGC 117029-1	*Indica*	Peru	Lowland	Y
IRGC 122272	UPL RI 7::IRTP 9897-C1	*Intermed.*	Philippines	Upland	Y
IRGC 127212	BARKHE TAULI::IRGC 16116-1	*Indica*	Nepal	-	Y
IRGC 127444	ITA 117::IRGC 75235-1	*Indica*	Nigeria	Upland	Y
IRGC 128023	DADKHANI::IRGC 45454-2	*Indica*	India	Paddy	Y
IRGC 128059	IR 1813-694-2::IRGC 32656-2	*Aus/boro*	Bangladesh	Upland	Y
IRGC 128304	GUANG XUAN LIU HAO::IRGC 77341-1	*Indica*	China	Paddy	N
IRGC 132361	O. SATIVA::IRGC 10164-2	*Indica*	India	Upland	N

D **E** **F**

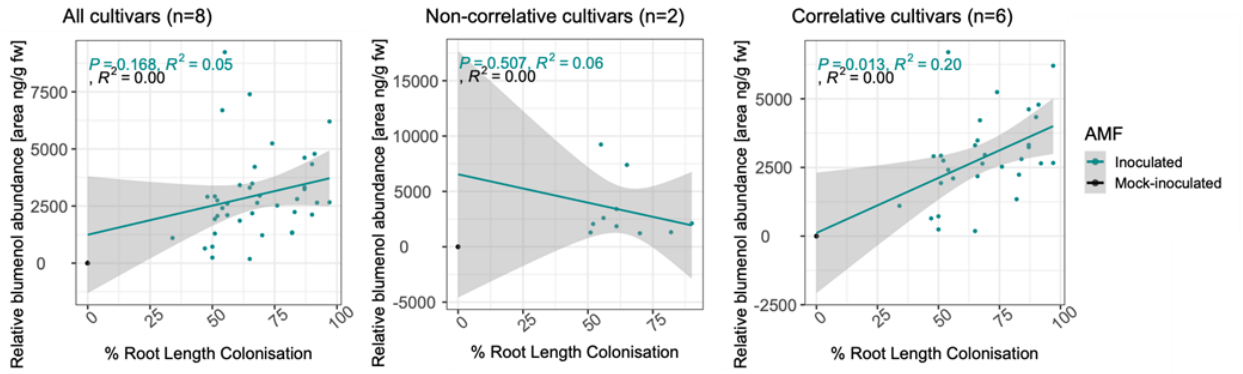

Figure 3.4. Correlation of aerial AMF-indicative blumenol derivatives in genetically diverse rice accessions from 3K-RG panel. *AM colonization data of diverse rice genotypes selected from 3K-RG analysed at 6 weeks post inoculation by (A) microscopic analysis of the percentage of root length colonization (%RLC) and (B) blumenol accumulation (11-carboxyblumenol C-Glc) in foliar material from the same samples. Genotypes are*

named by IRRI accession ID for the 3K-RG panel. (A) Bar charts show root colonization data, Percentage of Total Colonisation, Extraradical Hyphae (EH), Hyphopodia (H), Intraradical Hyphae (IH), Arbuscules (A), Vesicles (V) and Spores (S) is indicated per percent total in root length. Error bars represent mean ± standard error. Data points of 4-5 biological replicates of each genotype are shown, with 10 technical replicates used in root counting. (B) Bar charts show foliar blumenol accumulation. Data points of 4-5 biological replicates are shown. Error bars represent mean ± standard error. A Kruskal-Wallis test was performed, followed by post-hoc pairwise comparison using the agricolae R package. Different letters represent significant difference (p-value <0.05) between genotype conditions (C) Table indicates Accession Name, Cultivar, Country of Origin and Cultivation method and correlation success (blumenol compared to root colonisation relative to global mean) of accessions analysed. (D-F) Correlation analysis between (A) and (B) identifies overall correlation of AMF-indicative blumenol markers. A linear regression model was fit to (D) all data (E) non-correlating cultivars and (F) correlating cultivars. R^2 and p value of regression is denoted. Black dots indicate mock-inoculated samples and teal indicate inoculated samples.

To guide my decision about the suitability of blumenol as a foliar marker for AM fungal root colonisation, a better representation of genetically diverse rice cultivars was needed. Therefore, correlation was compared between eight additional diverse lines from the 3K-RG (Z. Li et al., 2014) and *Nipponbare* and *Shiokari* model cv. *japonica* cultivars. The eight lines were again selected according to the following criteria: diversity in country of origin, cultivation history and subpopulation (Figure 3.5C). Total arbuscular AM colonisation varied significantly between the cultivars, from 0.00 ± 0.00% in *IRGC 125958* to 55.6 ± 13.3% in *IRGC 125836* (KW, $p < 0.05$, Figure 3.5A).

Overall, a positive correlation between foliar blumenol abundance and total arbuscular colonisation, relative to model cultivars *Nipponbare* and *Shiokari* was observed for all the diverse cultivars. For example, in *IRGC 125658, IRGC 127404, IRGC 127836* and *IRGC 125842,* both root colonisation and blumenol abundance were statistically comparable to *Nipponbare* model (KW, $p < 0.05$, Figure 3.5A-B). Root colonisation in *IRGC 125958* and *IRGC 127361* was significantly lower than in model *Nipponbare*, and similarly blumenol abundance was reduced (KW, $p < 0.05$, Figure 3.5A-B). In *IRGC 127278* and *IRGC 127772,* root colonisation was decreased and increased compared to *Nipponbare* model cultivar, although not statistically significant (KW, $p > 0.05$) and blumenol abundance significantly decreased and increased respectively (KW, $p < 0.05$, Figure 3.5A-B).

Notably, comparison of linear regression of foliar blumenol abundance against root colonisation between model (n=2) and diverse cultivars (n=8) found significant positive correlation in both cases. Importantly, the correlation observed in diverse lines (R^2=0.52, $p < 0.001$, Figure 3.5D) was comparable to that observed in model *cv. japonica* lines (R^2=0.66, $p < 0.001$, Figure 3.5D).

Overall, foliar abundance of blumenol exclusively accumulated in AMF-inoculated lines in all diverse cultivars measured. A trend for positive correlation between blumenol abundance and variable degrees of mycorrhizal colonisation was observed between different model cultivars and genetically diverse rice plants, advocating for use as a HTP marker of AM colonisation in rice. Notably, variation in correlation was observed in some cultivars, and thus the potential for genetic variation in the induction of blumenol production and/or accumulation in some cases should be considered in resultant phenotypes observed in large-scale screens.

A

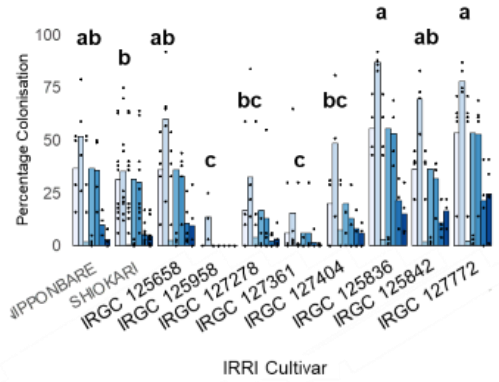

B

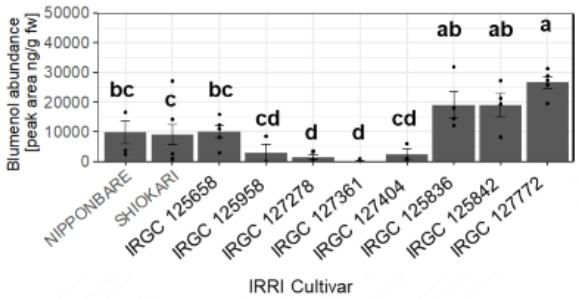

C

IRGC No.	Accession Name	Subpop.	Country	Cultivation	Correlation of blumenol to root colonisation?
Model	Nipponbare	*japonica*	Japan		Y
Model	Shiokari	*japonica*	Japan		Y
IRGC 125658	ASU::IRGC 62154-1	*indx*	Bhutan	Traditional	Y
IRGC 125958	CHAMA (DWARF)::IRGC 69487-1	*ind1B*	Zambia	Traditional	Y
IRGC 127278	CHING CH'UNG::IRGC 65002-1	*indx*	Taiwan	Traditional	Y
IRGC 127361	ESCONDE CACHO::IRGC 74305-1	*ind3*	Brazil		Y
IRGC 127404	HEGAR MANAH::IRGC 17733-1	*indx*	Indonesia	Traditional	Y
IRGC 125836	MEI FENG 9::IRGC 63735-1	*indx*	China		Y
IRGC 125842	MIN ZAO 6::IRGC 63772-1	*ind1A*	China		Y
IRGC 127772	RUS RUSSEI::IRGC 94341-1	*ind3*	Cambodia		Y

D

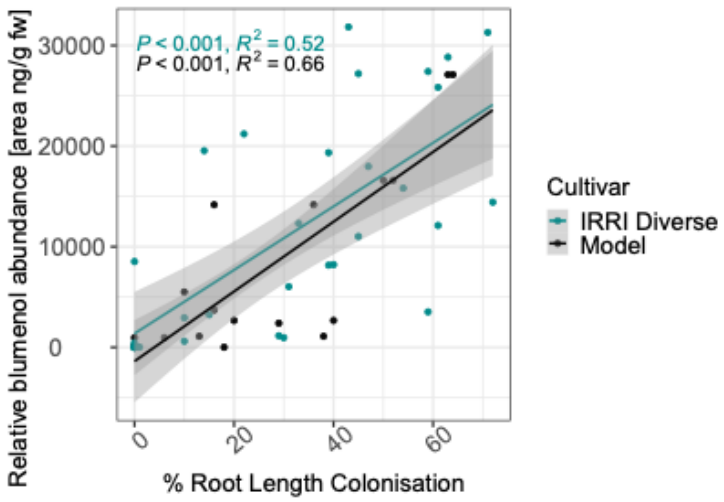

Figure 3.5 Correlation of AMF-indicative blumenol derivatives in model cultivars and genetically diverse rice accessions from 3K-RG panel. *AM colonization data of AMF-inoculated model cultivars Nipponbare and Shiokari and diverse rice genotypes selected from 3K-RG analysed at 8 weeks post inoculation by (A)*

microscopic analysis of the percentage of root length colonization (%RLC) and (B) blumenol accumulation (11-carboxyblumenol C-Glc) in foliar material from the same samples. Genotypes are named by IRRI accession ID for the 3K-RG. panel. (A) Bar charts show root colonization data, Percentage of Total Colonisation, Extraradical Hyphae (EH), Hyphopodia (H), Intraradical Hyphae (IH), Arbuscules (A), Vesicles (V) and Spores (S) is indicated per percent total in root length. Error bars represent mean ± standard error. Data points of 4-5 biological replicates of each genotype are shown, with 10 technical replicates used in root counting. (B) Bar charts show foliar blumenol accumulation. Data points of 4-5 biological replicates are shown. Error bars represent mean ± standard error. A Kruskal-Wallis test was performed, followed by post-hoc pairwise comparison using the agricolae R package. Different letters represent significant difference (p-value <0.05) between genotype conditions (C) Table indicates Accession Name, Cultivar, Country of Origin, Cultivation method and Correlation success (blumenol compared to root colonisation relative to global mean) of accessions analysed. (D) Linear regression between (A) and (B) identifies overall correlation in all cultivars. Diverse lines (n=8) are noted in teal and model (n=2) in black. R^2 and p value of regression is denoted in each case.

3.1.3 Discussion

I found that the blumenol C glucoside 11-carboxyblumenol C-Glc accumulates strictly in AMF-inoculated model and genetically diverse cultivars of rice, mirroring previous findings of AMF-indicative blumenol derivatives in *N. attenuata* (M. Wang et al., 2018). The sensitivity of such is similarly comparable, for example, a time course experiment confirmed that accumulation increased over time post inoculation with AMF in correlation to root colonisation. This corroborates previous findings in *N. attenuata,* where time lapse accumulations of blumenol were identified after three wpi and reflected increasing colonisation of root over time (M. Wang et al., 2018). In addition, foliar blumenol abundance best correlated to percentage of intraradical structures such as intracellular hyphae, arbuscules and vesicles rather than extracellular hyphae and spores. This has been found previously in other plant species, where accumulation correlated to formation of intraradical structures, such as arbuscules and vesicles (Fester et al., 2002; M. Wang et al., 2018). Whether blumenol production and/or accumulation is dependent on formation of specific stages of AM symbiosis development, fungal structures and/or associated signalling, remains to be elucidated.

In previous work, linear regression of foliar blumenol abundance against intraradical colonisation in *N. attenuata* was observed in the ranges of R^2 = 0.41-0.61 compared to percentage intraradical colonisation and R^2 = 0.67-0.89 compared to root expression of AM marker genes, dependent on AMF structure and blumenol

derivative measured (M. Wang et al., 2018). Such ranges are comparable to linear regression analyses identified in this study in model rice cultivars, which ranged from R^2 = 0.47-0.61 in comparisons with percentage intraradical colonisation, dependent on AMF structure and blumenol derivative. This further advocates for similar success as a foliar marker of root colonisation in rice as previously described for other crop and model plant species (Mindt et al., 2019; M. Wang et al., 2018).

Although reported in a population of field-grown recombinant inbred lines (RILs) in *N. attenuata* (M. Wang et al., 2018), correlation of blumenol to root colonisation has not yet been reported in diverse germplasms of other species. I found that analysis of foliar AMF-indicative blumenol abundance is an easy, HTP and minimally destructive method for interrogating AM colonisation rate in genetically diverse rice accessions. I noted a large variation in root colonisation between the diverse lines of the 3K-RG, as has been reported previously in the Rice Diversity Panel 1 (Davidson et al., 2019). In this study, an overall trend for positive correlation of blumenol abundance to such diverse root colonisation is reported. Analysis of blumenol abundance to percent intraradical root colonisation in a panel of eight diverse cultivars found correlation (R^2 = 0.52) was comparable to ranges observed in model rice cultivars (R^2=0.66) and to those observed previously in *N. attenuata* R^2 = 0.41-0.61 (M. Wang et al., 2018). Such correlation facilitated use of AMF-indicative blumenols in identifying AM-associated quantitative trait loci in RILs of *N. attenuata* (M. Wang et al., 2018), suggesting the potential for correlation within such ranges for successful use in HTP screens.

Importantly, variation in correlation was evident and less stringent in some of the diverse cultivars. Of all cultivars analysed, including 3 model and 16 diverse lines, 2 lines (11% of total) showed uncoupled correlation of blumenol accumulation to colonisation rates, which could be due to natural variation in genes required for blumenol accumulation or production. This suggests that up to 11% of values measured in HTP screens may be due to differences in blumenol induction and/or accumulation as compared to differences in root colonisation. Assessment of the suitability of blumenol for HTP screens requires placement of this degree of variation compared to variation present in use of current methods for determining root colonisation.

Notably, screening of large populations introduces potential for variation in current methods as microscopic quantification or gene expression analysis are confounded by time investment, causing limitation in sample number either by number of genotypes or number of biological replicates per genotype. Reduction in genotype number is unfavourable as it reduces power in association mapping studies (Tibbs Cortes et al., 2021). Conversely, AM symbiosis is a dynamic trait that can vary between plant biological replicates (standard deviations of ~4.7-16.9% are recorded in mean total intraradical colonisation in diverse lines with 4-5 biological replicates in this study, 3.1.2.2.) and reduction of replicate number would affect accurate estimation of mean colonisation per cultivar. Variation in measurement of root colonisation is therefore possible in use of either method for large scale screens of AM trait. Technical variation confounds current methods and potential for genetic variation confounds the blumenol method, as described in this study.

A focus on the increasing need for HTP phenotyping of AM symbiosis has resulted in application of new methods for determination of root colonisation in recent years. Pioneering work attempting to quantify AM colonisation based on pixel-based image segmentation was described in 2019. W_{IN}RHIZO software was successfully used to determine fungal coverage, but cannot determine ratio to colonised surface or distinguish canonical AMF structures (Kokkoris et al., 2019; Stoian et al., 2019). In 2021, Evangelisti et al. describe application of deep learning computational models to develop Automatic Mycorrhiza Finder (AMFinder), an automatic, user-supervised tool using computer-vision for automatic identification and quantification of canonical AMF structures in ink-stained root images. The method successfully enabled reproducible analysis of root colonisation in multiple plant hosts and captured altered colonisation in mutants with aberrant phenotypes (Evangelisti et al., 2021). Despite this, AMFinder is currently semi-automatic and requires user supervision of predictions (Evangelisti et al., 2021), meaning it is not yet applicable in larger scale analyses requiring HTP assessment. Further, the method has not yet been tested in diverse germplasms of rice. In addition, Timoneda et al. report use of betalain pigments as in vivo visual markers of AM colonisation. Using multigene vectors in which AM-responsive promoters drive expression of core betalain biosynthesis genes, betalain coloration is induced specifically in root tissues and cells hosting AM colonisation. The method, MycoRed, has clear potential for application in non-

destructive visualisation of colonisation in roots over time (Timoneda et al., 2021). Despite this, it requires transformation of the plant host with the construct and the approach has not yet been described for monocot crops such as rice (Timoneda et al., 2021). The methods are exciting new tools for quantification of AM colonisation in future studies but are not yet applicable for large scale screens of diverse germplasms of rice.

Considering such, despite variation, the potential for use of blumenols as AM-indicative markers in genetic screens is endorsed by ease and ability to screen large, diverse populations with appropriate replicate number beyond that which is currently possible with other methods. In addition, exclusive accumulation under AMF-inoculation and previous successful use in mapping to AM-associated genes (M. Wang et al., 2018) further highlights the potential for use of blumenol as an exciting tool for HTP screening of AM symbiosis in rice. Importantly, this study highlights natural variation in the correlation in diverse cultivars and HTP screens; using blumenol to probe AM colonisation should thus also consider that phenotypes observed could be due to variation in blumenol biosynthesis or accumulation. AM phenotypes in interesting lines should accordingly be complemented with visual and molecular diagnoses of root colonisation (Montero et al., 2018).

3.2 Investigating the role of AM signalling pathways and phosphate suppression in blumenol accumulation during AM symbiosis

3.2.1 Introduction

Blumenol accumulation during AM symbiosis has been reported in multiple plant species (Strack & Fester, 2006; M. Wang et al., 2018), which I confirmed for rice (Section 3.1), but the function and role of such in symbiosis development and/or functioning remains unknown. Independent reports indicate a strong correlation of foliar abundance with intraradical AMF structures such as intraradical hyphae, arbuscules and vesicles (Fester et al., 2002; M. Wang et al., 2018), as I further

described in rice (Section 3.1). In addition, previous analysis of AM signalling mutant, *ccamk* in *N. attenuata* found abolished accumulation of blumenol in AM-inoculated plants (M. Wang et al., 2018). Notably, only some aberrant intraradical hyphal colonisation is present in *ccamk* mutants; no cortical invasion or canonical intraradical structures such as arbuscules and vesicles establish (C. Gutjahr et al., 2008; Levy et al., 2004). This could suggest that blumenol accumulates according to presence of intraradical colonisation or associated signalling, which is further supported by my observations of reduced correlation to extraradical hyphae and spores (Section 3.1.2.2).

A suite of AM mutants is available in rice that allow for probing of different AM signalling pathways and canonical AMF structures for a given phenotype. Study of mutants of AM signalling genes expressed at different stages of root colonisation allows for segregation of different canonical structures produced during the AMF life cycle in the host root. For example, *CCAMK*, *POLLUX* and *CERK1* are genes that form integral parts of the CSP, the downstream signalling of which is lost in their respective mutants (Carotenuto et al., 2017; C. Gutjahr et al., 2008). The receptor-like kinase *CERK1* is required for perception of Myc-COs. Rice *cerk1* have morphologically normal AM colonisation but overall levels are reduced, representing a temporal or quantitative phenotype (Carotenuto et al., 2017; Miyata et al., 2014; X. Zhang et al., 2015). In mutant alleles of both rice CSP *ccamk-1* and *pollux-2,* hyphopodia form for initial root contact and penetration but intracellular hyphae are aberrant in structure and overall AM symbiosis is blocked at the intracellular cortical invasion stage (C. Gutjahr et al., 2008).

Downstream of the CSP, transporters required for the reciprocal exchange of nutrients and carbon are localised on the periarbuscular membrane and required for normal arbuscule formation and function (C Gutjahr et al., 2012; Yang et al., 2012; Q. Zhang et al., 2010; X. Zhang et al., 2015). For example, rice mutants of the AM-specific P_i-transporter *PT11,* have normal hyphopodia and intracellular hyphae but arbuscules are smaller and less branched than in wild type (Yang et al., 2012). Similarly, mutants of half-size ABC fatty acid transporters, *STR1* and *STR2* are deficient at the arbuscule formation stage: arbuscules appear small and stunted and function in fatty acid transport to AMF is perturbed (C Gutjahr et al., 2012).

In addition, rice mutants can further aid in elucidating the role of AM symbiosis signalling components. D14L/SMAX1 signalling facilitates AMF perception and is essential to symbiosis. Components of the pathway were elucidated in rice using mutant analysis (Choi et al., 2020; C. Gutjahr et al., 2015). In the D14L/SMAX1 pathway, binding of an unknown AM-associated ligand, KL, to the D14L receptor suppresses the negative regulator, SMAX1. This facilitates downstream signalling and expression of CSP transcription factors *CYCLOPS* and *NSP2*, which regulate the CSP and induction of SL biosynthesis to promote AM symbiosis. Suppression of SMAX1 is essential to regulation of such signalling in response to AMF, as evidenced by upregulated expression of CSP signalling and SL biosynthesis genes in *smax1* mutants, even in the absence of AMF (Choi et al., 2020; X.-R. Li et al., 2022; W. Liu, et al., 2011; van Zeijl et al., 2015). Overall, this collection of mutants allows for study of different AM stages and signalling, as summarized in Figure 3.6.

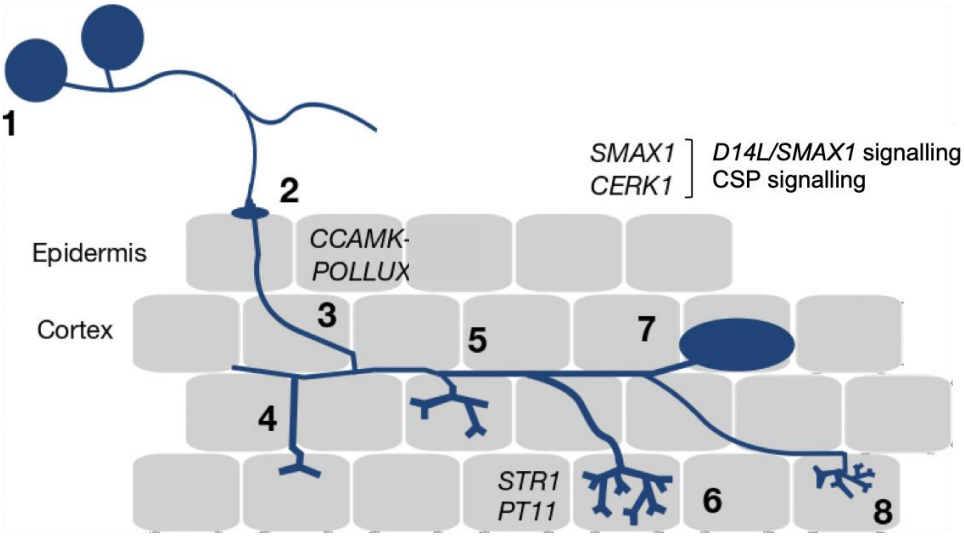

Figure 3.6 Genes noted on the diagram represent aberrant AM symbiosis at different stages of the AMF life cycle. *CCAMK-1 and POLLUX-2 are required during rhizodermal penetration, Stage 1. STR1 and PT11 are essential transport proteins required to facilitate symbiotic exchange at the arbuscule, Stages 4-6. SMAX1 and CERK1 are proteins involved in CSP and D14L/D3/SMAX1 signalling required for the regulation of AM symbiosis and the AMF life cycle.*

Notably, AMF preferentially colonise plant roots in Pi limited conditions and symbiosis is suppressed by the host if supply is otherwise abundant (Balzergue et al., 2013; Breuillin et al., 2010; S. E. Smith, 2003). Accordingly, host phosphate status is integrated into signalling pathways. In rice, the phosphate starvation

response transcription factor PHR2 is required for root colonisation and targets regulation of AM genes, such as *CERK1* and *NSP2* in CSP, AM-specific Pi-transporter *PT11* and SL and zaxinone biosynthesis genes. The D14L/SMAX1 pathway is thought to be downstream of PHR2 signalling and facilitates expression of genes regulating CSP signalling (Choi et al., 2020; Das et al., 2022; Shi et al., 2021).

Regulated production and exudation of SLs under P_i limitation is implicated in plant growth and pre-symbiotic signalling required for effective establishment of colonisation (C Gutjahr et al., 2012; Kobae et al., 2018; López-Ráez et al., 2015; López-Ráez et al., 2008). Zaxinone is additionally required for effective AM symbiosis and plant growth and the apocarotenoid negatively regulates SL biosynthesis and release under P_i-limitation (J. Y. Wang et al., 2019). Since blumenols are also apocarotenoids implicated in AM symbiosis, accumulation may also be regulated by P_i-deficiency to promote establishment of colonisation.

In this study, I made use of the above-described suite of mutants to examine functional requirement of blumenol for AM symbiosis in rice, particularly addressing the requirement for canonical AMF structures. In addition, the hypothesis that blumenol production is regulated by phosphate condition or the D14L/SMAX1 pathway, equivalent to observations in other AM-associated apocarotenoids, was tested.

3.2.2 Results

3.2.2.1 Is blumenol accumulation dependent on a particular stage of AMF life cycle?

The suite of mutants forming different canonical AMF structures, described in Figure 3.6, were interrogated to determine if blumenol accumulation during AM colonisation is dependent on a particular life cycle stage of AMF in the host root. An inoculation-gradient experiment with *R. irregularis* was used to promote different levels of colonisation in wildtype plants, allowing for comparison of relative root colonisation and blumenol levels in mutants. All mutants were inoculated with 300 spores per plant. In wild-type, root length colonisation increased from 29.8 ± 29.1% in lower

inoculum strength to 61.8 ± 15.5% and 77.2 ± 19.1% at higher concentrations (KW, $p < 0.05$, Figure 3.7B). Similarly, foliar blumenol increased at greater inoculum strengths compared to lower inoculum concentration, indicating correlation (KW, $p < 0.05$, Figure 3.7B).

As previously found in *N. attenuata ccamk* mutants (M. Wang et al., 2018), blumenol was completely abolished in *ccamk-1* and *pollux-2* CSP mutants, despite surface hyphal colonisation of 6.4 ± 5.8% and 4.0 ± 4.0% observed respectively (Figure 3.7A-B). Aberrant hyphae and hyphopodia were observed on rhizodermal cells but neither mutant formed intraradical arbuscules or vesicles, as previously published (C. Gutjahr et al., 2008). This suggests that colonisation of the root surface and outer root cell layers is not sufficient for blumenol production during symbiosis. Conversely, delayed AM colonisation of 24.8 ± 17.2% was observed in *cerk1,* which was statistically reduced compared to wild-type and equivalent to levels observed in wild type in lower inoculation strength. Similarly, blumenol abundance in *cerk1* was reduced and comparable to wild-type at lower inoculation strength, indicating correlation is maintained despite the temporal AM phenotype (KW, $p < 0.05$, Figure 3.7A-B).

In addition, a significant reduction in intraradical colonisation of 5.0 ± 7.4% was observed in AMF-inoculated *str1* fatty acid transporter mutants, which was lower than wild-type levels both at the equivalent and lower inoculum concentration (KW, $p < 0.05$, Figure 3.7A). Similarly, blumenol abundance was lower than wild-type at the equivalent and lower inoculum strength, but detected as opposed to abolished in AMF-absence (KW, $p < 0.05$, Figure 3.7B). Since *str1* mutants form stunted, un-folded arbuscule structures with loss of essential function in transport of fatty acids to AMF in reward for nutrient gain (C Gutjahr et al., 2012), I report that normal arbuscule unfolding and function are not required for blumenol accumulation.

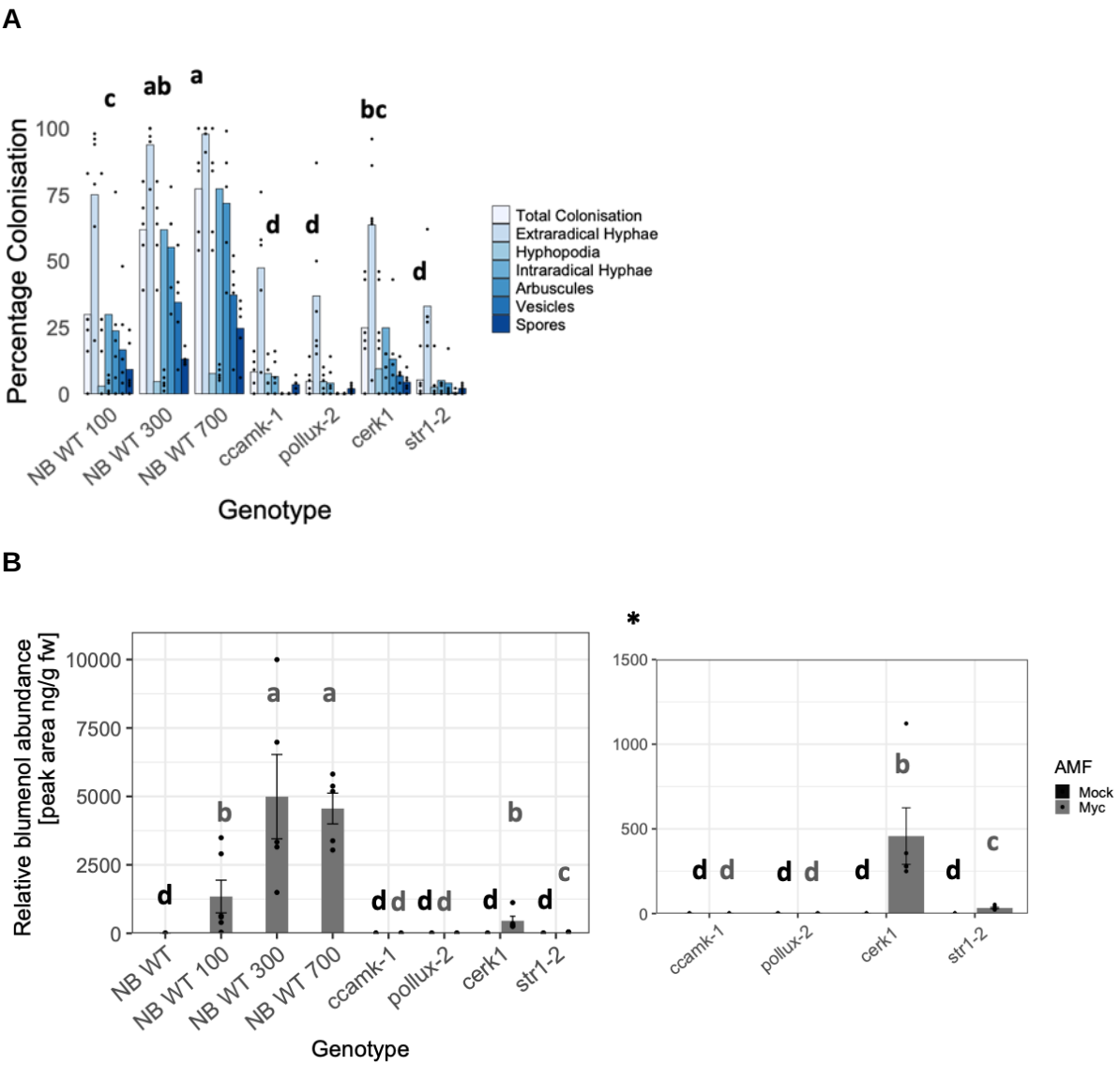

Figure 3.7 Blumenol accumulation during AM symbiosis in mutants with aberrant AMF life cycle stages. *AM root colonization data at weeks post inoculation analysed by (A) microscopic analysis of the percentage of root length colonization (%RLC) and (B) blumenol accumulation (11-carboxyblumenol C-Glc) in shoot material from the same samples. An inoculum gradient of 0 (NB WT, mock), 100, 300, and 700 spores was included for Nipponbare (NB) wild-type (WT). All mutants were inoculated with 300 spores, meaning NB WT 300 is the equivalent WT references. (A) Percentage of Total Colonisation, Extraradical Colonisation (EH), Hyphopodia (H), Intraradical Hyphae (IH), Arbuscules (A), Vesicles (V) and Spores (S) is indicated per root length. Data points of 5-6 biological replicates of each genotype are shown, with 10 technical replicates used in root counting. Error bars represent mean ± standard error. (B) Blumenol accumulation (11-carboxyblumenol C-Glc) in shoot material of the same samples. Data points of 5-6 biological replicates are shown. Black bars indicate mock- inoculated samples and grey bars indicate inoculated samples. Error bars represent mean ± standard error. * denotes zoomed in axis of genotypes with lower blumenol abundance. For comparison of mutant and WT, a Kruskal-Wallis test was performed followed by post-hoc pairwise comparison using the agricolae R package. Different letters represent significant difference (p-value <0.05), with colour indicating mock (NB WT, black) or AMF-inoculated (myc, grey) value to allow relative comparisons.*

3.2.2.2 Is blumenol accumulation dependent on D14L/D3/SMAX1 signalling pathway?

The D14L/ SMAX1 pathway was additionally interrogated using mutants of the negative regulator *SMAX1,* which exhibits increased fungal colonisation levels (Choi et al., 2020). Again, an inoculation-gradient experiment with *R. irregularis* in *Dongjin* wild-type background was used to promote different levels of colonisation, allowing for comparison of relative root colonisation and blumenol levels. In wild-type, root length colonisation increased from 11.0 ± 4.4% in lower inoculum strength to 61.3 ± 15.1% and 75.0 ± 10.2% at higher concentrations (KW, $p < 0.05$, Figure 3.8A). Similarly, foliar blumenol accumulation statistically increased as inoculum strength increased (KW, $p < 0.05$, Figure 3.8B).

Normal formation of AMF structures was observed in *smax1* and total colonisation was increased (86.4 ± 5.8%) compared to wild-type. In fact, root colonisation was statistically comparable to wild-type at highest inoculum strength (75.0 ± 10.2%) (KW, $p < 0.05$, Figure 3.8A), corroborating the published phenotype as a negative regulator of AM symbiosis (Choi et al., 2020). Notably, no blumenol accumulation was observed in AMF-absence (mock) in *smax1* (KW, $p < 0.05$, Figure 3.8B), revealing that blumenol production is not under control of the D14L/SMAX1 signalling pathway. Similarly, blumenol accumulation was increased in AMF-inoculated plants compared to wild-type and statistically equivalent to wild-type accumulation in the highest inoculum strength (KW, $p < 0.05$, Figure 3.8B), further suggesting that correlation is maintained and neither SMAX1 nor normal function of D14L/SMAX1 signalling pathway are not required for blumenol accumulation during AM symbiosis.

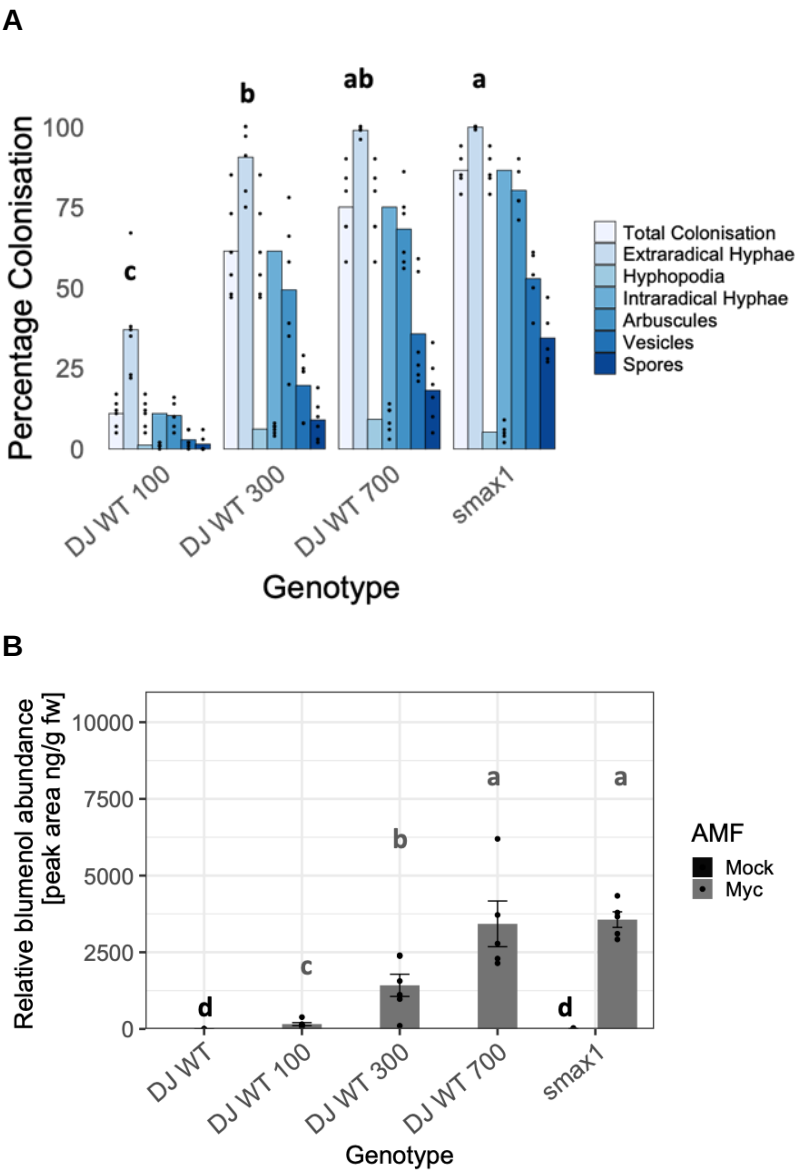

Figure 3.8 Blumenol accumulation in smax1 mutants. *AM root colonization data at six weeks post inoculation analysed by (A) microscopic analysis of the percentage of root length colonization (%RLC) and (B) blumenol accumulation (11-carboxyblumenol C-Glc) in shoot material from the same samples. An inoculum gradient of 0 (DJ WT, mock), 100, 300, and 700 spores was included for Dongjin (DJ) wild-type (WT). All mutants were inoculated with 300 spores, meaning DJ WT 300 is the equivalent WT references. (A) Percentage of Total Colonisation, Extraradical Colonisation (EH), Hyphopodia (H), Intraradical Hyphae (IH), Arbuscules (A), Vesicles (V) and Spores (S) is indicated per root length. Data points of 4-6 biological replicates of each genotype are shown, with 10 technical replicates used in root counting. Error bars represent mean ± standard error. (B) Blumenol accumulation (11-carboxyblumenol C-Glc) in shoot material of the same samples. Data points of 4-6 biological replicates are shown. Black bars indicate mock- inoculated samples and grey bars indicate inoculated samples. Error bars represent mean ± standard error. * denotes zoomed in axis of genotypes with lower blumenol abundance. For comparison of mutant and WT, a Kruskal-Wallis test was performed followed by post-hoc pairwise comparison using the agricolae R package. Different letters represent significant difference (p-value <0.05). Different letters represent significant difference (p-value <0.05), with colour indicating mock (DJ WT, black) or myc (grey) value for relative comparisons.*

3.2.2.3 Is blumenol accumulation during AM symbiosis dependent on phosphate availability?

Next, the impact of phosphate condition on foliar blumenol abundance was assessed in wild-type plants grown over time under increasing P_i fertilisation. Expression of a marker gene of phosphate starvation, *INDUCED BY PHOSPHATE STARVATION 1 (IPS1)* (X. L. Hou et al., 2005) was analysed to define the P_i status (deficiency vs proficiency) of the plant. Transcript level of *IPS1* increased with P_i limitation and was highest in plants grown in deplete conditions of $25\mu M$ P_i (KW, $p < 0.05$, Figure 3.10A). In such P_i-limited conditions, AM colonisation increased over time post inoculation, with average total root colonisation increasing from 15.8 ± 6.2% at four wpi to 69.4 ± 9.1% at seven wpi (KW, $p < 0.05$, Figure 3.9A). Suppression of AM colonisation was observed in plants grown in increasing P_i sufficiency, with total intracellular colonisation of 6.0 ± 7.6% and 1.4 ± 1.3% in $250\mu M$ and $2500\mu M$ P_i respectively at four wpi. Root colonisation increased slightly over time to 15.5 ± 5.3% and 2.8 ± 2.8% at seven wpi respectively, but never reached levels observed in P_i-limited condition (KW, $p < 0.05$, Figure 3.9A). Expression of fungal marker gene (*RiEF1a)* and early (*AM3)* and late (*AM14)* AM marker genes confirmed microscopic quantification, with greater expression in P_i-limited condition than in $250\mu M$ and $2500\mu M$ P_i (Figure 3.10B-D). The suppression of AM colonisation in high P_i conditions is well-recorded and reflects previous findings in multiple plant species (Balzergue et al., 2013; Breuillin et al., 2010; Mosse, 1973; S. E. Smith & Read, 2008).

Blumenol abundance was assessed in foliar material of the same plants. In all P_i conditions, blumenol accumulation in accordance with AM colonisation rates was observed (KW, $p < 0.05$, Figure 3.9A-B). For example, at seven wpi, total colonisation in P_i deficient, $25\mu M$ condition was 69.4 ± 9.1% and blumenol abundance corresponded to 7260.8 ± 3618.5 ng/g fw. In $250\mu M$ P_i, colonisation was reduced to 15.5 ± 5.3% and blumenol accordingly to 884.8 ± 1015.2 ng/g fw. In $2500\mu M$ P_i, colonisation was strongly reduced to 2.8 ± 2.8% and blumenol similarly to 68.9 ± 21.4 ng/g fw (Figure 3.9A&B). These data reveal that the induction of blumenol indeed occurs in response to AM fungal root colonisation and not due to elevated Pi nutrition of the plant.

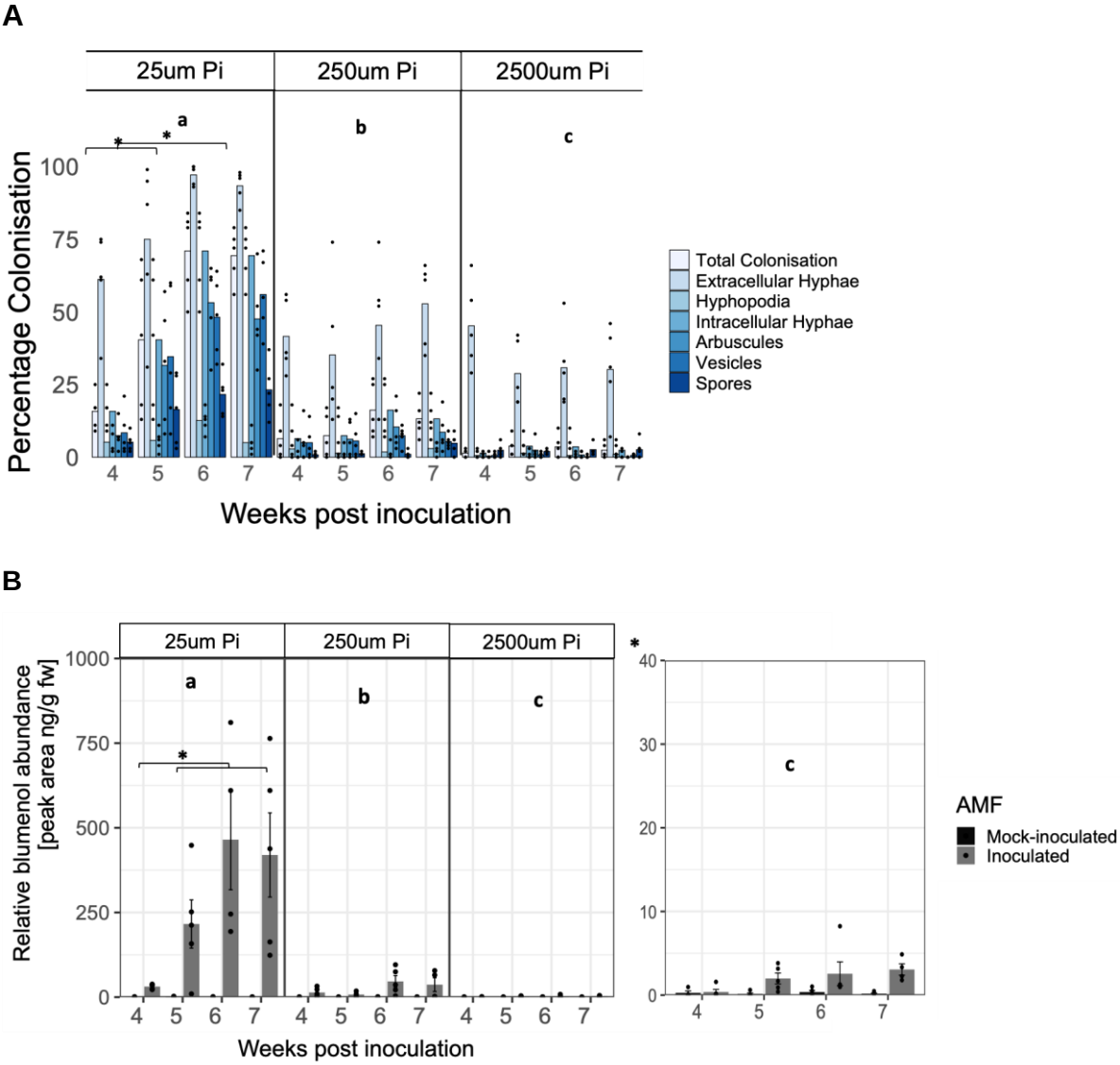

Figure 3.9. Aerial AMF-indicative blumenol derivatives correlate to % root length colonization; independent to phosphate status. *AM root colonization data analysed at 6 weeks post inoculation by (A, C) microscopic analysis of the percentage of root length colonization (%RLC) and (B) blumenol accumulation (11-carboxyblumenol C-Glc) in shoot material from the same samples. (A) Bar charts show root colonization data for Nipponbare (NB) WT grown in different phosphate conditions (25 µM, 250µM and 2500 µM Pi). Percentage of Total Colonisation, Extraradical Colonisation (EH), Hyphopodia (H), Intraradical Hyphae (IH), Arbuscules (A), Vesicles (V) and Spores (S) is indicated per root length. Error bars represent mean ± standard error. Data points of 4-5 biological replicates of each genotype are shown, with 10 technical replicates used in root counting. (B) Bar charts show foliar blumenol accumulation for Nipponbare (NB) WT grown in different phosphate conditions (25µM, 250µM and 2500µM Pi). Data points of 4-5 biological replicates are shown. Black bars indicate mock-inoculated samples and teal indicate inoculated samples. Error bars represent mean ± standard error. * denotes zoomed in axis of values at 2500 µM P_i with lower blumenol abundance A Kruskal-Wallis test was performed, followed by post-hoc pairwise comparison using the agricolae R package. Different letters represent significant difference (p-value <0.05) between condition and asterixis represent significant different (p<0.05) between time post inoculation within a given condition.*

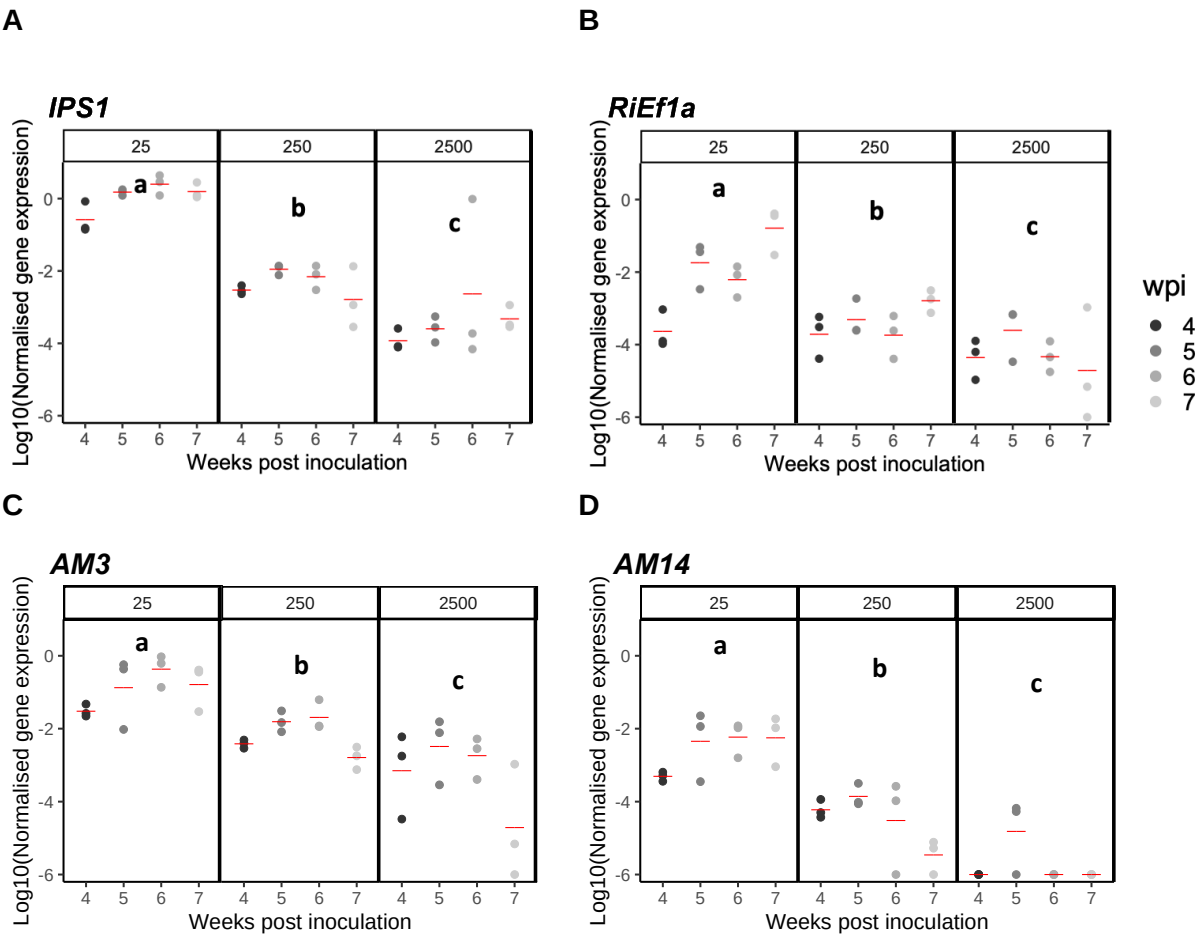

Figure 3.10. Gene expression analysis of phosphate starvation and AM marker genes. (*A-D) Gene expression data for (A) phosphate starvation marker IPS1, (b) fungal housekeeping gene RiEF1a, (C) early AM marker gene AM3 and (D) late AM marker genes AM14 in AMF-inoculated plants. Point colour corresponds to weeks post inoculation (wpi) with R. irregularis. Graphs are faceted by different phosphate conditions (25 µM, 250µM and 2500 µM Pi). Expression levels represent a GEOmean normalized to Cyclophilin housekeeping gene and were log_{10} transformed. Data points of 3 biological replicates, each with 3 technical replicates, for each time point are shown. Each dot and red bar indicate values from an individual plant and the mean value of each time point. A Kruskal-Wallis test was performed, followed by post-hoc pairwise comparison using the agricolae R package. Different letters represent significant difference (p-value <0.05) between phosphate condition.*

3.2.3 Discussion

In this study, use of rice mutants to probe blumenol accumulation at different life stages of AMF identified that colonisation of the root surface and outer root cell layers is not sufficient for blumenol production during symbiosis. Interestingly, intraradical colonisation and arbuscule presence was sufficient for blumenol accumulation. Correlation of blumenol to root colonisation was maintained in *str1,*

despite formation of stunted arbuscules (C Gutjahr et al., 2012), suggesting that blumenol production and/or accumulation occurs independently to arbuscule morphology. Notably, unlike *ccamk* and *pollux, str1* mutants retain normal arbuscule-related gene expression when inoculated with *R. irregularis*; genes such as *OsPT11* are still expressed at later time points (C. Gutjahr et al., 2008; C Gutjahr et al., 2012). Arbuscule biogenesis is associated with expression of symbiotic-specific phosphate transporters, such as *PT11* and putative lipid exporters *STR1* and *STR2* on the PAM covering the fine branches of the arbuscule (Genre et al., 2008; Kobae & Hata, 2010; Pumplin & Harrison, 2009; Roth et al., 2018). Maintenance of blumenol accumulation in *str1* suggests that normal arbuscule formation and function is not required for blumenol accumulation. Instead, I found that accumulation relies either on formation of intraradical colonisation structures and/or associated gene signalling pathways initiated by the formation of arbuscules specifically, the expression of which are lost in rice *ccamk* and *pollux* (C. Gutjahr et al., 2008; Pimprikar et al., 2016).

Such a finding validates previous reports of strong correlation of blumenol accumulation to intraradical colonisation structures such as arbuscules and vesicles (Fester et al., 2002; M. Wang et al., 2018) and further points towards a function in maintenance at later stages of AM colonisation, accumulating only after intraradical colonisation and related signalling are established. A specific requirement of arbuscule formation and subsequent signalling for blumenol biosynthesis and accumulation would corroborate data described here, but this degree of specification beyond necessity for general intraradical colonisation cannot be disentangled. Such a study would require a mutant with high hyphal colonisation but low arbuscule accumulation, which is currently not available in rice.

In addition, since no blumenol accumulated in absence of AMF in *smax1,* it is further reported that blumenol production and/or maintenance is not under regulation by the SMAX1 negative regulator during AM symbiosis (Choi et al., 2020; X.-R. Li et al., 2022). In addition, blumenol accumulation was independent to P_i fertilisation of the plant and not regulated by P_i deficiency. In other mycorrhizal-associated apocarotenoids, namely SLs and zaxinone, accumulation occurs in AMF absence and *de novo* biosynthesis and production are regulated by P_i deficiency and AMF through the phosphate starvation response network involving CSP signalling

downstream of D14L/SMAX1 signalling (Ablazov et al., 2020, 2022; Das et al., 2022; X.-R. Li et al., 2022; Votta et al., 2022; J. Y. Wang et al., 2019). Independence of blumenol to phosphate deficiency and strict accumulation in AMF presence is unlike zaxinone and SL and could suggest a functional, AM-specific role in intraradical colonisation rather than pre-symbiotic signalling or additional plant growth and development responses. As described, such roles as for instance in arbuscule maintenance, were not addressed in this study but would corroborate correlation to intraradical colonisation, independence to nutrient status and insufficiency of root surface contact in promoting accumulation.

Overall, it is reported that blumenol accumulates independently to D14L/ SMAX1 and P_i-starvation response signalling. Root surface contact is insufficient to promote accumulation, and instead abundance correlates robustly with intraradical colonisation and associated signalling. The role of blumenol during AM symbiosis remains unknown but could facilitate later stage intraradical accommodation and maintenance of AMF within host roots.

3.3 Investigating the role of SL biosynthesis and signalling genes in blumenol accumulation during AM symbiosis

3.3.1 Introduction

The current model for biosynthesis of apocarotenoids implicated in AM symbiosis, including SLs, zaxinone and blumenol, is summarized in Figure 3.11. The blumenol biosynthesis pathway has been partially elucidated. It is thought that a C_{40} carotenoid is cleaved by CCD enzymes (CCD7 and possibly CCD4), leading to a C_{27} apocarotenoid and C_{13} cyclohexenone. The C_{27} apocarotenoid is cleaved into rosafluene-dialdehyde (C_{14}), the precursor of mycorradicin, and C_{13} cyclohexenone blumenols by CCD1 (Floss et al., 2008; Ilg et al., 2014; Vogel et al., 2008). Mutant analysis has identified involvement of both CCD1 (Floss et al., 2008) and CCD7 (Vogel et al., 2010), the latter of which has an additional role in SL biosynthesis

(Alder et al., 2012; Vogel et al., 2010). Since CCD7 has specificity for *cis* isomer cleavage (Bruno et al., 2014), an isomerisation step is additionally required. It has been suggested that D27 may facilitate this, although no direct evidence has been reported (Fiorilli et al., 2019; M. Wang et al., 2018).

In addition, D3-mediated SL signalling through the D14 SL receptor regulates AM symbiosis, as SL is an important pre-symbiotic signal for stimulating effective colonisation (Yoshida et al., 2012). D3 is an F-box E3 ubiquitin ligase protein that binds D14 during SL signalling and subsequently targets D53/SMXL6/7/8 transcriptional repressors (SMXL1) for degradation (Stirnberg et al., 2007; Tal et al., 2022; Zhou et al., 2013). D3 is additionally involved in D14L-mediated repression of the AM symbiosis negative regulator SMAX1 (Choi et al., 2020; C. Gutjahr et al., 2015). Since no blumenol was observed in *smax1* in AMF absence (Section 3.1), it is suggested that the D14L/D3/SMAX1 signalling pathway is not required in blumenol production. The role of the SL signalling pathway, however, remains unknown.

This study aimed to characterise the interplay between SL and blumenol signalling and biosynthesis pathways during AM colonisation. The approach included analysis of intracellular colonisation and blumenol accumulation in mutants of *D10/CCD8, D17/CCD7, D27* genes required for SL biosynthesis and *D14* and *D3* genes required for SL signalling inoculated with *R. irregularis*. AM phenotypes have been previously reported for all mutants except *d27,* meaning this is additionally the first report of interrogation of the *β*-carotene isomerase *D27* for a role in AM symbiosis in rice.

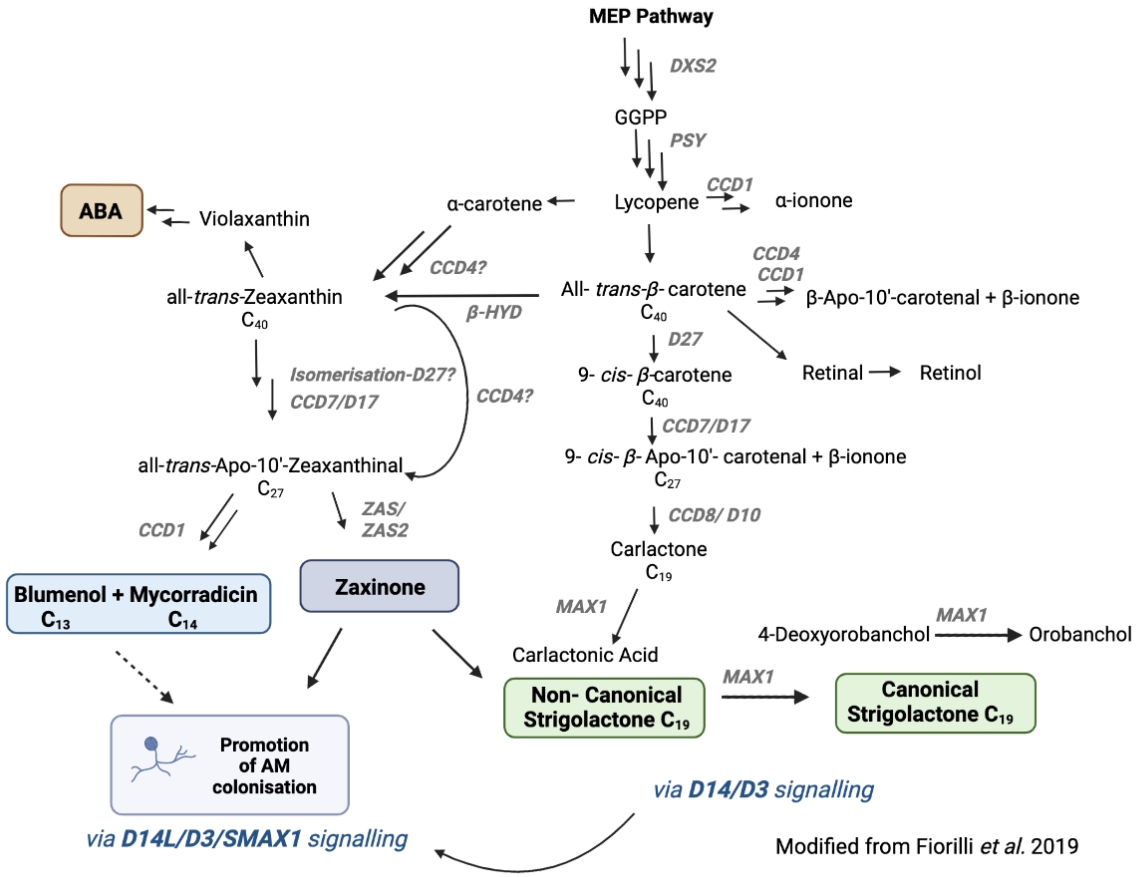

Figure 3.11 Summary of the current model of biosynthesis of AM-associated apocarotenoids, including ABA, SLs, blumenol and mycorradicin and zaxinones.

3.3.2 Results

3.3.2.1 Are SL biosynthesis and signalling genes required for blumenol accumulation during AM symbiosis?

An inoculation-gradient experiment with *R. irregularis* in *Shiokari* wild-type was used to promote different levels of colonisation, allowing for comparison between relative root colonisation and blumenol levels in SL biosynthesis and signalling mutants. In wild type, intraradical AM colonisation increased with increasing concentration from 4.2 ± 5.9% at 100 spores/plant to 77.4 ± 20.8% at 700 spores/plant (KW, $p < 0.05$, Figure 3.13A). As previously observed (Section 3.1), foliar blumenol similarly increased with greater inoculation concentrations from 15.0 ± 22.1 ng/g fw at 100 spores/plant to 3475.6 ± 2419.8 ng/g fw at 700 spores/plant (KW, $p < 0.05$, Figure 3.13B). All mutant plants were inoculated at 500 spores/plant for relative

comparisons. Total intracellular colonisation of 53.4 ± 26.5% and blumenol abundance of 619.4 ± 226.0 ng/g fw was observed in wild type inoculated with 500 spores/plant (Figure 3.13A).

Short height and tillering were observed in the SL biosynthesis mutants, *d27-1, d17-1* and *d10-1* grown to flowering stage (Figure 3.12), confirming the developmental and impaired SL production phenotypes previously reported (Arite et al., 2007; Ishikawa et al., 2005; H. Lin et al., 2009). In the colonisation experiment, *d10-1* mutants had 88.2 ± 9.2% total intraradical colonisation, which was increased compared to wild-type and statistically equivalent to wild type levels at greater inoculum strength of 700 spores/plant (KW, $p < 0.05$, Figure 3.13A). Similarly, blumenol abundance was increased compared to wild-type and statistically equivalent to wild type abundance at 700 spores/plant concentration (KW, $p < 0.05$, Figure 3.13B). D10/CCD8 is therefore likely not required for blumenol biosynthesis during AM symbiosis. In *d27-1,* total intraradical colonisation was significantly increased compared to wild-type, at 68.8 ± 18.8%, and comparable to wild type levels at 700 spores/plant concentrations (KW, $p < 0.05$, Figure 3.13A). In contrast, blumenol abundance was considerably reduced compared to wild-type and was comparable to wild type abundance at lower inoculation concentration of 100 spores/plant. The equivalent total colonisation of wild-type at this lower inoculation concentration was 6.4 ± 5.6%, which is 10-fold lower colonisation than colonisation observed in *d27-1* (KW, $p < 0.05$, Figure 3.13A-B). In *d17-1,* total intraradical colonisation was reduced compared to wild-type, with average of 40.3 ± 23.4%. This was equivalent to levels observed in wild-type both at 500 and 300 spores/plant (KW, $p < 0.05$, Figure 3.13A). In contrast, blumenol accumulation was entirely abolished (Figure 3.13B). Severely reduced and abolished blumenol abundance observed in *d27-1* and *d17-1* respectively, despite AM colonisation, could suggest a role of these genes in blumenol production and/or accumulation. Such a role for D17/CCD7 corroborates previous findings of reduced blumenol accumulation in *ccd7* mutants in tomato (Vogel et al., 2010). This is the first report of AM colonisation and blumenol abundance in D27 mutants.

In SL signalling mutants *d3-1* and *d14-1,* intraradical colonisation rates were reduced and increased compared to wild-type (KW, $p < 0.05$, Figure 3.13A), with 7.7 ± 5.1%

and 87.5 ± 15.8% relative to 53.4 ± 26.5% in the wild type, respectively. This corroborates AM colonisation phenotypes previously reported in these mutants (Choi et al., 2020; Yoshida et al., 2012). In *d3-1,* total intraradical colonisation was statistically equivalent to wild-type levels at lower inoculum strength of 100 spores/plant (KW, $p < 0.05$, Figure 3.13A). Similarly, blumenol abundance was reduced compared to wild-type and statistically equivalent to abundance observed in wild-type at 100 spores/plant (KW, $p < 0.05$, Figure 3.13B). In *d14-1,* total intraradical colonisation was statistically equivalent to levels observed in wild-type at greater inoculum strength of 700 spores/plant (KW, $p < 0.05$, Figure 3.13A). Blumenol abundance was additionally increased compared to wild-type and statistically equivalent to wild-type abundance at 700 spores/plant (KW, $p < 0.05$, Figure 3.13B). Together, this suggests that neither *D3* nor *D14* are required for blumenol accumulation during AM symbiosis. This further corroborates that normal function of the D14L/D3/SMAX1 pathway is not required for blumenol accumulation. In addition, it is reported that the SL signalling pathway is not required for accumulation of blumenol during AM symbiosis.

Figure 3.12 Growth phenotypes of SL biosynthesis mutants. *Representative image of Shiokari wild-type (SK WT) and SL biosynthesis mutants d27-1, d17- 1 and d10-1 at the reproductive stage*

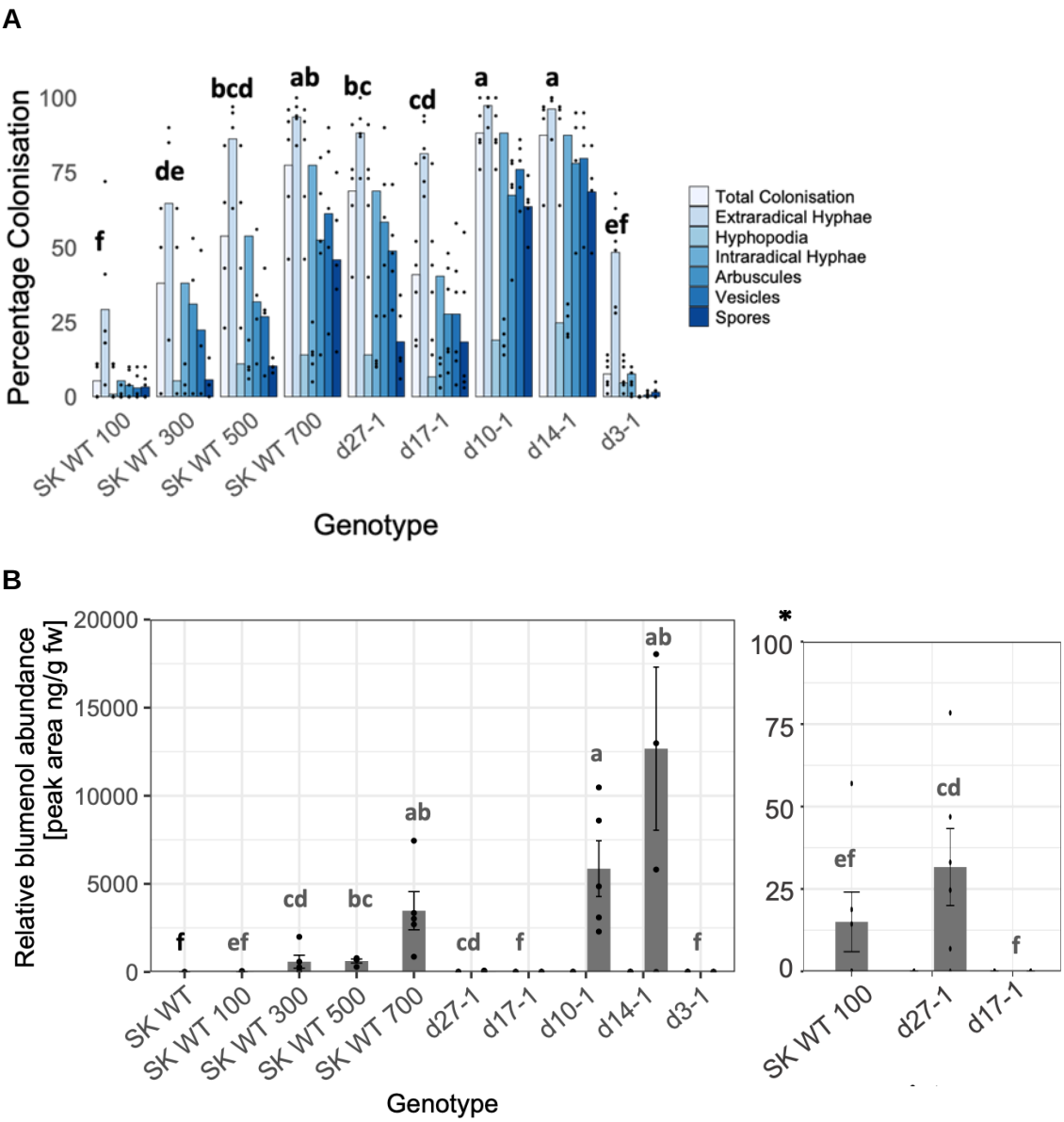

Figure 3.13. AM colonisation and blumenol accumulation during AM symbiosis in strigolactone signalling and biosynthetic genes. *(A) AM colonisation rate in Shiokari wild type (SK WT), SL biosynthesis mutants d10- 1, d17-1 and d27-1 and SL signalling mutants d14-1 and d3-1. Bar chart indicates total root length colonisation. An inoculum gradient of 0, 100, 300, 500 and 700 spores was included for SK WT (SK WT, SK WT 100, SK WT 300, SK WT 500 & SK WT 700 respectively). All mutants were inoculated with 500 spores, meaning SK WT 500 is the equivalent WT reference. Percentage of Total Colonisation, Extraradical Colonisation (EH), Hyphopodia (H), Intraradical Hyphae (IH), Arbuscules (A), Vesicles (V) and Spores (S) is indicated per root length. Data points of 4-6 biological replicates of each genotype are shown, with 10 technical replicates used in root countingError bars represent mean ± standard error. (B) Blumenol accumulation (11-carboxyblumenol C-Glc) in shoot material of the same samples. Data points of 4-6 biological replicates are shown. Black bars indicate mock- inoculated samples and grey indicate inoculated samples. Error bars represent mean ± standard error. * denotes zoomed in axis of genotypes with lower blumenol abundance. A Kruskal-Wallis test was performed, followed by post-hoc pairwise comparison using the agricolae R package. Different letters represent significant difference (p-value <0.05) and colour corresponds to mock (SK WT, black) or inoculated (grey) plants.*

3.3.2.2 Is reduction of foliar blumenol in *d27-1* and *d17-1* due to impaired biosynthesis and transport processes?

Previous work in *N. attenuata* suggested that foliar blumenol most likely originates from roots (M. Wang et al., 2018). Wang et al. (2018) found leaves of plants genetically manipulated in carotenoid biosynthesis accumulated blumenol despite lack of upstream carotenoid genes required for production. In addition, they found candidate genes for blumenol biosynthesis, such as *D27, CCD7* and *CCD1* were upregulated in roots but not leaves during AM colonization. Finally, blumenol was found in stem sap of AM-colonized plants and could be detected in shoot material of non-mycorrhizal seedlings when roots were incubated overnight in aqueous blumenol solutions, indicating the root as the site of biosynthesis and export in stem to leaves. It was therefore suggested that blumenol is produced in roots upon AMF-detection and exported to vasculature for systematic transport to foliar material (M. Wang et al., 2018).

To verify if reduced accumulation of foliar blumenol in *d27-1* and *d17-1* previously identified (Figure 3.13B) was due to reduced transport from root rather than aberrant biosynthesis, accumulation of blumenol in root material of the same plants was assessed in wild-type and SL biosynthesis mutants. The aglyconic derivative of 11-carboxyblumenol C-glc (m/z 241) was assessed for blumenol abundance measurements, due to greater root accumulation, allowing for comparison between root and shoot abundance. Notably, some blumenol accumulated to low levels in the absence of AMF in wild type root, although this was not statistically different to zero abundance observed in other genotypes in AMF-absence (KW, $p > 0.05$, Figure 3.14A). Overall root abundance of blumenol was lower than identified in foliar material (Figure 3.14B-C), as previously found in other plant species (M. Wang et al., 2018). In both root and shoot material, blumenol accumulation was severely reduced in *d27-1*, abolished in *d17-1* and increased in *d10-1* relative to wild type (KW, $p < 0.05$, Figure 3.14B-C). This suggests that impairment is not due to transport and instead D27 and D17/CCD7 are likely required for blumenol biosynthesis during AM symbiosis in the plant host root.

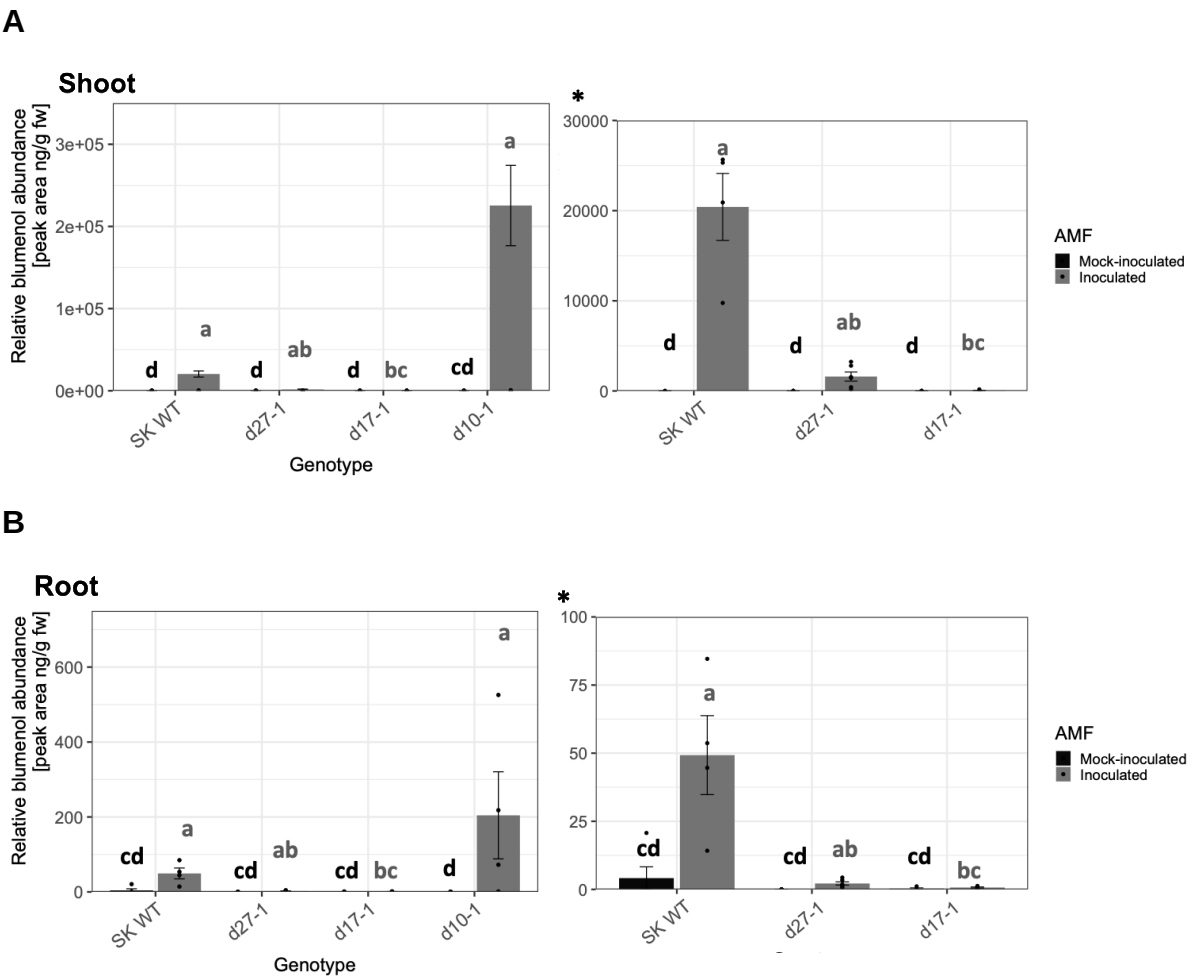

Figure 3.14. Comparison of blumenol accumulation in root and shoot material in SL biosynthesis mutants. *Blumenol accumulation (11-carboxyblumenol C) in shoot (A) and root (B) material of the same samples. Data points of 4-6 biological replicates are shown. Black bars indicate mock- inoculated samples and teal indicate inoculated samples. Error bars represent mean ± standard error. * denotes zoomed in axis of genotypes with lower blumenol abundance. A Kruskal-Wallis test was performed, followed by post-hoc pairwise comparison using the agricolae R package. Different letters represent significant difference (p-value <0.05) and colour corresponds to mock (WT) or inoculated sample.*

3.3.2.3 Is there transcriptional crosstalk between SL and blumenol biosynthesis pathways?

Since SL biosynthesis genes *D27* and *D17/CCD7* are identified to have dual roles in blumenol (Figure 3.10) and SL biosynthesis in rice (C Gutjahr et al., 2012; Hao et al., 2009; Shindo et al., 2018; Stauder et al., 2018), transcriptional feedback in the mutants was determined. An independent replicate experiment of wild type and SL biosynthesis mutant plants inoculated with 500 spores/ plant was conducted. AM colonisation and root expression of the AM marker genes *RiEF1a, AM3, AM14* and

PT11 were determined to confirm AM phenotypes of the SL biosynthesis mutants. In addition, blumenol biosynthesis genes *D27, D17* and *CCD1* were interrogated to determine if there is transcriptional feedback within SL and blumenol biosynthesis pathways.

Intraradical root colonisation of 38.5 ± 21.4% was observed in wild-type and this was statistically equivalent to *d27-1* and *d10-1* at 38.8 ± 23.4% and 42.4 ± 23.4% respectively (KW, $p < 0.05$, Figure 3.15A). In contrast, reduced intraradical colonisation of 13.7 ± 13.5% was observed *d17-1,* but this was not statistically significant, likely due to limited biological replicates (N=3), (KW, $p > 0.05$, Figure 3.15A). The colonisation phenotypes of the SL biosynthesis mutants (Figure 3.15A) were confirmed by AM marker gene expression. Expression of early colonisation marker *AM3* and late colonisation makers *AM14* and *PT11* were statistically comparable to wild-type levels in all the SL biosynthesis mutants (KW, $p < 0.05$, Figure 3.15B). A tendency for reduced expression of *AM3* and *PT11* compared to wild-type was observed in both *d27-1* and *d17-1* but this was not significant (KW, $p > 0.05$, Figure 3.15B). In addition, expression of the fungal housekeeping gene *RiEF1a* was significantly reduced in *d27-1* and *d17-1* compared to wild-type (KW, $p < 0.05$, Figure 3.15B), suggesting that fungal biomass was reduced in these mutants. This concurs observations of reduced colonisation in *d17-1* and wild-type level colonisation in *d10-1* but contrasts the observed wild-type colonisation in *d27-1.* Further gene expression analysis is required to determine the correlation of marker gene expression in *d27-1* compared to phenotypes observed by microscopic quantification.

As found in previous studies in rice (C. Gutjahr et al., 2008; C Gutjahr et al., 2012; Kobae et al., 2018; M. Wang et al., 2018), expression of AM associated marker genes *RiEF1a, AM3, AM14* and *PT11* and SL biosynthesis genes *D27, D17, D10* was upregulated in mycorrhizal wild type plants (KW, $p < 0.05$, Figure 3.16). In addition, as previously shown in *N. attenuata,* maize and Medicago (Z. Sun et al., 2008; Walter et al., 2007; M. Wang et al., 2018), the blumenol biosynthesis gene *CCD1* is additionally found to be upregulated in mycorrhizal rice roots (KW, $p < 0.05$, Figure 3.16). Interestingly, AMF-enhanced expression of SL and blumenol biosynthesis genes *D27, D17, D10* and *CCD1* was lost in *d27-1, d17-1* and *d10-1*

mutants (KW, $p > 0.05$, Figure 3.17), suggesting that transcriptional response to AMF is impaired in the mutants.

Since blumenol abundance was severely reduced and abolished in *d27-1* and *d17-1* respectively (Figure 3.13), expression of proposed blumenol biosynthesis genes *D27, D17* and *CCD1* was additionally compared between wild-type and the SL biosynthesis mutants. Expression of *D17* and *CCD1* did not significantly differ between AMF-inoculated wild type and *d27-1, d17-1* and *d10-1* plants (KW, $p > 0.05$, Figure 3.17B,D), suggesting that there is limited transcriptional feedback for these blumenol biosynthesis genes. Interestingly, *D27* expression was reduced in mycorrhizal *d17-1* and *d27-1* compared to *d10-1* and wild type. Average $\log_{10}$-normalised expression decreased from -1.51 ± 0.14 and -1.56 ± 0.27 in wild type and *d10-1* respectively to -1.70 ± 0.29 in *d17-1* and -2.2 ± 0.20 in *d27-1* (KW, $p < 0.05$, Figure 3.17A). This suggests that there is some transcriptional feedback in *D27* expression, which is regulated by *D17* and *D27,* but not *D10*.

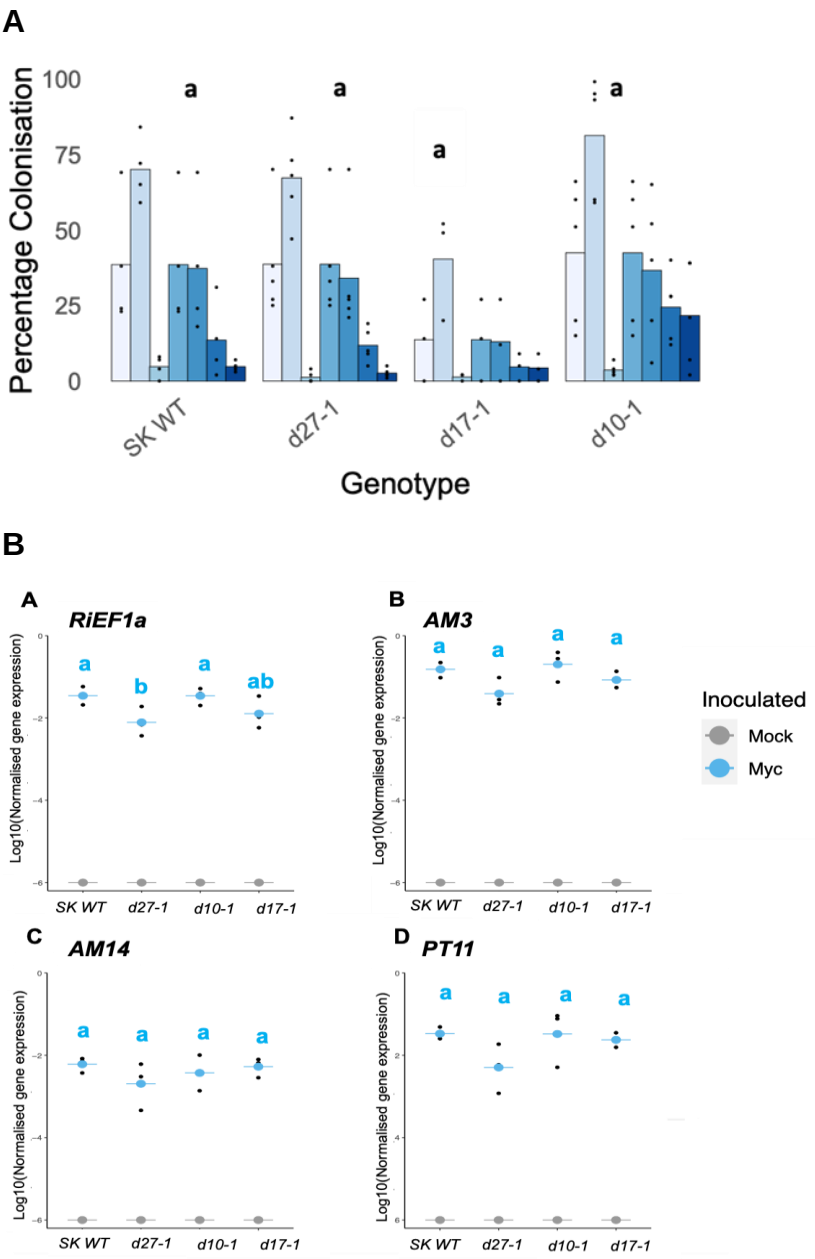

Figure 3.15 Gene expression analysis in SL biosynthesis mutants. *(A) AM colonisation rates in Shiokari wild type (SK WT) and SL biosynthesis mutants d27-1, d10- 1 and d17-1 inoculated with 500 spores/plant of R.irregularis, harvested 6 weeks post inoculation. Bar charts indicate Percentage of Total Colonisation, Extraradical Hyphae (EH), Hyphopodia (H), Intraradical Hyphae (IH), Arbuscules (A), Vesicles (V) and Spores (S) per root length. Data points of 3-4 biological replicates of each genotype are shown, with 10 technical replicates used in root counting. A Kruskal-Wallis test was performed, followed by post-hoc pairwise comparison using the agricolae R package. Different letters represent significant difference (p-value <0.05). (B.A-D) qRT-PCR based gene expression data for AM marker genes RIEF1a, AM3, AM14 and PT11 was assessed in WT and SL biosynthesis mutants d27-1, d17-1 and d10-1. Grey and blue colours correspond to mock-inoculated and AMF-inoculated (myc) respectively. Expression levels represent a GEOmean normalized to Cyclophilin and were log10 transformed to ensure equal variance in Kruskal- Wallis and post hoc tests. Data points of 3 biological replicates, each with 3 technical replicates, for each genotype are shown. Asterix indicates significant difference between mock and myc conditions within genotype and letters represent significant differences in myc, AMF-inoculated expression between genotypes.*

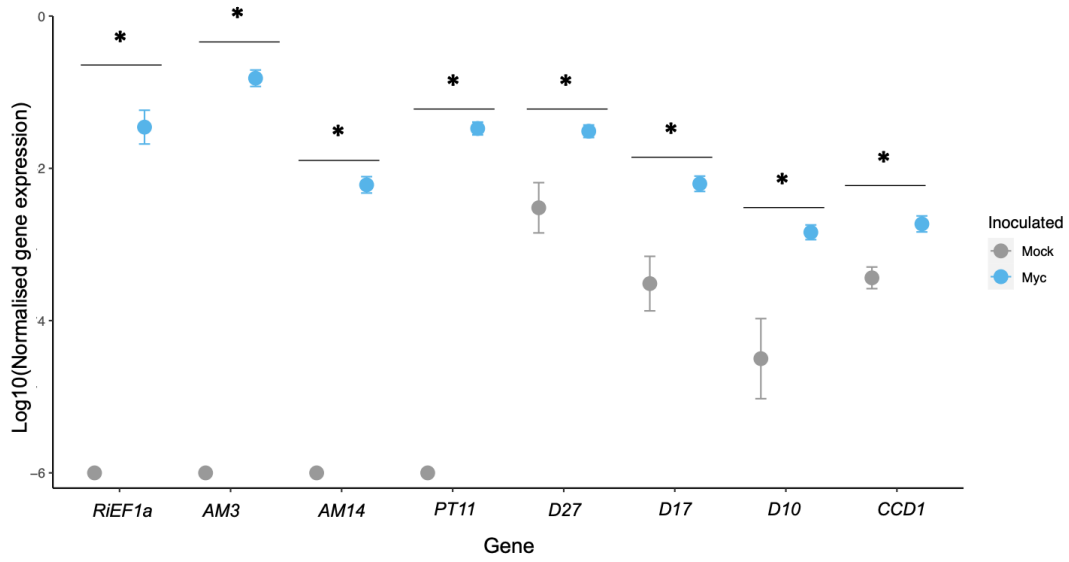

Figure 3.16 AM marker gene and SL/blumenol biosynthesis gene expression analysis in wild type plants. *qRT-PCR based gene expression data for AM marker genes RiEF1a, AM3, AM14 and PT11, SL biosynthesis genes D27, D17, D10 and blumenol biosynthesis gene CCD1 was assessed in WT Shiokari plants. Grey and blue colours correspond to mock-inoculated and AMF-inoculated (myc) respectively. Expression levels represent a GEOmean normalized to Cyclophilin and were log10 transformed to ensure equal variance in Kruskal- Wallis and post hoc tests. Data points of 3 biological replicates, each with 3 technical replicates, for each genotype are shown. Asterix indicates significant difference between mock and myc conditions.*

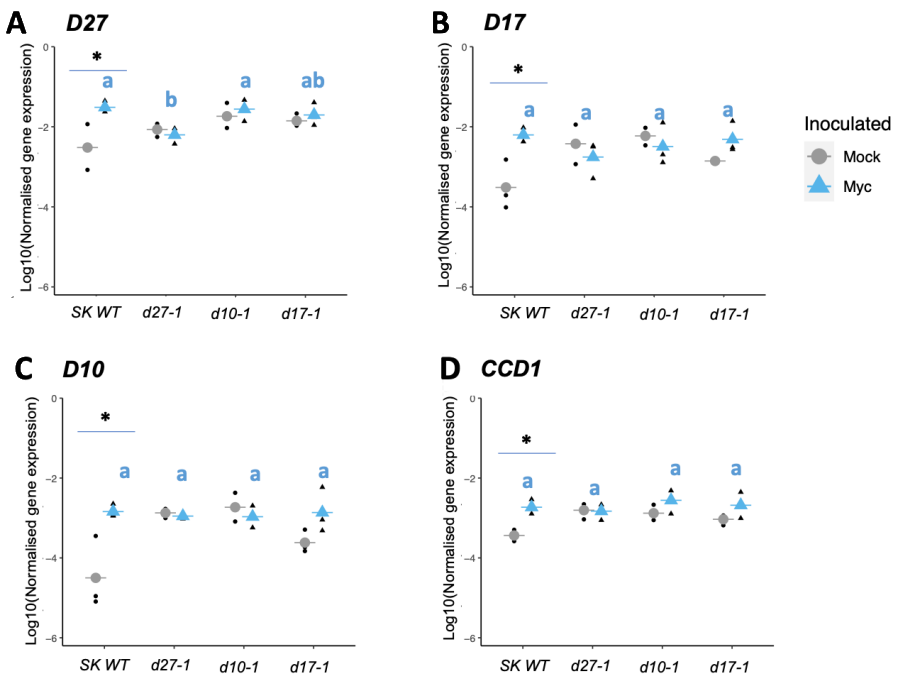

Figure 3.17. Gene expression analysis in SL biosynthesis mutants. *(A-D) qRT-PCR based gene expression data for SL and blumenol biosynthesis genes D27, D17 and CCD1 as well as SL biosynthesis gene D10 was assessed in WT and SL biosynthesis mutants d27-1, d17-1 and d10-1. Grey and blue colours correspond to mock-inoculated and AMF-inoculated (myc) respectively. Expression levels represent a GEOmean normalized to*

Cyclophilin and were log_{10} transformed to ensure equal variance in Kruskal- Wallis and post hoc tests. Data points of 3 biological replicates, each with 3 technical replicates, for each genotype are shown. Asterix indicates significant difference between mock and myc conditions within genotype and letters represent significant differences in myc, AMF-inoculated expression between genotypes.

3.3.3 Discussion

Although some crosstalk between mycorrhizal-associated apocarotenoids has previously been suggested, the interplay between SL biosynthesis and signalling and blumenol remained unknown beyond the proposed dual function of CCD7 and D27 in their biosynthesis pathways (Fiorilli et al., 2019; Vogel et al., 2010; J. Y. Wang et al., 2019). Here I report that SL signalling is not required for blumenol production. Neither the α/β hydrolase receptor D14 nor the F-box protein D3 were required for blumenol accumulation in mycorrhizal roots. This additionally corroborates previous results that SMAX1 and the D14L/D3/SMAX1 signalling pathway are not essential to blumenol accumulation (Choi et al., 2020; Yoshida et al., 2012) Overall, I report that D14/D3 SL signalling and D14L/D3/SMAX1 AM signalling pathways are not essential for blumenol accumulation during AM symbiosis.

The first stage of blumenol biosynthesis is thought to involve cleavage of a common C_{40} precursor by CCDs (CCD4 or D17/CCD7) to form a C_{27} intermediate and C_{13} cyclohexanone. Reduction of blumenol and mycorradicin in tomato *ccd7* mutants implicated CCD7 as the enzyme required for biosynthesis (Vogel et al., 2010). I additionally found blumenol production required the *CCD7* rice homolog, *d17*, further supporting that D17/*CCD7* is essential to the blumenol biosynthesis pathway (Bruno & Al-Babili, 2016; M. Wang et al., 2018). It is interesting to note that other blumenol biosynthesis mutants, such as *dxs2*, have been reported to have increased amounts of dead and degenerative arbuscules (Floss et al., 2008). Although delayed root colonisation has been identified in *d17,* no arbuscule phenotype has been reported (C Gutjahr et al., 2012; Kobae et al., 2018), nor was seen in these experiments, suggesting that blumenol biosynthesis genes are not required for normal arbuscule turnover.

To date, *D27* has only directly been implicated in SL biosynthesis, where it catalyses the reversible isomerization of all-*trans*- and 9-*cis*- *β*-carotene (C_{40}). Since products of CCD7 cleavage are *cis* configured, it has previously been suggested that D27 may additionally be required for an isomerisation step in blumenol biosynthesis (Bruno & Al-Babili, 2016; Bruno et al., 2014; Fiorilli et al., 2019; M. Wang et al., 2018). I report severe reduction in blumenol abundance in AMF-inoculated *d27-1*, further suggesting that D27 is required in blumenol biosynthesis. In addition, there appears to be transcriptional regulation of *D27* expression by *D27* and *CCD7* blumenol biosynthesis genes, although this requires further elucidation. In the proposed biosynthesis pathway, D27 likely isomerises all-*trans-zeaxanthin* (C_{40}) to *cis* configuration to allow stereoisomer specificity of cleavage by CCD7. Zeaxanthin (C_{40}) is cleaved into a C_{27} intermediate, all-*trans*-Apo-10'-zeaxanthinal, which is then cleaved to blumenol (C_{13}) and mycorradicin (C_{14}) products by CCD1. The proposed model in rice is summarized in Figure 3.18 and concurs previously suggested pathways for blumenol biosynthesis (Fiorilli et al., 2019; M. Wang et al., 2018). Notably, the potential for additional biosynthesis by other suggested CCDs, such as CCD4, remains to be elucidated.

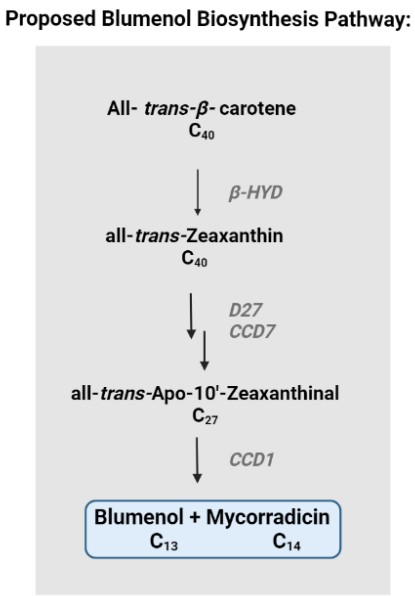

Figure 3.18 Proposed pathway for blumenol biosynthesis during AM symbiosis in rice. *As suggested previously* (Fiorilli et al., 2019; M. Wang et al., 2018)*, β-carotene is likely cleaved by β-carotene hydroxylase to produced zeaxanthin. CCD7 has been previously implicated in the formation of all-trans-β-apo-10'-carotenoids* (Alder et al., 2012; Bruno et al., 2014; Vogel et al., 2010)*, and likely cleaves zeaxanthinThis study identified that D27 likely fulfils as the required isomerisation step . Downstream, CCD1 has been implicated in production of C_{13} blumenols and C_{14} mycorradicin from the apo-10'-zeaxanthinal product* (Floss et al., 2008; M. Wang et al., 2018).

Previous publications of AM phenotypes in SL biosynthesis mutants suggested that colonisation is initially reduced in D17/CCD7 and D10/CCD8 but can recover to wild type levels (C Gutjahr et al., 2012; Kobae et al., 2018). No AM phenotype has been reported in D27 to date. It is significant to point out that independent replicate experiments identified plastic AM phenotypes in *d27-1* and *d10-1* mutants of wild-type and increased colonisation compared to wild type. Such phenotypes have not been reported previously and advocate for the need of greater spatiotemporal resolution of the requirement for SL in AM symbiosis. In addition, the presence of AM colonisation in *d27-1* and *d17-1* mutants, indicates that the production and/or accumulation of SLs and root and foliar blumenol derivatives are not essential for AM symbiosis.

Overall, while SL biosynthesis and signalling are not necessary for accumulation of blumenol during AM symbiosis, SL biosynthesis genes *D17* and *D27* are each required for biosynthesis of blumenol C glycosides during AM symbiosis.

3.4 Investigating the requirement for SL and blumenol biosynthesis genes for efficient AM colonisation in rice

3.4.1 Introduction

Previous studies have reported that AM colonization levels are reduced in SL biosynthesis mutants *d10/ccd8* and *d17/ccd7* in rice (C Gutjahr et al., 2012; Kobae et al., 2018). Gutjahr et al. first reported AM colonization of *d10-1* and *d17-1* by *R. irregularis* (formerly *Glomus intraradices)* was reduced by more than half with respect to the corresponding *Shiokari* wild type (C Gutjahr et al., 2012). Later, Kobae et al. reported a similar phenotype of reduced number and length of hyphal-colonized regions per plant in *d10-2*, *d17-2* and *d10-2/d17-2* compared to wild type (cv. *Nipponbare).* In addition, length of colonized regions in *d17-2* were significantly shorter than that in *d10-2.* Similarly, reduced extension of colonized regions was observed in *d10-1* and *d17-1* (cv. *Shiokari)* mutants compared to wild

type, with greater reduction in *d17-1.* Notably, it was reported that although growth of colonised regions occurred at a slower pace, colonisation could eventually reach wild type levels in both mutants. Kobae et al. (2018) suggested that reduced growth of colonized regions in SL-deficient mutants was due to reduced hyphal entry into roots and the phenotypic severity in *d17* was thought to be due to a distinct role of D17 in development of intraradical hyphae (Kobae et al., 2018). Since few experiments have further tested this assumption, and a plasticity of AM phenotypes were reported in the mutants in Section 3.3, further resolution of the role of SL biosynthesis genes in promoting AM colonisation is essential for understanding the role of SL and blumenol in AM symbiosis.

The current understanding of the requirement for AM-associated apocarotenoids for AM colonisation in rice can be summarised as follows. Previous analysis in rice found that endogenous, canonical SL 2′-epi-5-deoxystrigol (*epi*-5DS) was undetectable in roots of *d10-1* and *d17-1* (Umehara et al., 2008) and *d27-1* (H. Lin et al., 2009). In addition, reduced canonical 4-deoxyorobanchol (4-DO) and non-canonical *MeO-5-DS is1* was observed *d27-1* but not measured in *d17-1* or *d10-1* (Choi et al., 2020). Recent reports similarly indicate that canonical SLs 4-DO and orobanchol and non-canonical *MeO-5-DS is1* are not required. *Os900-KO* mutants lacking production of these derivatives, but that still produce a novel non-canonical SL derivative (CL+30), don’t show tillering and reduced shoot height but exhibit a delay in AM symbiosis at early time point, which recovers to wild type levels over time post inoculation. The authors reported that canonical SLs are required for efficient establishment of AM symbiosis (Ito et al., 2022), but loss of non-canonical *MeO-5-DS is1* in the mutant suggests that a clear distinction cannot be made. Although delayed, AM colonisation can establish in SL biosynthesis mutants, suggesting that *epi*-5DS and likely 4-DO and *MeO-5-DS is1* and SL derivatives are not essential for colonisation.

Similarly, blumenol is abolished in *d17-1* and severely reduced in *d27-1* but AM colonisation still occurs (Section 1.3), suggesting that blumenol is not essential for AM symbiosis. A reduction in mycorradicin alone does not abolish AM symbiosis establishment (Floß et al., 2008; Floss et al., 2008) but, since a mutant with abolished mycorradicin accumulation has not yet been reported, essentiality for

colonisation cannot be determined. Similarly, root colonisation is reduced in *zas* and *zas2* mutants despite increased root expression of SL biosynthesis genes and accumulation of canonical SLs in root exudates. The essentiality for zaxinone in AM symbiosis remains to be determined in mutants where zaxinone is completely abolished (Ablazov et al., 2020, 2022; Votta et al., 2022; J. Y. Wang et al., 2019). Overall, the requirement for AM-associated apocarotenoids requires further investigation and could help to elucidate apocarotenoid signatures required for AM symbiosis. In addition, the dual role of D17 and D27 biosynthesis enzymes in accumulation of apocarotenoids in AM symbiosis promotes the need for comprehensive study of the apocarotenoid profiles of CCD and isomerase enzymes implicated in apocarotenoid biosynthesis. Since CCDs required for some biosynthesis pathways have not yet been elucidated, apocarotenoid signatures could differ from current, assumed function in CCD mutants (Fiorilli et al., 2019).

This study aimed to further explore the roles of SL biosynthesis genes in AM symbiosis using time and inoculation-gradient assessments of AM phenotypes in *d27-1, d17*-1 and *d10-1* mutants. In addition, a metabolomics study aimed to assess AM-associated apocarotenoid accumulation in mutants to provide greater resolution to differential AM phenotypes observed.

3.4.2 Results

3.4.2.1 What is the requirement for SL and blumenol biosynthesis genes in AM symbiosis in rice?

A time-course of AM colonisation in wild type and SL biosynthesis mutant plants inoculated with 500 spores per plant was conducted. The results at six weeks post inoculation were previously described in Figure 3.15 but are recapitulated in Figure 3.19 for ease of time course comparison. A tendency for reduced colonisation was observed in *d17-1,* although not significant, and wild-type colonisation was observed in *d27-1* and *d10-1* (KW, $p < 0.05$, Figure 3.15 & 3.19A). At nine weeks post inoculation, all SL biosynthesis mutants had wild type levels of total intraradical colonisation (KW, $p > 0.05$, Figure 3.19B), suggesting that delayed AM colonisation can recover over time, as has previously reported in other SL biosynthesis mutants (Ito et al., 2022; Kobae et al., 2018).

To further assess whether AM phenotypes can be recovered by increased spore concentration, I conducted an inoculation gradient experiment comparing wild-type and SL biosynthesis mutants. AM colonisation was reduced in all mutants at all spore concentrations, with the most severe reduction consistently in *d17-1* (KW, $p < 0.05$, Figure 3.20A-B). Intriguingly, a reduction in colonisation was also seen at higher spore concentration of 700 spores/plant. Intraradical colonisation of 72.2 ± 7.3% was observed in wild-type and this was reduced in *d27-1* and *d10-1* to 40.8 ± 24.9% and 56.6 ± 11.6% respectively and severely reduced in *d17-1* to 14.5 ± 9.0% (KW, $p < 0.05$, Figure 3.20A-B). This suggests that a higher spore concentration is not sufficient to recover AM colonisation in SL biosynthesis mutants.

Overall, I report that the reduction in AM colonisation in SL biosynthesis mutants reported is clearly more plastic than previously published (C Gutjahr et al., 2012; Kobae et al., 2018), as seen by different AM phenotypes observed between independent replicate experiments. Recovery of root colonisation to wild type levels is observed by increased time post inoculation, as suggested previously (Ito et al., 2022; Kobae et al., 2018), but not by greater spore concentrations. Since it is widely understood that the requirement for SL biosynthesis is at early stages of AM symbiosis, where pre-communication facilitates effective establishment of symbiosis (reviewed by (Hull et al., 2021)), I hypothesize that plasticity occurs due to the ability for colonisation to recover over time once sufficient symbiosis has been established and independent experiments may capture different phenotypes dependent on timing of recovery post establishment, causing plasticity. In addition, I repeatedly observed that *d17-1* exhibits a more severe AM phenotype at the establishment phase compared to *d27-1* and *d10-1.* I therefore report that there is a greater requirement for D17/CCD7 in pre-symbiotic communication facilitating efficient establishment of AM symbiosis. Since colonisation levels recover to wild-type in all mutants, SL biosynthesis is required but not essential for AM symbiosis.

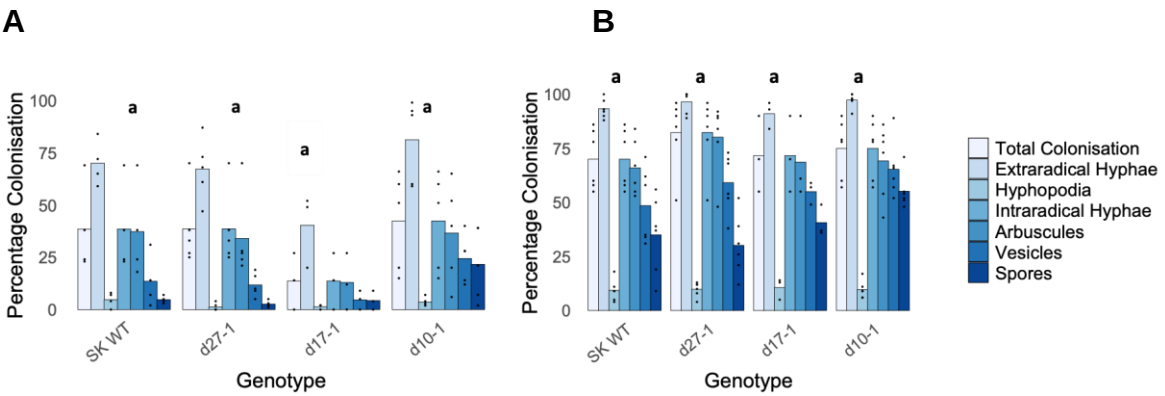

Figure 3.19. AM colonisation in SL biosynthesis gene mutants in rice. *AM colonisation rates in Shiokari wild type (SK WT) and SL biosynthesis mutants d27-1, d10- 1 and d17-1 inoculated with 500 spores/plant of R.irregularis. (A and B) experiments harvested at 6- and 9-weeks post inoculation respectively. Bar charts indicate Percentage of Total Colonisation, Extraradical Hyphae (EH), Hyphopodia (H), Intraradical Hyphae (IH), Arbuscules (A), Vesicles (V) and Spores (S) per root length. Data points of 3-6 biological replicates of each genotype are shown, with 10 technical replicates used in root counting. A Kruskal-Wallis test was performed, followed by post-hoc pairwise comparison using the agricolae R package. Different letters represent significant difference (p-value <0.05).*

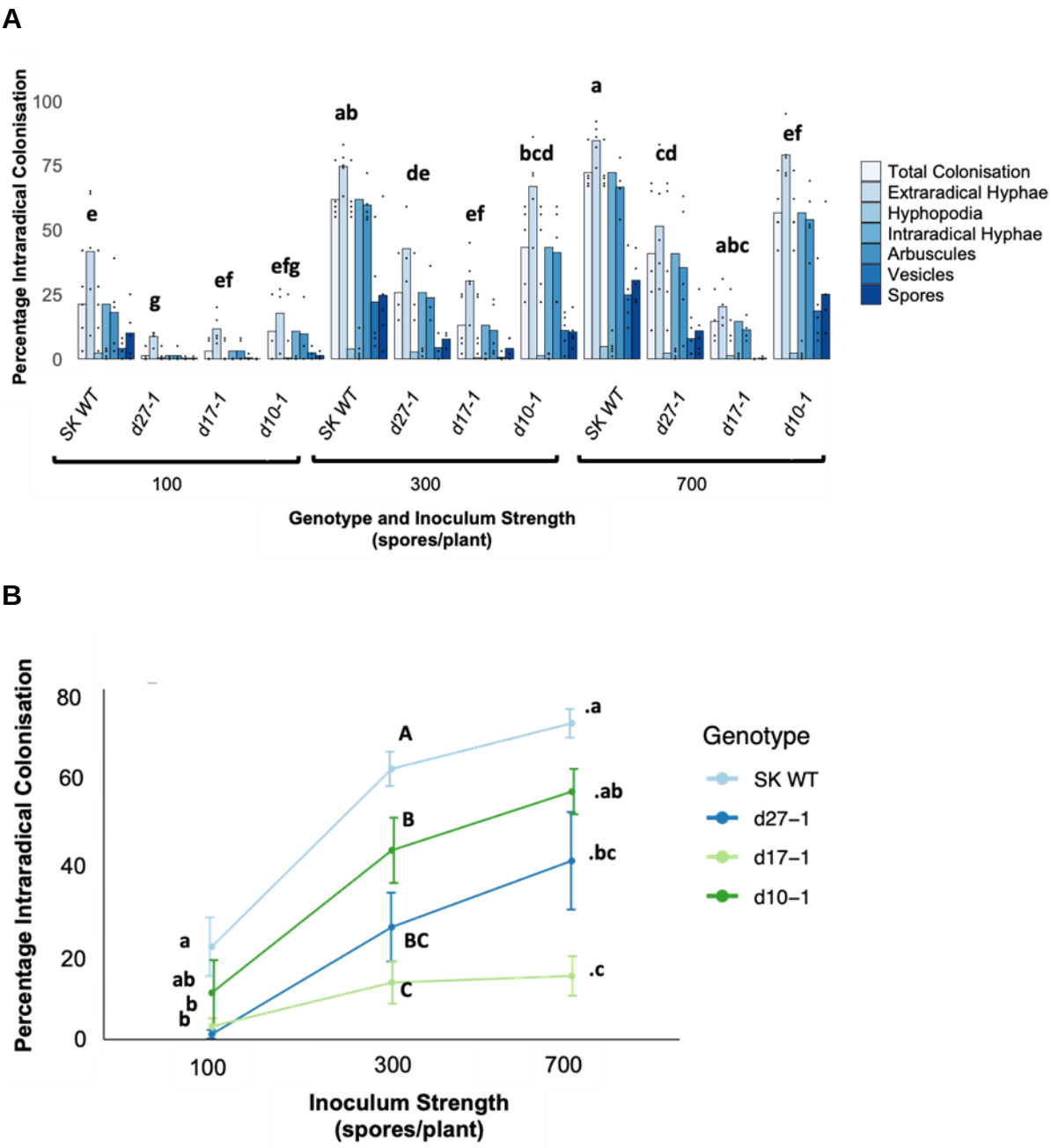

Figure 3.20. Inoculation gradient analysis of AM colonisation in SL biosynthesis gene mutants. *Experiment interrogating AM colonisation in WT and SL mutants grown in different spore inoculation concentrations. (A) AM colonisation rate in Shiokari wild type (SK WT) and SL biosynthesis mutants d27-1, d10-1 and d17-1. Bar chart indicates Percentage of Total Colonisation, Extraradical Colonisation (EH), Hyphopodia (H), Intraradical Hyphae (IH), Arbuscules (A), Vesicles (V) and Spores (S) per root length. Data points of 4-6 biological replicates of each genotype are shown, with 10 technical replicates used in root counting. A Kruskal-Wallis test was performed, followed by post-hoc pairwise comparison using the agricolae R package. Different letters represent significant difference (p-value < 0.05). Error bars represent mean ± standard error. (B) Graph comparing mean percent colonisation between WT and SL mutants when inoculated with 100, 500 and 700 spores of R.irregularis per plant. Data points of 3-6 biological replicates of each genotype are shown. A Kruskal-Wallis test was performed per inoculation strength, followed by post-hoc pairwise comparison using the agricolae R package. Different letters represent significant difference within inoculum concentration (p-value <0.05). Error bars represent mean ± standard error.*

3.4.2.2 Do SL and blumenol biosynthesis genes differ in accumulation of apocarotenoids and SL derivatives in rice roots during AM symbiosis?

I observed that both *d17-1* and *d27-1* have abolished accumulation of some SLs and 11-carboxyblumenol C-Glc derivatives and intraradical colonisation still occurs, suggesting that neither blumenol nor SLs are essential for maintenance of AM colonisation. In addition, it seems the requirement for D17 for efficient AM colonisation is greater than for D27 and D10. All mutants have previously been reported to be SL deficient, through small, bushy stature, as observed in Figure 3.12, and abolished root production of 2′-*epi*-5-deoxystrigol (*epi*-5DS), a known canonical SL that has been identified in hydroponic culture media in rice (Hao et al., 2009; Umehara et al., 2008). It is therefore suggested that differences in AM colonisation may be driven by apocarotenoid signatures beyond blumenol or canonical SLs measured in *d17-1*. In addition, the CCD enzymes involved in biosynthesis of many apocarotenoid pathways remain unknown, meaning the apocarotenoid pools of CCDs and isomerases including *D17*, *D10* and *D27,* and their implication for AM symbiosis, are elusive.

To assess apocarotenoid pools of the SL biosynthesis mutants, wild type, *d27-1, d17-1* and *d10-1* mutants (cv. *Shiokari*) grown in the inoculation gradient experiment (Figure 3.20) were assessed using a metabolite analysis of endogenous canonical and non-canonical SLs and short apocarotenoids including mycorradicin, blumenol and beta-ionone/ol derivatives (Table 3.1). Extraction of root material used an optimized method for SL detection (Floková et al., 2020) and root accumulation of apocarotenoids was analysed by Liquid Chromatography Mass Spectrometry coupled with electrospray ionisation (LCMS-ESI+). A total of 48 predicted apocarotenoid compounds were identified (Table 3.1), most of which ionized as sodium (Na) adducts. Principal component analysis (PCA) of the 48 predicted compounds in WT and SL biosynthesis mutants identified overlap in accumulation in all cases, with clear segregation of WT and *d10-1* compared to *d27-1* and *d17-1*. Principal component 1 (PC1; 70.6% variance explained) clustered SK WT and *d10-1* into wide 95% confidence ellipses, whilst PC2 (22.9% variance explained) clustered

d27-1 and *d17-1* into an additional wide 95% confidence ellipses, depicting separate population means (Figure 3.21A).

Clear segregation of *d27-1* and *d17-1* from wild type and *d10-1* was most evident when SLs were excluded from the apocarotenoid pools (Figure 3.21C) and less overlap was present between mutants in analysis of SL derivatives only (Figure 3.21B). This corroborates previous findings of different blumenol accumulation between D10 and enzymes D27 and D17. In addition, it further suggests differences in accumulation of SL-independent apocarotenoids between the SL biosynthesis mutants. Notably, the LC-MS analysis was run in positive ESI mode, which achieves maximal resolution and ionization efficiency for SLs but is not optimised for blumenols and other apocarotenoids. The analysis is in the process of being repeated in negative mode to confirm and further analyse the identity of the potential apocarotenoids segregating between the mutants.

Table 3.1 Table of 48 potential apocarotenoid compounds identified by LCMS-ESI+. *Compound name, apocarotenoid 'family' and molecular weight (m/z) measured in collaboration with Prof. Paul Fraser and Dr. Laura Perez at Bourne Laboratory, Royal Holloway, University of London are given.*

Compound Name	Apocarotenoid family	m/z
GR24-Na	Strigolactone	4.74
CarlactoneNa	Strigolactone	5.15
11-carboxyblumenol C-9-O-glucosideNa	Blumenol	3.46
11-hydroxyblumenol C-9-O-glucosideNa	Blumenol	2.87
11-hydroxyblumenol C-9-O-glucosideNa	Blumenol	3.25
3-OH-carlactoneNa	Strigolactone	5.06
4-deoxyorobancholNa	Strigolactone	4.39
7-OH-orobancholNa	Strigolactone	3.43
7-OH-orobancholNa	Strigolactone	3.05
7-OH-orobancholNa	Strigolactone	4.87
7-OH-orobancholNa	Strigolactone	4.01
7-OH-orobanchyl acetateNa	Strigolactone	4.77
7-OH-orobanchyl acetateNa	Strigolactone	4.21
7-oxo-orobancholNa	Strigolactone	4.02
7-oxo-orobancholNa	Strigolactone	4.6
7-oxo-orobanchyl acetateNa	Strigolactone	3.87
7-oxo-orobanchyl acetateNa	Strigolactone	4.39
7-oxo-orobanchyl acetateNa	Strigolactone	3.51
ABANa	ABA	2.56
beta-apo-13-carotenone	beta-apo-13-carotenone	5.91
beta-apo-13-carotenone	beta-apo-13-carotenone	4.26
beta-apo-13-carotenone	beta-apo-13-carotenone	5.15
beta-apo-13-carotenoneNa	beta-apo-13-carotenone	5.14
Blumenol C 9-O-beta-(6-O-rhamnosyl-2-O-beta-glucuronosylglucoside)Na	Blumenol	3
Blumenol C-9-O-glucose-glucosideNa	Blumenol	3.14
Blumenol C-9-O-glucosideNa	Blumenol	3.6
Blumenol C-9-O-glucosideNa	Blumenol	3.31
Blumenol C-9-O-glucosideNa	Blumenol	4.71
CarlactoneNa	Strigolactone	5.15
Methyl carlactonoateNa	Strigolactone	6.42
Methyl carlactonoateNa	Strigolactone	5.2
Methyl carlactonoateNa	Strigolactone	5.59
Mycorradicin	Mycorradicin	3.5
Mycorradicin	Mycorradicin	2.99
Mycorradicin	Mycorradicin	2.74
Mycorradicin glucosideNa	Mycorradicin	3.05
Mycorradicin glucosideNa	Mycorradicin	3.48
Mycorradicin glucosideNa	Mycorradicin	3.9
Mycorradicin glucosideNa	Mycorradicin	2.69
Mycorradicin glucosideNa	Mycorradicin	4.9
Mycorradicin-diglycosylatedNa	Mycorradicin	2.89
MycorradicinNa	Mycorradicin	4.16
MycorradicinNa	Mycorradicin	4.64
MycorradicinNa	Mycorradicin	0.93
OrobancholNa	Strigolactone	3.81
OrobancholNa	Strigolactone	3.16
Orobanchyl acetateNa	Strigolactone	3.57
Retinal	Retinal	5.59

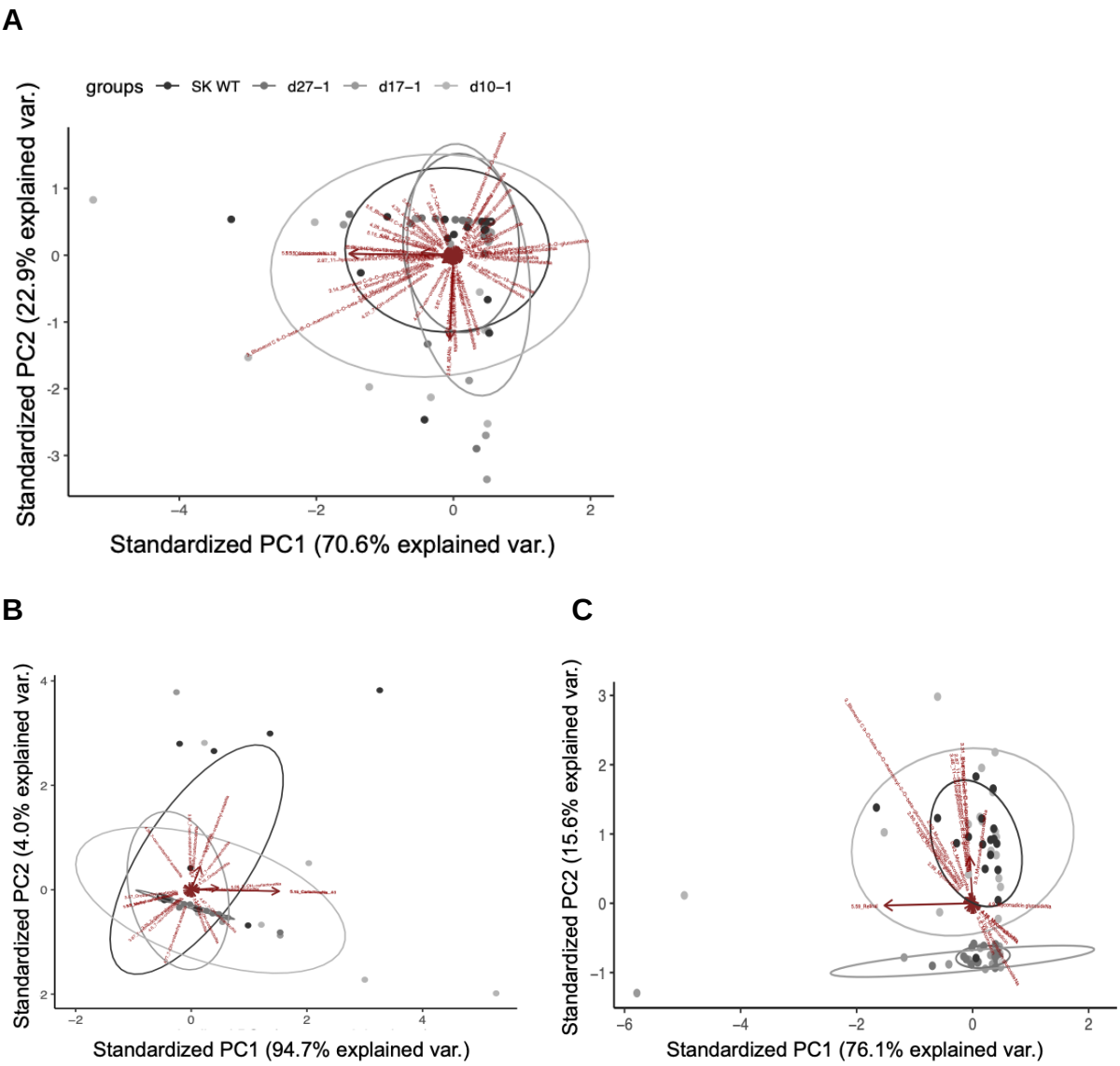

Figure 3.21 Principal component analysis (PCA) of 48 apocarotenoid compounds. PCA of compounds (red arrows) of (A) total apocarotenoids, (B) SL family apocarotenoids and (C) non-SL family apocarotenoids. Each point indicates a compound. Colour of point and 95% confidence ellipses represent clusters dependent on genotype including SK WT, *d27-1, d17-1* and *d10-1.* Data points of 4-5 biological replicates per genotype are included. Percentage variance explained by each principal component (PC) is given on axes.

3.4.3 Discussion

Overall, it is suggested that the SL biosynthesis genes, particularly *D17*, are required but not essential for ensuring efficient establishment of AM colonisation. The severity of reduced infection being strongest in *d17-1* mutants has been seen consistently and corroborates reports in *d17-2 (cv. Nipponbare)* (Kobae et al., 2018). In addition, this report newly indicates an AM phenotype in *d27-1.* The phenotype resembles that of *d10*, where in conditions where root colonisation establishment is suppressed,

intraradical colonisation is reduced but to a less severe extent than in *d17.* Importantly, this study additionally highlights that wild type or wild type-like colonisation can be achieved in all mutants, particularly in *d10-1* and *d27-1*, as reported in *d17-2* and *d10-2* previously (Kobae et al., 2018). In addition, I suggest that the AM colonisation delay observed in the mutants previously (C Gutjahr et al., 2012; Kobae et al., 2018) is likely a more plastic phenotype than had been anticipated. This concurs previous suggestions that SL biosynthesis mutants D17 and D10 are required for 'punctual internalization of hyphae into roots' and that colonisation progression once established is normal (Kobae et al., 2018). Discrepancy between the phenotype of *d17* compared to *d10* and *d27* could be due to different requirement for such internalization (Kobae et al., 2018) or due to differential SL or apocarotenoid signatures in these mutants, which requires further analysis.

Pools of SLs and other AM-associated apocarotenoids were determined in *d27-1, d17-1* and *d10-1*. PC analysis suggested that apocarotenoid pools of *d10-1* are most like wild-type whilst *d27-1* and *d17-1* have different signatures, particularly of non-SL apocarotenoids. This corroborates findings of the involvement of D27 isomerase and D17/CCD7 carotenoid cleavage dioxygenases in other apocarotenoid biosynthesis pathways, namely blumenol (and likely its mycorradicin by-product). It also advocates for further analysis of other apocarotenoid biosynthesis pathways that these enzymes may be involved in. Identification of such will allow for appropriate interpretation of AM phenotypes with respect to essential or required AM-associated apocarotenoids.

3.5 Conclusions

This analysis used a combination of targeted metabolomics and classic microscopy and AM marker gene expression techniques to confirm that hydroxy- and carboxyblumenol C glycosides are accurate foliar markers of AM colonisation in rice, suitable for HTP diversity screens. Genetic and physiological manipulation suggest a blumenol accumulation occurs strictly after intraradical colonisation is established. AMF-regulated production and/or accumulation is independent to phosphate status

and AM-associated signalling pathways such as D14/D3 SL signalling and the D14L/D3/SMAX1 AM signalling. A model for blumenol biosynthesis (Figure 3.18) was confirmed using genetic manipulation of enzymes known to contribute to SL biosynthesis. D27 and D17/CCD7 were found to be essential for blumenol biosynthesis and accumulation.

Genetic manipulation of SL and blumenol biosynthesis genes suggest that AM colonisation phenotypes are more plastic than previously reported. Delayed colonisation is reported in all mutants under some experimental conditions and is consistently most severe in *d17-1.* Importantly, this can recover to normal levels as root colonisation progresses. Apocarotenoid signatures corroborate SL-independent roles of D27 and D17/CCD7 and invite the further analysis of AM-associated apocarotenoids and their function in AM symbiosis. Such analysis could elucidate the reasoning for greater requirement of D17/CCD7 in AM symbiosis.

Acknowledgments

The blumenol measurements throughout this chapter was done in collaboration with Prof. Ian Baldwin, Dr. Rayko Halitschke and Catarina Rocha at Max Planck Institute for Chemical Ecology, Jena, Germany (Mindt et al., 2019; M. Wang et al., 2018). Plant growth, harvest, root colonisation and gene expression were assessed by myself at University of Cambridge, UK. Blumenol extraction and abundance analysis was completed by myself, Dr. Rayko Halitschke and Catarina Rocha using facilities at Max Plank Institute for Chemical Ecology, Jena, Germany.

The apocarotenoid metabolomics was done in collaboration with Prof. Paul Fraser and Dr. Laura Perez at Royal Holloway, University of London, UK. Plant growth, harvest, root colonisation and gene expression were assessed by myself at University of Cambridge, UK. Root apocarotenoid abundance was analysed by myself and Dr. Perez at Bourne Laboratory, Royal Holloway, University of London, UK.

4 Chapter Four– Genetic analysis of AM symbiosis establishment and benefit in a diverse panel of rice

4.1 Selection of a diverse *Indica* rice panel from the 3K-RG

4.1.1 Introduction

In 2002, cultivated Asian rice (*Oryza sativa)* was the first crop genome to be fully sequenced (Goff et al., 2002; Matsumoto et al., 2005; J. Yu et al., 2002). Twenty years later the available rice genomes now extend to diverse panels that describe extensive genetic and phenotypic variation in global cultivars. The Rice Diversity Panels 1 and 2 (RDP1, RDP2), include ~1500 accessions of landrace and elite *O. sativa* rice genotyped using genome-wide high density rice array (HDRA) (McCouch et al., 2016). In addition, international effort through the 3,000 Rice Genome Project (3K-RG) produced a giga-dataset of publicly available genome sequences, genotyped using Illumina resequencing technology. The 3K-RG panel combines 3,024 *O. sativa* rice accessions with global representation of both genetic and functional diversity from 89 countries (J. Y. Li et al., 2014). More recently, the Bengal and Assam Aus panel (BAAP) containing 226 *aus* accessions collected from Bangladesh and India was described (Norton et al., 2018). Together, this provides considerable genomic annotation to aid in trait genetic analysis studies, such as genome-wide association studies (GWAS), in rice (W. Wang et al., 2018).

Significant natural variation in agronomic yield traits is present across the diverse rice panels, including the RDP1 (Cobb et al., 2021; Eizenga et al., 2014; K. Zhao et al., 2011; Zhong et al., 2021) and BAAP (Norton et al., 2018). Over 75 agronomic traits have been recorded for the 3K-RG (IRRI GRIN-GLOBAL, https://gringlobal.irri.org/gringlobal) and studies have also begun to use this resource to report natural variation in the full panel (Y. L. Lin et al., 2021). In addition, subsets of the 3K-RG have been developed in order to more manageably define phenotypic

variation (Abbai et al., 2019; A. Kumar et al., 2019; Y. L. Lin et al., 2021; Menard et al., 2021; Tnani et al., 2021). This includes development of a Mini-Core collection of 520 lines that captured natural variation of agronomic traits and facilitated GWAS mapping to genomic regions of interest (A. Kumar et al., 2019).

Since one of the aims of the PhD was to analyse the genetic diversity of AM-associated phenotypes in a diverse panel of rice, the first objective was to identify a diverse subset of rice cultivars that would be representative of global subpopulation and country diversity whilst being efficient for phenotype screening.

4.1.2 Results

4.1.2.1 Selection of a diverse *Indica* panel from the 3K-RG

The 3K-RG was chosen as the reference panel as, although one study has mapped genetic associations in AM traits in rice using the RDP1 (Davidson et al., 2019), no studies have yet explored natural variation in AM traits across diversity represented in the 3K-RG panel. The 3K-RG contains over 3,000 accessions with huge genetic diversity characterised in over 2 million single nucleotide polymorphisms (SNPs) and a core set of 404K SNPs for genetic analysis (W. Wang et al., 2018). In addition, cultivar and variant data are available through the online SNP-Seek (Alexandrov et al., 2015) and RiceVarMap2 (H. Zhao et al., 2015) databases, with tools that easily allow exploration of genomic variants and allelic diversity at genome regions of interest.

The above described 3K-RG panels (Abbai et al., 2019; A. Kumar et al., 2019, 2020; Y. L. Lin et al., 2021; Menard et al., 2021; Tnani et al., 2021) were not published in 2018, when panel selection occurred for the PhD. Instead, the first objective was to create a panel of lines that captured diversity of the 3K-RG in a manageable number of cultivars that could be interrogated for AM phenotypes.

The panel was selected from the 3K-RG using the following criteria:

1. *Rice race/sub-population*

Five subpopulations of Asian rice, *O.sativa,* including *indica, aus/boro, temperate japonica, aromatic (basmati/sadri)* and *tropical japonica* have been described (Garris et al., 2005; Glaszmann, 1987; Kato et al., 1928). Previous phylogenetic analysis of the 3K-RG segregated this further into nine sub-populations, most of which correspond to geographical origin. These included four clusters of *Indica* (XI-1A from East Asia, XI-1B of modern varieties of diverse origins, XI-2 from South Asia and XI-3 from Southeast Asia*);* three clusters of *Japonica* (GJ-tmp from East Asia, GJ-sbtrp from Southeast Asian subtropical and GJ-trip from Southeast Asian tropical); and single clusters for South Asian cA and cB accessions (W. Wang et al., 2018).

Accession choice for the panel focused on the sub-population *Indica* as AMF most often form associations to rice in upland conditions (Ilag et al., 1987) and recent focus has noted the potential for *Indica* as sources of genetic diversity for improved upland rice performance (Saito et al., 2018). *Indica* accounts for ~70% of global rice trade (USDA, 2021) and is produced globally in tropical, sub-tropical and partly temperate zones, such as in India, Bangladesh, Thailand, Viet Nam, Indonesia, Myanmar, the Philippines, and southern provinces of China (Koizumi et al., 2021). The *aus* subpopulation is also well known for inclusion of upland varieties (Glaszmann, 1987), however ecotype distribution is primarily in Bangladesh, northern Myanmar and north-eastern India (Norton et al., 2018; W. Wang et al., 2018). Since previous reports have noted that differences in AM colonisation level can be partially driven by country or region (Davidson et al., 2019), the *Indica* subpopulation was instead selected to ensure global diversity in the 3K-RG was captured.

2. *Geographical Diversity*

After sub-setting the 3K-RG for *Indica* accessions, the next criterion was that the panel maintained all 89 countries and a similar distribution of *Indica* subpopulations as represented in the full 3K-RG *Indica* population (1,760 accessions; 58.2% of 3K-RG) (Z. Li et al., 2014). A total of 218 cultivars was selected that maintains global representation (Figure 4.1A) by inclusion of at least one cultivar from each of the 89

countries. In addition, all five *Indica* subpopulations from the 3K-RG, K=9, including *indx* (admixture), *ind1A, ind1B, ind2* and *ind3* were included with the same distribution as in the full panel (Figure 4.1B).

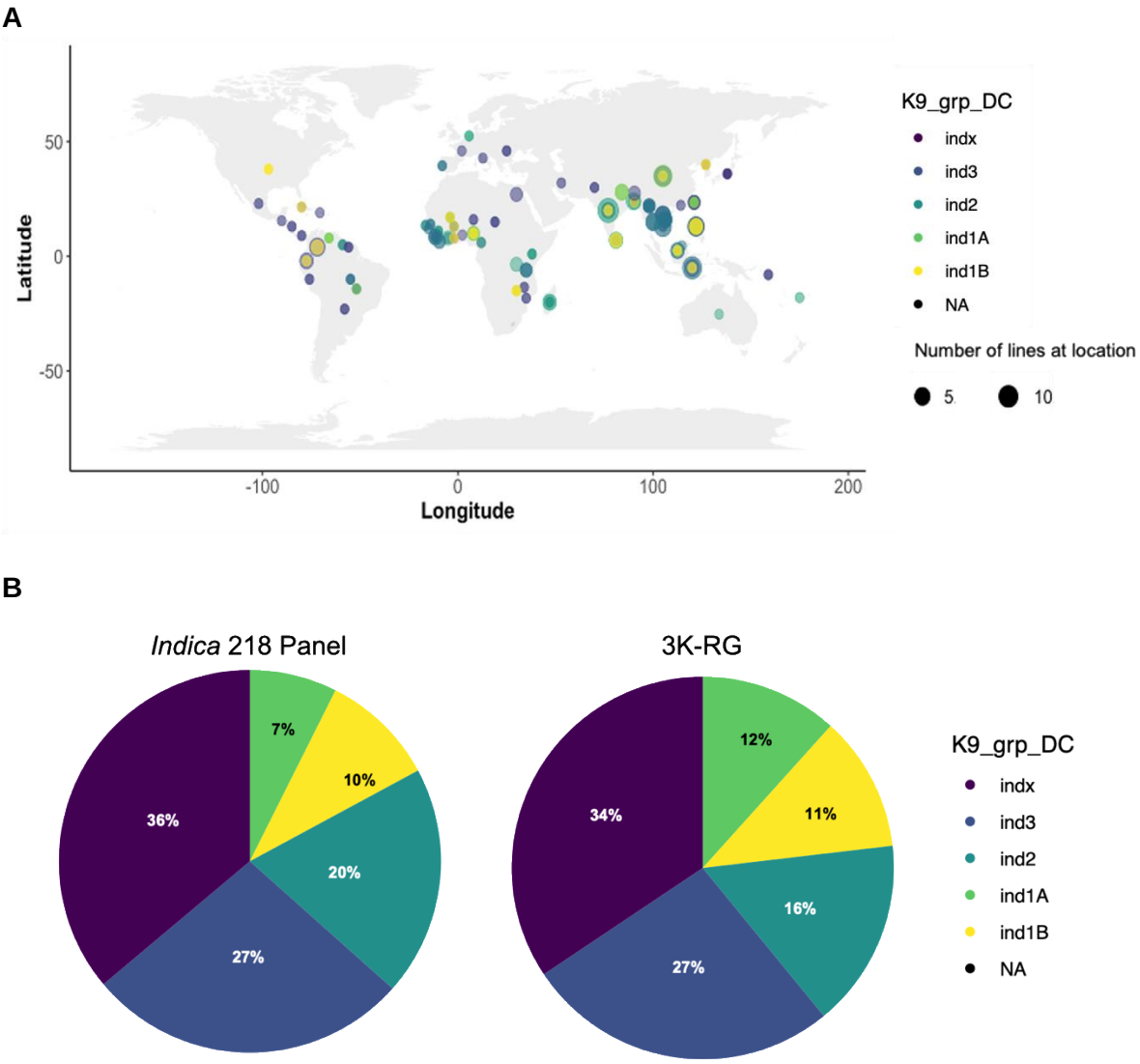

Figure 4.1 Global and subpopulation diversity represented in panel of 218 Indica lines. *(A) World map showing countries represented in diverse* Indica *panel selected. Each of 89 countries present in 3K-RG are represented. Colour of point indicates K9 subpopulation group from 3K-RG and size indicates number of lines represented at each location. (B) Pie chart representing percentage of each indica subgroup in both 218 panel and full 3K-RG panel. K9_grp_DC refers to indica subpopulation denominated in 3KRG as indx (admixture), ind1A, ind1B, ind2 and ind3.*

4.1.2.2 Population structure analysis in selected panel

Previous analysis of population structure in the *Indica* lines in the 3K-RG found five *Indica* subpopulations in K=9, including an admixture, and nine in K=15 (W. Wang et

al., 2018). To further determine the distribution of these in the selected panel, a population component analysis (PCA) was conducted. PCA analysis included 196 accessions from the 218 lines (Table 2.18), chosen as those with available seed that were used for my subsequent GWAS analyses. The accessions were extracted from the publicly available 3K-RG set of ~4.8 million SNPs, 'Filtered 3K-RG SNP set' (W. Wang et al., 2018). The SNPs were then further filtered by the following thresholds: minor allele frequency (MAF) >5%, missing data < 10%, minor allele count > 8. Since many SNPs were in very high linkage disequilibrium (LD), a "non-redundant" subset was selected after LD pruning very highly correlated SNPs (R^2=0.95, $p < 0.05$). A total of 386,173 SNPs in the non-redundant set were mapped to *Nipponbare* reference sequence and used for population structure and kinship analysis.

PC1 vs PC2 indicated five clusters that described the five subpopulations in the 3K-RG, K=9 (W. Wang et al., 2018) (Figure 4.2A). It is unsurprising that some overlay of indx (purple) was seen with all subgroups as this in an admixture likely containing accessions from all subgroups (Figure 4.2A). A further PCA overlaying the chosen *Indica* panel (red) across the full 3K-RG *Indica* panel, K=15 (green) further confirmed that the panel had good representation of the full diversity present in *Indica* (Figure 4.2B). Both PC analyses indicated a wide spread of cultivars across all *Indica* subpopulations in the 3K-RG (Figure 4.1 & Figure 4.2).

Kinship analysis between individuals in the panel was performed to estimate co-ancestry. A kinship matrix of the panel was constructed using TASSEL software with the Centered IBS method of Endelman and Jannink, 2012 to estimate additive genetic variance (Bradbury et al., 2007; Endelman et al., 2012). The kinship value for all accessions exhibited a weak level of genetic relatedness, with most values falling ~0% (Figure 4.3). Together with the reduced population structure, this suggests that the panel diverse in genetic structure and will have a reduced frequency of spurious marker-trait associations in analyses such as GWAS.

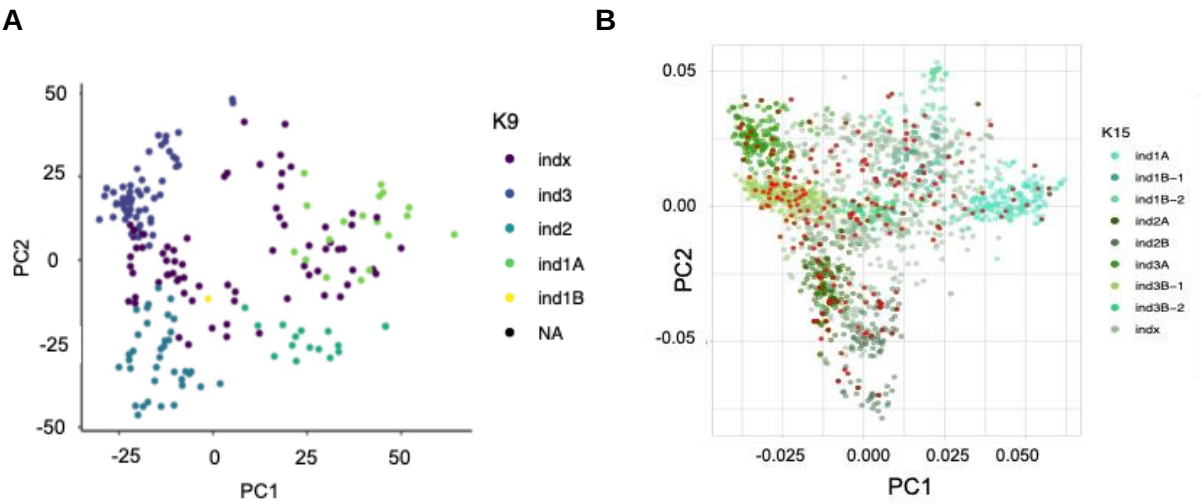

Figure 4.2 Diversity of rice in subpanel selected. *(A-B) Principal component analysis of four principal components (PC) in the (A) selected panel. Colour refers to indica subpopulation denominated in 3KRG K=9 as indx (admixture), ind1A, ind1B, ind2 and ind3. compared to all indica represented in 3K-RG (B) Genotypes are coloured by 3KRG K=15 subpopulation of* Indica *lines, with lines from the selected panel represented in red. K15 Indica graph is courtesy of Dr. Dmytro Chebotarov, IRRI.*

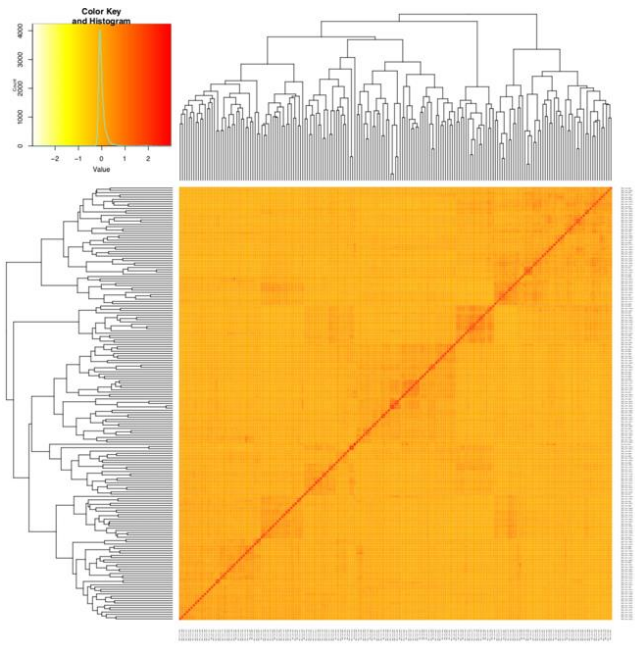

Figure 4.3 Kinship among the selected Indica panel used in the GWAS (196 lines). *A kinship matrix of the panel was constructed using TASSEL software with the Centered IBS method of Endelman and Jannink, 2012 to estimate additive genetic variance (Bradbury et al., 2007; Endelman et al., 2012). Heatmap indicates kinship value across accessions.*

4.1.2.3 Summary of phenotypic diversity in seed traits identified in selected panel

The selected *Indica* panel was next assessed for coverage of known natural variation in agronomic traits represented in the full 3K-RG dataset. This method is as described previously in development of the 'MiniCore' of the 3K-RG (A. Kumar et al., 2019). Phenotypic data was retrieved from the publicly available qualitative morpho-agronomic data available for the 3K-RG (IRRI GRIN-GLOBAL, https://gringlobal.irri.org/gringlobal/), and four agronomic traits were selected for the analysis: seed coat colour at post-harvest (SCCO_REV), seedling height (SDHT_CODE), spikelet fertility (SPKF) and panicle length at post-harvest (PLT_CODE_POST). The distribution of trait variation was compared between available data for the 3K-RG cultivars (Figure 4.4), namely 207 of the 218 accessions in the selected *Indica* panel, 1,337 of the 1,760 total *Indica* in the 3K-RG and 2,266 accessions in the 3,024 accessions of the 3K-RG.

Despite inclusion of significantly less accessions, the selected *Indica* panel represented similar quantitative distribution of variation in the agronomic traits as was seen in the full 3K-RG panels (Figure 4.4A). Notably, some extremes of the categories such as variable purple seed coat colour, completely sterile spikelet fertility and very short (<11cm) panicle length at post-harvest, that are present at reduced counts in the full sets were not represented in the smaller panel. Considering the wide genetic diversity included in a small number of genotypes compared to the full *Indica* and 3K-RG panel, and the small number of counts of these in the full sets (Figure 4.4A), it is suggested that phenotypic diversity is appropriately reflected in the selected panel. In addition, seed of cultivars in the selected *Indica* panel were obtained from IRRI Genebank (https://www.irri.org/international-rice-genebank) and significant variation in coat colour, grain shape, appearance, and size was observed, complementing the GRIN-GLOBAL results (Figure 4.4B). Overall, agronomic trait diversity provides further evidence for successful design of an *Indica* panel that represents both natural genotypic and variation present in the full 3K-RG.

A

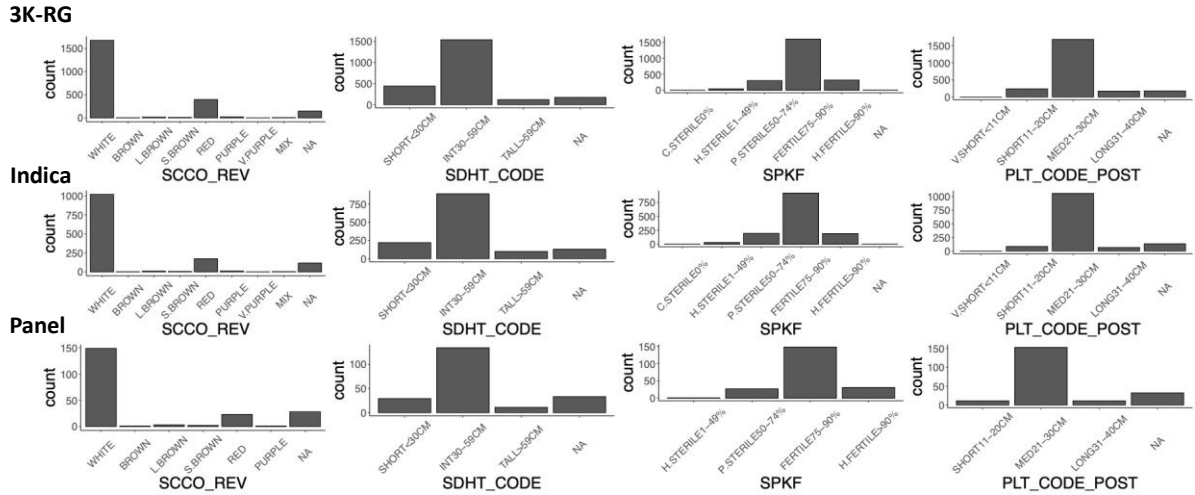

B

Figure 4.4 Phenotypic variation in agronomic traits assessed across selected panel compared to full Indica and 3K-RG. *(A) Seed coat colour at post-harvest (SCCO_REV), seedling height (SDHT_CODE), spikelet fertility (SPKF) and panicle length at post-harvest (PLT_CODE_POST) were compared. All qualitative categories are as defined by IRRI. For seed coat colour, pericarp colour is either white, brown, light brown, speckled brown, red, purple, variable purple or mixed. Seedling height was categorized as short (<30cm), intermediate (30-59cm) and tall (>59cm). Spikelet fertility ranged from completely sterile (0%), highly sterile (1-49%), partially sterile (50-74%), fertile (75-90%) to highly fertile (>90%). Panicle length from axis was categorized as very short (<11cm), short (11-20cm), medium (21-30cm) and long (31-40cm). (B) Variation in seed coat colour (caryopsis-pericarp) was observed for the selected panel. Cultivar ID is noted on white labels and seed hull and seed caryopsis-pericarp of each cultivar is below label. 60 lines with representative variation of the 207 are shown.*

4.1.3 Discussion

An *Indica* panel of ~200 accessions that maintains full representation of 89 countries and nine *Indica* subpopulations present in the 3K-RG was selected. The panel has significant genotypic diversity and low population structure and kinship among individuals, as shown by PCA and kinship analysis. In addition, phenotypic diversity

in agronomically relevant traits that are characterised in the full 3K-RG and *Indica* subpopulation of the 3K-RG are well represented.

The availability of the small, diverse *Indica* panel allows for efficient trait evaluation and genetic association analyses of the *Indica* subpopulation in rice.

4.2 Analysis of natural variation in AM colonisation and response in a diverse panel of rice

4.2.1 Introduction

Much of the research on AMF-rice interactions has focused on molecular characterisation of the components driving efficient symbiosis (Choi et al., 2020; Guimil et al., 2005; C. Gutjahr et al., 2008; C. Gutjahr et al., 2012; C. Gutjahr et al., 2009, 2015; Kobae et al., 2018; Miyata et al., 2014; Shi et al., 2021; Yang et al., 2012). Despite this, limited knowledge is available for the understanding of cultivar differences in AM colonisation level. Diversity in root colonisation has been primarily described in pot experiments comparing limited genotype numbers (Gao et al., 2007; H. Li et al., 2016; Suzuki et al., 2015). Importantly, studies in field conditions have additionally noted variation, although in some cases no change in colonisation level was identified between cultivars (Diedhiou et al., 2016; Jeong et al., 2015; Sisaphaithong et al., 2017; M. Vallino et al., 2009). More recently, larger numbers of rice cultivars have been compared. Davidson et al., assessed 334 accessions of the RDP1 for growth and colonisation responses to *R. irregularis* inoculation. Hyphal root colonisation varied from 22 to 90% across the cultivars and varied between subpopulations. Mean colonization rates between *indica, temperate japonica and tropical japonica* were greater than in *aus* and there was large variation within each subgroup, partially mapping to country and region of origin (Davidson et al., 2019).

In addition to root colonisation, natural variation in plant response to AMF-inoculation ‘mycorrhizal responsiveness’ has been observed in traits such as growth, stature, dry weight, nutrition and yield (Fester et al., 2011; Sawers et al., 2008; Taylor et al., 2015). It has been suggested that cultivar response to root colonisation falls on a

continuum between mutualism and parasitism (Johnson et al., 1997), determined by environment and plant and AMF genetic factors. Accordingly, positive and negative responsiveness have been reported across many plant species (Galván et al., 2011; B. A. D. Hetrick et al., 1992; Kaeppler et al., 2000; Lehmann et al., 2012; Lehnert et al., 2018; Suzuki et al., 2015; Thirkell et al., 2022; Watts-Williams et al., 2019; Xavier & Germida, 1998; Y. G. Zhu et al., 2001).

In rice, field-trials in Senegal identified ecotype-specific responses to AMF inoculation. Some upland cultivars had an enhanced response to inoculation in terms of grain yield, harvest index and spikelet fertility (Diedhiou et al., 2016). In addition, varietal differences in yield responsiveness were observed in a panel of rice seedlings pre-colonised with AMF before growth in the field in India (Sisaphaithong et al., 2017). In a larger-scale study in the glasshouse comparing 64 rice cultivars inoculated with *F. mossae* AMF, positive and negative growth responses were observed, dependent on cultivar (Suzuki et al., 2015). Similarly, in a comparison of over 300 diverse rice cultivars in the RDP1, Davidson et al. report variation in shoot dry weight between subpopulations and within *Indica* lines inoculated with *R. irregularis* AMF (Davidson et al., 2019). Environmental factors have also been mapped. For example, differences in mycorrhizal responsiveness in terms of growth promotion and resistance to the rice blast fungus *Magnaporthe oryzae* was observed in some elite rice cultivars grown in flooded fields in the USA (Campo et al., 2020). A recent study found shading and flooding caused negative MGR in two rice cultivars (Y. Wang et al., 2021). Overall, diversity in AM colonisation and mycorrhizal responsiveness has been previously described, although only few studies compare large numbers of genotypes, and the effects of environment are still being explored.

The hallmark benefit of AMF on the plant host is the potential for enhanced phosphorous (P) nutrition through the symbiotic route (Bucher, 2007; Yang et al., 2012). Genetic diversity in root colonisation and phosphate transporter expression has been noted previously in rice, and suggested that host ability to profit from symbiosis is genetically driven (Jeong et al., 2015). Natural variation in shoot P content, root colonisation and mycorrhizal phosphorous uptake has been noted previously in six maize cultivars, and superior lines correlated with increased root hyphae and high P uptake (Sawers et al., 2017). In contrast, variation in mycorrhizal

growth response has been reported in a spring wheat mapping population and was independent to mycorrhizal shoot P content (Thirkell et al., 2022). Previous reports in rice found that varietal differences in biomass and grain yield response to AMF inoculation in three cultivars were independent to shoot P content (Sisaphaithong et al., 2017) and that additional factors are involved. Such differences in the profit of increased P on biomass should be further explored to determine genetic factors involved.

Host response to AMF inoculation is commonly described as the relative performance of AMF-inoculated plants compared to plants growth in AMF absence. Changes in biomass are described as mycorrhizal growth response (MGR) (B. A. D. Hetrick et al., 1992) and several studies have reported QTLs associated to such responsiveness (Galván et al., 2011; B. A. Hetrick et al., 1995; Kaeppler et al., 2000; Thirkell et al., 2022). Notably, a seemingly equivalent large positive response could be due an increased response relative to very poor performance under non-AM conditions (dependence) or a boosted performance beyond typical levels (benefit), as described in Figure 4.5. This is evidenced in recent work in spring wheat that found a negative correlation of MGR to biomass in non-mycorrhizal state, suggesting that large responses are confounded by dependence (Thirkell et al., 2022). It is non-dependence driven benefit that is the most agronomically relevant in the potential for use of AMF as natural biofertilizers promoting plant performance (Ramírez-Flores et al., 2020; Sawers et al., 2017). Methods have been reported to distinguish dependence and benefit (Ramírez-Flores et al., 2020; Sawers et al., 2010) and allow for identification of positively benefitting lines in responsiveness analyses. In addition, plant host factors specifically associated to host dependence and benefit can be determined and, accordingly, QTLs associated to benefit have recently been described in maize (M. Li et al., 2022; Ramírez-Flores et al., 2020). Such methods have exciting applications for the potential to facilitate breeding for predictable nutrition and yield responses in mycorrhizal crop plants.

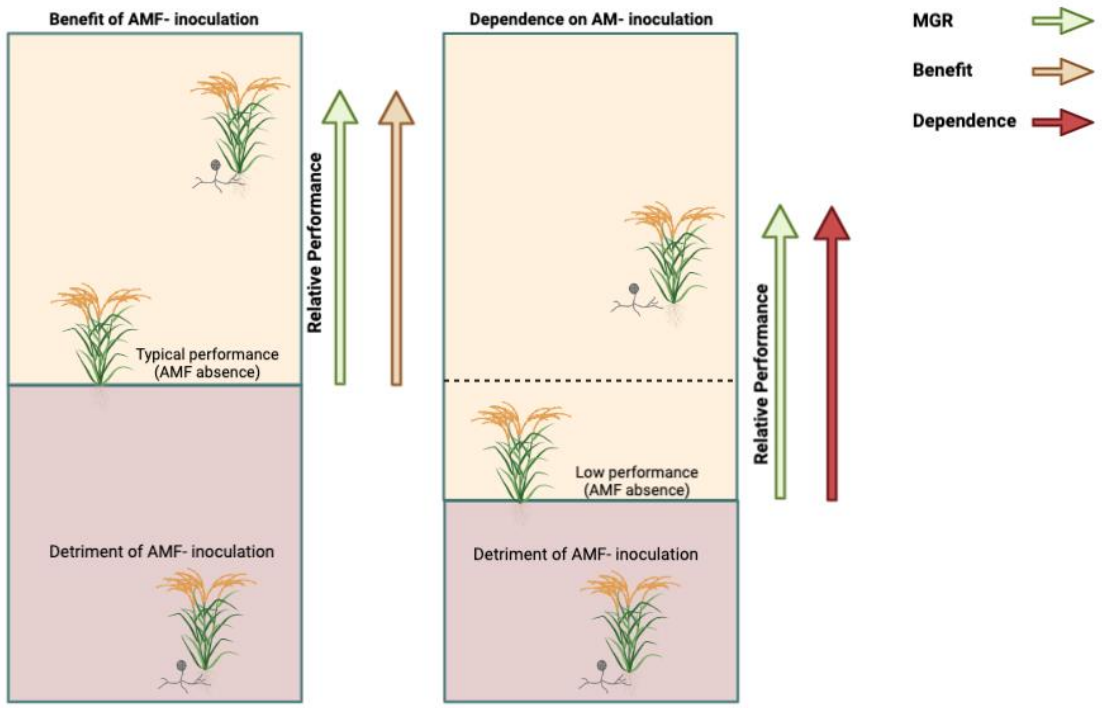

Figure 4.5 Relative mycorrhizal response confounds benefit and dependence. *A seemingly equivalent host response to AMF-inoculation (MGR, green arrow) can represent a boosted performance of a plant that performs poorly under AMF absence in given condition (dependence, red arrow) or it can be due to a boosted performance of a plant that already grows typically in the condition (benefit, yellow arrow). Figure adapted from* (Ramírez-Flores et al., 2020).

In this study, the hypothesis that there is natural variation in AM colonisation level and response across cultivars of the 3K-RG was assessed in the diverse *Indica* panel. The effect of AMF inoculation on plant biomass and shoot mineral content was further determined, allowing comparison of over 200 cultivars. The study also aimed to use targeted analyses to identify lines that are highly responsive to AMF-inoculation, specifically pursuing variation that is not correlated with non-mycorrhizal performance but specific to beneficial response.

4.2.2 Results

4.2.2.1 Experimental design for phenotype screen of the diverse *Indica* panel

The selected *Indica* panel (Table 2.19) was screened under both mock- and *R. irregularis* AMF-inoculated conditions in a glasshouse experiment grown in the Cambridge University Botanic Garden Experimental Glasshouse, Summer 2021 (Figure 4.6). A randomized block design was used in order to account for spatial variation in the glasshouse (Montgomery, 1984).

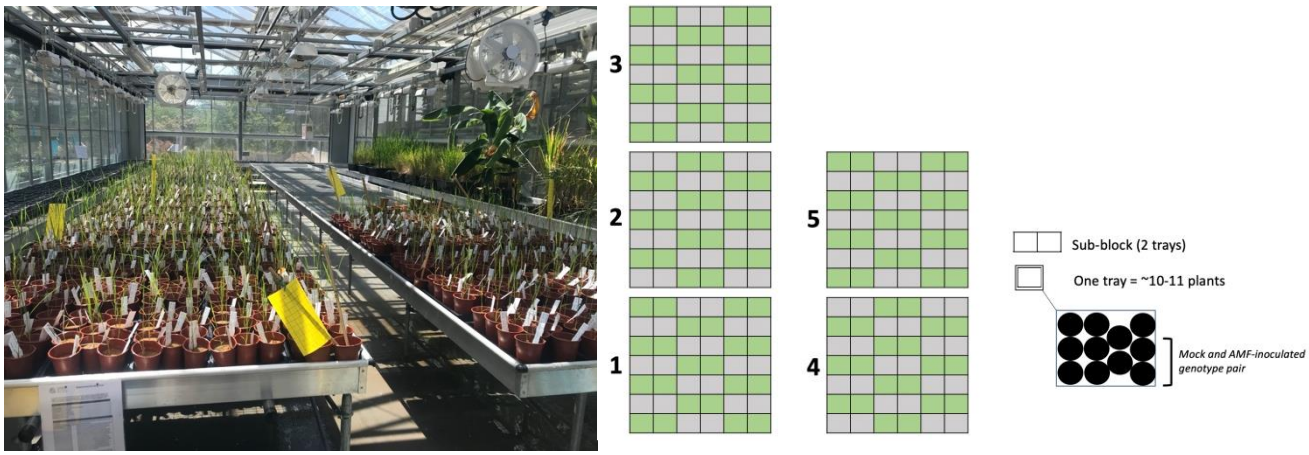

Figure 4.6 Randomized block design of the phenotypic screen conducted in the Indica panel. *The experiment was grown in a randomized block design in the glasshouse, including five 'genotype pair' (mock and AMF-inoculated) biological replicates per cultivar. Each replicate was in a block and included 42 sub-blocks of 10-11 plants, with ~2000 plants grown in total in the experiment. Plants were grown for eight weeks in pots of sterile quartz-sand medium mock and AMF-inoculated with R. irregularis spores suspended in H_2O.*

4.2.2.2 Investigating natural variation in AM abundance in diverse rice lines

To identify natural variation in AM symbiosis, AM colonisation was assessed the selected *Indica* panel. Since a correlation of blumenol abundance and root colonisation in AMF-inoculated plants of diverse rice accessions was confirmed earlier in the PhD project (Chapter Three), foliar abundance of blumenol was assessed only in AMF-inoculated lines and used as a high throughput marker of root colonisation.

Abundance of both 11-carboxyblumenol C-Glc and 11-hydroxyblumenol C-Glc was assessed in the panel. Significant natural variation in blumenol abundance was identified, as seen in histograms representing data distribution of the derivatives (Figure 4.7A-B). 11-carboxyblumenol C-Glc abundance ranged from 0.00 ng/g fw to 42,673.63 ng/g fw and 11-hydroxyblumenol C-Glc from 2.69 ng/g fw to 3,537.04 ng/g fw (Figure 4.7C).

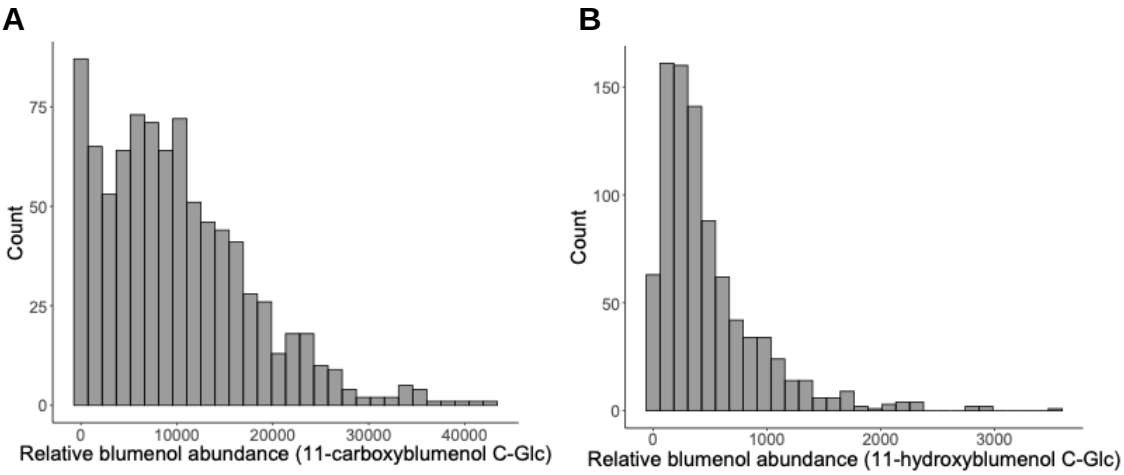

C

Variable	N	Mean	Std. Dev.	Min	Max
11-carboxyblumenol C-Glc	877	9920.75	7717.56	0.00	42673.63
11-hydroxyblumenol C-Glc	877	484.00	461.52	2.69	3537.04

Figure 4.7 Histograms of distribution of blumenol abundance. *Count of (A) 11-carboxyblumenol C-Glc and (B) 11-hydroxyblumenol C-Glc abundance in the selected panel (peak area ng/g fw). (C) Table of summary statistics for blumenol abundance. Global mean standard deviation, minimum and maximum valurs were analysed per trait, with N the number of observations. 4-5 biological replicates per cultivar were included. Data represents AMF-inoculated plants only.*

In order to determine the relative range of root colonisation corresponding to blumenol abundances observed across the panel, I assessed root colonisation in nine cultivars that were representative of low, average and high blumenol abundance compared to the global population mean of 9,920 ± 7,717.56 ng/g fw. A subset of these lines were used previously for correlation analyses described in Chapter Three (Figure 3.5). The data is replicated in Figure 4.8 and includes additional cultivars that were selected to determine relative intraradical colonisation in lines with the highest and lowest blumenol abundances of the panel. *ESCONDE CACHO, CHING*

C'HUNG, *CHAMA (DWARF)* and *HEGAR HANAH* had the four lowest abundances of blumenol at 199.68 ± 191.01 ng/g fw, 1569.21 ± 750.27 ng/g fw, 2160.00 ± 1637.25 ng/g fw, and 2399.62 ± 1849.14 ng/g fw respectively (Figure 4.8B). In contrast, *RUS RUSSEI, MEI FENG 9, SICAN* and *MIN ZAO 6* had the third, seventh, eighth and eleventh highest abundances at 26,587.18 ± 1976.48 ng/g fw, 22,995.67± 5192.63 ng/g fw, 2,1560.00 ± 6,574.53 ng/g fw and 18,996.31 ± 3,962.21 ng/g fw respectively (Figure 4.8B). Blumenol abundance in *ASU* was similar to global average at 10,050.62 ± 2,161.90 ng/g fw.

In low blumenol abundance lines, intraradical colonisation was statistically equivalent in *ESCONDE CACHO* and *CHAMA (DWARF)* at 6.2 ± 13.31% and 0.00 ± 0.00% respectively. Similarly, equivalent intraradical colonisation of 16.8 ± 24.5% and 20.00 ± 17.35% was observed in *CHING C'HUNG*, and *HEGAR HANAH* respectively. It is striking that *CHAMA(DWARF)* appears to have lost capability to associate with AMF and the line is an intriguing candidate for further analysis (Figure 4.8A). In high blumenol lines, average root colonisation was statistically equivalent at 55.3 ± 22.6%, 55.8 ± 13.3%, 56.25 ± 17.88% in *RUS RUSSEI, MEI FENG 9* and *SICAN* respectively. Intraradical colonisation of 36.20 ± 16.57% and 36.50 ± 10.02% was observed in *ASU* and *MIN ZAO 6* respectively (Figure 4.8A).

As observed previously, a good correlation between root colonisation and abundance of 11-carboxyblumenol C-Glc was observed (R^2=0.41, $p < 0.001$, Figure 4.8C). The strength of correlation was within the same range observed previously (M. Wang et al., 2018) and, slightly weaker, but comparable to model cultivars *Nipponbare* and *Shiokari,* n=2, included in the GWAS (R^2=0.64, $p < 0.001$, Figure 4.8C), corroborating previous findings (Chapter 3). This suggested that blumenol accumulation was representative of root colonisation in the panel and thus was used in further analyses of genetic variation in AM traits.

Natural variation in AM colonisation was therefore assessed further in the whole *Indica* panel by considering 11-carboxyblumenol C-Glc abundance. Significant variation in abundance was identified across subpopulations within the *Indica* panel (Figure 4.9A), with mean foliar 11-carboxyblumenol C-Glc abundance ranging over 150-fold from 199.68 ± 191.02 ng/g fw in *ESCONDE CACHO* to 32,762.78 ± 6449.69 ng/g fw in

BONG SEN (Supplementary Table 4.1). Root colonisation analysis in cultivars with highest and lowest blumenol abundance (Figure 4.8A) suggests this is likely equivalent to a range of ~0-56% root colonisation. Such natural variation in root colonisation has been observed previously in diverse lines of RDP1 (Davidson et al., 2019). In addition, since it was previously found that ecotype had a significant effect on root colonisation, with similar levels in *indica, temperate japonica* and *tropical japonica* but reduced colonisation in *aus* (Davidson et al., 2019), the effect of *Indica* subpopulation was assessed. Since the data was not normally distributed (Shapiro-Wilk, $p < 0.05$), a non-parametric Kruskal-Wallis test was performed to determine the impact of subpopulation on blumenol abundance. There was no significant difference in blumenol abundance between the *Indica* subpopulations (KW, $p > 0.05$, Figure 4.9B) or compared to the cv. *japonica* model cultivars *Nipponbare* and *Shiokari* (KW, $p < 0.05$, Figure 4.9B), although as only two cultivars are included, compared to over 200 *Indica* cultivars, a full comparison between the *indica* and *japonica* ecotypes cannot be determined.

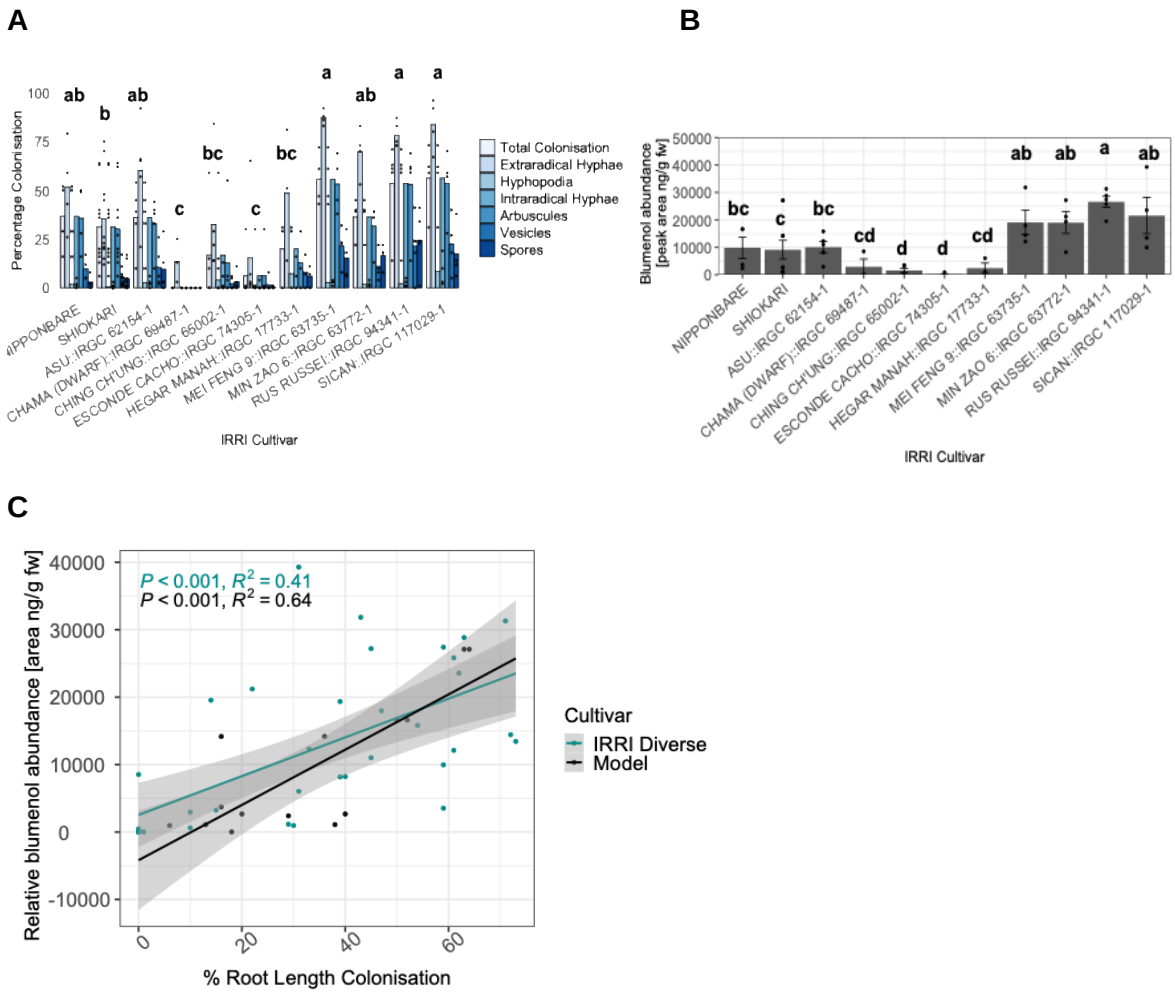

Figure 4.8 Correlation of AMF-indicative blumenol derivatives in model cultivars and genetically diverse rice accessions from GWAS. *AM colonization data of AMF-inoculated model cultivars Nipponbare and Shiokari and diverse rice genotypes selected from 3K-RG analysed at 8 weeks post inoculation by (A) microscopic analysis of the percentage of root length colonization (%RLC) and (B) blumenol accumulation (11-carboxyblumenol C-Glc) in foliar material from the same samples. (A) Bar charts show root colonization data, Percentage of Total Colonisation, Extraradical Hyphae (EH), Hyphopodia (H), Intraradical Hyphae (IH), Arbuscules (A), Vesicles (V) and Spores (S) is indicated per percent total in root length. Error bars represent mean ± standard error. Data points of 3-5 biological replicates of each genotype are shown, with 10 technical replicates used in root counting. (B) Bar charts show foliar blumenol accumulation. Data points of 3-5 biological replicates are shown. Error bars represent mean ± standard error. A Kruskal-Wallis test was performed, followed by post-hoc pairwise comparison using the agricolae R package. Different letters represent significant difference (p-value <0.05) between genotype conditions (C) Linear regression identifies overall correlation in all cultivars. Diverse lines (n=9) are noted in teal and model (n=2) in black. R^2 and p value of regression is denoted in each case.*

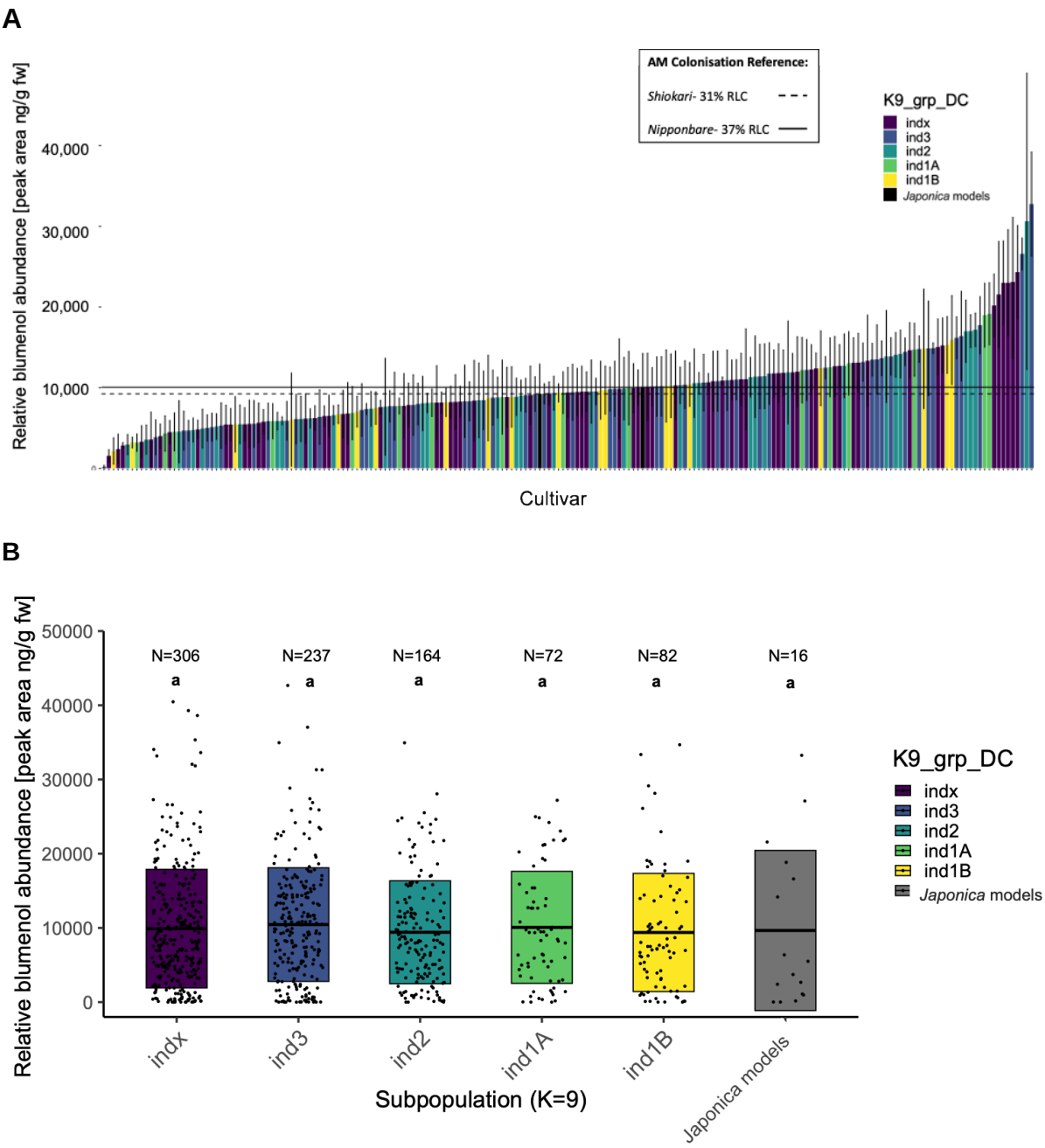

Figure 4.9 Mean abundance of 11-carboxyblumenol C-Glc identified in shoot material of 198 genotypes of Indica* panel *inoculated with AMF. *(A) Bar chart height shows mean 11-carboxyblumenol C-Glc abundance and error bars show mean ± standard error. Colour of bar represents Indica subpopulation as defined by 3K-RG, K=9 sub-populations. Bars are ordered by abundance and cultivar on the axis. Data points of 4-6 biological replicates are shown for indica lines and 7-8 biological replicates for japonica models. Black lines indicate abundance of blumenol in model cv japonica cultivars Nipponbare (solid) and Shiokari (dashed). (B) Data are presented as box plots displaying mean +- SEM, split by the mean. Individual black points correspond to one data point, N is the number of observations per group. A Kruskal-Wallis test was performed, followed by post-hoc pairwise comparison using the agricolae R package. Different letters represent significant difference (p-value <0.05) between genotype conditions.*

4.2.2.3 Growth trait response to AMF inoculation

To assess growth responses to AMF, the following growth and biomass traits were measured and compared between mock- and AMF-inoculated plants: seedling height (4 weeks post inoculation, wpi), vegetative height (eight wpi) and vegetative biomass including root fresh weight (RFW), root dry weight (RDW), shoot fresh weight (SFW) and shoot dry weight (SDW). Significant phenotypic variation was identified for all traits, as seen in histograms representing data distribution for mock- and AMF- inoculated plants (Figure 4.10).

A two-way ANOVA revealed the effects of cultivar and AMF inoculation on variation in growth traits (Table 4.1). Whilst cultivar explained a large extent of variation (ANOVA, $p < 0.01$), the effect of AMF inoculation was trait dependent (Table 4.1). For example, inoculation had a very small significant effect on seedling height (ANOVA, $F(1, 1177) = 6.66$, $p = 0.010$) and increased the global population mean 3.57% from 15.4 ± 5.0 cm to 15.95 ± 5.1 cm. In contrast, inoculation had a non-significant effect on variation in vegetative height (ANOVA, $F(1, 1168) = 1.82$, $p = 0.177$).

A non-significant effect of inoculation was observed for RDW (ANOVA, ($F(1, 1120) = 0.98$, $p = 0.323$) but a small, significant effect was evident for RFW (ANOVA, $F(1, 1173) = 24.98$, $p < .001$). AMF-inoculation increased global population mean RFW 9.0% from 0.956 ± 0.37g to 1.042 ± 0.40g (Table 4.1) The interaction of cultivar and inoculation was non-significant (ANOVA, $F(198, 1173) =0.95$, $p = 0.685$). Similarly, inoculation had a small, significant effect on both SDW (ANOVA, $F(1, 1164) = 9.72$, $p = 0.002$) and SFW (ANOVA, $F(1, 1149) = 43.70$, $p < .001$), but the interaction with cultivar was non-significant in both cases, (ANOVA, $p > 0.05$). AMF inoculation increased shoot biomass 4.73% from 0.148 ± 0.05g to 0.155 ± 0.05g SDW and 10.75% from 0.735 ± 0.26g to 0.814 ± 0.287g SFW (Table 4.1).

Overall, a large diversity in height and biomass parameters was observed between the *Indica* cultivars. This concurs previous reports of phenotypic diversity in growth traits observed in panels representing the 3K-RG (Abbai et al., 2019). The effect of inoculation was small but significant and increased global population seedling height

by 4% and vegetative biomass by ~ 10%. This concurs previous findings of AMF inoculation affecting biomass parameters in host rice plants (Campo et al., 2020; Davidson et al., 2019; Diedhiou et al., 2016; Sisaphaithong et al., 2017; Suzuki et al., 2015).

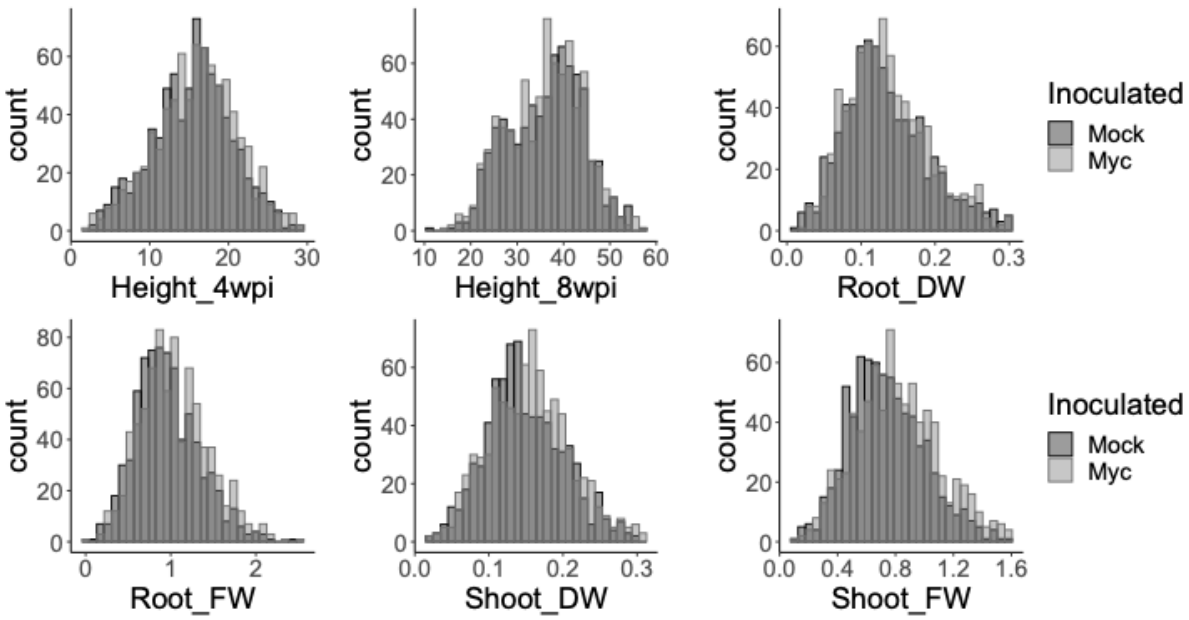

Figure 4.10 Histograms of distribution of growth traits screened in the panel in mock- and AMF-inoculated conditions. *Count of height at 4 (Height_4wpi) and 8 weeks (Height_8wpi) post inoculation (wpi), shoot dry weight (Shoot_DW), root dry weight (Root_DW), shoot fresh weight (Shoot_FW), root fresh weight (Root_FW), root to shoot ratio of fresh and dry weight were measured (Root:Shoot_FW/Root:Shoot_DW) is given. 4-5 biological replicates per cultivar per condition was included. Colour indicates mock- (black) or AMF- (grey) inoculated plants.*

Table 4.1 Descriptive summary and statistics in growth traits. *Height at 4 (Height_4wpi) and 8 weeks (Height_8wpi) post inoculation (wpi), shoot dry weight (Shoot_DW), root dry weight (Root_DW), shoot fresh weight (Shoot_FW), root fresh weight (Root_FW were measured. 4-5 biological replicates per cultivar per condition was measured. Global mean and standard deviation were analysed per trait, with N the number of observations. A Two-way ANOVA of cultivar and inoculation was performed, and p value significance is indicated: ** p < 0.001, * p < 0.05, NS not statistically significant, p > 0.05*

Variable	Cultivar	Inoculation	Cultivar x Inoculation	Treatment	N	Mean	Std. Dev.
Height_4wpi	**	*	NS	Mock	768	15.4	4.979
				AMF-inoculated	806	15.945	5.137
Height_8wpi	**	NS	NS	Mock	762	36.204	7.966
				AMF-inoculated	803	35.972	8.046
Root_DW	**	NS	NS	Mock	731	0.134	0.057
				AMF-inoculated	786	0.136	0.054
Root_FW	**	**	NS	Mock	759	0.956	0.37
				AMF-inoculated	811	1.042	0.4
Shoot_DW	**	*	NS	Mock	751	0.148	0.053
				AMF-inoculated	810	0.155	0.054
Shoot_FW	**	*	NS	Mock	749	0.735	0.259
				AMF-inoculated	796	0.814	0.287

A correlation analysis was used to identify the relationship between blumenol abundance and growth in AMF-inoculated plants. Although a positive correlation was identified between 11-carboxyblumenol C-Glc and 11-hydroxyblumenol C-Glc, abundance was not directly equivalent (r=0.69, p < 0.01, Figure 4.11). This concurs previous observations of differences in abundance of the derivatives reported in Chapter Three. Among growth traits, a weak positive correlation was identified between abundance of 11-carboxyblumenol-C-glc and shoot (r=0.38 fresh, r=0.34 dry, respectively, p < 0.01, Figure 4.11A-B) and root biomass (r=0.32 fresh, r=0.23 dry, p < 0.01, Figure 4.11C-D). A weak positive correlation to height was also observed (r < 0.16, p < 0.01, Figure 4.11E). This suggests that AM colonisation level partially correlates to increased biomass and height, but that this is not the only factor involved. Such an observation of lack of simple correlation has been reported previously, where differences in biomass in mycorrhizal plants was observed in maize and wheat cultivars with equivalent levels of root colonisation (Sawers et al., 2017; Thirkell et al., 2022).

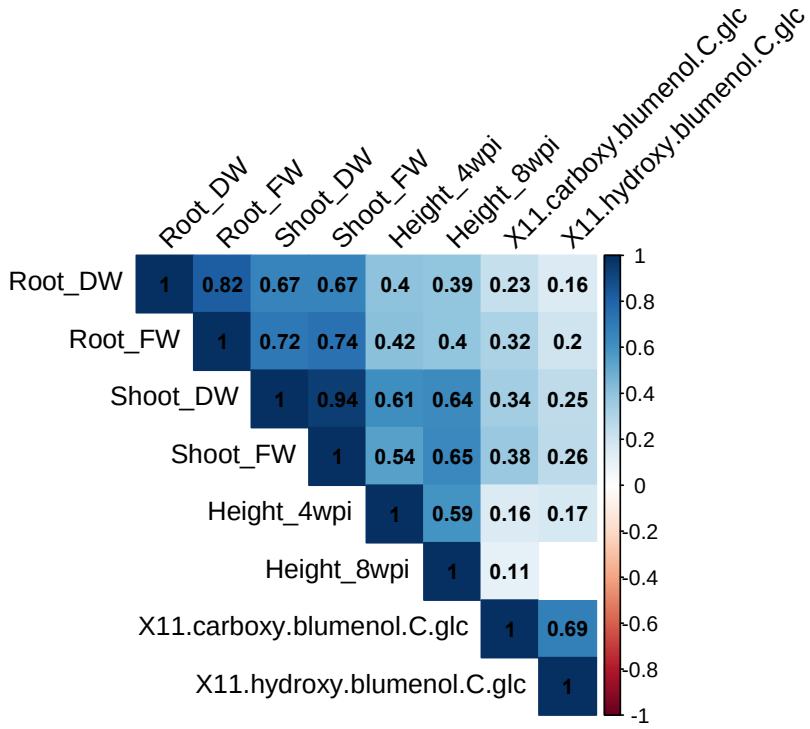

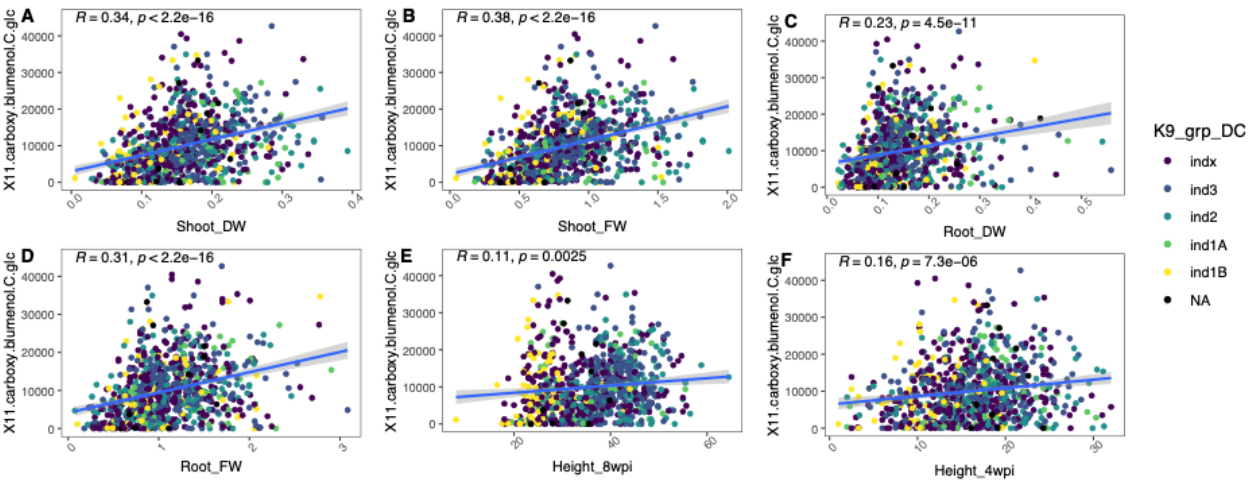

Figure 4.11 Correlations between blumenol abundance and traits measured in AMF-inoculated plants only. *Correlation matrix of traits including height at 4 (Height_4wpi) and 8 weeks (Height_8wpi) post inoculation with AMF, shoot dry weight (Shoot_DW), root dry weight (Root_DW), shoot fresh weight (Shoot_FW), root fresh weight (Root_FW), AMF-indicative blumenols 11-carboxyblumenol C-Glc (X11.carboxy.blumenol.C.glc) and 11-hydroxyblumenol C-Glc (X11.hydroxy.blumenol.C.glc) The blue colour shows positive association and red colour indicates negative association, with the intensity of the colour intensity and size of circle indicating degree of association, p<0.01. Non-significant correlations are blank. (A-F) Linear regression plots show correlation of total data. Pearsons correlation coefficient (R) and significance value are shown. Each point indicates individual plant measurements and colour represents Indica subpopulation as defined by 3K-RG, K=9 sub-populations.*

4.2.2.4 Ionome trait screening

To investigate natural variation in the foliar ionome, the mineral element composition of the leaf, of the diverse *Indica* panel, foliar concentration of 16 mineral elements (Li, Na, Mg, P, S, K, Ca, Mn, Fe, Co, Ni, Cu, Zn, Rb, Sr and Mo) was assessed. Natural variation in concentration was observed across all elements, as evidenced in histograms of data distribution for mock- and AMF inoculated plants (Figure 4.12).

A two-way ANOVA revealed the effects of cultivar and AMF inoculation on mean foliar ion concentration, summarised in Table 4.2. Data was $\log_{10}$ transformed to fit assumptions of normality and no interaction term was included since replicates were pooled for ICP analysis. First, macronutrients, namely phosphorous, potassium, calcium, magnesium, and sulphur were assessed. Cultivar had a large effect on concentration of all macronutrients (ANOVA, $p < 0.001$, Table 4.2), but the size and significance of the effect of inoculation was element dependent. For example, inoculation had a non-significant effect on foliar potassium (ANOVA, $F(1, 201) = 0.15$, $p = 0.702$) and a small, significant effect on foliar sulphur concentration

(ANOVA, $F(1, 201) = 9.69$, $p = 0.002$). Global mean foliar sulphur concentration increased 3.14% from 2866.76 ± 588.12 to 2956.78 ± 470.73 ppm upon AMF inoculation (Figure 4.12, Table 4.2).

A significant, medium effect of inoculation was observed in foliar magnesium (ANOVA, $F(1,201) = 23.13$, $p < .001$) and calcium concentration $F(1, 201) = 26.91$, $p < .001$). Global mean foliar magnesium concentration increased 4.83% from 2594.74 ± 502.70 to 2720.28 ± 512.64 ppm upon AMF inoculation (Figure 4.12, Table 4.2) and global mean foliar calcium concentration increased 9.10% from 4441.04 ± 1009.76 to 4876.27 ± 1096.92 ppm upon AMF inoculation (Figure 4.12, Table 4.2). Notably, inoculation had a large, significant effect on foliar phosphorous concentration (ANOVA, $F(1, 201) = 127.57$, $p < .001$). Global population mean increased 16.63% from 848.43 ± 123.31 ppm to 989.54 ± 188.35 ppm upon AMF-inoculation (Figure 4.12, Table 4.2).

The effect of cultivar and inoculation on mean micronutrient and other mineral element concentrations was additionally assessed. Cultivar had a significant effect on all elements (ANOVA, $p<0.001$, Table 4.2), but the effect of inoculation was again element dependent. For example, inoculation had a significant, medium effect on foliar manganese (ANOVA, $F(1, 201) = 13.13$, $p < .001$), iron (ANOVA, $F(1, 201) = 27.10$, $p < .001$) and strontium (ANOVA, $F(1, 201) = 19.70$, $p < .001$) and a significant, large effect on foliar nickel (ANOVA, $F(1, 201) = 48.82$, $p < .001$), copper ($F(1, 201) = 53.08$, $p < .001$) and molybdenum (ANOVA, $F(1, 201) = 50.62$, $p < .001$), (Figure 4.12, Table 4.2).

Overall, natural variation in the shoot ionome was observed across the diverse *Indica* panel, as evidenced by the wide spread of data observed on histograms and the significant effect of cultivar on foliar concentration of 13 of the 16 mineral elements measured. In addition, AMF-inoculation affected the shoot ionome, as reported recently in maize (M. Li et al., 2022). The largest positive effect of AMF inoculation was observed for foliar phosphorous content. This corroborates reports that AMF can provide an alternative, symbiotic route for increased phosphate uptake in the rice host in low nutrient conditions (Yang et al., 2012).

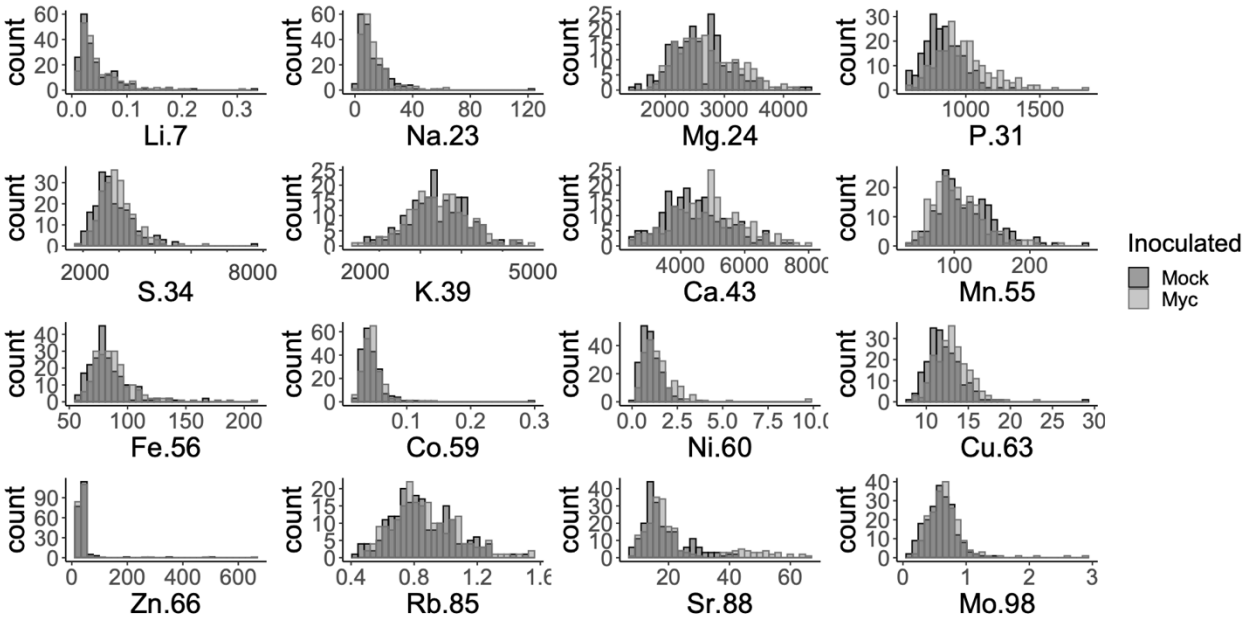

Figure 4.12 Histograms of distribution of growth traits screened in the panel in mock- and AMF-inoculated conditions.. *Phenotypic distribution of the following foliar ion concentrations (ppm) were measured: lithium (Li.7), sodium (Na.23), magnesium (Mg.24), phosphate (P.31), sulphur (S.34), potassium (K.39), calcium (Ca.43), manganate (Mn.55), iron (Fe.56), cobalt (Co.59), nickel (Ni.60), copper (Cu.63), zinc (Zn.66), rubidium (Ru.85), strontium (Sr.88) and molybdenum (Mo.98). Histograms show count of mean foliar concentration. 5 biological replicate plants were pooled per cultivar for ICP analysis.. Colour indicates mock- (black) or AMF- (grey) inoculated plants.*

Table 4.2 Descriptive summary and statistics in foliar ionome. *The following foliar ion concentrations (ppm) were measured: lithium (Li.7), sodium (Na.23), magnesium (Mg.24), phosphate (P.31), sulphur (S.34), potassium (K.39), calcium (Ca.43), manganate (Mn.55), iron (Fe.56), cobalt (Co.59), nickel (Ni.60), copper (Cu.63), zinc (Zn.66), rubidium (Ru.85), strontium (Sr.88) and molybdenum (Mo.98). Log_{10} transformed for normal distribution. ** $p < 0.001$, * $p < 0.05$, NS not statistically significant, $p > 0.05$. 5 biological replicate plants were pooled per cultivar for ICP analysis. Global mean and standard deviation were analysed per trait, with N the number of observations. A Two-way ANOVA of cultivar and inoculation was performed, and p value significance is indicated: ** $p < 0.001$, * $p < 0.05$, NS not statistically significant, $p > 0.05$*

Variable	Cultivar	Inoculation	Type	Inoculated?	N	Mean	Std. Dev.
Ca.43	**	**	Macronutrient	Mock	202	4441.04	1009.76
				AMF-inoculated	202	4876.27	1096.92
Co.59	**	*	Element	Mock	202	0.05	0.02
				AMF-inoculated	202	0.05	0.02
Cu.63	**	**	Element	Mock	202	12.14	2.20
				AMF-inoculated	202	13.13	2.05
Fe.56	**	**	Element	Mock	202	82.58	16.94
				AMF-inoculated	202	88.75	20.32
K.39	**	NS	Macronutrient	Mock	202	27127.85	3614.76
				AMF-inoculated	202	27249.76	3752.13
Li.7	**	*	Element	Mock	202	0.04	0.04
				AMF-inoculated	202	0.05	0.04
Mg.24	**	**	Macronutrient	Mock	202	2594.74	502.70
				AMF-inoculated	202	2720.28	512.64
Mn.55	**	**	Element	Mock	202	115.21	36.67
				AMF-inoculated	202	104.26	33.98
Mo.98	**	**	Element	Mock	202	0.60	0.23
				AMF-inoculated	202	0.69	0.33
Na.23	**	*	Element	Mock	202	12.49	11.66
				AMF-inoculated	202	13.09	10.41
Ni.60	**	**	Element	Mock	202	1.05	0.55
				AMF-inoculated	202	1.53	1.14
P.31	**	**	Macronutrient	Mock	202	848.43	123.31
				AMF-inoculated	202	989.54	188.35
Rb.85	**	NS	Element	Mock	202	0.85	0.20
				AMF-inoculated	202	0.87	0.21
S.34	**	*	Macronutrient	Mock	202	2866.76	588.12
				AMF-inoculated	202	2956.78	470.73
Sr.88	**	**	Element	Mock	202	18.47	7.23
				AMF-inoculated	202	23.06	13.49
Zn.66	*	NS	Element	Mock	202	41.16	42.57
				AMF-inoculated	202	42.98	58.93

Next, a Pearson's correlation analysis was used to identify the relationship between blumenol abundance and ion composition in AMF-inoculated plants. A weak positive correlation was identified between abundance of 11-carboxyblumenol C-Glc and foliar P concentration ($r = 0.24$, $p < 0.01$, Figure 4.13B) and Cu concentration ($r = 0.23$, $p < 0.01$, Figure 4.13B). This concurs the positive effect of AMF inoculation on foliar concentration of these ions (Table 4.2). In addition, a weak negative correlation between abundance of 11-carboxyblumenol C-Glc and foliar Co ($r = 0.15$, $p < 0.01$, Figure 4.13B) was also observed.

The experiment was conducted in P_i deplete conditions and it was therefore expected that variation in shoot biomass would be driven by increased nutrient uptake from established symbiosis. A weak positive correlation of shoot biomass to rubidium was observed ($r = 0.15$, $p < 0.01$, Figure 4.13A) and surprisingly, no correlation was observed with foliar phosphorous content ($r = -0.041$, $p = 0.57$, Figure 4.12 & 4.13). Independence of yield response to AMF to shoot phosphorous content has been observed previously in field trials in rice, suggesting other factors are involved (Sisaphaithong et al., 2017). This is unlike maize, where previous studies identified correlation of increased shoot biomass with increased shoot P content in six AMF-inoculated diverse cultivars (Sawers et al., 2017).

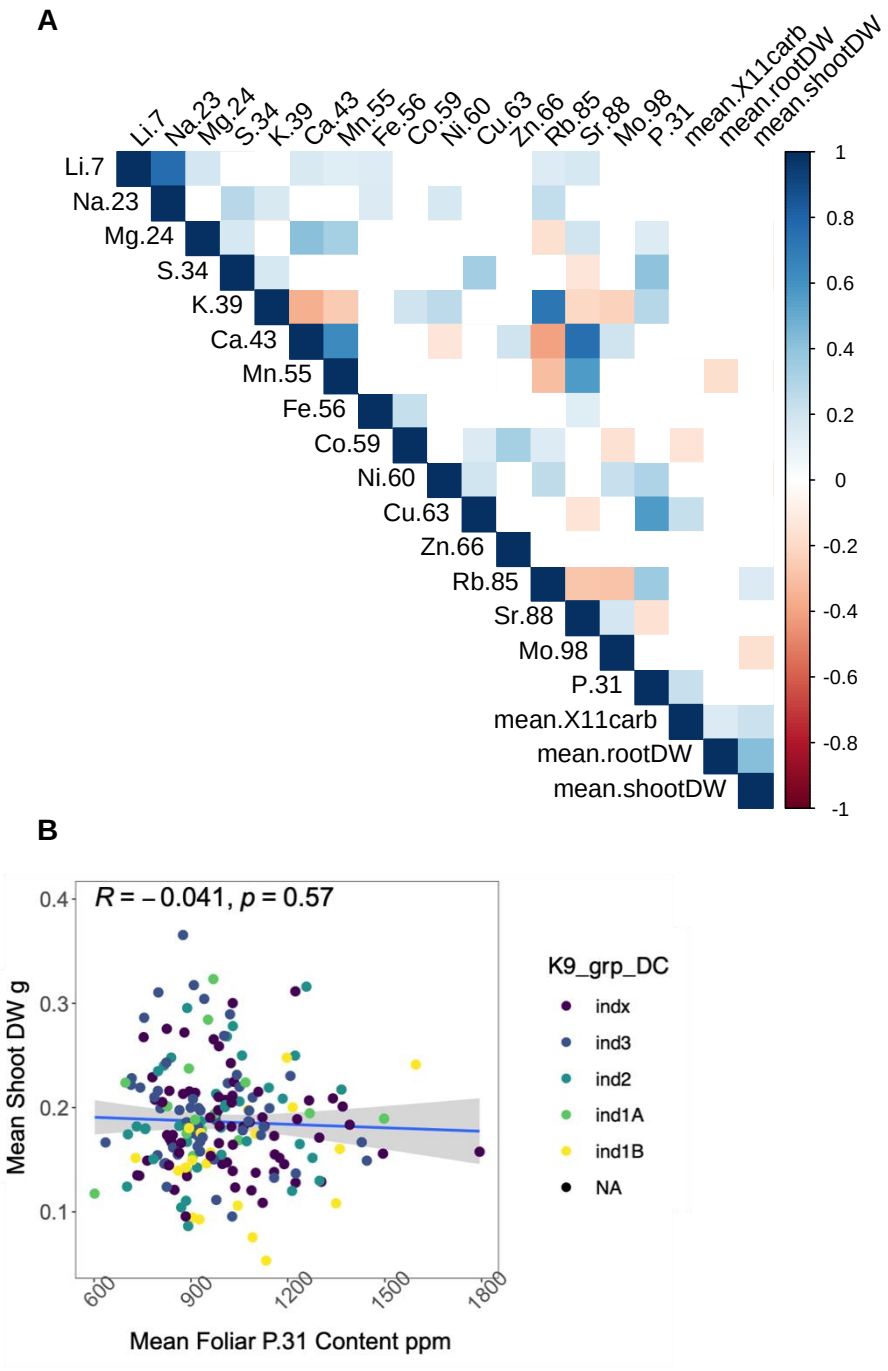

Figure 4.13 Correlation of blumenol, growth parameters and foliar ion composition. *(A) Correlation matrix of mean shoot dry weight (mean.shootDW), root dry weight (mean.rootDW), 11-carboxyblumenol C-Glc abundance (mean.X11carb) and foliar ion concentration (ppm) of lithium (Li.7), sodium (Na.23), magnesium (Mg.24), phosphate (P.31), sulphur (S.34), potassium (K.39), calcium (Ca.43), manganate (Mn.55), iron (Fe.56), cobalt (Co.59), nickel (Ni.60), copper (Cu.63), zinc (Zn.66), rubidium (Ru.85), strontium (Sr.88) and molybdenum (Mo.98). The blue colour shows positive association and red colour indicates negative association, with the intensity of the colour intensity and size of circle indicating degree of association, p<0.01. Non-significant correlations are blank. (B) Linear regression plot shows correlation of mean data per cultivar of shoot DW and foliar P content, with 4-5 biological replicates included in mean calculation. Pearson's correlation coefficient (R) and significance value are shown. Each point indicates cultivar and colour represents Indica subpopulation as defined by 3K-RG,K=9 sub-populations.*

4.2.2.5 Summary of diversity in AM responsiveness identified in diverse rice lines

Diversity in growth response to AMF-inoculation was further evaluated across the lines using 'relative mycorrhizal responsiveness' MGR (Janos, 2007) :

$$Relative\ mycorrhizal\ responsiveness\ (\%), mycorrhizal\ growth\ response\ (MGR) = \frac{(Mean\ AMF\ inoculated - Mean\ Mock\ inoculated)}{Mean\ Mock\ inoculated}\ x\ 100$$

Natural variation in shoot and root dry weight responsiveness was evident across the *Indica* panel, with negative and positive responsiveness observed in both cases (Figure 4.14). For example, SDW MGR ranged from -70.45% in *PERUBAK LUEY* and -48.56% in *ALAGUSAMBA* to 196.00% in *SABRAN* and 160.65% in *ORIONE.* Similarly, RDW MGR ranged from -60.60% in *HEGAR MANEH* and -57.94% in *VEN THAP* to 126.17% in *CHANDINA* and 123.15% in *PERUBAK LUEY.* Since the data was not normally distributed (Shapiro-Wilk, $p < 0.05$), a non-parametric Kruskal-Wallis rank sum test was performed to determine if subpopulation influenced shoot and root DW MGR. *Indica* subpopulation had no significant effect on shoot or root DW MGR (KW, $p > 0.05$) (Figure 4.14).

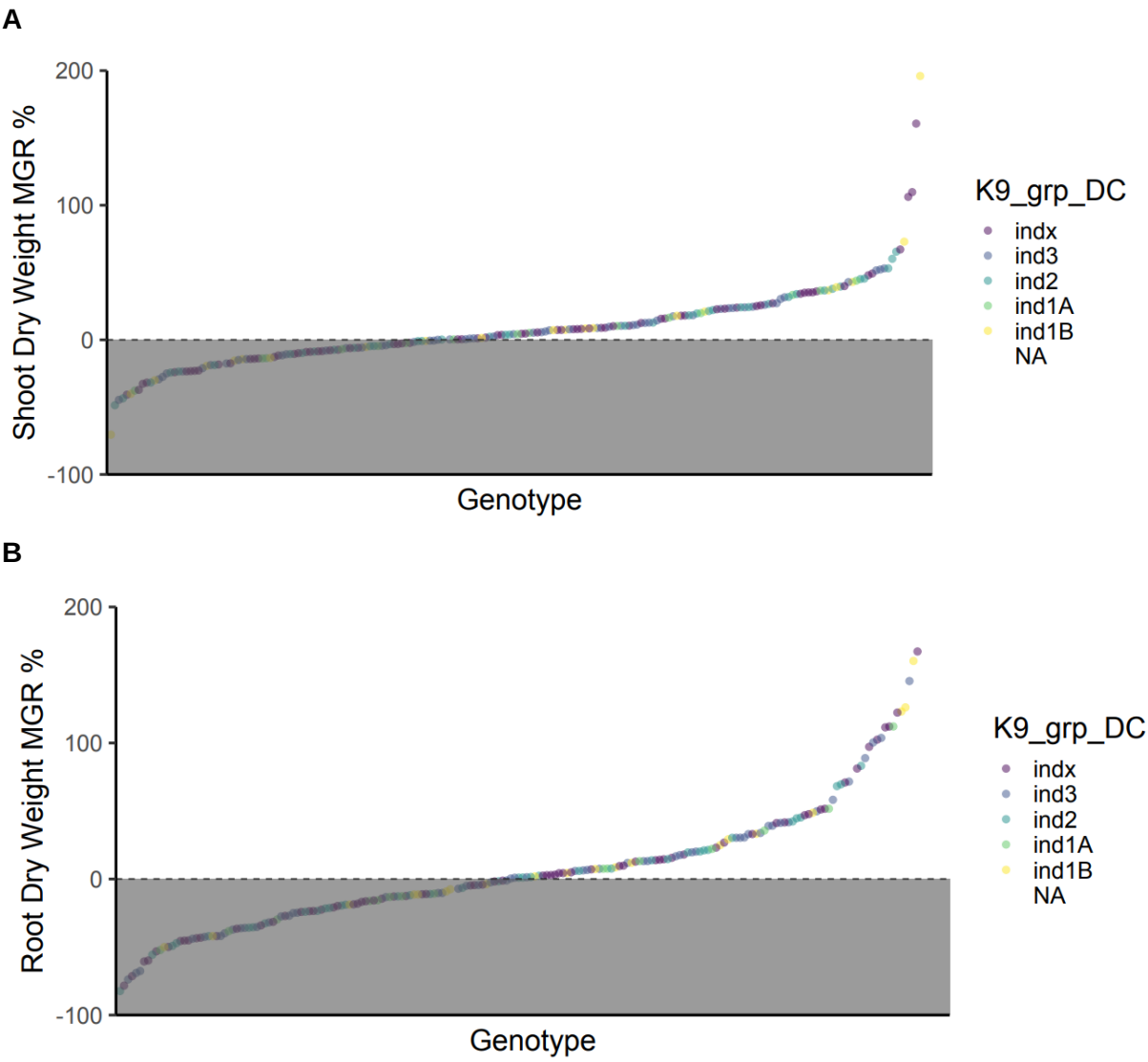

Figure 4.14 Distribution of mycorrhizal growth response (MGR) among the diverse Indica lines*. MGR in terms of (A) shoot dry weight biomass and (B) root dry weight biomass is given. Grey indicates negative biomass response. Each point indicates genotype means and colour represents Indica subpopulation as defined by 3K-RG, K=9 sub-populations.*

Natural variation in foliar ionome responsiveness to AMF was also observed across all 16 mineral elements measured, with both negative and positive responses in all elements (Figure 4.14). Since AM symbiosis is known to provide a source of phosphate to the plant, response of foliar phosphorous concentration upon AMF-inoculation was further analysed. Again, both positive and negative response of foliar phosphorous to AMF inoculation was observed (Figure 4.15). Since the data was not normally distributed (Shapiro-Wilk, $p < 0.05$), a non-parametric Kruskal-Wallis test was performed to determine if subpopulation influenced foliar P response. *Indica*

subpopulation had no significant effect on foliar P response to AMF inoculation (KW, $p > 0.05$) (Figure 4.16).

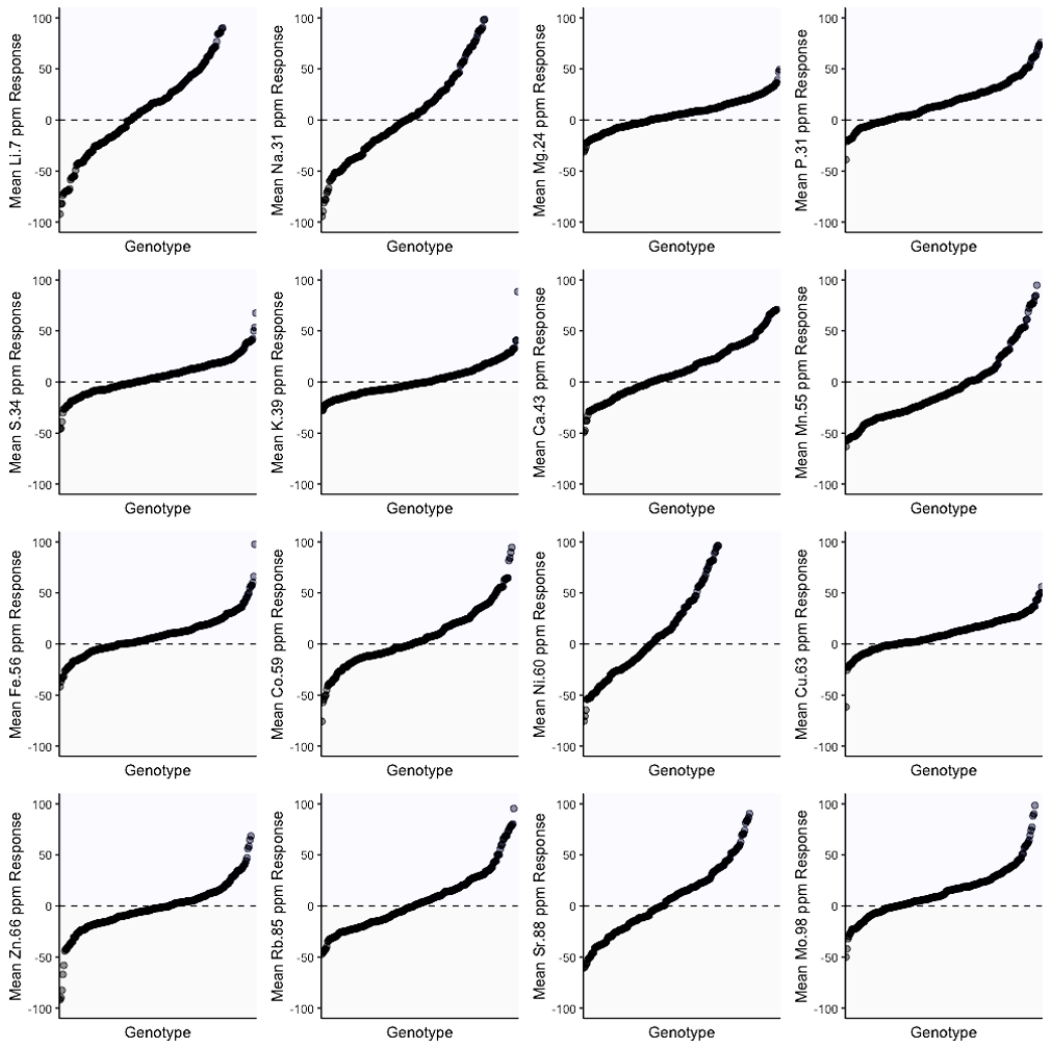

Figure 4.15 Responsiveness of foliar ion content to AMF inoculation. *Responsiveness in terms of mean foliar content of the following foliar ion concentrations (ppm) were measured: lithium (Li.7), sodium (Na.23), magnesium (Mg.24), phosphate (P.31), sulphur (S.34), potassium (K.39), calcium (Ca.43), manganate (Mn.55), iron (Fe.56), cobalt (Co.59), nickel (Ni.60), copper (Cu.63), zinc (Zn.66), rubidium (Ru.85), strontium (Sr.88) and molybdenum (Mo.98). Grey indicates negative biomass response. Each point indicates genotype mean per cultivar.*

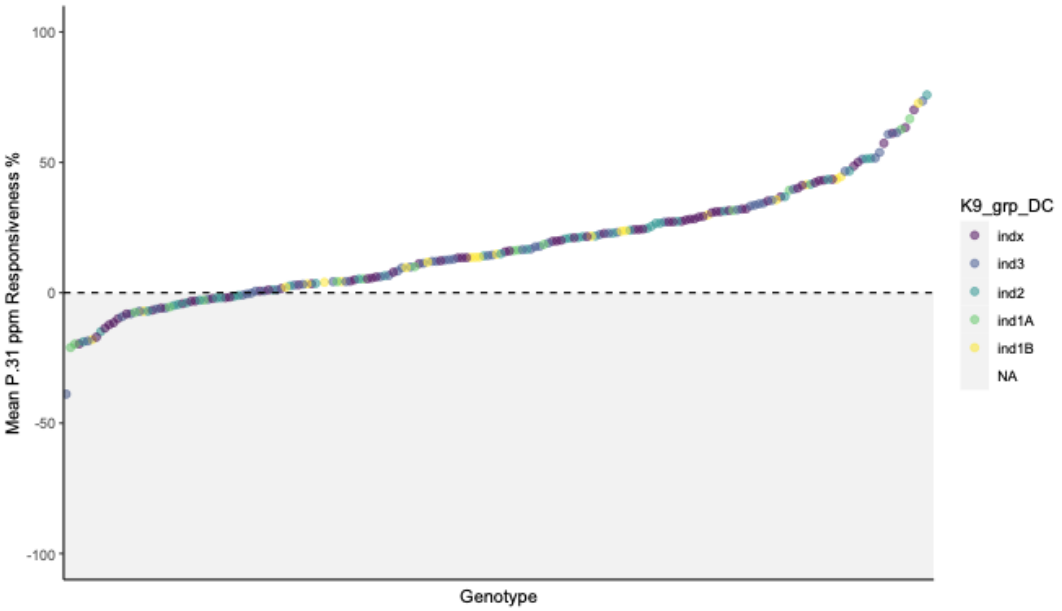

***Figure 4.16 Distribution of foliar phosphorous response among the diverse Indica lines**. (A) Mean foliar P concentration response to AMF (ppm) is given. Grey indicates negative biomass response. Each point indicates genotype mean per cultivar and colour represents Indica subpopulation as defined by 3K-RG, K=9 sub-populations.*

A Pearson's correlation analysis was used to identify the relationship between blumenol abundance and host plant responsiveness. Among growth traits, a weak positive correlation was identified between mean abundance of 11-carboxyblumenol C-Glc and SDW responsiveness ($r=0.22$, $p < 0.01$, Figure 4.17A). Similarly, increased foliar phosphorous upon AMF-inoculation weakly correlated to blumenol abundance ($r=0.18$, $p<0.01$, Figure 4.17C). In contrast, no correlation to RDW responsiveness was observed ($r = 0.061$, $p=0.39$, Figure 4.17B). The weak correlation in SDW and foliar phosphorous responsiveness and lack of change in RDW responsiveness, further advocates against a simple correlation of greater root colonisation resulting in greater host benefit, as observed previously in differences in response across diverse rice cultivars (Campo et al., 2020; Davidson et al., 2019; Diedhiou et al., 2016; Sisaphaithong et al., 2017).

Overall, this suggests that there is significant natural variation in biomass and foliar phosphorous assimilation in response to AMF inoculated in rice. In addition, growth responsiveness to AMF-inoculation only partially relates to root colonisation level and instead is likely driven by additional genetic factors.

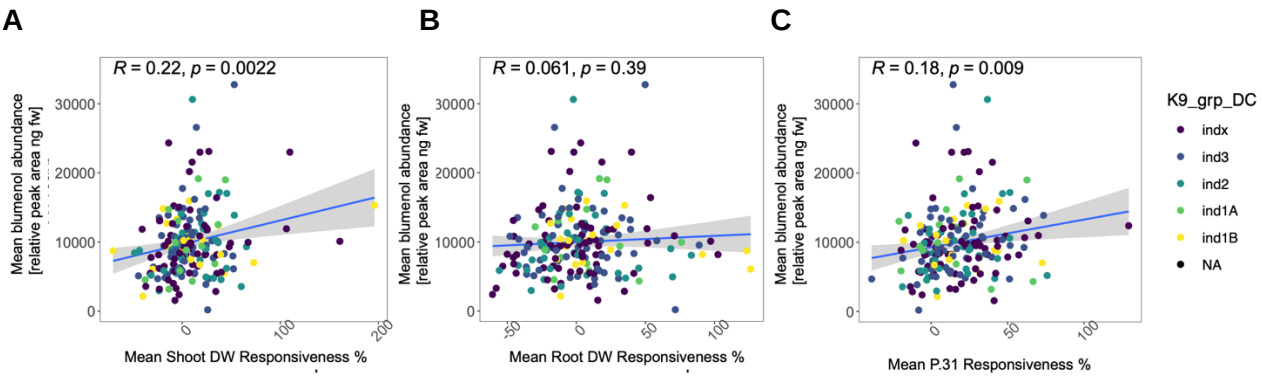

Figure 4.17 Correlation of blumenol abundance to plant host responsiveness. *Linear regression plots show correlation of blumenol abundance (11-carboxyblumenol C-Glc) to (A) SDW, (B) RDW and (C) foliar P responsiveness. Pearson's correlation coefficient (R) and significance value are shown. Each point indicates mean cultivar measurement in AMF-inoculation condition and colour represents Indica subpopulation as defined by 3K-RG, K=9 sub-populations.*

4.2.2.6 Identification of cultivars with contrasting response to AMF inoculation

To identify lines with superior and inferior response, diverse cultivars with contrasting MGR in terms of both positive or negative SDW and RDW response were selected. These included *ALAGUSAMBA, SRAU KHSAI, MOSHI, CHAMA(DWARF),CRILLO LA FRIA, INAP 6 and HAM MOON* with negative MGR and *SABRAN, ORIONE, TOC 5430, CHING LUI, MOUI SAMBA*, *BONG SEN and SAM SI* with positive MGR, summarised in Figure 4.18A.

Both negative and positive foliar P responsiveness was observed across all the selected cultivars, regardless of MGR. For example, negative P responsiveness of -4.89 and -2.84 was observed in *MOSHI* and *CRILLO LA FRIA* and SDW MGR was negative at -43.50% and -37.69% respectively (Figure 4.18A-B). In contrast, positive foliar P response of 4.03% and 31.09% was observed in *CHAMA(DWARF)* and *HAM MOON* despite reduced SDW MGR of -40.13% and -31.76% respectively (Figure 4.17A-B). This was also observed in superior lines. For example, in *MOUI SAMBA, CHING LUI* and *SABRAN*, positive foliar P responsiveness of 72.68%, 27.39% and 23.79% and SDW MGR of 72.94%, 106.22% and 196.00% respectively was observed (Figure 4.18A-B). In contrast, despite increased SDW MGR of 160.65%, foliar P responsiveness was reduced by 3.26% upon AMF inoculation in *ORIONE* (Figure 4.18A-B). This matches previous findings where a weak positive correlation

between SDW MGR and foliar P responsiveness was observed and suggests that additional factors are involved in host biomass response to AMF.

Since dependence (relative growth in the absence of AMF) can drive plant host response (Figure 4.6), mean SDW in mock-inoculated plants of the selected cultivars was compared to the global panel mean, 0.148 ± 0.053g (Table 4.1). Some of the superior lines had reduced SDW compared to the global mean (Figure 4.18C). For example, mean SDW of 0.069 ± 0.018g and 0.075 ± 0.010g was observed in *ORIONE* and *SABRAN* respectively (Figure 4.18C). This suggests that the response in these cultivars is likely driven by a poor performance in absence of AMF, representing dependence. In contrast, mean SDW in cultivars such as *CHING LUI* and *BONG SEN* 0.134 ± 0.014g and 0.131 ± 0.01g respectively was near global population mean (Figure 4.18C). These cultivars therefore exhibit typical dependence and the positive MGR represents benefit of AMF inoculation on plant performance.

Overall, this corroborates previous findings of a weak correlation of foliar P content and SDW in AMF-inoculation. In addition, positive response to AMF-inoculation was found to be driven by both dependence and benefit in the superior lines. This corroborates the need for use of caution in relative measures of response such as MGR when identifying lines with superior capacity to benefit from symbiosis.

A

Cultivar	Country	P.31.resp	X11carb	K9_grp_DC	mean.rootDWresp	mean.shootDWresp
ALAGUSAMBA::IRGC 8944-2	Sri Lanka	1.14	8437.374	ind2	-1.648987	-48.55649
SRAU KHSAI::IRGC 29896-2	Cambodia	0.68	5115.85	ind3	-30.711297	-44.58258
MOSHI::IRGC 70648-1	Kenya	-4.89	8801.342	ind2	-21.616162	-43.50476
CHAMA (DWARF)::IRGC 69487-1	Zambia	4.03	2160.006	ind1B	-11.386482	-40.12553
CRILLO LA FRIA::IRGC 10793-1	Venezuela	-2.84	4540.531	ind1A	-16.104869	-37.69382
INIAP 6::IRGC 117002-1	Ecuador	1.63	5477.916	indx	-43.523316	-32.65954
HAM MOON::IRGC 9135-2	Hong Kong	31.09	7762.444	indx	-45.544889	-31.76418
SAM SI::IRGC 99020-1	Lao	0.63	6126.194	ind3	15.206612	52.26913
BONG SEN::IRGC 7011-1	Viet Nam	14.44	32762.78	ind3	49.822695	53.10338
MOUI SAMBA::IRGC 75751-1	Burkina Faso	72.68	7030.124	ind1B	4.40613	72.93686
CHING LIU::IRGC 65018-1	Taiwan	27.39	11915.88	indx	51.131222	106.22079
TOC 5430::IRGC 70487-1	Panama	13.42	22997.81	indx	39.889706	109.73924
ORIONE::GERVEX 333-C1	Italy	-3.26	10104.56	indx	97.187376	160.65326
SABRAN::IRGC 34630-1	Indonesia	23.79	15310.34	ind1B	34.92823	196.00281

B

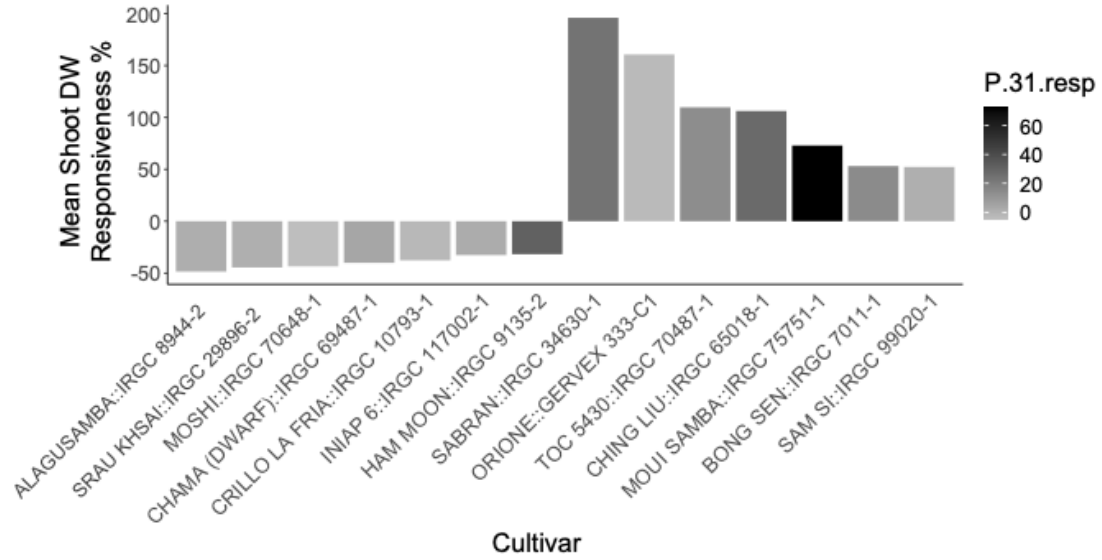

C

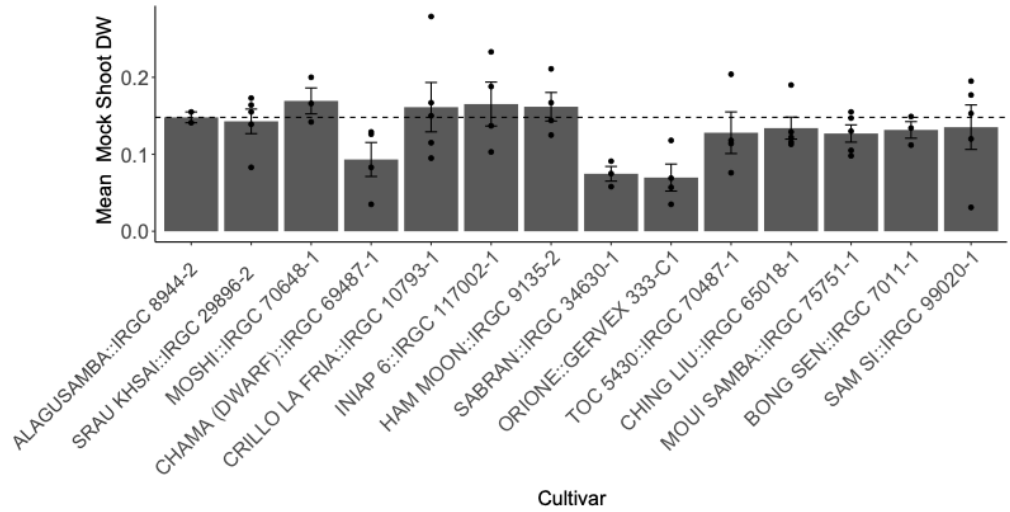

Figure.18 Identification of responsiveness in superior and inferior lines from the diverse Indica panel. *Six superior lines and six inferior lines in terms of MGR were analysed. (A) Table indicates cultivar, country of origin, foliar P content responsiveness (P.31.resp), indica subgroup (K9_grp_DC), mean RDW responsiveness (mean.rootDWresp) and mean SDW responsiveness (mean.shootDWresp) (B) Bar chart of mean SDW*

responsiveness in the cultivars. Bar colour indicates extent of foliar P responsiveness, with darker grey a more positive response. Mean response was calculated per cultivar. (C) Bar chart indicates mean SDW in AMF absence (mock) per cultivar. Global population mean is represented by dashed line. Individual plant measurements are given as points and bar indicates cultivar mean, with error bars indicating standard deviation ± mean.

I next implemented an approach noted previously to identify lines with superior capacity for benefit. The method uses a linear model to describe population-level variation in the relationship of non-mycorrhizal to AMF-inoculated plant performance. Residuals from the model are extracted to determine outlying variation that describes specific variation acting on either non-colonised or AMF-inoculated plants. The latter allows for determination of beneficial, non-dependence based variation (Sawers et al., 2010).

A linear regression of AMF-inoculated SDW against non-inoculated SDW was performed. A weak positive correlation between mock and AMF-inoculated SDW was observed (r^2=0.28, $p < 0.05$, Figure 4.19A) with a positive intercept and a positive slope. This suggests that most of the variation in SDW response is due to specific, non-dependence variation in the *Indica* panel. Outlying lines with large variation were identified using residual values plotted against non-inoculated SDW (Figure 4.19B). Large positive and negative residuals indicated cultivars which are highly and poorly performing in response to AMF-inoculation respectively, independent of dependence. The top 15 are labelled (Figure 4.19B) and the highest performing lines included *ANADI WHITE, DUDRE, IA CUBA 17, DUD KUNING* and *BONG SEN*. Lines that performed most poorly include *INIAP 6, CHANDINA, ALAGUSAMBA, HAM MOON* and *HEGAR MANAH* (Figure 4.19B).

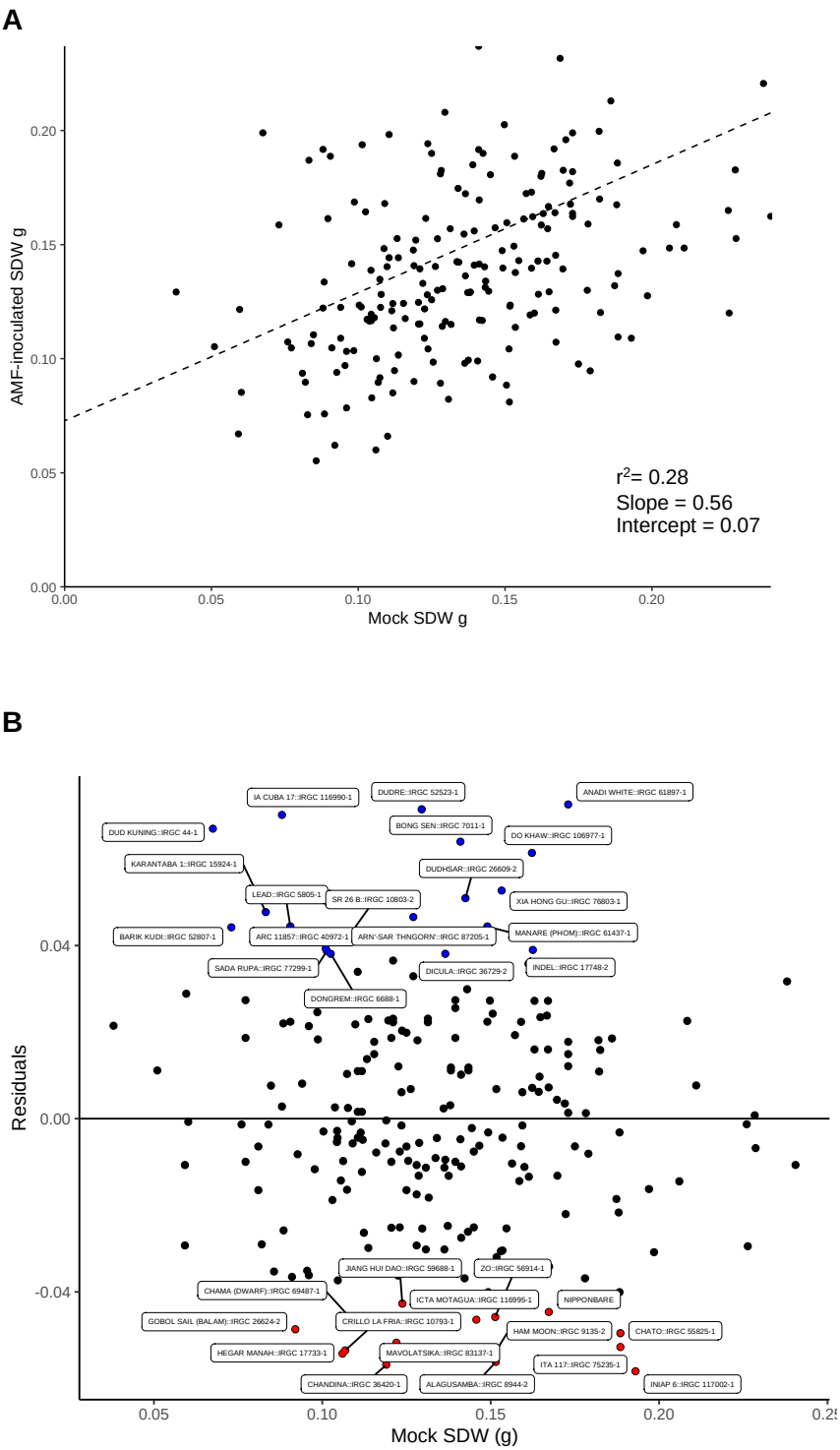

Figure 4.19 Regression of shoot dry mass of AMF-inoculated and mock-inoculated plants for the Indica panel.*(A) linear regression of SDW in AMF-inoculated plants against mock-inoculated plants. Cultivars are shown as filled black circles, with a dashed line indicating the linear model. R^2, slope and intercept of linear model are denoted. (B) Residuals of linear model plotted against Mock SDW. Top fifteen most positive (blue filled circles) and negative (red filled circles) are labelled with genotype name.*

4.2.3 Discussion

This study identified significant variation in AMF-indicative blumenol abundance across the diverse *Indica* panel, independent to subpopulation. This concurs previous identification of significant variation in hyphal root colonisation in rice diversity panels (RDP1), (Davidson et al., 2019) and additionally suggests that there is great natural genetic diversity across *Indica* cultivars of the 3K-RG.

The effect of cultivar and AMF inoculation on biomass and ionome parameters was assessed in the diverse *Indica* panel. Cultivar significantly affected all traits measured, indicating that there is natural variation in height, biomass and shoot mineral element content in *Indica* rice grown in P_i limited environments. This has been observed previously (Chin et al., 2011) but has not been measured directly in lines of the 3K-RG. Analysis of genetic factors driving such differences, as identified previously in the RDP1 (M. Wissuwa et al., 2015), could aid in future breeding of P-efficient rice varieties.

AMF inoculation caused a 4% increase in seedling height, a 10% increase in biomass and a significant increase in foliar content of many mineral elements, including a 16% increase in foliar P. In addition, correlation of blumenol abundance to foliar P and Co was observed in AMF-inoculated plants. This lends further support for the potential of AMF to increase plant growth and mineral uptake (Bucher, 2007; S. E. Smith & Read, 2008; Yang et al., 2012). Correlation analysis allowed further interpretation of the importance of AM colonisation level on biomass traits. Foliar blumenol abundance weakly correlated to shoot and root biomass suggesting that there is not a simple correlation and additional factors are involved in determining response.

Notably, host root architecture can change upon AM symbiosis- lateral roots are preferentially colonised by AMF and their formation is induced by symbiosis establishment (Chiu et al., 2018; C. Gutjahr et al., 2009; Oláh et al., 2005). The correlation of root biomass to blumenol abundance observed in the panel could suggest that (a) there is natural variation in extent of root density and biomass changes caused by AMF or (b) root architecture, particularly lateral root number, is

partially driving differences in root colonisation level. Such cannot be distinguished without measurements of root architecture across the panel, which was beyond the scope of this project. Natural variation in *OsCERK1* has been found to drive root colonisation level (R. Huang et al., 2020), and CERK1 is known to facilitate lateral root induction in AMF presence (Chiu et al., 2018). Lateral root differences were not measured in the beneficial *CERK1* haplotypes (R. Huang et al., 2020) but it would be again interesting again to see if changes in root architecture were partially responsible for the genetic response.

While AM symbiosis is known to increase phosphate acquisition efficiency (S. E. Smith & Read, 2008; Yang et al., 2012), and a positive impact of AMF on foliar P concentration was observed, such benefit is not without cost. Unlike previous studies in maize (Sawers et al., 2017), no correlation between shoot biomass and P content was observed in the diverse panel, suggesting other factors contribute to growth benefit from symbiosis. In addition, a large variation in foliar phosphorous responsiveness was identified across the panel. Diversity in increased phosphorous absorption and grain yield upon AMF inoculation of diverse rice cultivars has been noted previously (Maiti et al., 2012; S. Zhang et al., 2015) and further indicates a continuum of detriment to benefit of AMF to both plant host growth and nutrition, dependent on environmental and plant genetic factors. In addition, changes in shoot ionome in response to AMF-inoculation was observed, with natural variation in such responsiveness evident across the diverse panel. This corroborates previous identification of mycorrhizal status impacting natural variation in ionome in maize (M. Li et al., 2022).

Additional analysis of mycorrhizal growth response (MGR) identified both positive and negative biomass effects of AMF presence on SDW and RDW. Natural variation in host supply of carbohydrate sources to AMF could affect the resultant biomass impact. In addition, the efficiency with which plants convert P to yield is dependent both on uptake, phosphate acquisition efficiency (PAE) and efficiency of internal use into biomass, phosphate utilisation efficiency (PUE) (Rose et al., 2011). Natural variation in PAE and PUE of P obtained from hyphal sources could additionally explain the lack of correlation of SDW and P responsiveness observed in diverse *Indica* rice cultivars. Such genetic differences in PUE and PAE have been reported

previously in rice (N. K. Fageria et al., 1988; Hedley et al., 1994; Saleque et al., 2008; M. Wissuwa et al., 2001). Measurement of PAE and PUE of hyphal P was beyond the scope of this project but could aid in elucidating the extent to which certain cultivars derive greater benefit from AMF inoculation than others.

Importantly, measures of MGR confound benefit and detriment of AMF inoculation that could be due to poor performed under non-inoculation conditions, which is not of agronomic importance. A linear model was used to separate population-level variance with specific variance related to benefit from AMF-inoculation. A large amount of variance in SDW was attributed to specific mock- or AMF-inoculated performance. Lines with great benefit and detriment in AMF-inoculation were identified as outlying residuals of the model. This analysis has previously been used to identify benefit of AMF-inoculation in diverse plant species (Sawers et al., 2010) and is additionally used here for identifying positively benefiting lines in rice, including *ANADI WHITE, DUDRE, IA CUBA 17, DUD KUNING* and *BONG SEN*. Since plant response to mycorrhizae is dependent on environmental condition, it is additionally important to note here that benefit is reported in plants grown in pots in non-flooded, P_i deplete conditions in the glasshouse.

4.3 A Genome Wide Association Study (GWAS) interrogating genetic variation in establishment of AM symbiosis in rice

4.3.1 Introduction

Despite increasing understanding of factors that control AM symbiosis, such as cell signalling, morphological changes and nutrient uptake regulation (Choi et al., 2018; Das et al., 2022; Shi et al., 2021), little is known about the host genetic factors determining the extent of interaction and host response. Genetic association studies have started to elucidate genetic factors in multiple plant species. In wheat, large genetic variation in AM colonisation has been reported and six QTLs mapping to colonisation level were identified on four chromosomal regions, including a chloride

channel protein, assumed pathogen defence genes and a gene encoding a callose synthase, important for cell wall composition (Lehnert et al., 2017). An additional study in durum wheat found seven putative QTLs associated to mycorrhizal colonisation. Many chromosomal regions co-mapped with QTLs associated to disease resistance genes and root traits, and predicted protein function included host-parasite infection, plant growth and homeostasis were identified, as well as nodulin proteins and calcium-related genes, which have previously been implicated in AM symbiosis (De Vita et al., 2018). More recently, a GWAS interrogating AM traits in a tetraploid wheat collection identified four QTLs associated to symbiosis (Ganugi et al., 2021). Six QTLs associated to AM colonisation of soybean have been identified and candidate genes again include homologs of known nodulin proteins and genes encoding proteins that have previously been associated to AM colonisation, such as serine/threonine protein kinases, a UDP-glycosyltransferase and a cytochrome P450 (Pawlowski et al., 2020). Such studies are in their infancy, and require further candidate gene validation, but reflect the great potential for further understanding of genetic factors driving AM colonisation in multiple crop species.

In rice, Davidson et al., found 23 putative QTLs mapping to diverse hyphal colonisation rates in a panel of 334 cultivars in the RDP1. Candidate genes included a calcium/calmodulin serine/threonine protein kinase and two ammonium transporters (Davidson et al., 2019). The study clearly demonstrated that there is large variation in AM colonisation rates in diverse cultivars and evidenced potential to identify genetic regions associated to colonisation establishment and mycorrhizal responsiveness. To date, this is the only known report of genome-wide mapping of AM traits in rice.

GWAS are a powerful tool for identifying genetic variants and single nucleotide polymorphisms (SNPs) associated to a given traits, quantitative trait loci (QTLs). QTLs are identified by examining the strength of linkage disequilibrium (LD) (the degree of non-random association between alleles at different loci) between markers and functional polymorphisms across a set of diverse germplasm. Typically, GWAS in crop species are performed using a panel of lines, with multiple replicates of each line and an average of these phenotypes used as the response variable. The

success of such a study is pertinent on germplasm choice. Population structure can generate false positives in mapping and thus high phenotypic diversity should be maintained whilst minimizing genetic structure. In addition, extent of LD decay will determine the ability to map QTLs to genes/genetic regions of interest. In rice, LD decay is estimated ~200Kb and candidate genes within this region of the lead SNP are commonly reported (McNally et al., 2009).

Since a large amount of genetic data is available for the 3K-RG and selected panel, the AM phenotypes observed across the *Indica* panel in Section 4.2 was subjected to GWA mapping to further identify genetic drivers of AM colonisation in *Indica* rice.

4.3.2 Results

4.3.2.1 GWA Mapping of AM colonisation traits

Due to seed availability, a total of 196 accessions from the selected *Indica* panel were analysed in the GWAS. Genotype data was obtained from available 3K-RG SNP datasets (IRRI, https://snp-seek.irri.org/_download.zul). The ‘Filtered SNP set’ of the 3K-RG was chosen as it contains ~4.8 million filtered SNPs and is used in IRRI SNPSeek data analysis software (https://snp-seek.irri.org/download.zul). SNP data for the 196 genotypes in the selected panel were extracted from the ‘Filtered SNP set’ with the following thresholds: minor allele frequency (MAF) >5%, missing data < 10%, minor allele count > 8. This gave ~ 2,088,720 SNPs. These were then pruned to reduce highly correlative SNPs ($R^2 = 0.95$, $p < 0.05$), creating a "non-redundant" subset that would be computationally efficient whilst representing variation across the whole genome. A total of 386,173 SNPs in the non-redundant set were mapped to *Nipponbare* reference sequence and used for population structure analysis and GWA mapping of AM traits.

For AM colonisation trait data, foliar abundance of 11-carboxyblumenol C-Glc and 11-hydroxyblumenol C-Glc was assessed in AMF-inoculated plants of the 196 cultivars in the panel. Best unbiased linear predictors (BLUPs) were calculated using a linear model with glasshouse block as a random effect to account for spatial differences. Normal distribution of BLUPs of each trait was assessed using Shapiro-wilk test with a significance threshold of $p < 0.05$. Since both were not normally

distributed, transformations were performed. A $\log_{10}$ (X + 100) transformation was performed for 11-hydroxyblumenol C-Glc (Shapiro wilk, p=0.492) and a square root (X + 1000) transformation for 11-carboxyblumenol C-Glc (Shapiro-wilk, p = 0.083) (Figure 4.20).

Broad-sense heritability, the proportion of phenotypic variation due to genetic factors, was calculated based on the linear model results, as described previously (M. Li et al., 2022). Moderate heritability of 38% was observed for 11-carboxyblumenol C-glc and strong heritability of 72% for 11-hydroxyblumenol C-Glc (Figure 4.20). It is perhaps unsurprising that heritability of 11-carboxyblumenol-C-Glc is lower, as the derivative correlates more strictly to AM colonisation and low heritability of AM colonisation has been noted previously (Leiser et al., 2016; M. Li et al., 2022). Regardless, genetic factors clearly determine some extent of phenotypic variation in abundance in both cases.

A

Trait	Mean	SD	H^2
11-carboxyblumenol-C-glc	9508.98	6968.42	0.38
11-hydroxyblumenol-C-glc	444.95	370.12	0.72

B

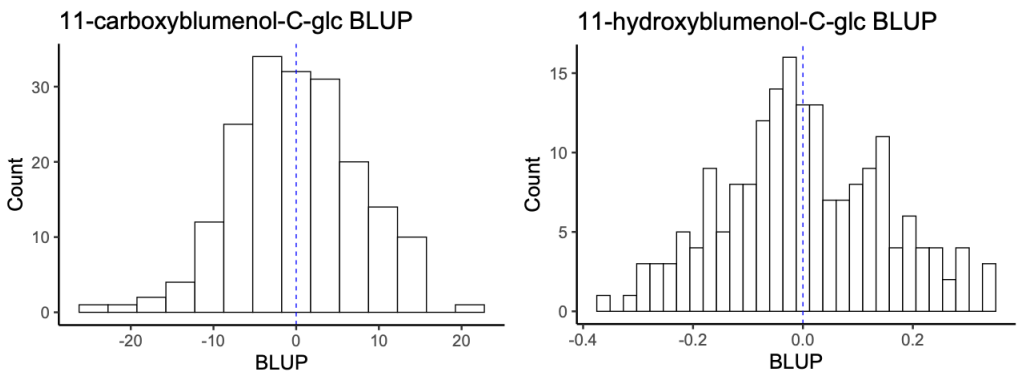

Figure 4.20 Summary statistics and frequency distribution of blumenol abundance traits. *(A) Table represents mean and standard deviation of abundance of 11-carboxyblumenol C-Glc and 11-hydroxyblumenol C-Glc. BLUPs were estimated using the following model: Y ~ (1|sub.block) + (1|Cultivar). Broad sense heritability H^2 measured using BLUPs is noted per trait. (B) Frequency distribution of BLUPs after transformation for normal distribution. A log10 (X + 100) transformation was performed for 11-hydroxyblumenol C-Glc and a square root (X + 1000) transformation for 11-carboxyblumenol C-Glc.*

The blumenol abundance traits were analysed by multivariate GWAS using a BLINK model implemented in the GAPIT package (Lipka et al., 2012). Principal components (PC) were included to reduced false positives due to population stratification. PC = 4 was selected as analysis of the scree plot of eigenvalues for each PC identified this as the 'elbow' after which additional PCs would add relatively little information (Figure 2.4). The BLINK model selects associated markers based on LD and multiple tests, and iteratively incorporates them as covariates in a fixed effects model to eliminate their connection to the cryptic relationship among individuals. This provides a computationally efficient and powerful statistical method for GWAS (Lipka et al., 2012). Notably, BLINK relies strongly on LD and the output of the model reduces SNPs in high LD with lead SNPs to low significance. This means that it is difficult to distinguish whether lead SNPs are lone peaks, which are prone to false association. A widely used, univariate Mixed Linear Model (MLM) was therefore also fit to compare associations and corroborate that lead peaks are associated with multiple SNPs of a similar signal. Both PC = 4 and a relatedness matrix were included in the MLM model to account for population structure and kinship to reduce false positives.

A Bonferroni-correction of 1/N, with N independent markers of 386,173 SNPs and α = 0.05, was used to determine a stringent genome-wide *P*-value significance threshold of $1.3e^{-7}$ ($-\log_{10}(P) = 6.88$). A significant lead SNP associated to 11-hydroxyblumenol C-Glc was identified by both the BLINK and MLM models (Figure 4.21A). The SNP explained 27.4% and 24.6% of phenotypic variance in the models respectively (Figure 4.21B). A significant lead SNP associated to 11-carboxyblumenol C-Glc abundance was also identified using the BLINK model (Figure 4.21B). This was established not to be a lone peak using the MLM results to confirm that there were peaks of a lower significance in a similar region. The lead SNP explained 39.6% of phenotypic variance in the BLINK model (Figure 4.21C).

Further, since the Bonferroni correction is considered a conservative significance threshold, it is possible that additional SNPs associated to blumenol abundance may be eliminated. To identify potential candidates, SNPs in MLM model above a widely used threshold of $P < 0.0001$, $-\log_{10}(P) > 4$ were considered 'suggestive' of association. Such a method has been reported previously in mapping of AM traits in rice (Davidson et al., 2019). Five suggestive SNPs associated to 11-

hydroxyblumenol C-Glc abundance were identified on chromosomes 1,3,6,7 and 11 and seven suggestive SNPs on chromosomes 3,5,7 and 11 were found to be associated to 11-carboxyblumenol C-Glc abundance (Figure 4.21A-C).

Notably, there was no overlap in the significant or suggestive SNPs associated to either blumenol derivatives (Figure 4.21). This could be due to their differences in stringent accumulation in AMF-inoculated plants, as described in Chapter Three. It should be noted that whether a SNP is associated to biosynthesis of the blumenol derivatives and/or extent of AM symbiosis cannot be uncoupled in this analysis. Since 11-hydroxyblumenol C-Glc accumulates less strictly to AM symbiosis and has a higher broad sense heritability than 11-carboxyblumenol C-Glc, it could be speculated that candidate genes associated to this derivative may be more likely to refer to genetic variation in blumenol biosynthesis than AM symbiosis signalling than in SNPs associated to 11-carboxyblumenol C-Glc, which has a strict accumulation in AMF-inoculated plants.

A

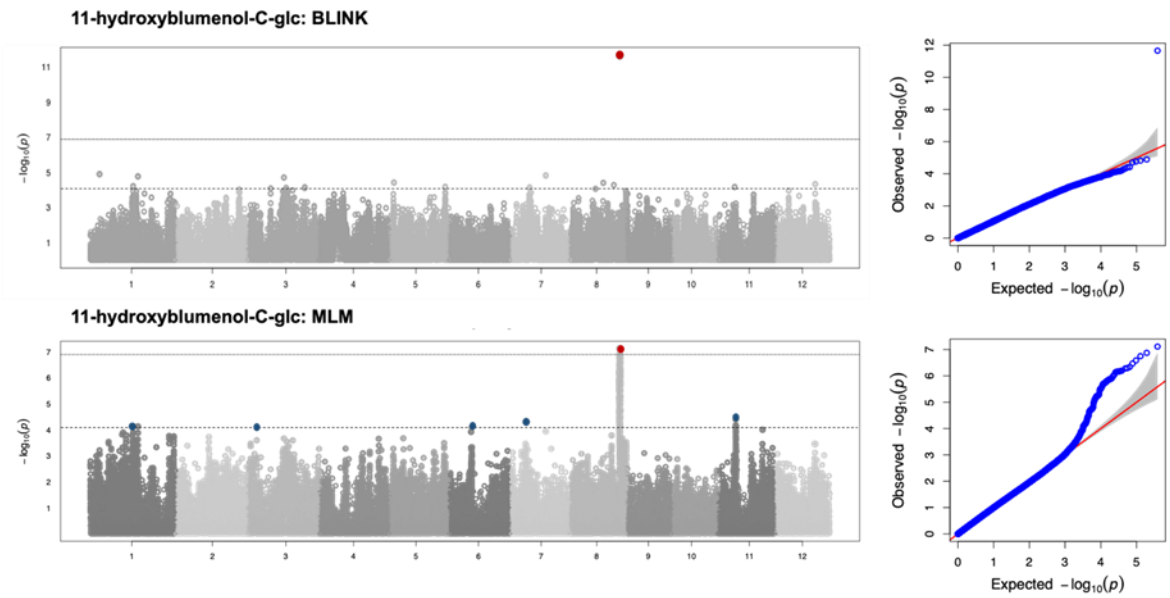

B

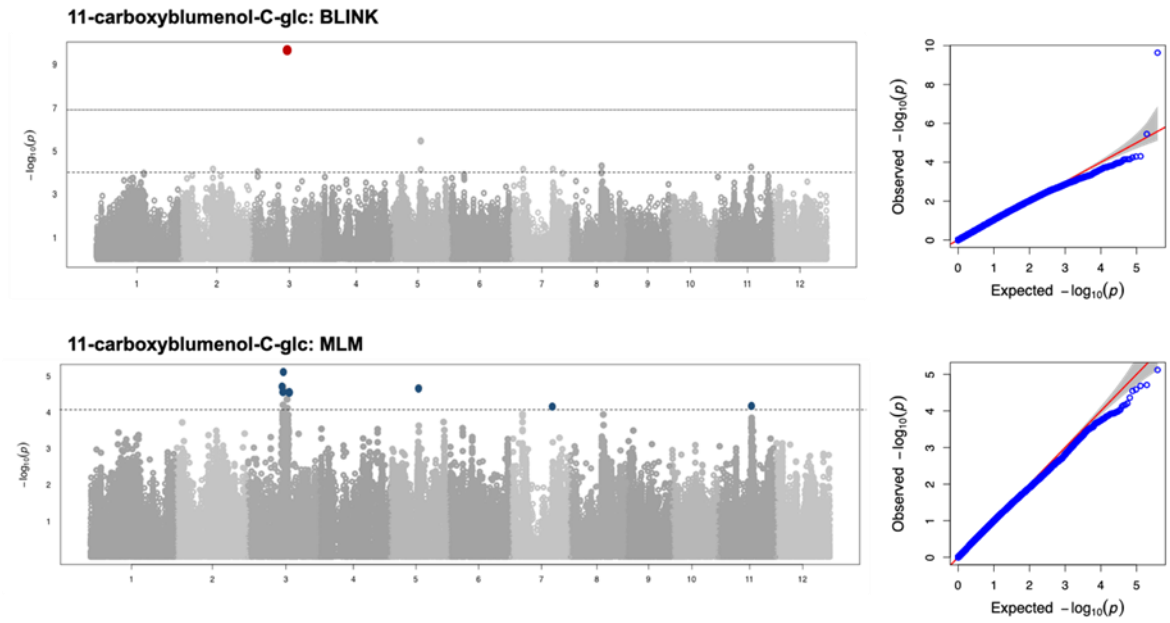

C

Trait	Model	SNP Type	SNP	Chromosome	Position	P.value	MAF	Effect	PVE %
11-hydroxyblumenol-C-Glc	BLINK	Significant	267148437	8	25118909	2.20E-12	0.377	-0.065	27.494
	MLM	Significant	267148437	8	25118909	7.73E-08	0.346	-0.071	24.666
	MLM	Suggestive	325725188	11	9032631	3.25E-05	0.233	-0.053	
	MLM	Suggestive	219830683	7	7498776	4.62E-05	0.102	-0.086	
	MLM	Suggestive	21198820	1	21198820	7.11E-05	0.112	-0.081	
	MLM	Suggestive	192559721	6	11476601	8.00E-05	0.118	0.071	
	MLM	Suggestive	84030417	3	4822244	8.05E-05	0.107	0.073	
11-carboxyblumenol-C-Glc	BLINK	Significant	97371344	3	18163171	2.32E-10	0.083	-5.521	39.619
	MLM	Suggestive	97371344	3	18163171	7.58E-06	0.083	-5.283	
	MLM	Suggestive	165664927	5	14540241	2.07E-05	0.187	-4.145	
	MLM	Suggestive	100150657	3	20942484	2.86E-05	0.091	-4.859	
	MLM	Suggestive	333352073	11	16659516	6.83E-05	0.086	4.518	
	MLM	Suggestive	233130513	7	20798606	7.02E-05	0.254	3.349	
	MLM	Suggestive	99417592	3	20209419	7.64E-05	0.051	-5.680	
	MLM	Suggestive	97987052	3	18778879	9.32E-05	0.051	5.761	

Figure 4.21 GWAS results of significant SNP-trait associations for blumenol traits. *BLINK and MLM Manhattan and quantile-quantile (Q-Q) plots showing associations to (A) 11-hydroxyblumenol C-Glc and (B) 11-carboxyblumenol C-Glc. Red points indicate SNPs above the Bonferroni-corrected threshold of -log$_{10}$(P) > 6.88 (solid line) and blue points represent SNPs suggestive of association at -log$_{10}$(P) > 4 (dashed line). (C) Table summarising significant and suggestive SNPs associated to the traits for each model. SNP ID, chromosome, position on chromosome, P value, minor allele frequency (MAF), effect of BLUP (Effect) are noted. Percentage variance explained (PVE %) is noted for significant SNPs.*

4.3.2.2 Mining candidate genes

Notably, the GWAS analysis used a non-redundant LD pruned set of SNP markers, meaning that each SNP is representative of large genomic regions. It is well appreciated that effects are not always associated to the lead SNP position, which is especially true in this analysis where a non-redundant SNP set was used. Since rice is estimated to have an average LD value of ~200 Kb (McNally et al., 2009), a region 100 Kb up- and down-stream of the lead SNP position was interrogated by the following pipeline to identify candidate genes for further analysis:

Firstly, functional SNP annotation was performed to identify putative effects associated to the lead position. This was estimated using SNP SEEK tool (https://snp-seek.irri.org), which incorporates SnpEff program to categorise variants based on their predicted effects on coding regions within a defined region (Cingolani et al., 2012). SNPEff reports effects as modifier, low, moderate, and high impact. Modifier usually refers to non-coding variants or variants affecting non-coding genes, where predictions are difficult or there is no evidence of impact. Low effects include synonymous SNPs (variant causes a codon that produces the same amino acid), moderate effects include missense variants (variant causes a codon that produces a different amino acid). High impact effects refer to a predicted non-synonymous change in coding region (Cingolani et al., 2012).

In addition, RiceVarMap2 was used to identify the potential effect of SNPs in non-coding gene regions (H. Zhao et al., 2015). Enhancers are non-coding intergenic DNA regions that have a central role in control of gene expression. Since an enhancer has previously been defined in rice to be in the proximity of a gene if it is within 5 Kb of the gene body (J. Sun et al., 2019), a region 5 Kb upstream and downstream of each SNP peak was interrogated for effect. RiceVarMap2 includes

chromatin accessibility profiles from six tissues of 2-week-old plants of *Zhenshan97* cultivar, measured using an Assay for Transposase-Accessible Chromatin with high-throughput sequencing (ATAC-seq assay), and gives a score from -2 to 2 for predicted change in accessibility using a logarithmic ratio of the predicted accessibility of the alternative genotype to the value of the reference genotype. The more extreme the score the more likely the variant affects chromatin accessibility (H. Zhao et al., 2015).

Next, all genes within the 200 Kb region were annotated using Rice Gene Hub tool (https://rice-genome-hub.southgreen.fr/find/genes). Their potential to be related to AM traits was assessed by comparison of gene ID with (a) a list of 205 genes with a genetically determined or putative function in AM symbiosis (Das et al., 2022) and (b) transcriptomic data of genes differentially expressed in rice inoculated with *R. irregularis* and grown similarly to this GWAS experiment (S. Wang et al., 2020). SNPEff was used to determine variants, namely SNPs and insertion or deletions (INDELs) in the genes. A candidate gene list was then produced and assessed for potential to be associated to variation blumenol abundance and AM symbiosis.

4.3.2.3 Candidate genes associated to 11-hydroxyblumenol C-Glc abundance

Firstly, the lead SNP on chromosome 8 at position 25118909 associated to 11-hydroxyblumenol C-Glc abundance (Figure 4.21) was interrogated. Mean 11-hydroxyblumenol C-Glc abundance was compared between haplotypes of the SNP (Figure 4.22). A significant increase in mean 11-hydroxyblumenol C-Glc abundance from 346.47 ± 14.56 ng/g fw in cultivars with reference GG haplotype to 528.37 ± 32.81 ng/g fw and 596.08 ± 26.57 ng/g fw in cultivars with heterozygous G/A and AA haplotype respectively was identified (KW, $p < 2.2\ e^{-16}$, Figure 4.22A). Functional SNP annotation was performed on a region 100 Kb up- and down-stream of the lead position and SNPEff identified potential coding effects. The G → A or A/G mutation is predicted to be a silent, intergenic modification upstream of LOC_Os08g39694, a putative, expressed cytochrome P450 monooxygenase (CYP). Further analysis using RiceVarMap2 identified that the position is within a region ~2.3 Kb upstream of the gene with increased chromatin accessibility. The G → A mutation is predicted to

reduce chromatin accessibility by a score of -0.04 and -0.05 in root and flag leaf tissues respectively. This suggests that the SNP could influence an enhancer region of the gene (Figure 4.22B). Notably, a CYP has previously been identified as a candidate gene for mycorrhizal colonisation in GWAS in soybean (Pawlowski et al., 2020). In addition, CYPs are the largest enzyme family involved in hydroxylation and play crucial roles in biosynthesis of secondary metabolites, including strigolactone (Zheng et al., 2021). The enzymes may be required for biosynthesis of AM associated apocarotenoids or blumenol C glycosides themselves (Fiorilli et al., 2019). LOC_Os08g39694 is therefore recommended as a strong candidate for further analysis.

Next, since other associative SNPs could be in LD with the lead position, genes in the 200 Kb region of the lead SNP position were annotated for potential function in AM symbiosis. 16 candidate genes were identified, including three additional CYPs, a putative receptor-like cytoplasmic kinase RLCK257, FLOWERING basic helix-loop-helix (bHLH) transcription factor FBH1, ETHYLENE INSENSITIVE 3-LIKE PROTEIN transcription factor (EIL4), and lipoxygenase enzyme LOX9 (Table 4.3A). None of the annotated genes were found previously to be regulated by AM symbiosis.

To narrow down the candidate gene list, coding variants that may disrupt protein structure and function, were mined (Table 4.3B). For each candidate gene, the genomic locus plus 5 Kb upstream and downstream was interrogated. Effects of ‘Filtered 3K-RG’ SNPs associated to each candidate gene was estimated using SNP SEEK tool (https://snp-seek.irri.org) and SnpEff. The following modifier effect variants were identified: downstream gene variant (< 5 Kb downstream of gene); upstream (< 5 Kb upstream of gene); intergenic (variant in intergenic region); intron (variant in intron); 3’ UTR variant (variant in 3’ UTR); 5’ prime UTR (variant in 5’ UTR). Low effects included synonymous SNPs and moderate effects included missense variants. All candidate genes contained variants with multiple potential moderate or modifying effects, as summarised in Table 4.3.

To narrow the candidate list, potential function in AM symbiosis or blumenol biosynthesis was interrogated. The EIL4 ethylene insensitive transcription factor is an excellent candidate for further analysis, as multiple SNP effects, including non-

synonymous missense variants, are predicted. In addition, ethylene signalling has previously been implicated in AM symbiosis and is reported to be crucial to integration of phosphate status into AM establishment, as described in a recent review (Müller & Harrison, 2019). Similarly, receptor like kinases (RLKs) have previously been associated to AM symbiosis and have roles in perception of symbiotic 'Myc' factors to facilitate AM-associated signalling (Chiu & Paszkowski, 2020). The implication of receptor-like cytoplasmic kinases acting in phosphorylation cascades downstream of such perception, as recognised in immunity and stress response signalling, has been noted recently (Chiu & Paszkowski, 2020). For example, an RLCK acting downstream of AM-associated RLK *NFR5* was recently described in *L. japonica* to be essential for root nodule symbiosis signalling (Wong et al., 2019). The putative cytoplasmic receptor, RLCK247, is therefore additionally an interesting candidate for roles in AM symbiosis.

In addition, *LOX9* encodes a lipoxygenase, which is a ubiquitous family of enzymes required for regulated plant defence. LOX enzymes have previously been implicated in resistance to blast fungus in rice (Marcos et al., 2015; Marla & Singh, 2012). AM symbiosis is widely described to interplay with plant immunity (Antolín-Llovera et al., 2014; Chiu & Paszkowski, 2020; Miyata et al., 2014; X. Zhang et al., 2015) and thus the *LOX9* is additionally a good candidate gene for further analysis.

Table 4.3 Analysis of the region associated to the significant SNP for 11-hydroxyblumenol C-Glc. *(A) Table summarises genes annotated with 100 Kb up- and down-stream of the significant position on chromosome 8. (B) SNPEff results for SNP variants present 5kb up- and down-stream of each of the genes identified within the region. The number of non-synonymous SNPs (No. NS SNPs) and insertion/deletion (No. INDELs) is given. Predicted effects of all SNPs is noted, including whether the impact is predicted to be low, moderate, high or modifying to gene expression.*

A

MSU	RAP-DB	Gene	Function
	Os08g0506000		OTU-like cysteine protease family protein, putative
	Os08g0506100		Conserved hypothetical protein
LOC_Os08g39580			Zinc knuckle family protein
	Os08g0506350		Conserved hypothetical protein
LOC_Os08g39590	Os08g0506400	OsRLCK257	Receptor like protein kinase-like protein
	Os08g0506500		RNA methyltransferase
LOC_Os08g39630	Os08g0506700	OsFBH1	BHLH TF
LOC_Os08g39640	Os08g0507000		Cytochrome P450 monooxygenase
	Os08g0507200		Hypothetical conserved gene
LOC_Os08g39680			Hypothetical protein
LOC_Os08g39694	Os08g0507702		Putative Cytochrome P450 monooygenase
	Os08g0508000		Cytochrome P450 monooxygenase
	Os08g0508100		Conserved hypothetical protein
	Os08g0508600		Pre-rRNA-processing protein TSR2, putative
LOC_Os08g39830	Os08g0508700	EIL4	Similar to ethylene-insensitive 3 TF
LOC_Os08g39840	Os08g0508800	LOX9	Lipooxygenase 7

B

Gene	No. NS SNPs	No. INDELs	SNP Effects	EFFECT
Os08g0506000	1	156	intergenic, upstream, intron, missense	modifier, moderate
Os08g0506100	16	389	intron, missense, downstream	modifier, moderate
LOC_Os08g39580	0	31	synonymous, downstream	low, modifier
Os08g0506350	0	133	intergenic	modifier
OsRLCK257	0	108	upstream, downstream, intergenic	modifier
Os08g0506500	2	164	downstream, intergenic, missense, intron, synomymous	low, modifier, moderate
OsFBH1	0	231	upstream, intergenic, 5' prime UTR, missense, intron, 3' prime U	modifier, moderate
Os08g0507000	8	72	upstream, intergenic, missense, intron, downstream,	modifier, moderate
Os08g0507200	2	44	upstream, downstream, intergenic, missense	modifier, moderate
LOC_Os08g39680	8	208	upstream, downstream, intergenic, missense, intron	modifier, moderate
LOC_Os08g39694	6	397	missense, upstream, intergenic, intron, synonymous, downstrea	low, moderate, modifier
Os08g0508000	0	77	upstream, downstream, intergenic, synonymous	low, modifier
Os08g0508100	0	91	downstream, intron	modifier
Os08g0508600	2	136	upstream, intergenic, missense	modifier, moderate
EIL4	2	138	upstream, downstream, intergenic, missense, 3' UTR	modifier, moderate
LOX9	6	259	downstream, intergenic, missense, intron	modifier, moderate

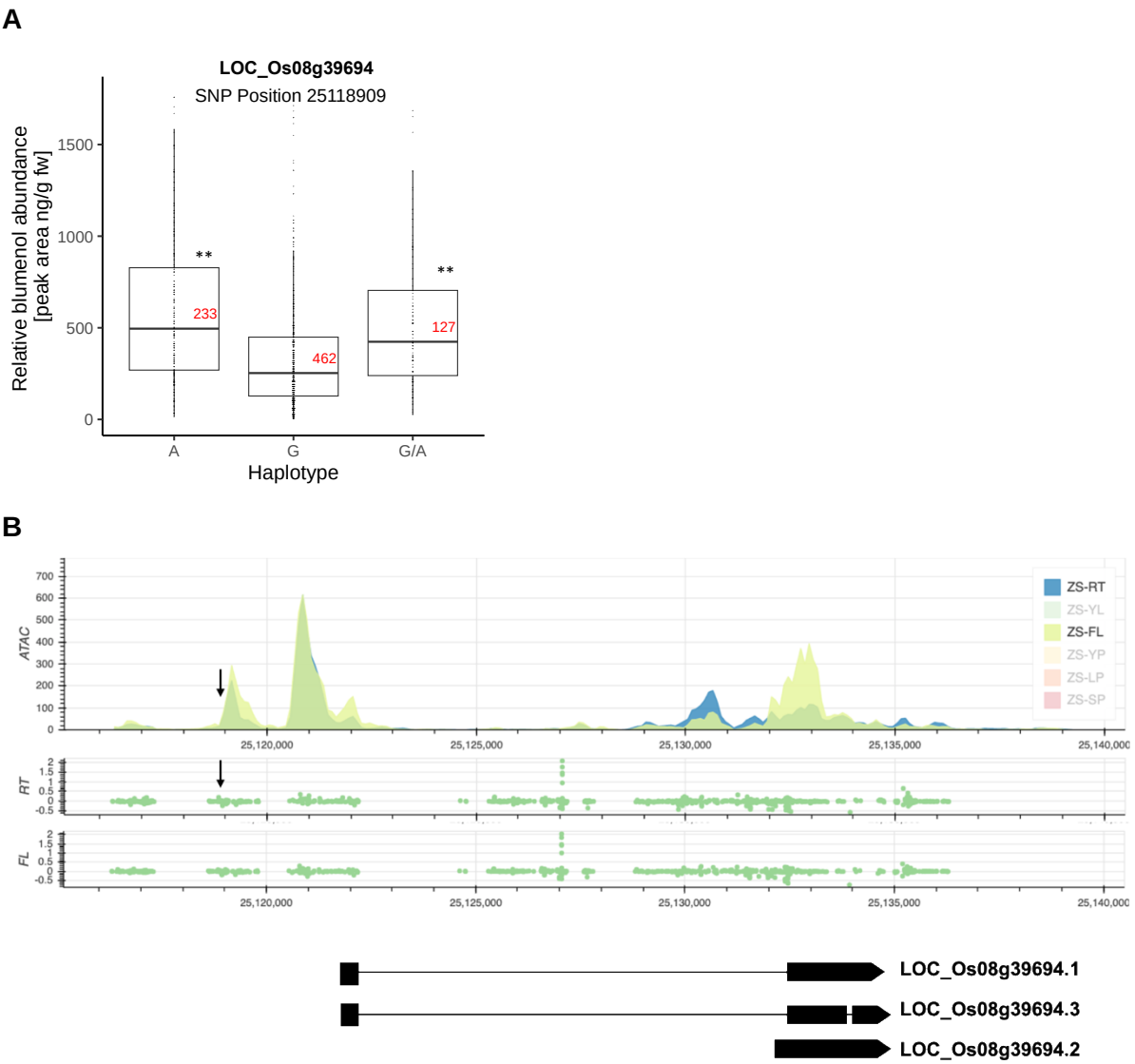

Figure 4.22 Haplotype analysis of a putative CYP at LOC_Os08g39684 identified to be associated to 11-hydroxyblumenol C-Glc. *(A) Abundance of 11-hydroxyblumenol C-Glc in haplotypes of a SNP upstream of LOC_Os08g39684. Haplotypes identified in cultivars of the panel include reference allele G, alternative allele heterozygous G/A and G. Significant differences of blumenol abundance in alternative compared to reference alleles was analysed by Kruskal Wallis test and asterixis denote statistically significant differences (p < 0.05). (B) Gene model and chromatin accessibility data from RiceVarMap2 for 5 Kb up- and down-stream of LOC_Os08g39684. The chromatin accessibility ATAC-Seq score is denoted for root (RT) and flag leaf (FL). Green points indicate SNP variants affecting chromatin accessibility and black arrows indicate position of the SNP identified in GWAS.*

4.3.2.4 Candidate genes associated to 11-carboxyblumenol C-Glc abundance

Next, the significant lead SNP at position 18163171 on chromosome 3 (Figure 4.21) was analysed for effect on 11-carboxyblumenol C-Glc abundance. Comparison of mean 11-carboxyblumenol C-Glc abundance between haplotypes of the SNP found abundance significantly decreased from 9868.77 ± 13.74 ng/g fw and 8359.53 ± 49.74 ng/g fw in cultivars with reference AA haplotype or missing call respectively to 5067.09 ± 27.36 ng/g fw in cultivars with TT haplotype (KW, $p = 9.87e^{-8}$, Figure 4.23). Functional SNP annotation was performed 100 Kb up- and down-stream of the peak and a SNP at position 18163171 was identified as having potential effects (Figure 4.23). The A → T mutation is predicted to be a silent, intergenic modification ~3 Kb upstream of *LOC_Os03g31750* a PYRUVATE PHOSPHATE DIKINASE (PPDKA). Notably, chromatin accessibility analysis using RiceVarMap2 didn't predict a score for the effect of the variant (Figure 4.23). The chromatin accessibility score is a prediction based on analysis of tissue after two weeks of growth (H. Zhao et al., 2021). Since chromatin accessibility can be affected by development and environment (Alvarez et al., 2019; Liang et al., 2021; H. Zhao et al., 2021), it is possible that the region becomes accessible and is required for regulation of gene expression at different life stages of the plant or in different environments, such as upon P_i deficiency or AMF recognition.

PPDK is an enzyme responsible for production of phosphoenolpyruvate, the primary acceptor of CO2 during CAM and C_4 photosynthesis. PPDK also contributes to NADH to NADPH conversion and has roles in nitrogen assimilation and synthesis of fatty acids. In rice, which has C_3 photosynthesis, it has previously been implicated in starch metabolism (Moons et al., 1998). Notably, PPDKA is a cytosolic isoform of one of three PPDK-encoding genes in rice, including two cytosolic and chloroplast PPDKB enzymes. Recently, a SNP in the PPDKB isoforms has associated to endosperm development. The role of PPDKB in such function is unknown but is hypothesized to regulate provision of energy through supplying pyruvate for lipid synthesis and hexoses for starch biosynthesis (H. Wang et al., 2020). PPDKA has previously been noted to be required for inducible metabolic responses to ABA, low oxygen stress and water deficit in non-photosynthetic tissues (Moons et al., 1998).

Thus, PPDK enzymes have hypothesized function in regulation of energy sources in plants. Notably, *LOC_Os03g31750* was previously found to be upregulated 2.3-fold upon inoculation with *R.irregularis* (S. Wang et al., 2020), Table 4.4. It could be speculated that PPDKA is associated to changes in carbon allocation occurring during association with AMF, required for regulated establishment of symbiosis. The region ~3 Kb upstream may be required for normal transcription, which when perturbed affects function in AM symbiosis and thus reduced root colonisation and 11-carboxyblumenol C-Glc abundance. Such a hypothesis would require analysis of mutants of PPDKA.

16 additional genes were annotated within the region, including two more genes that were previously found to be differentially expressed upon inoculation of rice with *R. irregularis* (S. Wang et al., 2020), Table 4.4A. Previously, expression analysis of rice inoculated with *R. irregularis* found *LOC_Os03g31679*, a bHLH transcription factor regulated gene, WINDHOSE2 (WIH2) was downregulated 0.76-fold while *LOC_Os03g31880,* SHORT ROOT TRANSCRIPTION FACTOR 2 (SHR2) expression was upregulated ~1.69-fold (S. Wang et al., 2020). In addition, a putative mechanosensitive ion channel protein, a GCN5-related N-acetyltransferase and a glycosyltransferase were identified (Table 4.4A).

Again, to narrow down the candidate gene list, coding variants were mined using SNP Seek tool (https://snp-seek.irri.org) and SNPEff annotation. Modifier effects caused by upstream, downstream, intron, 3’ UTR, 5’ UTR and intergenic variants were identified. In addition, moderate effects caused by missense variants were evident in some genes and a possible high effect variant caused by splice donor variation was identified in *LOC_Os03g31730,* an expressed protein of unknown function. 16 of the 17 candidate genes contained variants with the potential to cause high, moderate, or modifying effects, as summarised in Table 4.4B.

Next, potential candidate genes were interrogated for function. Firstly, *SHR2* is a gene that encodes a GRAS family transcription factor known to be required for cortical cell division. Current models assumed SHR modulates ground tissue division to generate clonally related endodermis and cortex cell layers (Henry et al., 2017). Many GRAS domain proteins have been associated with having essential regulatory

roles AM symbiosis, including RAM1, NSP1 and NSP2, as reviewed by (A. M. Maclean et al., 2017). In addition, the GRAS transcription factor MIG1 has been identified to have roles in facilitating AM symbiosis, as together with DELLA, it controls cortical radial cell expansion during arbuscule development (Heck et al., 2016). Since expression of *SHR2* has previously been reported to increase ~1.69-fold during AM symbiosis (S. Wang et al., 2020) and the transcription factor is implicated in control of cortical cell development, it is an excellent candidate gene for further analysis.

In addition, expression of a bHLH transcription factor regulated gene, *WIH2* has been reported to be downregulated 0.76-fold during AM symbiosis (S. Wang et al., 2020). WIH2 has previously been described in rice as a class of small peptides with GYPPX repeats. WIH2 has been implicated in drought tolerance through interaction with HOTHEAD transcription factor to regulate long chain fatty acid biosynthesis and increase cuticular wax composition (Gu et al., 2021). Since fatty acid biosynthesis is implicated in lipid transfer during AM symbiosis (Bravo et al., 2017; C Gutjahr et al., 2012; Luginbuehl et al., 2017), *WIH2* is additionally a good candidate gene for further study.

Table 4.4 Analysis of the region associated to the significant SNP for 11-carboxyblumenol C-Glc. *(A) Table summarises genes annotated with 100 Kb up- and down-stream of the significant position on chromosome 3. Log fold change (Log FC) of previously identified in rice inoculated with R. irregularis* (S. Wang et al., 2020) *is given where identified. (B) SNPEff results for SNP variants present in each of the genes identified within the region. The number of non-synonymous SNPs (No. NS SNPs) and insertion/deletion (No. INDELs) is given. Predicted effects of all SNPs is noted, including whether the impact is predicted to be low, moderate, high or modifying.*

A

MSU	RAP-DB	Gene	Function	logFC in AMF (Wang et al. 2020)
LOC_Os03g31679	Os03g0431100	WIH2	BHLH TF, drought tolerance	-0.764038807
LOC_Os03g31690	Os03g0431200		GCN5-related N-acetyltransferase, putative	
LOC_Os03g31730	Os03g0431800		expressed protein	
LOC_Os03g31760			expressed protein	
LOC_Os03g31880	Os03g0433200	SHR2	SHR transcription factor	1.694385081
LOC_Os03g31750	Os03g0432100	PPDKA	Similar to Pyruvate, phosphate dikinase 2	2.353124562
LOC_Os03g31706			expressed protein	
LOC_Os03g31740			ZCF37, putative, expressed	
LOC_Os03g31790			hypothetical protein	
	Os03g0432277		hypothetical protein	
	Os03g0431550		Glycosyl transferase, family 20 domain .	
LOC_Os03g31640				
LOC_Os03g31839	Os03g0432900		mechanosensitive ion channel protein 2	
	Os03g0432666		hypothetical gene	
LOC_Os03g31670			hypothetical protein	
LOC_Os03g31870			hypothetical protein	
LOC_Os03g31700			expressed protein	

B

Gene	No. NS SNPs	No. INDELs	SNP Effects	EFFECT
WIH2	0	84	upstream, downstream, intron	modifier
LOC_Os03g31690	1	82	downstream, intron, missense	modifier, moderate
LOC_Os03g31730	9	627	intron, missense, splice donor	modifier, moderate, high
LOC_Os03g31760	6	105	3' UTR, missense, downstream	modifier, moderate
SHR2	2	42	missense, upstream, 5' UTR, synoymous	low, modifier, moderate
PPDKA	1	107	intron, missense, splice donor	modifier, moderate
LOC_Os03g31706	1	49	missense, 5' UTR	modifier, moderate
LOC_Os03g31740	2	8	missense, downstream	modifier, moderate
LOC_Os03g31790	3	2	missense	moderate
Os03g0432277	0	22	upstream, intergenic	modifier
Os03g0431550	0	165	upstream, intergenic	modifier
LOC_Os03g31640	20	27	missense, downstream	modifier, moderate
LOC_Os03g31839	1	8	missense	moderate
Os03g0432666	0	32	-	-
LOC_Os03g31670	2	61	missense, upstream, downstream, intron	modifier, moderate
LOC_Os03g31870	3	36	missense, downstream	modifier, moderate
LOC_Os03g31700	10	44	missense, intron	modifier, moderate

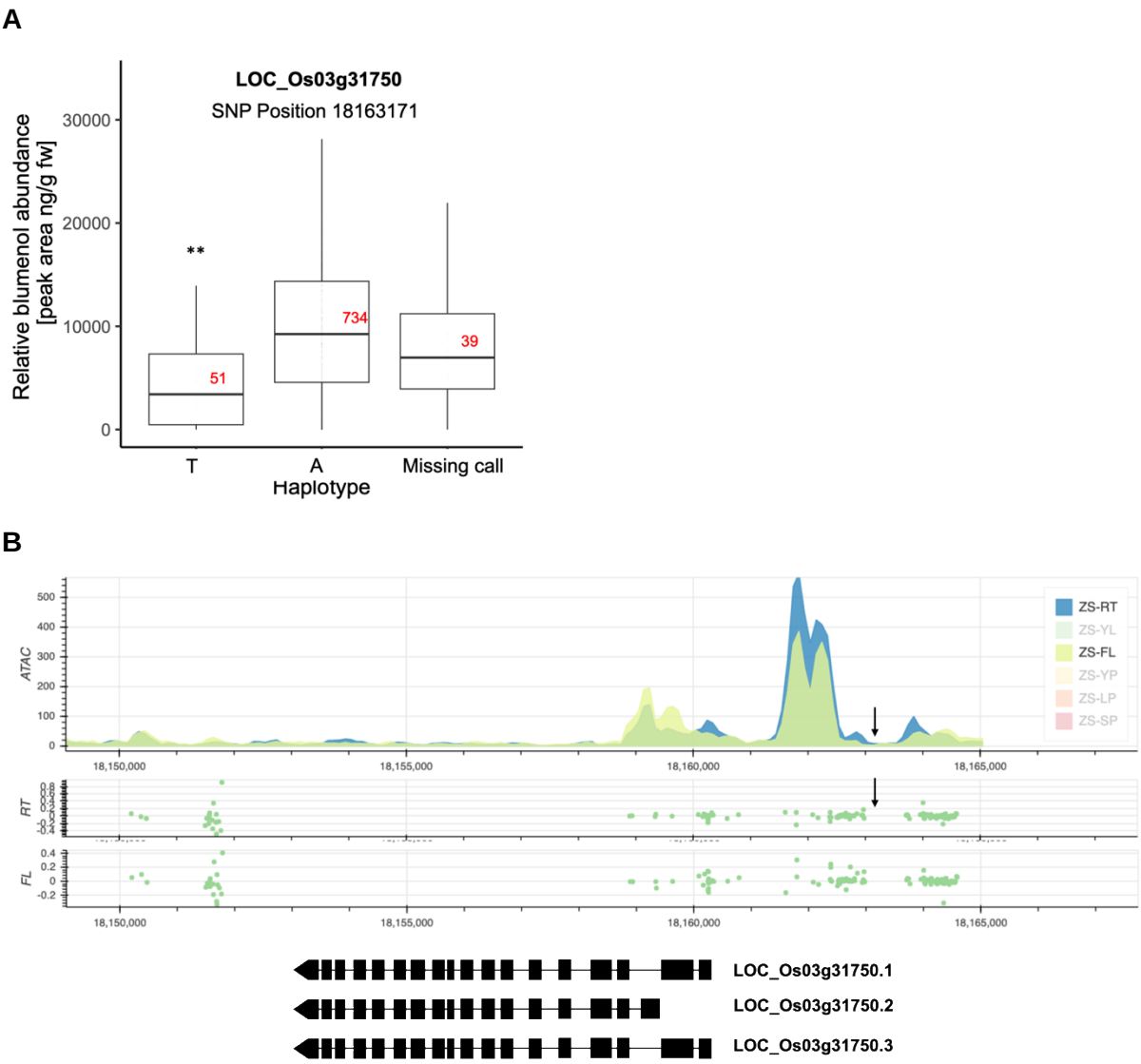

Figure 4.23 Haplotype analysis of PPDKA at LOC_Os03g31750 identified to be associated to 11-carboxyblumenol C-Glc. *(A) Abundance of 11-carboxyblumenol C-Glc in haplotypes of a SNP upstream of LOC_Os03g31750. Haplotypes identified in cultivars of the panel include reference allele A, missing call and alternative allele T. Significant differences of blumenol abundance in alternative compared to reference alleles was analysed by Kruskal Wallis test and asterixis denote statistically significant differences (p < 0.05). (B) Gene model and chromatin accessibility data from RiceVarMap2 for 5 Kb up- and down-stream of LOC_Os03g31750. The chromatin accessibility ATAC-Seq score is denoted for root (RT) and flag leaf (FL). Green points indicate SNP variants affecting chromatin accessibility and black arrow indicates position of the SNP identified in GWAS.*

4.3.3 Discussion and a comment on future analyses

This study clearly notes an exciting list of candidate genes associated to blumenol abundance during AM colonisation, including transcription factors regulated by AM symbiosis and genes involved in lipid biosynthesis, root development and plant defence. In addition, haplotype analysis found differences in mean blumenol abundance in cultivars with SNP variations in regions proximal to strong candidate genes. A putative CYP associated to 11-hydroxyblumenol C-Glc abundance, with potential function in biosynthesis of AM-associated apocarotenoids including blumenols, is reported. In addition, a PPDK enzyme with potential function in control of carbon resources during AM symbiosis is highlighted as being associated to 11-carboxyblumenol C-Glc. These genes are recommended candidates for further analysis.

Next, analyses should focus on further investigating candidate genes in the significant and suggestive SNP regions by running the GWAS models again using the larger set of ~2M SNPs. Haplotype blocking should then be performed to narrow the associated region and reduce the gene list to strong candidates. This work was beyond the timeframe of this project but is currently ongoing as a collaboration with Prof Ruairidh Sawers and Dr. Meng Li at Penn State College of Agricultural Sciences. In addition to QTLs associated to variation in root colonisation, the analysis will focus on mapping genetic regions associated to host growth and nutrient responses. This will use a previously described method that identified QTLs associated to beneficial host response to AMF in maize (M. Li et al., 2022; Ramírez-Flores et al., 2020). Briefly, four models are used in mapping, including separate analysis of non- and AMF-inoculated data and models considering AMF as an additive or interactive covariate (M. Li et al., 2022). The GRID LMM package will be used to fit the linear mixed models for GWAS (Runcie & Crawford, 2019) and candidate genes annotated using MAGMA (de Leeuw et al., 2015). Such analyses will be used to further identify QTLs and candidate genes associated to blumenol abundance (root colonisation) and additionally identify QTLs associated to beneficial host response in terms of the growth and nutrient uptake in rice.

Once candidates are confirmed, functional experimentation including analysis of root length colonisation and blumenol abundance in knock out mutants is required to identify if the genes have a role specifically in AM symbiosis signalling and/or blumenol accumulation during AM symbiosis. Such analysis will allow for identification of genetic regions associated to beneficial response to AMF in nutrient limited conditions, which will be important in the potential for use as AMF in future sustainable agriculture systems.

4.4 Conclusions

This study represents the first description of a globally distributed, diverse panel of *Indica* rice representative of phenotypic diversity in the 3K-RG. Physiological and ionomic analyses identified natural variation in height, biomass and foliar ionome composition. This provides preliminary support for genetic factors determining plant growth and metabolic response in P deplete conditions.

There was also significant natural variation in AM colonisation and response across the panel, clearly demonstrating that the outcome of AMF-inoculation is genetically determined in *Indica* rice. Further analysis used the extensive resources available for the 3K-RG to identify genetic regions and candidate genes associated to colonisation and the accumulation of blumenol during AM symbiosis. Several exciting candidate genes were highlighted as targets for future study.

Host plant response is partially driven by extent of colonisation but likely determined by genetic factors. Notably, unlike in maize (Sawers et al., 2017), shoot biomass responses were independent to shoot P content and likely dependent on additional factor such as PUE. Further analyses of data described in this project are ongoing for mapping of such genetic factors and QTLs associated to beneficial growth and nutrient response to AMF inoculation. Identification of genetic determinants driving crop benefit in aerobic, P deplete environments will be important in the potential for use as AMF in future sustainable agriculture systems.

4.5 Supplementary Figures

Supplementary Figure 4.1 Mean blumenol abundance in selected Indica panel. *Cultivar name, subpopulation (K=9), country of origin is indicated. Mean and standard error of abundance of 11-hydroxyblumenol C-Glc and 11-carbocyblumenol C-Glc in AMF-inoculated plants is indicated, with 4-5 biological replicates per cultivar.*

Cultivar	K9	Country	11-hydroxyblumenol C-Glc		11-carboxyblumenol C-Glc	
			Mean	SE	Mean	SE
ESCONDE CACHO::IRGC 74305-1	ind3	Brazil	112.34	18.01	199.68	191.02
CHING CH'UNG::IRGC 65002-1	indx	Taiwan	107.18	60.06	1569.22	750.28
CHAMA (DWARF)::IRGC 69487-1	ind1 B	Zambia	123.22	66.93	2160.01	1637.25
HEGAR MANAH::IRGC 17733-1	indx	Indonesia	66.44	22.2	2399.62	1849.14
RIZ INDETERMINE::IRGC 69014-1	indx	Niger	562.87	116.75	2852.61	358.92
GOBOL SAIL (BALAM)::IRGC 26624-2	ind2	Bangladesh	126.96	47.53	2965.04	1242.92
ITA 117::IRGC 75235-1	ind1 B	Nigeria	60.78	19.26	3206	662.6
CHIAYI WU-K'O::IRGC 64974-1	ind1 A	Taiwan	197.74	51.08	3208.23	1075.33
VEN THAP::IRGC 56138-1	indx	Viet Nam	154.47	72.03	3301.82	1996.63
MALAGASY::IRGC 69717-1	ind2	Zambia	363.24	170.18	3572.51	1807.88
EX SANDEMA::IRGC 79964-1	indx	Ghana	35.12	22.67	3592.15	3393.31
KOLUBA::IRGC 30463-3	ind3	Sierra Leone	425.92	82.19	3866.79	2168.84
CAMPONI::IRGC 116963-1	indx	Surinam	173.13	55.6	4006.92	1500.21
SATHIYA::IRGC 59225-1	ind1 A	Nepal	351.92	102.28	4335.03	2192.95
MAMORIAKA::IRGC 77867-1	indx	Madagascar	447.6	179.6	4508.12	1430.26
CRILLO LA FRIA::IRGC 10793-1	ind1 A	Venezuela	292.44	75.85	4540.53	2358.57
DUDHSAR::IRGC 26609-2	ind2	Bangladesh	94.09	65.87	4565.16	3841.95
LUBUK LINGGAU::IRGC 20000-2	ind3	Indonesia	154.14	41.29	4694.78	2402.28
GLAM::IRGC 47978-2	ind3	Thailand	328.95	53.41	4698.82	1262.41
PURA BINNI::IRGC 26772-1	ind2	Bangladesh	427.92	142.82	4766.43	1490.15
BALIBUD::IRGC 26871-1	indx	Philippines	83.85	29.37	4832.18	1156.26
MODDAI KARUPPAN::IRGC 15465-1	ind2	Sri Lanka	190.34	37.59	4942.85	2402.61
KERITING TINGGI::IRGC 19972-1	ind3	Indonesia	318.13	131.92	5020.58	1624.73
SRAU KHSAI::IRGC 29896-2	ind3	Cambodia	517.61	244.6	5115.85	1722.27
MAVOLATSIKA::IRGC 83137-1	ind2	Madagascar	191.47	66.77	5206.45	1580.59
KILOMBERO::IRGC 69698-1	ind3	Tanzania	286.54	106.83	5318.06	2825.03
MERLE::GERVEX 1685-C1	indx	France	447.54	85.58	5443.09	2400.15
GAJA BARU::IRGC 17586-1	indx	Indonesia	290.32	69.23	5443.14	1994.28
ADNY 11::C1	ind1 B	Mali	137.53	72.9	5463.44	3425.46
LALKA (LAL DHAN)::IRGC 64946-1	ind2	Fiji	58.38	20.91	5475.18	2393.47
INIAP 10::IRGC 117000-1	indx	Ecuador	237.11	55.95	5477.92	2051.54
SOLOMON RED RICE::IRGC 50950-1	indx	Solomon Islands	206.56	110.05	5518.7	2952.84
SAMON::IRGC 44735-2	ind3	Philippines	351.64	152.57	5529.46	2899.2

IA CUBA 17::IRGC 116990-1	indx	Cuba	199.6	76.45	5652.11	2441.34
NASAENG::IRGC 107818-1	indx	Lao People's Democratic Republic	291.53	66.91	5781.46	1510.25
GOJOT::IRGC 17669-1	ind3	Indonesia	284.5	70.07	5848.62	2238.71
SAN BAO GU::IRGC 76732-1	ind1 A	China	289.24	87.59	5860.22	2177.82
PARA NELLU::IRGC 50009-1	ind2	India	343.93	85.63	5876.83	1082.93
LARHA MUGAD::IRGC 52339-1	ind2	India	126.63	29.37	5907.25	492.51
NIAW NARAI::IRGC 71353-1	ind3	Thailand	370.85	156.73	5915.55	2392.48
CHANDINA::IRGC 36420-1	ind1 B	Sri Lanka	180.24	140.04	6067.27	5770.73
SAM SI::IRGC 99020-1	ind3	Lao People's Democratic Republic	471.13	158.58	6126.19	3055.82
DUDA MONOR::IRGC 26335-2	ind2	Bangladesh	344.87	120.47	6133.13	2787.58
ICTA MOTAGUA::IRGC 116995-1	indx	Guatemala	124.38	43.01	6179.67	3076.4
MILAGROSA::IRGC 44634-2	ind2	Philippines	363.19	55.15	6212.15	1184.02
ARIANA::GERVEX 396-C1	indx	Romania	261.34	107.96	6250.81	1526.43
B 38::IRGC 34409-1	ind3	Liberia	713.14	305.54	6383.12	3377.81
INDEL::IRGC 17748-2	indx	Indonesia	262.19	82.08	6489.67	1273.86
531::IRGC 82643-1	indx	Philippines	441.19	148.87	6506.62	2596.88
DONGREM::IRGC 6688-1	ind2	India	325.02	81.82	6602.25	1176.58
SIGARDIS::IRGC 15555-1	ind1 B	Sri Lanka	198.95	59.57	6723.38	1160.2
GIZA 178::GERVEX 1681-C1	indx	Egypt	257.65	102.5	6746.83	2938.89
LUA DUC::IRGC 16718-1	indx	Viet Nam	376.55	159.74	6821.16	3822.82
ANADI WHITE::IRGC 61897-1	ind1 A	Nepal	432.79	64.93	6867.9	3278.2
MOUI SAMBA::IRGC 75751-1	ind1 B	Burkina Faso	476.24	212.39	7030.12	1889.4
UTRI DELI::IRGC 19182-1	ind3	Indonesia	338.2	103.55	7248.47	3260.55
RUJAK DANAN::IRGC 35446-2	ind3	Indonesia	356.11	87.78	7366.4	685.6
SAMBA::IRGC 11993-1	ind2	Sri Lanka	235.74	47.01	7400.09	2144.46
WAGWAG PUTI::IRGC 44804-2	ind1 B	Philippines	154.2	30.66	7482.27	2007.97
YADU BARA::IRGC 86912-1	indx	Bhutan	399.84	48.92	7601.47	836.55
TANDAKAY FINGO::IRGC 69793-1	ind2	Gambia	537.04	271.52	7652.29	5998
CHE MAH::IRGC 79480-1	ind3	Malaysia	288.88	83.28	7721.13	1932.16
PUEY TAW::IRGC 71405-1	ind3	Thailand	526.85	292.82	7722.31	4190.48
EX MARABA GURUKU::IRGC 69582-1	ind1 A	Nigeria	316.7	44.12	7750.76	978.3
HAM MOON::IRGC 9135-2	indx	Hong Kong	280.29	98.23	7762.44	3995.17
PA FADAYA::IRGC 58524-1	indx	Sierra Leone	298.49	107.54	7863.43	2708.49
GADABUNG (GUNDIL)::IRGC 17569-2	ind3	Indonesia	354.73	124.67	7865.1	3744.87
TUI (KIDAYAN)::IRGC 79058-1	ind3	Philippines	114.79	34.95	7986.53	2565.2
BARIK KUDI::IRGC 52807-1	ind2	India	351.6	132.86	8072.82	3351.16
IB 11::IRGC 74420-2	ind2	Burundi	244.77	94.43	8116.28	1184.15
IH PEN SHIM MING::IRGC 26067-1	ind1 A	Brazil	170.9	37.3	8148.73	1688.47
CEA 3::IRGC 116965-1	indx	Paraguay	353.91	154.56	8156.33	4573.75
LEAD::IRGC 5805-1	indx	Malawi	350.5	82.93	8171.18	1292.29
SADA RUPA::IRGC 77299-1	ind1 B	Bangladesh	194.4	80.34	8190.21	1766.76
ARC 11857::IRGC 40972-1	indx	India	246.6	51.47	8226.71	1973.03

ALTAMIRA 9::IRGC 116953-1	indx	Nicaragua	183.86	48.28	8244.19	3374.47
EA HOUM::IRGC 11783-1	indx	Lao People's Democratic Republic	209.76	41.45	8284.46	1911.46
BATU::IRGC 71508-1	ind3	Malaysia	521.23	208.43	8323.07	4494.68
DICULA::IRGC 36729-2	ind3	Philippines	654.7	104.02	8325.66	2413.28
WAGWAG::IRGC 44802-1	indx	Philippines	203.28	114.55	8397.79	4991.24
ALAGUSAMBA::IRGC 8944-2	ind2	Sri Lanka	508.36	257.18	8437.37	4633.68
ZO::IRGC 56914-1	ind3	Cote d'Ivoire	308.22	86.98	8452.28	3626.87
PERUBAK LUEY::IRGC 86436-1	ind1 B	Malaysia	247.33	173.8	8733.09	5299.78
PULUT SELEMYAM::IRGC 71820-1	ind3	Malaysia	272.36	32.23	8781.33	3397.8
MOSHI::IRGC 70648-1	ind2	Kenya	167.36	47.31	8801.34	2523.26
YA NONG ZAO 4::IRGC 63908-1	ind1 A	China	760.77	237.5	8844.98	4584.66
ARC 12884::IRGC 22417-1	indx	India	230.91	105.04	8851.74	3680.73
ARC 11663::IRGC 42695-1	ind1 B	India	252.8	143.84	8858.79	3735.7
NS 1515::IRGC 68947-1	ind2	Madagascar	159.18	52.3	8882.05	2317.61
NS 199::IRGC 68864-1	ind2	Cote d'Ivoire	363.7	108.01	9024.76	1922.94
BORIZINA 640::IRGC 68382-1	ind3	Madagascar	1340.37	211.62	9086.44	2086.76
CT 9506-18-7-1T-2::IRGC 116973-1	indx	Colombia	610.34	253.83	9100.11	3591.32
HOING CANTEL::IRGC 19282-2	ind3	Indonesia	481.38	108.96	9226.7	2139.67
SHIOKARI	NA	NA	459.06	149.95	9246.53	3700.88
KAMPTI::IRGC 75626-1	ind3	Burkina Faso	525.49	52.18	9256.7	1248.86
DA GANG ZHAN::IRGC 67103-1	indx	China	275.06	49.38	9317.24	1415.54
BK 26::IRGC 45197-1	ind2	India	181.75	53.19	9327.83	2106.61
DAA MANSA::IRGC 67559-1	ind1 B	Ghana	402.68	109.3	9372.66	1127.46
WI BIR SHUN::IRGC 4602-1	ind1 A	China	530.07	178.1	9393.12	2587.12
PJ 110::IRGC 68981-1	indx	Cameroon	753.62	262.28	9417.66	3098.69
FELEGBASEH::IRGC 58443-1	ind3	Sierra Leone	539.64	183.63	9449.09	3475.51
MATHOLUWA::IRGC 8901-1	indx	Sri Lanka	419.08	130.24	9476.4	2933.81
JIANG HUI DAO::IRGC 59688-1	indx	China	634.16	135.05	9508	3175.7
PICO NEGRO::IRGC 55849-1	indx	Ecuador	569.29	176.11	9517.73	2449.86
MENAHARA 505::IRGC 68709-1	ind2	Madagascar	291.72	177.89	9521.12	3909.44
KARANTABA 1::IRGC 15924-1	ind3	Senegal	1148.22	147.21	9543.99	1644.65
IR 1813-694-2::IRGC 32656-2	ind1 B	Philippines	201.92	65.73	9696.5	3581.41
IRGA 318-11-6-9-2B::IRGC 117339-1	ind1 B	Colombia	245.11	74.45	9721.78	2970.02
KA SAEN::IRGC 11642-1	ind3	Lao People's Democratic Republic	242.47	96.12	9842.94	2716.11
P 41::IRGC 68987-1	ind3	Liberia	784.05	273.6	9866.91	3416.01
WAGWAG RAOIS::IRGC 44805-1	indx	Philippines	222.48	154.73	9873.61	6190.7
WANGKOD::IRGC 71646-1	ind2	Malaysia	274.59	53.5	9910.34	3865.18
TSAO SHENG LI 1::IRGC 1309-1	ind1 A	China	1113.56	466.87	9953.98	4548.14
EX FOILAEIN (NAPUTO)::IRGC 81675-1	indx	Mozambique	437.92	85.36	9960.17	3022.24
ASU::IRGC 62154-1	indx	Bhutan	479.11	147.92	10050.62	2161.9
NIPPONBARE	NA	NA	281.6	67.92	10062.64	4175.66
ORIONE::GERVEX 333-C1	indx	Italy	424.31	141.92	10104.56	4161.87

GAO LIANG ZAO::IRGC 59563-1	indx	China	272.3	27.48	10123.71	2373.66
ARNG'-KAR PHAR ONG::IRGC 87196-1	ind3	Cambodia	283.32	83.65	10154.4	3682.9
BANDI::IRGC 17214-1	ind3	Indonesia	429.75	122.21	10177.16	3682.21
ZACATEPEC::IRGC 16901-2	ind1B	United States of America	464.83	211.05	10223.18	4464.85
ECIA 24-107-1::IRGC 116978-1	ind1B	Cuba	223.76	77.48	10250.34	3940.79
DELI POCONG::IRGC 35265-1	indx	Indonesia	1234.95	516.38	10294.99	4264.22
O. SATIVA::IRGC 10164-2	ind2	India	439.74	72.35	10304.36	2254.36
SRAU THMOR::IRGC 29904-1	ind3	Cambodia	862.53	500.7	10387.61	2966.47
MILYANG 77::IRGC 69340-1	ind1B	Korea, Republic of	184.93	49.86	10415.75	2703.36
FACAGRO 64::IRGC 82059-1	ind2	Burundi	430.55	180.89	10574.54	4254.15
RAJHUSAI (ACR 12)::IRGC 53630-1	ind2	India	353.74	40.26	10592.82	1296.28
MANARE (PHOM)::IRGC 61437-1	ind3	Guinea	1148.77	296.88	10632.89	3491.07
AM BEUS::IRGC 87189-1	indx	Cambodia	324.41	58.72	10668.67	1092.84
ARC 11901::IRGC 21727-1	indx	India	337.96	145.39	10814.28	3722.92
QUERO ASSAN::IRGC 28860-1	ind3	Portugal	308.99	68.32	10820.79	3723.84
HURANG ARISO LUTA::IRGC 26055-1	indx	Brazil	253	33.36	10886.97	447.4
SANPATONG NYAY::IRGC 99050-1	ind3	Lao People's Democratic Republic	731.74	143.79	10932.27	3736.55
DALSUNG 41::IRGC 79385-1	indx	Korea, Republic of	237.69	31.73	10971.9	2479.72
PAN DAWK MAHK::IRGC 71380-1	ind3	Thailand	621.81	117.64	11009.33	2481.11
INIAP 6::IRGC 117002-1	indx	Ecuador	411.53	168.14	11045.06	3219.5
BOHOTO BALOOCHESTAN::IRGC 66237-1	indx	Iran	568.68	327.44	11054.45	6247.95
FOFFI::IRGC 68438-1	ind2	Cote d'Ivoire	550.75	147.64	11321.03	2467.3
GEANT W 7::IRGC 9620-1	ind2	Netherlands	446.39	150.97	11382.18	5039.91
KETAN SERANG::IRGC 14615-1	ind3	Indonesia	659.61	165.49	11404.87	3978.59
DISSI::IRGC 101346-1	ind2	Cameroon	563.83	167.06	11433.55	4010.76
EKAYIN SAW::IRGC 97468-2	ind3	Myanmar	633.86	173.99	11759.12	3817.14
MAGSIING::IRGC 5211-1	indx	Philippines	635.57	195.24	11777.06	2909.15
JUMA 62::IRGC 117011-1	indx	Dominican Republic	656.92	362.17	11816.49	3634.3
BANTA TIMA::IRGC 69474-1	indx	Gambia	708.21	149.42	11850.66	2826.42
KAZALSAIL::IRGC 37161-2	ind2	Bangladesh	1002.29	307.33	11908.25	6364.14
CHING LIU::IRGC 65018-1	indx	Taiwan	272.26	49.54	11915.88	2323.73
UPL RI 7::IRTP 9897-C1	indx	Philippines	382.02	73.88	11985.71	4335.61
BARKHE TAULI::IRGC 16116-1	ind1A	Nepal	503.83	170.1	12186.78	4052.8
DIAMBARANG::IRGC 56726-1	ind3	Guinea-Bissau	400.73	158.77	12212.8	3771.72
MOVE (MOKOLE)::IRGC 69739-1	indx	Benin	325.5	103.55	12257.16	3082.65
MURGI BRINJ::IRGC 73109-1	indx	Pakistan	402.41	64.42	12392.77	1926.16
FEDEARROZ 50::G1	ind1B	Colombia	674.62	141.1	12419.62	4639.97
MINDANAO::IRGC 44642-2	ind3	Philippines	538.22	116.99	12484.79	1395.28
LANG QIAN CHE::IRGC 59730-1	ind1A	China	426.66	122.47	12533.25	3649.4
R 762::IRGC 70531-1	indx	Colombia	1250.36	327.23	12665.51	3699.22
IRGA 346-111-2-1F::IRGC 117341-1	indx	Colombia	221.28	50.86	12705.36	2635.22
MEKENZIE SMALL::IRGC 49895-1	ind2	Guyana	613.63	158.39	12714.47	3952.03

NAN ERH AI 5::IRGC 34255-1	ind1 A	China	575.34	199.29	13028.78	3923.98
H 15-23-DA::C1	indx	Mali	779.03	96.99	13081.12	3107.39
TOURBE::IRGC 47066-1	indx	Chad	546.7	161.96	13107.26	3633.16
MARAMAY::IRGC 82628-1	ind3	Philippines	750.02	139.89	13185.69	2365.56
CT 9737-6-1-1-2-2P-M::IRGC 117330-1	indx	Colombia	605.12	226.25	13339.5	5669.86
PA RABICHINA::IRGC 58609-1	ind3	Sierra Leone	808.76	254.06	13485.98	2022.91
DUD KUNING::IRGC 44-1	ind3	Indonesia	804.04	187.73	13519.59	4274.99
SRAU KHGNAERNG::IRGC 87073-1	ind3	Cambodia	899.03	183.39	13660.95	2150.3
DUDRE::IRGC 52523-1	ind2	India	686.69	147.27	13881.88	5694.21
DAMNOEUB KRACHAK SESS::IRGC 87380-1	ind3	Cambodia	640.77	118.41	13886.85	2317.08
XITTO::IRGC 6671-1	ind2	India	560.63	59.66	14083.19	2750.21
DISSIGBE::IRGC 66916-1	ind2	Guinea	841.05	175.84	14182.4	2956.41
ARN'-SAR THNGORN'::IRGC 87205-1	ind3	Cambodia	1153.95	309.41	14453.75	1718.81
MALOBA (DISSI ROUGE)::IRGC 75700-1	indx	Burkina Faso	635.43	144.81	14653.18	3413.24
KWANG LU AI 4::IRGC 28480-2	ind1 A	China	1091.92	88.68	14719.85	3284.48
DO KHAW::IRGC 106977-1	ind3	Lao People's Democratic Republic	520.05	141.4	14799.81	1623.03
CHATO::IRGC 55825-1	ind1 B	Ecuador	555.29	308.7	14832.09	7402.45
EX EBOKOZURU::IRGC 79912-1	ind3	Nigeria	722.51	172.8	14883.75	5860.9
KATUMANI::IRGC 69695-1	ind3	Tanzania	1452.09	200.38	14901.87	666.44
TE SAN AI 2::IRGC 93355-1	indx	China	529.22	60.64	15049.39	3470.08
EX AUBERGE::IRGC 79898-1	indx	Egypt	365.17	66.38	15237.26	3421.88
SABRAN::IRGC 34630-1	ind1 B	Indonesia	324.86	124.84	15310.34	3526.01
E 2024::IRGC 67958-1	ind1 B	China	370.59	134.88	15935.5	5489.96
TAMBAS JANGKOK::IRGC 78724-1	ind3	Brunei Darussalam	1633.92	262.57	16185.35	2594.64
TRANG LUA::IRGC 16781-1	ind3	Viet Nam	1106.09	456.04	16411.92	5547.63
ADANKARU::IRGC 79842-1	ind2	Nigeria	1352.14	356.15	17000.16	3861.19
MULLIKURUVA::IRGC 77529-1	ind2	India	381.9	30.9	17027.16	2020.47
HD 10::IRGC 6638-1	ind2	Australia	645.94	129.62	17186.29	2068.22
ASFALA::IRGC 70650-1	ind3	Kenya	745.76	165.41	17753.06	3550.09
MIN ZAO 6::IRGC 63772-1	ind1 A	China	1259.31	245.87	18996.31	3962.21
XIA HONG GU::IRGC 76803-1	ind1 A	China	970.07	221.69	19161.5	3842.66
CHAM LEK::IRGC 89387-1	indx	Lao People's Democratic Republic	1333.72	242.65	20195.26	3888.86
SICAN::IRGC 117029-1	indx	Peru	1125.77	450	21560	6574.54
MEI FENG 9::IRGC 63735-1	indx	China	1232.99	168.44	22995.67	5192.63
TOC 5430::IRGC 70487-1	indx	Panama	638.52	192.56	22997.81	6580.29
CHAMPION::IRGC 66327-1	indx	Guyana	554.12	254.22	23101.53	9505.78
AI JIAO ZI::IRGC 82255-1	indx	China	784.31	170.33	24333.89	5765.92
RUS RUSSEI::IRGC 94341-1	ind3	Cambodia	2704.6	300.84	26587.18	1976.48
SR 26 B::IRGC 10803-2	ind2	India	1174.71	587.47	30627.2	18355.94
BONG SEN::IRGC 7011-1	ind3	Viet Nam	677.17	66.86	32762.78	6449.69

5 Chapter Five- AM symbiosis in the rice field

5.1 Investigating the potential for AM colonisation in direct-seeded rice cultivation at IRRI, Philippines

5.1.1 Introduction

In the late 1950s, a shift towards plant breeding for high yielding varieties; improved agricultural practices, irrigation methods and machinery; herbicide and pesticide developments and application of synthetic nutrient fertilisers including nitrogen and phosphorous facilitated the near doubling of food production, termed the 'Green Revolution' (Conway, 1997). Despite huge success in reducing hunger and malnutrition, it is becoming apparent that such practices are causing widespread natural ecosystem loss, reduced soil quality and aquatic and terrestrial pollution and toxicity issues (D. Tilman et al., 2001; Vitousek et al., 1997). The goal of future, sustainable agriculture is now to maximise the net benefit of agricultural food production with improved ecosystem services through a balance of increasing yield, efficiency of nitrogen, phosphorous and water use and promoting biodiversity for enhanced ecological function (Power, 1999; D. Tilman et al., 2002).

The potential for use of AM symbiosis in sustainable rice production requires understanding of the yielding capacity and ecosystem function of AMF in different agroecosystems of rice. Currently, over 75% of global rice production is from rice cultivated under flooded, submerged conditions in lowland fields (J. L. Maclean et al., 2002). Submerging lowland rice paddy fields limits pest spread, competition from weeds and increases the availability of nutrients in the soil. Despite this, the practice requires large amounts of labour for land preparation, cultivation and harvest and relies of use of huge amounts of water (Haefele et al., 2009). As these become increasingly limiting issues in rice production, cultivation methods in many countries are moving towards more sustainable practices. For example, alternate wetting and drying irrigation (AWD) involves intermittent irrigation of the field, with cycles of flooding and drying to reduce water use. Similarly, direct seeded rice (DSR) is a low-input demand method involving sowing pre-germinated seed into a puddled soil

surface (wet seeding), standing water (water seeding) or dry seeding into a seedbed/directly onto the field (dry seeding). DSR is then grown wet or dry, with irrigation ranging from fully flooded to rainfed conditions. A shift to practices such as AWD or DSR could substantially reduce crop water and labour requirements for rice production (Rahman, 2019).

Such reduced water cultivation systems will have important considerations for the potential of AMF as natural biofertilizers of rice. AMF respire aerobically and thus it was previously thought that anoxic, waterlogged paddy conditions were non-mycorrhizal. More recently, it is recognized that AMF are present in waterlogged systems but root colonisation is severely suppressed (Bernaola, et al., 2018; M. Vallino et al., 2009; Y. Wang et al., 2015). AMF have been found in many conventional, waterlogged rice growth systems, particularly at early growth stages or before flooding (Bernaola, et al., 2018; Y. Wang et al., 2015; Watanarojanaporn et al., 2013). It is suggested that AMF are viable in such systems as expression of fungal nutrient transporter genes such as the high-affinity *GintPT* is maintained (M. Vallino et al., 2014; Y. Wang et al., 2021).

Notably, a plasticity of AM colonisation in response to flooding has been described (Jeong et al., 2015; M. Vallino et al., 2014). Previous work at IRRI, Philippines grew rice plants in soil collected from three sites on the upland rice farm: from a typical paddy rice field, which was hypoxic due to continuous irrigation (IR soil); a rice paddy that was fallow for one season (F soil), and a farm border region with aerobic conditions and no rice cultivation for at least 5 years (NR soil). Natural AM colonisation was highest in F or NR soil, seen from 4 weeks post sowing. Although initially delayed, colonisation was later also seen in IR soil after 10 weeks post sowing (Jeong et al. 2015). Similarly, AMF presence and root colonisation has been identified in rice grown in AWD systems in Italy. Vallino et al. noted plastic adaptation of root architecture and functional symbiosis establishment to wetland or dried conditions, which was less evident if plants were maintained in one condition for long periods (M. Vallino et al., 2009). Together, this suggests that, although flooding initially suppresses AM colonisation, the relationship can recover once flooding has subsided. Further work is required to understand the abundance and plant host benefit of colonisation by such recovered AMF communities, but the findings

advocate for the potential of AMF fertilisation in limited input, sustainable cultivation systems.

Although the potential for AM colonisation has been described in AWD, currently, limited field studies have been conducted to identify native AMF and the potential for AM colonisation in DSR cultivation systems. Wet-DSR is commonly practiced in areas of Malaysia, Thailand, Vietnam, the Philippines, and Sri Lanka where labour shortages mean that transplanted, puddled rice growth is not financially viable. In addition, dry-DSR and water seeding accounts for a large proportion of rice grown in the United States. Notably, in many cases of dry-DSR, the soil is flooded after plants establish, although the timing of flooding can vary (Bernaola, et al., 2018). Dry-DSR with plants grown under aerobic, irrigation conditions is only traditionally practiced in rainfed, upland ecosystems across Asia (review: (V. Kumar & Ladha, 2011)). Previous studies have suggested that AMF may be favoured in dry-DSR systems, as they are particularly present in flooded, DSR systems in the period from seeding to flooding (Bernaola, et al., 2018; Campo et al., 2020; Dhillion, 1992; Secilia & Bagyaraj, 1994), but no comparison of AMF in anaerobic, flooded and aerobic, dryland DSR has yet been conducted in the field to current knowledge (Panda et al., 2021). As labour and water shortages become increasingly inhibitive to rice cultivation, there is increasing focus on cultivation using DSR practices with reduced flooding. Understanding the impact of irrigation and cultivation methods on maintaining crop yields and ecological function, including interactions with AMF, will be integral for future application prospects of AMF in these systems.

This study was a broad, first-look assessment of the native root colonisation potential in field-grown rice at IRRI, Philippines grown under different irrigation systems, comparing DSR to traditional transplanted paddy systems. The presence of native AMF and AM colonisation was assessed in *NSIC Rc222 (IRRI 154)*, locally known as *Tubigan 18,* a popular rice variety grown throughout the Philippines. The variety was released by IRRI in 2010 and has an average yield of 6.1 tonnes, with maximum 10 tonnes/hectare (Cabusora et al., 2022). A test of native AMF presence and root colonisation levels in *NSIC Rc222* grown in different cultivation systems was conducted in upland and lowland fields at IRRI, Philippines during the 2022 wet season.

5.1.2 Results

5.1.2.1 AM colonisation identified in different irrigation and planting methods in the direct seeded rice trial at IRRI, Philippines

Roots of *NSIC Rc222 (IRRI 154)* were sampled from different fields of the DSR breeding trials at IRRI, Philippines during 2022 wet season. The breeding trial included four plots with different growth regimes, including DSR in upland fields (with different irrigation regimes) and transplanted, paddy rice in lowland fields. The planting method, date, and irrigation of each regime is summarized in Figure 5.1A. Briefly, dry DSR trials were seeded directly onto dry soil and either irrigated (irrigated at field capacity of > 10kPa with no stagnant flooding) or rainfed (only watered when soil water content < - 50kPa). Wet DSR trials were directly seeded onto flooded soil and plants were grown in stagnant flooding (puddled). In comparison, a trial with traditional transplanting of seedlings into flooded, stagnant water was grown in lowland farm at IRRI. These comparisons are used routinely in DSR Breeding Trials at IRRI. All plots were fertilized with the recommended rate of 120:30:20 $N:P_2O_5:K_2O$ in kg/ha. Ten replicate plots of *NSIC Rc222* were sampled per regime (Figure 5.1B).

AMF presence and colonization was assessed in roots of *NSIC Rc222 (IRRI 154)* harvested at flowering stage from each of the regimes noted above (Figure 5.1B). This was approximately 12-13 weeks post seeding of DSR and 8 weeks post transplanting of lowland rice (Figure 5.1A). AM colonisation was assessed in pooled samples of three biological replicate plants per 10 replicate plots of each regime. Total intraradical colonisation and extraradical hyphal presence were similar within the dry DSR plots, regardless of irrigated or rainfed regime (Kruskal Wallis test, $p < 0.05$, Figure 5.2A-B). All canonical AMF structures were identified (Figure 5.2), with an average total intraradical colonization of 15.1 ± 15.3% and 19.4 ± 9.5% and extraradical hyphae of 24.8 ± 17.1% and 31.8 ± 8.4% in irrigated and rainfed dry DSR respectively (Figure 5.2A). In contrast, both stagnant flooded rice regimes (flooded wet DSR and flooded transplanted) had abolished intraradical colonization (KW, $p < 0.05$, Figure 5.2A). AMF were present but limited in both regimes, as evidenced by presence of some extraradical hyphae at 1.9 ± 2.6% and 1.8 ± 1.7% in wet, puddled DSR and transplanted, flooded plants respectively (Figure 5.2).

A

Study Code	Study Title	Planting method	Direct Seeding/ Transplanting Date	Irrigation Method
DSR22WS-08	Yield trial of selected fixed lines mid-early under dry DSR	dry DSR (irrigated)	May 24, 2022	Soil is kept at field capacity. When the tensiometer reading is at -10 kPa, irrigation must be given. No stagnant water.
DSR22WS-09	Yield trial of selected fixed lines mid-early under puddled DSR	wet DSR (puddled)	May 18, 2022	Stagnant flooding
DSR22WS-11	Yield trial of selected fixed lines mid-early under drought	dry DSR (rainfed)	May 25, 2022	Irrigation is only done when the tensiometer reading is at -50 kPa.
DSR22WS-13	Yield trial of selected fixed lines mid-early under transplanted condition	transplanted	June 17, 2022	Flooded

B

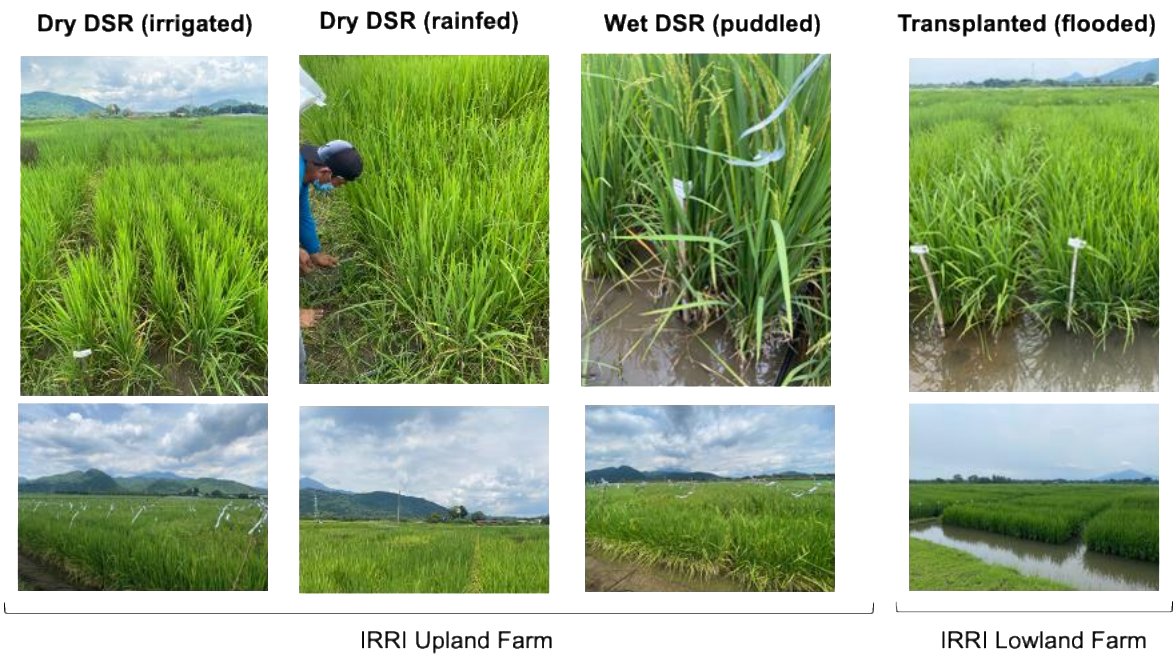

Figure 5.1 Representative images of irrigation and planting method in each field trial in the direct-seeded rice trials at IRRI, Philippines. *(A) Table indicates study code, description, planting method, planting date and irrigation method per regime. (B) Images represent NSIC Rc22 in representative plots of each regime and shows field conditions of irrigation method i.e. flooded or non-flooded.*

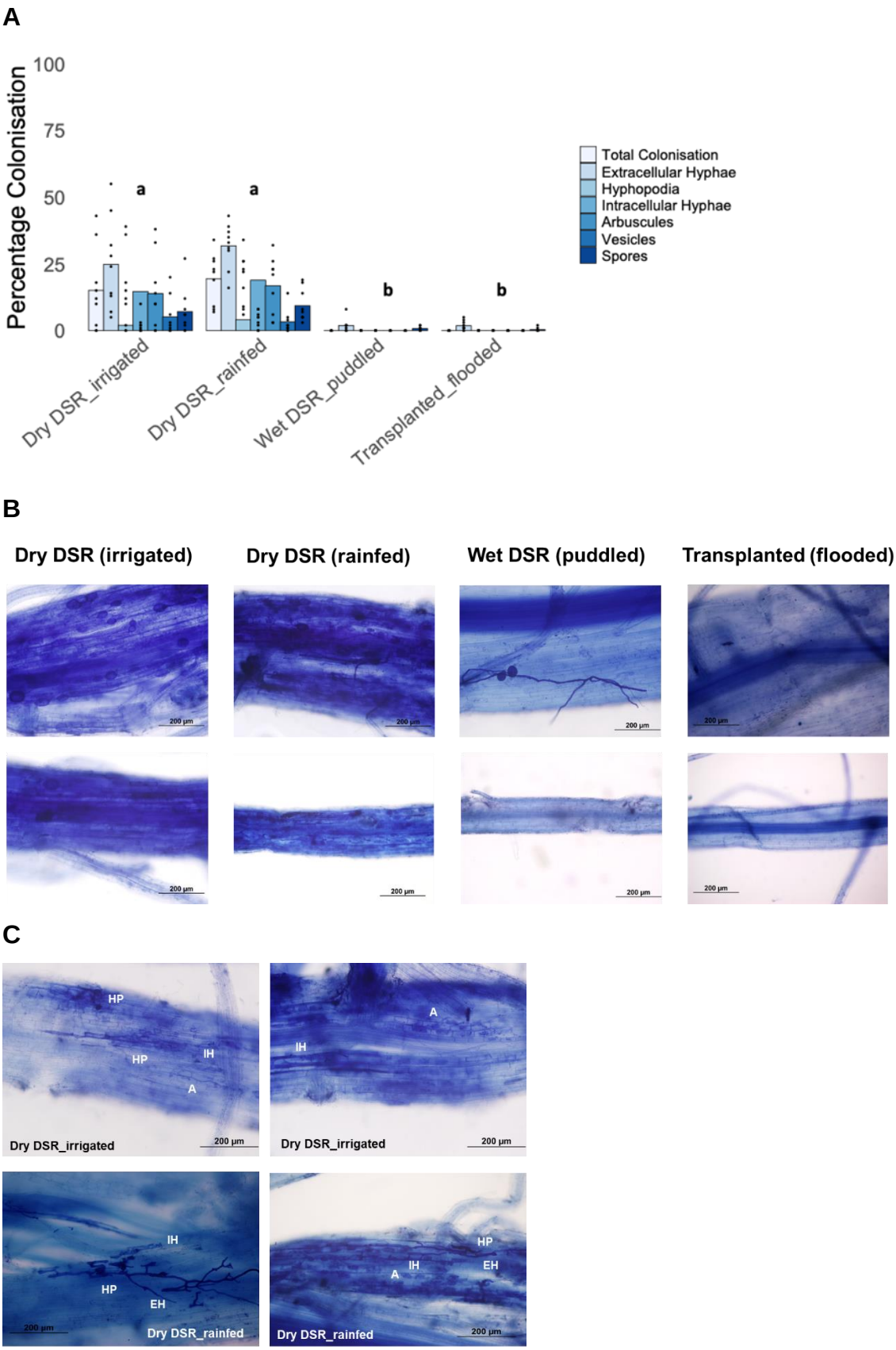

Figure 5.2 AM colonisation rate in NSIC Rc222 (IRRI 154) grown in different planting and irrigation methods*. DSR refers to direct seeded rice grown in upland fields and transplanted to transplanted seedlings grown in a lowland field. Fields were either rainfed (only irrigated if -50kPa), irrigated (irrigated if -10kPa),*

puddled (stagnant flooding) or flooded. (A) Bar chart indicates Percentage of Total Colonisation, Extraradical Hyphae (EH), Hyphopodia (H), Intraradical Hyphae (IH), Arbuscules (A), Vesicles (V) and Spores (S) per root length. Data points of 9-10 biological replicate pools of each regime are shown, with 10 technical replicates used in root counting. A Kruskal-Wallis test was performed, followed by post-hoc pairwise comparison using the agricolae R package. Different letters represent significant difference (p-value <0.05). (B) Representative images of overall AM colonisation identified by trypan blue staining of roots of NSIC Rc222 (IRRI 154) grown in different planting and irrigation methods. Upper panel shows crown root colonisation and lower panel is lateral root. (C) Representative images of canonical AMF structures identified in dry DSR regimes. The following AMF structures are labelled on the image: Extraradical Hyphae (EH), Hyphopodia (HP), Intraradical Hyphae (IH), Arbuscules (A), Scale bar indicates 200um.

5.1.3 Discussion

This study provides the first account, to current knowledge, of AM colonization in *NSIC Rc222 (IRRI 154),* one of the most popular varieties of rice grown in the Philippines. In addition, although native AMF have previously been identified in soil from the IRRI farm, colonization was assessed under glasshouse conditions (Jeong et al., 2015). I additionally report the presence of native AMF populations of soils at IRRI and their potential for natural colonization of field-grown rice. Further work should additionally assess the identity and abundance of such AMF communities.

Previous studies have identified that AMF are present but severely reduced in root colonisation in rice grown in flooded systems (Bernaola, et al., 2018; Campo et al., 2020; M. Vallino et al., 2014; Y. Wang et al., 2021). This study similarly identified AMF presence but abolished intraradical colonisation in planting and irrigation methods that promoted waterlogging of the field, such as in wet DSR and transplanted paddy rice. In contrast, AM colonisation was identified in rice grown in the field in aerobic, dry-direct seeded systems that were non-flooded, either by irrigated or rainfed regimes. It is significant that native AM colonisation was observed in a broad-look assessment of an elite, widely grown variety, cultivated under standard practices at the IRRI farm. Further assessments should include comparison of AM colonisation in more cultivars in the DSR breeding trials. In addition, changes to the standard practices for growth could promote greater levels of colonisation and should be further explored, as noted in regimes including reduced fertilisation (Breuillin et al., 2010; Nouri et al., 2014) and addition of AMF inoculum (Bernaola et al., 2018; Solaiman & Hirata, 1997; Y. Wang et al., 2021).

Biomass and grain assessment was beyond the timeframe of this project, but yield obtained in *NSIC Rc222 (IRRI 154)* grown in DSR should be compared to traditional, transplanted paddy cultivation. This is important as future consideration of AMF in rice production requires understanding of the potential yield and ecosystem function benefits in sustainable growth systems. The impact of AM colonisation on rice growth has been widely assessed in plants grown under flooded conditions, both in native conditions and with addition of AMF inoculum, and variable responses in terms of mycorrhizal growth response (MGR) and yield have been reported (Bernaola, et al., 2018; Campo et al., 2020; Secilia & Bagyaraj, 1994; Solaiman & Hirata, 1997).

The impact of AMF in other systems is less well understood. Studies have begun noting the potential for AMF in sustainable systems including AWD (M. Vallino et al., 2009) or in systems in which flooding and nutrient application is delayed (Lumini et al., 2011). In a comparison between conventional high-input wetland monocropping and organic farming in a 5-year rotation in Italy, Lumini et al. noted that organic management such as delayed flooding and reduced nutrient input increased AMF diversity and root colonisation. They also suggested that early experimental trials identified positive yield response in such systems (Lumini et al., 2011). Multiple studies report that increased flooding resulted in negative mycorrhizal response compared to positive or neutral response in dry conditions (Gewaily, 2019; Y. Wang et al., 2021). Flooding regime is therefore an important determinant of host response. In addition, AMF community (Y. Wang et al., 2015; Watanarojanaporn et al., 2013), rice cultivar (Campo et al., 2020; Diedhiou et al., 2016; R. Huang et al., 2020; Sisaphaithong et al., 2017) and additional environmental factors affect response. Further assessments of production systems, including DSR, with diverse cultivars grown with different irrigation, fertilizer and AMF inoculum inputs over multiple seasons are required. Such studies will facilitate understanding of the potential for AMF presence and root symbiosis to impact rice growth and production in sustainable growth systems globally.

Overall, this study pioneered the potential for AM colonisation in DSR grown in low input, non-flooded irrigation regimes. The potential for biofertilisation capabilities of

AMF in such systems is exciting but further studies are required to select the best responding cultivars and to ensure that appropriate yields can be obtained.

5.2 Investigating the impact of AMF inoculation on diverse *Indica* cultivars in the field

5.2.1 Introduction

Benefits of AM symbiosis include improved host plant nutrition, defence, and abiotic stress tolerance (Al-Karaki & Hammad, 2001; Cordier et al., 1998; Ruiz-Lozano et al., 2001, 2012; S. E. Smith & Read, 2008). In addition, AMF have direct, beneficial effects on ecosystem function and contribute improvement of soil structure and aggregation and composition of plant and microbial communities (Leifheit et al., 2014; Rillig et al., 2015; Rillig & Mummey, 2006; Van Der Heijden et al., 1998). It is generally thought that modern agricultural practices such as application of large amounts of fertilizers, intensive crop production and mechanical soil disruption has led to the disruption of mycorrhizal networks and altered AMF communities (Verbruggen & Kiers, 2010). Re-establishing natural AMF richness and diversity could be a promising, sustainable alternative to conventional fertiliser practices.

Such a view has been widely considered in mycorrhizal literature, but the application of AMF in agroecosystems is currently confounded by limited understanding of some core concepts. These include the genetic determinants of mycorrhizal growth responsiveness (MGR), benefit and dependence in crop cultivars; the impact of resource balance and environmental factors on MGR in the field and the complexity of interactions in diverse microbial communities (Ryan & Graham, 2018). This PhD has largely focused on understanding genetic determinants of AM colonisation and host response in rice using a glasshouse experiment to assess divers cultivars. Glasshouse experiments facilitate probing of AM symbiosis in conditions in which environmental extremes are controlled, nutrient and water availability are managed and noncolonised controls can be established. Despite this, it is important to additionally understand genetic variation and the impact of native AMF and inoculation on growth and agronomic traits in future, sustainable agroecosystems.

Such requires design of field experiments with conditions to ensure both colonisation and plant yield are optimised (Ryan & Graham, 2018).

In a study of rice grown in pots with field soil, AMF inoculation was reported to mitigate negative effects of phosphate deficiency on agronomic traits (Das et al., 2022). In addition, environmental, ecotype and cultivar-dependent benefits of AMF have been observed in the field. Early research noted that AMF inoculation increased nitrogen content of shoot and grain and increased yield by 14-21% compared to non-inoculated rice (Solaiman & Hirata, 1997). A similar increase in yield in AMF-inoculated rice grown in low fertiliser conditions has additionally been reported (S. Zhang et al., 2015). More recently, assessment of larger numbers of genotypes and diverse cultivars has noted genetic diversity in AM colonisation and response (Campo et al., 2020; Diedhiou et al., 2016; Sisaphaithong et al., 2017).

This study aimed to assess variation in plant performance in response to AMF-inoculation in diverse *Indica* cultivars grown in the field at IRRI, Philippines (Figure 5.3). A subset of lines representing the large extent of variation in AM colonisation and MGR observed in the glasshouse in the *Indica* panel were selected. Since it had previously been observed that AM colonisation is suppressed in flooded, paddy rice (Lumini et al., 2011; M. Vallino et al., 2014; Y. Wang et al., 2021), the experiment was designed to promote AMF by directly seeding rice onto dry soil grown in irrigated, non-flooded conditions. Notably, although AMF were later found to be present at the IRRI farm in the same season (Section 5.1), it was unclear at the time of planting the extent to which native AMF were present. In order to measure the impact of AMF, I conducted a comparative experiment of a plot with assumed native AMF and a neighbouring plot with addition of AMF inoculum.

Figure 5.3 Example of field rice at International Rice Research Institute (IRRI), Philippines. *Image of field rice breeding trials at IRRI taken during visit in August 2022.*

5.2.2 Results

5.2.2.1 Field experiment design and motivation

The field experiment was designed to promote AM colonisation and yield over the growing season. First, it was conducted in the IRRI rain-sheltered experimental plots at the lowland farm to ensure that flooding of the plot could be avoided, especially as the experiment was conducted during the wet season. Plants were direct-seeded and grown in irrigated, non-flooded conditions (dry DSR). In addition, the field had previously been low phosphate (2018) followed by three years fallow, meaning nutrient composition would be low and the fertilisation regime could be controlled. The experiment was conducted in P deplete conditions to promote AM symbiosis. A top dressing of urea was applied twice to avoid yellowing of plants, ensuring vigor and growth to flowering stage.

In comparison to glasshouse experiments, it is difficult to establish non-mycorrhizal controls in the field; methods such as sterilising the soil are not representative of native conditions as they impact soil properties and microbial communities (Ryan & Graham, 2018). Instead, the impact of AMF inoculation was compared against native AMF present in the soil. Native AMF were presumed to be present as they have previously been observed at multiple locations of the IRRI farm (Jeong et al., 2015).

Mykovam®, was selected as an AMF inoculum as it is a commercial inoculum produced locally to IRRI and contains spore propagules and root fragments of plants infected with a 12 species mix of AMF. The experimental design included direct seeding of cultivars into two plots, one with native AMF only (no addition to soil) and the other with addition of Mykovam® AMF inoculum. Plants were grown in a randomised design with three replicate rows per genotype in each plot (Figure 5.4A-B).

The soil composition of each plot was tested at six weeks post planting/inoculation to ensure uniformity (Figure 5.4B). Soil pH, availability of nitrate and ammonium are factors that affect rice growth and thus were tested in both plots. Overall, pH of the two plots were statistically equivalent at an average of pH 7.1 (ANOVA, $F(1,8) = 0.03$, $p= 0.872$, Figure 5.4B), which is within the optimal range for agricultural fields (Nand Kumar Fageria, 2016). In addition, the amount of available nitrate and ammonium can affect plant nutrition and is dependent on multiple factors including soil type, clay content and nutrient composition (Youngdahl et al., 1982). Mean soil nitrate (mg exch NO_3-N/kg soil) and ammonium (mg exch NH_4-N/kg soil) were more variable than soil pH and the difference between plots was thus assessed by non-parametric Kruskal Wallis test. Nitrate and ammonium content didn't significantly differ between the native and AMF-inoculated plots (KW, $p >0.05$, Figure 5.4B). Overall, the plots were considered relatively uniform such that differences could be attributed to the effect of AMF inoculum.

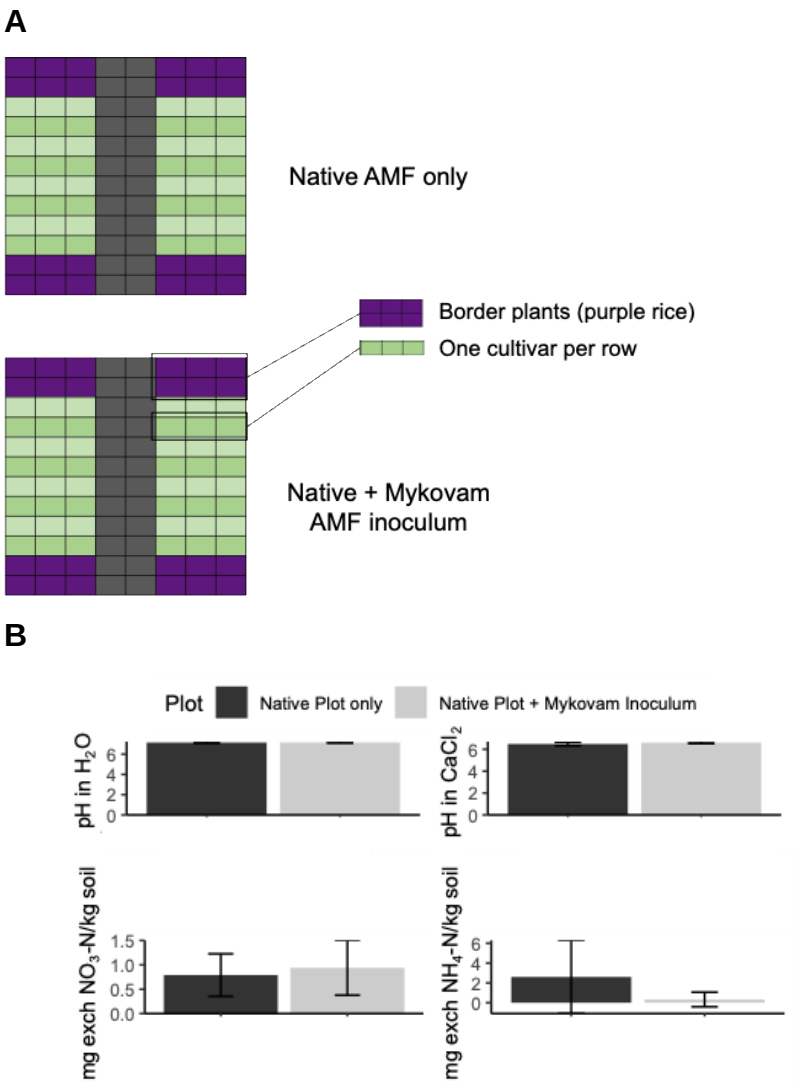

Figure 5.4 Representative diagram and soil composition of field experimental design at IRRI, Philippines. *(A) Diagram of randomised design of the trial. Plots were either native or AMF-inoculated with Mykovam 12 AMF species mix inoculum. Each genotype was planted in three replicate rows per plot, with 36 total rows per plot. Borders of purple rice were included for each plot. (B) soil composition of each plot. Soil pH measured in water and $CaCl_2$,* soil nitrate (mg exch NO_3-N/kg soil) and ammonium (mg exch NH_4-N/kg soil) was assessed. Bars indicate mean values with error bars for mean+- standard deviation. Five replicate soil samples per plot were assessed.

5.2.2.2 Identification of *Indica* cultivars with contrasting AM phenotypes

Cultivars were selected for the field trial based on being representative of diversity and variation in blumenol abundance and responsiveness observed during the glasshouse screen of ~200 diverse *Indica* cultivars described in Chapter Four. Twelve genotypes were selected, four that had contrasting blumenol abundance

(foliar 11-carboxyblumenol C-Glc) and six that had contrasting MGR in the glasshouse experiment (Chapter Four). In addition, the model cv. *japonica Nipponbare* and model cv. *indica* model *IR64* were included for reference (Table 5.1).

The selection criterion aimed to identify cultivars with contrasting phenotypes whilst also being diverse in subpopulation and country of origin. *BONG SEN* and *SICAN* were selected as cultivars with superior blumenol abundance as they had the highest and eight highest blumenol abundance across the whole panel in the glasshouse experiment and were diverse in subpopulation and country of origin (Table 5.1). For example, *BONG SEN* is a traditional Vietnamese deep-water, so-called floating rice, which remains as the only floating rice variety still grown in Vinh Phuoc commune, Vietnam (Hoa, 2015; N. Lang et al., 2009). In contrast, *SICAN* originates from Peru in Latin America, where rice is predominantly directly seeded and grown in dry, irrigated soil with conventional tillage (Chirinda et al., 2018). Similarly, *CHING CH'UNG* and *CHAMA(DWARF)* were selected as cultivars with low blumenol abundance as they had the second and third lowest abundance in the panel in the glasshouse experiment and were diverse in origin. *CHING CH'UNG* originates from Taiwan and, in contrast, *CHAMA(DWARF)* is an aromatic variety local to the Chama region in Zambia (Styger, 2014).

Equivalent root colonisation of some of the lines was determined during analysis that assessed blumenol correlation with fungal root colonisation in the glasshouse experiment, as described in Chapter Four. For reference, the *Nipponbare* model cultivar had average blumenol abundance of 10062.0 ng/g fw and percentage arbuscule colonisation of 37.1 ± 18.8% (Figure 5.5). Average foliar blumenol abundance ranged 20-fold between the low and high lines, from 1569.2 ± 740.3 ng/g fw in *CHING CH'UNG* and 2160.0 ± 1637.3 ng/g fw in *CHAMA(DWARF)* to 21560.0 ± 6574.5 ng/g fw in *SICAN* and 32762.8 ± 6449.7 ng/g fw in *BONG SEN* (Figure 5.5). Percentage arbuscular colonisation was severely reduced in low blumenol cultivars at 0.0 ± 0.0% in *CHAMA(DWARF)* and 18.8 ± 25.5% in *CHING CH'UNG* compared to *Nipponbare* reference (KW, $p < 0.05$, Figure 5.5A). Similarly, blumenol abundance was reduced compared to *Nipponbare* (KW, $p < 0.05$, Figure 5.5B). Increased arbuscular colonisation of 53.5 ± 17.9% compared to *Nipponbare* was observed in

SICAN (KW, $p < 0.05$, Figure 5.5A). Similarly, blumenol abundance was increased in *SICAN* and *BONG SEN* compared to *Nipponbare* reference (KW, $p < 0.05$, Figure 5.5B). Root colonisation analysis of *BONG SEN* was not included at the time of analysis. Overall, AM colonisation correlated well to blumenol abundance and suggests the selected cultivars are diverse in establishment of root colonisation.

In addition, cultivars representing contrasting MGR in terms of height, shoot dry weight (SDW) and root dry weight (RDW) observed in the panel during the glasshouse experiment were selected, again with the criterion that they were diverse in subpopulation and country of origin (Table 5.1). Three cultivars with AMF-enhanced plant height and biomass were identified: *LEAD; MODDAI KARUPPAN; PAN DAWK MAHK*. The cultivars originate from Malawi, Sri Lanka and Thailand respectively (Table 5.1). In *LEAD,* a MGR of 13% increase in height, 32.3% increase in SDW and 87.8% increase in RDW was observed in the glasshouse experiment (Table 5.1). Similarly, height, SDW and RDW increased by 6.3%, 27.8% and 69.6% respectively in *MODDAI KARRUPAN* and 15.8%, 13.6% and 30.4% respectively in *PAN DAWK MAKH* (Table 5.1). In addition, three cultivars with AMF-decreased plant height and biomass were identified: *HAM MOON; KILOMBERO; MOSHI*. *HAM MOON* originates from Hong Kong whilst *KILOMBERO* and *MOSHI* originate from Tanzania and Kenya respectively (Table 5.1). In *HAM MOON,* a MGR of -15.4%, -27.6% and -43.5% was observed in height, SDW and RDW respectively (Table 5.1). Similarly, height, SDW and RDW decreased by -6.7%, -17.7% and -35.9% respectively in *KILOMBERO* and -15.7%, -22.0% and -21.6% respectively in *MOSHI* (Table 5.1).

Since I previously found that foliar P responsiveness only weakly correlated to increased MGR, I additionally assessed the diversity of foliar P response in the selected lines. *LEAD, MODDAI KARRUPAN* and *PAN DAWK MAHK* were selected for positive MGR responses and had mean foliar P responsiveness of 57.3%, -2.0% and 12.9% ppm respectively (Table 5.1, Figure 5.6). Similarly, *HAM MOON, KILOMBERO* and *MOSHI* were selected for negative MGR and had mean foliar P responsiveness of 31.1%, 19.0% and -4.9% ppm respectively (Table 5.1, Figure 5.6). As observed in Chapter Four, foliar P responsiveness didn’t directly correlate to MGR response in the cultivars (Figure 5.6).

Overall, mean percentage blumenol, MGR and foliar P responsiveness were diverse across the panel selected for the field trial and representative of variation observed in the diverse *Indica* panel assessed in the glasshouse experiment (Table 5.1).

Table 5.1 Summary of selected lines and blumenol and MGR observations from glasshouse experiment at University of Cambridge, UK. *Table indicates lines selected, country of origin, K9 subpopulation in 3K-RG, mean foliar blumenol abundance and mycorrhizal growth response determined by height, root and shoot dry weight and foliar P response. No data for IR64 is available as the cultivar was not included in the selected panel for the glasshouse experiment.*

Cultivar	Country	Subpop	Selection Criteria	Mean Blumenol Abundance	Mean % MGR (Height)	Mean % MGR (Shoot DW)	Mean % MGR (Root DW)	Mean % Foliar P Response ppm
CHAMA (DWARF)::IRGC 69487-1	Zambia	ind1B	Low Blumenol	2160.0	-1.4	-16.4	-14.9	4.0
CHING CH'UNG::IRGC 65002-1	Taiwan	indx	Low Blumenol	1569.2	0.8	6.2	4.9	41.2
SICAN::IRGC 117029-1	Peru	indx	High Blumenol	21560.0	-4.3	20.8	14.8	40.1
BONG SEN::IRGC 7011-1	Vietnam	ind3	High Blumenol	32762.8	7.2	60.0	35.9	14.4
LEAD::IRGC 5805-1	Malawi	indx	Positive MGR	8171.2	13.3	32.3	87.8	57.3
MODDAI KARUPPAN::IRGC 15465-1	Sri Lanka	ind2	Positive MGR	4942.8	6.3	27.8	69.6	-2.0
PAN DAWK MAHK::IRGC 71380-1	Thailand	ind3	Positive MGR	11009.3	15.8	13.6	30.4	12.9
HAM MOON::IRGC 9135-2	Hong Kong	indx	Negative MGR	7762.4	-15.4	-27.6	-43.5	31.1
KILOMBERO::IRGC 69698-1	Tanzania	ind3	Negative MGR	5318.1	-6.7	-17.7	-35.9	19.0
MOSHI::IRGC 70648-1	Kenya	ind2	Negative MGR	8801.3	-15.7	-22.0	-21.6	-4.9
NIPPONBARE	Japan	temp	Model *japonica*	10062.6	-8.5	-14.3	-3.7	4.0
IR 64		ind1B	Model *indica*	-	-	-	-	-

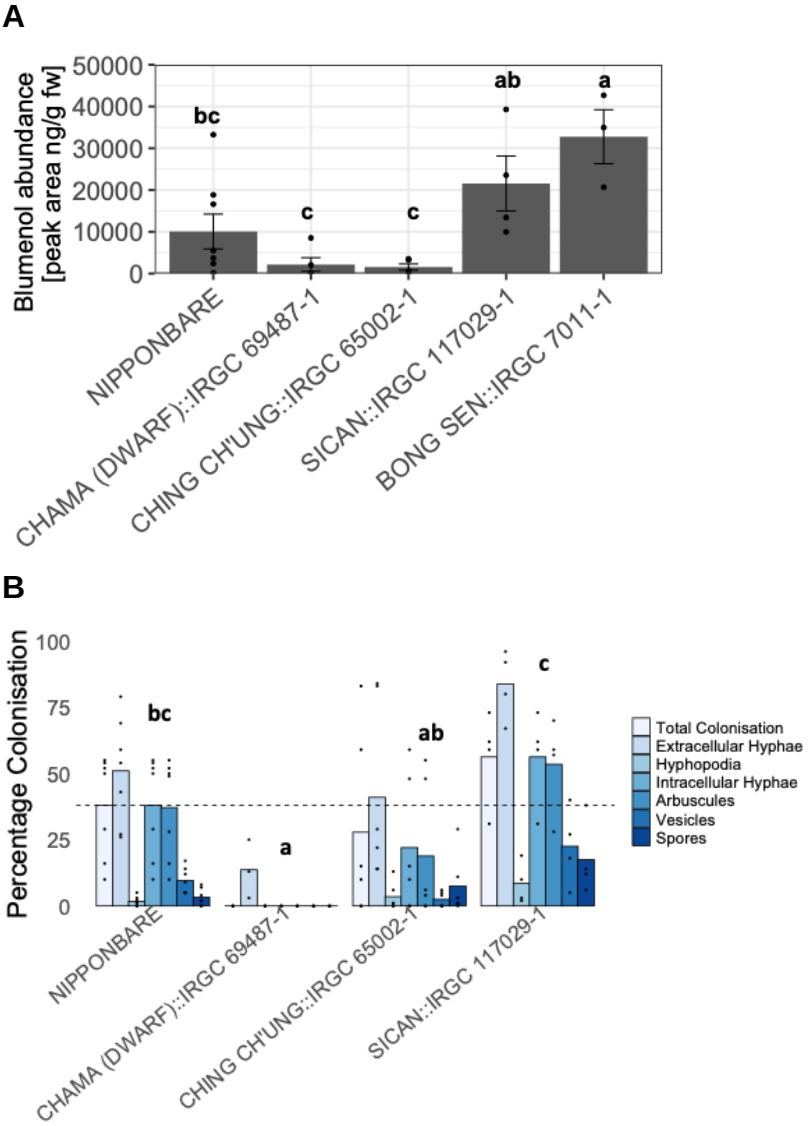

Figure 5.5 AM colonisation phenotypes of lines selected from GWAS due to contrasting blumenol abundance. *(A) Mean foliar 11-carboxyblumenol C-Glc abundance (peak area ng/g fresh weight) +- standard deviation per genotype (B) Mean percentage arbuscule colonisation in lines selected for blumenol phenotype. Error bars represent mean ± standard deviation. Dashed line indicates value for Nipponbare reference. Bar chart indicates Percentage of Total Colonisation, Extraradical Hyphae (EH), Hyphopodia (H), Intraradical Hyphae (IH), Arbuscules (A), Vesicles (V) and Spores (S) per root length. Data points of 4-5 biological replicates are shown, with 10 technical replicates used in root counting. A Kruskal-Wallis test was performed, followed by post-hoc pairwise comparison using the agricolae R package. Different letters represent significant difference (p-value <0.05).*

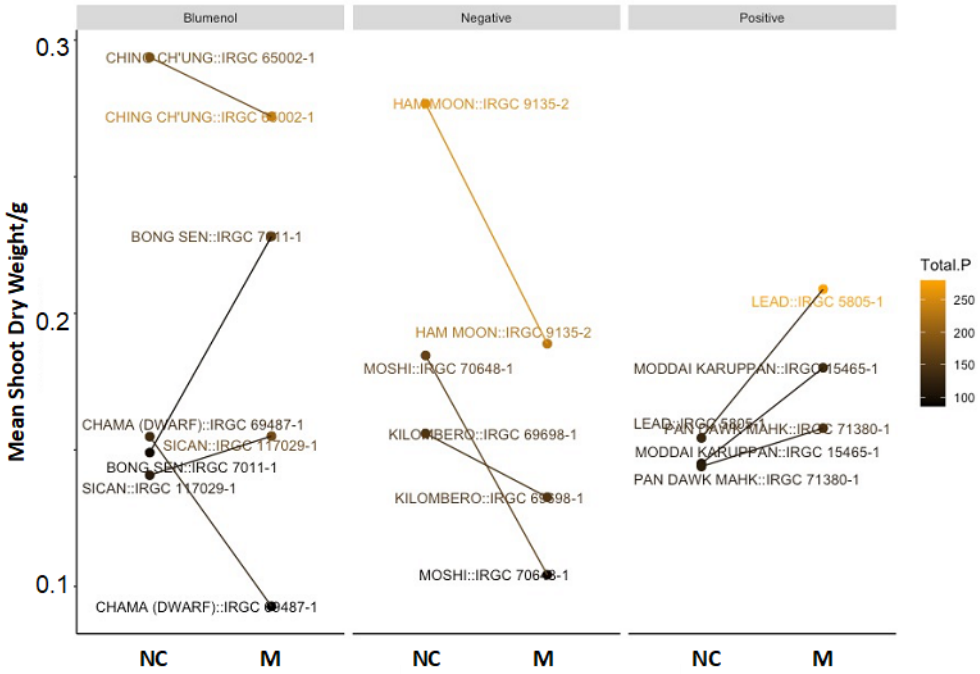

Figure 5.6 Growth phenotypes of lines selected from GWAS due to contrasting blumenol abundance and mycorrhizal responsiveness*. Shoot dry weight response and foliar phosphorous of lines in mock and AMF-inoculated conditions. Graphs indicate shoot dry weight in grams in mock and AMF-inoculated conditions. Graphs are faceted by selection criteria, namely contrasting blumenol abundance or negative and positive mycorrhizal growth response phenotypes identified in glasshouse experiment described in Chapter Four. Points indicate mean values per cultivar. NC indicates mock-inoculated and M indicates mycorrhizal, AMF-inoculated.*

5.2.2.3 Comparison of the effect of AMF inoculation in diverse rice cultivars grown in field conditions

The selected lines were grown in the experimental design described in Section 5.2.2.1. To assess growth and yield response to AMF-inoculation, biomass and yield traits were measured across the growing season and compared between the native AMF and native + AMF-inoculated plots (Figure 5.7).

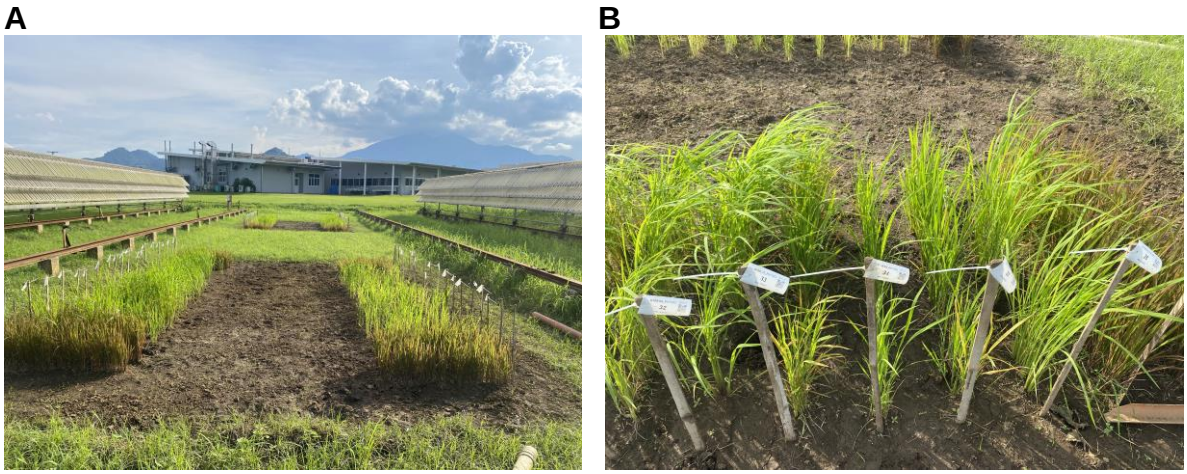

Figure 5.7 *Representative image of the (A) native and native + AMF inoculum plots and (B) cultivar rows of the field experiment conducted in the lowland farm at IRRI, Philippines.*

Six weeks post planting, vegetative traits including height, shoot dry weight (SDW) and total crown root number (TCR) were assessed. The number of days to flowering (DTF) was additionally recorded. Significant natural variation was observed across the panel, as observed in histograms representing data distribution of the traits (Figure 5.8).

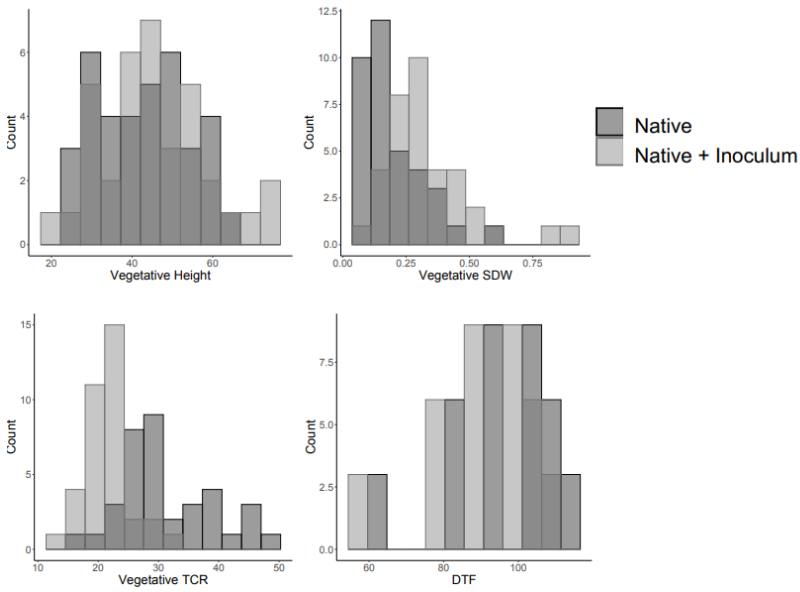

Figure 5.8 Histograms of distribution of growth and yield traits identified in native and native + AMF inoculation plots in the field. *Traits included vegetative height (cm); shoot dry weight (SDW, g) and total crown roots (TCR) and days to flowering (DTF, days). Three biological replicates per genotype replicate row were measured, with three biological replicates per genotype per plot. Colour indicates native only (black) or native +AMF-inoculum (grey) inoculated plants.*

For each trait, global population mean (Table 5.3) in native and native + AMF inoculum plots was identified, and a two-way ANOVA revealed the effects of cultivar and AMF inoculation. Where required, traits were $\log_{10}$ transformed to fit assumptions of normality (Table 5.2). To identify variation in response to AMF inoculation within cultivars, mean value per cultivar (Table 5.3) was additionally assessed and Tukey's least significant difference post-hoc comparisons of ANOVA model were used to identify statistical differences between native and AMF-inoculated plots.

Firstly, vegetative plant height, TCR and SDW were assessed. Cultivar had a significant effect on plant height (ANOVA, $F(11, 48) = 11.43$, $p < 0.001$, Figure 5.9B & Table 5.2) and vegetative SDW (ANOVA, $\log_{10}$ transformed, $F(11, 48) = 4.71$, $p = 1.40e^{-6}$, Figure 5.9C & Table 5.2) but not TCR. Notably, AMF-inoculation significantly affected SDW (ANOVA, $\log_{10}$ transformed, $F(1, 48) = 30.34$, $p = 7.36e^{-5}$, Figure 5.9C), decreasing global average from 0.33 ± 0.17g to 0.20 ± 0.13g. A tendency for decreased SDW upon AMF-inoculation was observed in all cultivars and post-hoc comparisons found a significant decrease in *SICAN* from 0.32g to 0.11g (Tukey, $p = 0.04$) and *PAN DAWK MAHK* from 0.51g to 0.18g (Tukey, $p = 0.002$, Figure 5.9C). In contrast, AMF-inoculation significantly increased TCR from an average of 21.6 ± 3.8 crown roots to 31.3 ± 8 crown roots (ANOVA, $\log_{10}$ transformed, $F(1, 48) = 50.87$, $p = 4.61e^{-9}$, Figure 5.9A & Table 5.2). Again, the effect was consistent across cultivars and post-hoc comparisons found a statistically significant increase of mean TCR from 25.8 to 40.2 in *MODDAI KARRUPAN* (Tukey, $p = 0.006$), 22.0 to 35.9 in *HAM MOON* (Tukey, $p = 0.008$), 19.0 to 34.0 in *KILOMBERO* ($p = 0.004$) and 19.8 to 34.3 in *MOSHI* (Tukey, $p = 0.006$), Figure 5.9A).

A significant effect of cultivar (ANOVA, $\log_{10}$ transformed, $F(11,59) = 1263.58$, $p< 2.2e^{-16}$, Figure 5.10 & Table 5.2) and AMF-inoculation (ANOVA, $\log_{10}$ transformed, $F(1,59) = 564.34$, $p< 2.2e^{-16}$, Figure 5.8 & Table 5.2) was observed for DTF. AMF inoculation increased DTF from an average of 91 ± 14 days to 96 ± 14 days (Figure 5.8 & Table 5.2). The increase was significant for all cultivars measured (Tukey, $p < 0.05$, Figure 5.10).

Overall, the effect of AMF inoculation compared to native AMF only appeared to be consistent across all cultivars measured, with addition of inoculum causing increased TCR and decreased SDW. In addition, AMF inoculation consistently increased DTF.

Table 5.2 Descriptive summary and statistics in growth traits. *Traits included vegetative height (Veg.Height, cm); total crown roots (Veg.TCR) and shoot dry weight (Veg.SDW, g); days to flowering (DTF) and post-harvest height (Harvest.Height, cm); grain dry weight (Grain.DW, g), straw dry weight (StrawDW, g); shoot biomass (SB, gm^{-2}), grain yield (GY, gm^{-2}) and harvest index (HI). Three biological replicates per genotype replicate row were measured, with three biological replicates per genotype per plot. Global mean and standard deviation were analysed per trait, with N the number of observations. A Two-way ANOVA of cultivar and inoculation was performed, and p value significance is indicated: ** $p < 0.001$, * $p < 0.05$, NS not statistically significant, $p > 0.05$*

Trait	Cultivar	Inoculation	Cultivar x Inoculation	Treatment	N	Mean	St.Dev
Veg.Height	**	NS	NS	Native	35	42.8	13.3
				Native + Inoculum	33	45.42	11.3
Veg.SDW	**	**	NS	Native	36	0.33	0.17
				Native + Inoculum	36	0.2	0.13
Veg.TCR	NS	**	NS	Native	25	21.6	3.8
				Native + Inoculum	27	31.3	8
DTF	**	**	-	Native	36	91	14
				Native + Inoculum	36	96	14
PH.Height	**	NS	NS	Native	35	91.6	27
				Native + Inoculum	34	87.6	26
Straw Biomass	**	NS	*	Native	36	1042.9	753.6
				Native + Inoculum	36	1106	756.3
Grain Yield	**	NS	NS	Native	34	40.4	121.1
				Native + Inoculum	34	31	78.7
Harvest Index	**	NS	NS	Native	34	0.016	0.038
				Native + Inoculum	35	0.014	0.024

Table 5.3 Summary of growth and yield traits measured in the field experiment. *Table indicates mean phenotypic data measured per cultivar in the native and native + AMF inoculum plots. Traits included vegetative height (Veg.Heigh, cmt); total crown roots (Veg.TCR) and shoot dry weight (Veg.SDW, g); days to flowering (DTF) and post-harvest height (Harvest.Height, cm); grain dry weight (Grain.DW, g), straw dry weight (StrawDW, g); shoot biomass (SB, gm^{-2}), grain yield (GY, gm^{-2}) and harvest index (HI). Three biological replicates per genotype replicate row were measured, with three biological replicates per genotype per plot.*

Cultivar	Plot	Veg.Height	Veg.TCR	Veg.SDW	DTF	Harvest.Height	GrainDW	StrawDW	SB	GY	HI
CHAMA (DWARF)::IRGC 69487-1	Native+AMF	26.83	31.00	0.08	102	66.67	0.16	49.51	660.09	2.33	0.003
	Native	28.89	24.00	0.20	97	63.22	0.10	37.07	494.27	1.36	0.004
CHING CH'UNG::IRGC 65002-1	Native+AMF	39.94	29.56	0.11	84	93.00	0.07	59.58	794.36	0.97	0.001
	Native	47.11	21.44	0.24	79	111.78	0.09	55.33	737.78	1.22	0.002
SICAN::IRGC 117029-1	Native+AMF	30.52	24.78	0.11	91	72.44	0.22	58.30	777.29	3.06	0.004
	Native	41.39	17.67	0.32	86	75.44	0.22	90.67	1208.89	3.11	0.002
BONG SEN::IRGC 7011-1	Native+AMF	46.12	32.33	0.20	84	105.22	0.30	100.26	1336.80	4.16	0.003
	Native	43.67	23.00	0.27	79	97.44	0.19	63.47	846.27	2.58	0.006
LEAD::IRGC 5805-1	Native+AMF	55.72	33.11	0.39	105	110.44	1.64	111.24	1483.16	22.74	0.014
	Native	60.17	23.22	0.46	100	97.44	2.19	98.75	1316.62	30.39	0.032
MODDAI KARUPPAN::IRGC 15465-1	Native+AMF	59.67	40.22	0.38	109	98.22	19.84	222.79	2970.58	277.27	0.087
	Native	61.22	25.78	0.56	104	137.56	31.22	217.91	2905.51	431.63	0.131
PAN DAWK MAHK::IRGC 71380-1	Native+AMF	46.22	26.00	0.18	116	94.67	0.14	66.01	880.13	2.00	0.002
	Native	62.00	22.22	0.51	111	80.22	0.34	74.54	993.91	4.73	0.005
HAM MOON::IRGC 9135-2	Native+AMF	44.90	35.89	0.24	91	98.89	0.25	108.09	1441.24	3.55	0.002
	Native	45.61	22.00	0.34	86	102.89	0.14	62.08	827.78	1.97	0.003
KILOMBERO::IRGC 69698-1	Native+AMF	51.69	34.00	0.24	102	118.33	2.35	111.59	1487.87	32.76	0.023
	Native	46.51	19.00	0.28	97	114.44	0.23	69.59	927.82	3.27	0.004
MOSHI::IRGC 70648-1	Native+AMF	47.61	34.33	0.23	109	92.44	1.35	65.50	873.29	18.80	0.020
	Native	44.44	19.78	0.25	104	106.00	0.20	60.05	800.67	2.77	0.004
NIPPONBARE	Native+AMF	29.78	27.11	0.11	64	41.55	0.11	11.26	150.09	1.47	0.010
	Native	31.80	19.44	0.25	59	39.33	0.02	18.55	247.33	0.35	0.001
IR 64	Native+AMF	34.22	26.89	0.11	91	59.67	0.23	31.30	417.33	3.22	0.009
	Native	32.28	21.67	0.31	86	73.67	0.06	90.63	1208.36	0.88	0.001

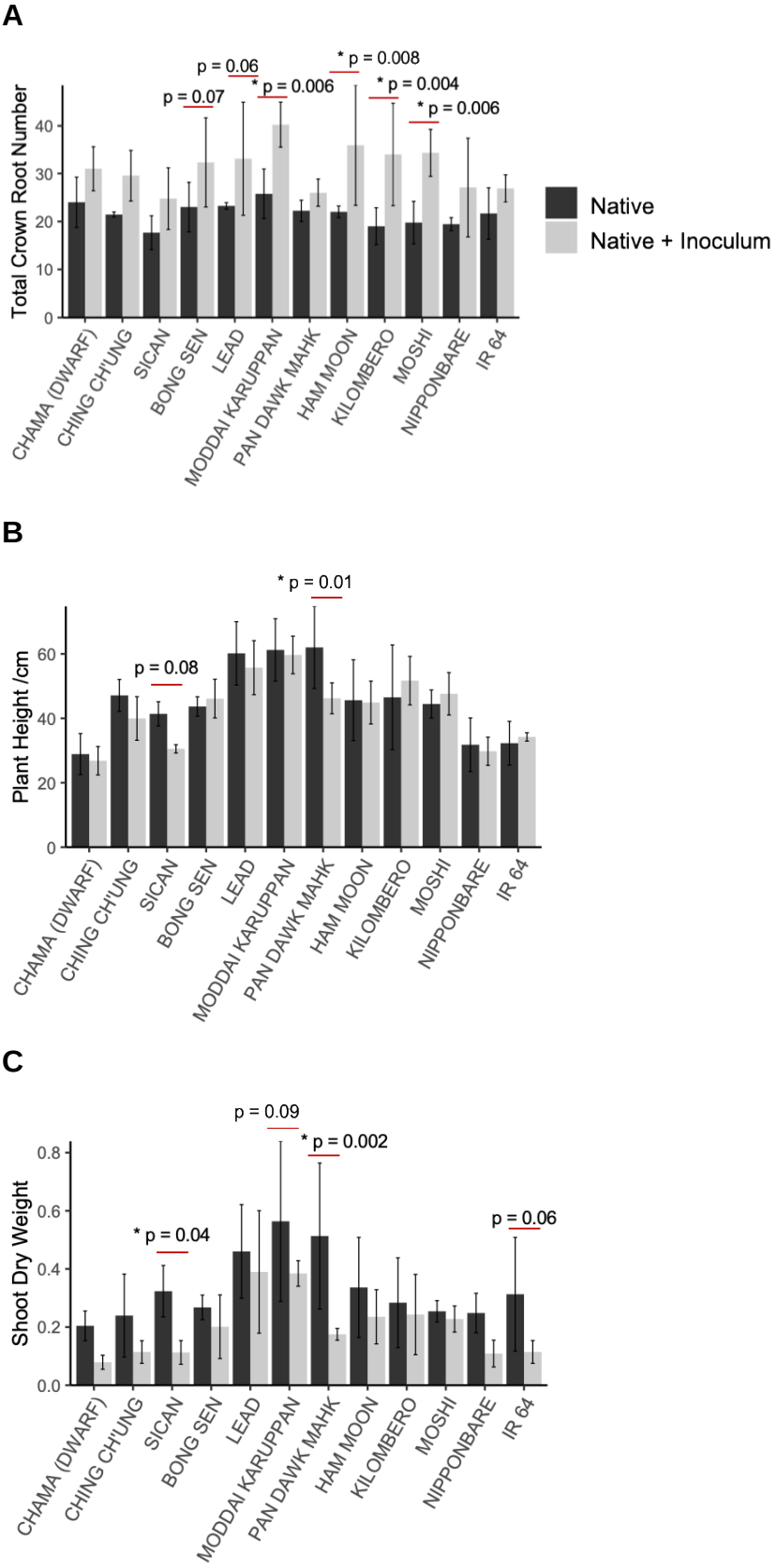

Figure 5.9 Growth phenotypes measured at vegetative stages in native and AMF-inoculated plots. *(A) Total crown root number, (B) plant height and (C) shoot dry weight was assessed in each cultivar and compared between native (black) and AMF-inoculated (grey) plots. Mean values are represented as bars with error bar of mean+- standard deviation. Three biological replicates per genotype replicate row were measured, with three*

biological replicates per genotype per plot. Statistically significant interaction of AMF-inoculation per genotype after post-hoc tests are indicated by asterix (*) and red lines. P-value of post-hoc (Tukey) test are indicated.

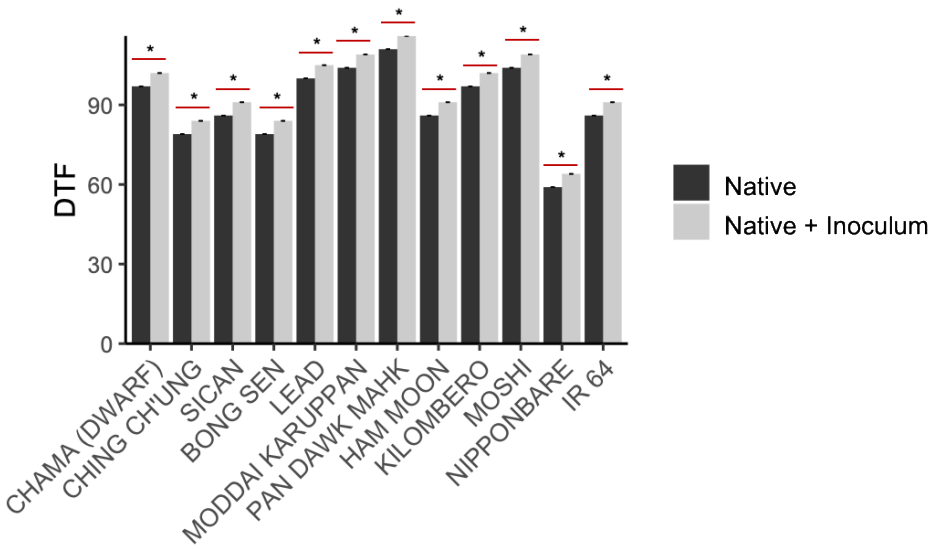

Figure 5.10 Days to flowering (DTF) measured in native and AMF-inoculated plots.. *Days to flowering was assessed in each cultivar and compared between native (black) and AMF-inoculated (grey) plots. Mean values are represented as bars with error bar of mean+- standard deviation. Three biological replicates per genotype per plot were measured. Statistically significant interaction of AMF-inoculation per genotype after post-hoc tests are indicated by asterix and red lines.*

Post-harvest, plant height, straw biomass (above-ground biomass post flowering, g), and grain yield (GY), grams of grain dry weight per m^2 were measured. Harvest index (HI), a ratio of grain yield to biomass yield was calculated by the following equation:

$$Harvest\ Index\ (HI) = \frac{Grain\ Yield\ (g\ per\ m^2\ )}{Grain\ Yield +\ Straw\ Biomass\ (g\ per\ m^2)}$$

Again, significant variation was observed across the panel, evident in large spread in histograms representing data distribution of the traits (Figure 5.11).

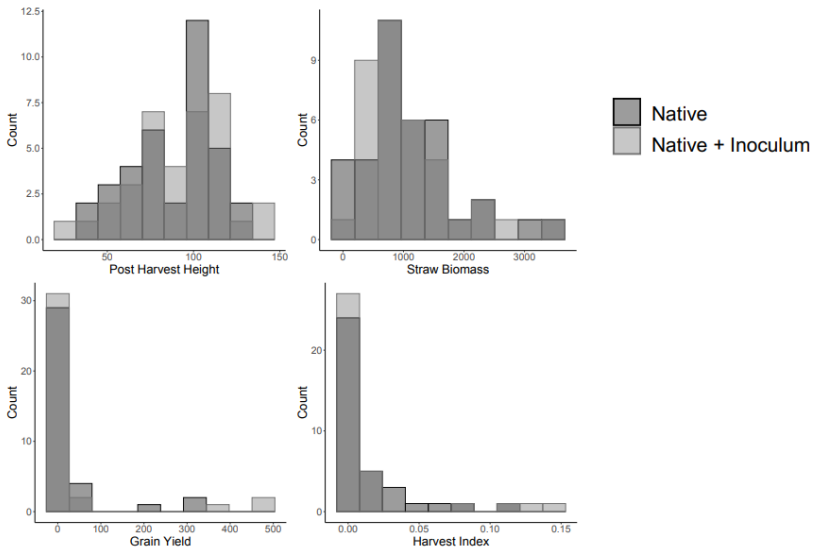

Figure 5.11 Histograms of distribution of growth and yield traits identified in native and native + AMF inoculation plots in the field. *Traits post-harvest height (cm); straw biomass (gm^{-2}), grain yield (GY, gm^{-2}) and harvest index (HI). Three biological replicates per genotype replicate row were measured, with three biological replicates per genotype per plot. Colour indicates native only (black) or native +AMF-inoculum (grey) inoculated plants.*

A two-way ANOVA revealed the effects of cultivar and AMF-inoculation on variation in post-harvest traits (Table 5.2). Cultivar had a significant effect on both plant height (ANOVA, $F(11,48) = 17.4$, $p = 3.53e^{-13}$, Figure 5.12A & Table 5.3) and straw biomass (ANOVA, log_{10} transformed, $F(11,48) = 13.8$, $p = 2.17e^{-11}$, Figure 5.12B & Table 5.2). AMF inoculation didn't significantly affect mean values of either trait but post-hoc comparisons found AMF-inoculation significantly increased straw biomass in *BONG SEN* (Tukey, $p = 0.03$) from 63.47 to 100.26 g/m^2 and decreased straw biomass in *IR64* from 90.63 to 31.3 g/m^2 (Tukey, $p = 0.001$, Figure 5.12B). A tendency for increase in straw biomass from 62.08 to 108.09 g/m^2 was also observed in *HAM MOON* (Tukey, $p = 0.08$, Figure 5.12B).

In addition, a significant effect of cultivar was observed for both grain yield (ANOVA, log_{10} transformed, $F(11,48) = 11.8$, $p = 2.6e^{-10}$, Figure 5.12C & Table 5.2) and harvest index (ANOVA, log_{10} transformed, $F(11,48) = 6.4$, $p = 2.0e^{-6}$, Figure 5.12D & Table 5.2). There was a non-significant effect of AMF-inoculation on both traits but post-hoc comparison found a tendency for increase in grain yield in *KILOMBERO* (Tukey, $p = 0.06$, Figure 5.12C) and *MOSHI* (Tukey, $p = 0.08$, Figure 5.12D), although this was not significant at $p < 0.05$ level. For harvest index, post-hoc

comparison found a significant increase in harvest index from 0.001 to 0.01 in *NIPPONBARE* (Tukey, p = 0.002) and 0.009 to 0.01 in *IR64* (Tukey, p = 0.02, Figure 12D). Overall, there was natural variation in the effect of AMF-inoculation on post-harvest biomass and yield traits across the diverse cultivars.

BONG SEN is highlighted as a cultivar with superior response to AMF-inoculation in the field. Although at first vegetative SDW was negatively influenced, a significant positive effect of inoculation on straw biomass was observed in the field, increasing from 63.4 to 100.3 g/m^2 (Tukey, p =0.03, Figure 5.12B, Table 5.3). In addition, a trend for increased grain yield from 2.6 to 4.2 g/m^2 was identified, although this was not statistically significant (Tukey, p > 0.05, Figure 5.12C, Table 5.3). Interestingly, *BONG SEN* was previously highlighted as a cultivar with superior response in the glasshouse experiment described in Chapter Four. Although there are many factors that differ between these experiments, particularly in the lack of 'mock, non-AMF' comparisons, soil substrate, climate and growing season, it is intriguing that a consistent positive response is observed. This cultivar is therefore recommended as a candidate for further interrogation of superior response.

A

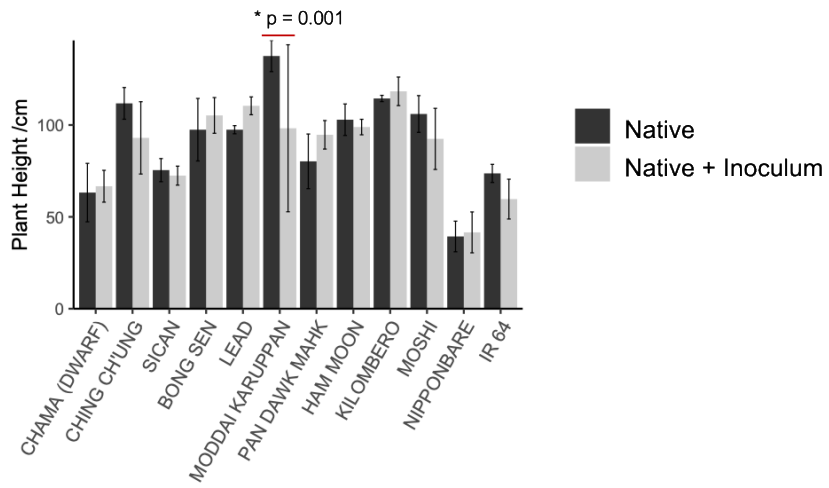

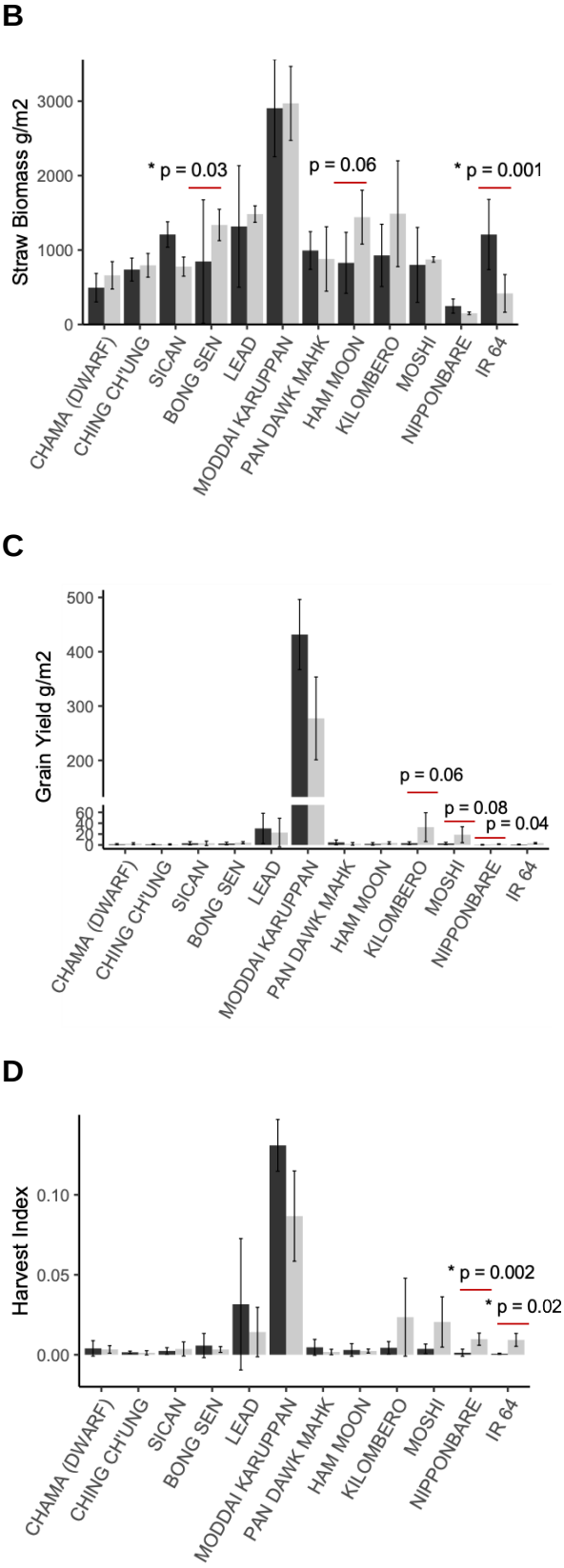

Figure 5.12 Growth and yield phenotypes measured post-harvest in native and AMF-inoculated plots. *(A) Plant height/cm (B) straw biomass g/m^2 (C) grain yield g/m^2, (D) harvest index (HI) was assessed in each cultivar and compared between native (black) and AMF-inoculated (grey) plots. Mean values are represented as bars with error bar of mean+- standard deviation. Three biological replicates per genotype replicate row were*

measured, with three biological replicates per genotype per plot. Statistically significant interaction of AMF-inoculation per genotype after post-hoc tests are indicated by asterix and red lines. P-value of post-hoc (Tukey) test are indicated.

5.2.3 Discussion

The aim of the study was to assess the effect of AMF-inoculation on growth and yield traits in diverse rice cultivars in the field. Notably, cultivar had a significant effect on all field traits except TCR, highlighting the great phenotypic diversity between the selected *Indica* cultivars. This is unsurprising considering they were diverse in country of origin and subpopulation (Table 5.1). Although the effect of AMF-inoculation was less widespread, some consistent global responses were evident in the field. For example, AMF-inoculation increased vegetative TCR number in all cultivars. Changes in root architecture upon AMF-inoculation have been previously observed in rice, with increased lateral root number, lateral root density and crown root length but not crown root number reported (Chiu et al., 2018; C. Gutjahr et al., 2009). The consistent trend for change in root architecture in the AMF-inoculated plot, observed in the field across the diverse cultivars, suggests that increased AMF-inoculation may increase crown root number in rice. Although an increased crown root number has not been observed in previous studies, this could be due to limitations due to pot size in glasshouse experiments. AMF-induced root changes such as total crown root observed here should be further assessed in the field in larger numbers of diverse rice cultivars over multiple growing seasons.

Similarly, days to flowering (DTF) was consistently increased upon AMF-inoculation. The effect of AM colonisation on flowering time is debated, with reports of AMF-inducing early flowering (Diedhiou et al., 2016), no difference in flowering or delayed flowering across different species (Bryla & Koide, 1990; Gaur et al., 2000; Howlin & Yates, 1999; Lu & Koide, 1994; Vaingankar & Rodrigues, 2015). The consistency of delayed flowering time of ~5-6 days observed across the diverse lines suggests that AMF-inoculation could delay flowering time in some diverse cultivars of *Indica* rice. Such an observation should be repeated across multiple seasons and environments to ensure vigorous analysis of the effect of AMF inoculation on DTF in *Indica* rice.

Notably, vegetative shoot dry weight was consistently decreased upon AMF-inoculation in the field. It could be that AMF causes a decrease in biomass at early vegetative stage of field grown *Indica* rice as photosynthetic carbon is exchanged from the plant host. The timing of nutrient and carbon exchange between the plant and AMF in the 'free-market' model (Kiers et al., 2011) remains to be better elucidated but is likely integral to host response. In contrast, cultivar-dependent effects of AMF-inoculation on post-harvest straw biomass, grain yield and harvest index were observed. Variation in the change in above-ground biomass, harvest index and spikelet fertility in AMF-inoculated field-grown rice has previously been identified in field trials in Senegal, with both positive and negative impact of AMF observed across different cultivars (Diedhiou et al., 2016). The similar cultivar-dependence observed here concurs observations of genetic variation in response to AMF-inoculation in the field and highlights diversity within the *Indica* ecotypes. In addition, it suggests that host responses to AMF in the field are dependent on plant life cycle, which has been observed previously in the paddy rice (Y. Wang et al., 2015). Wang et al. found that AM colonisation was low in seeding and tillering stages and increased over the plant life cycle. In addition, the composition of AMF communities colonising the root were dependent on the host developmental stage (Y. Wang et al., 2015).

A positive biomass and grain yield increase in the field upon AMF-inoculation, coupled with increased foliar phosphorous on AMF-inoculation and high blumenol abundance observed in the glasshouse experiment, suggests *BONG SEN* as a target cultivar for future analysis. *BONG SEN* was additionally highlighted in linear regression analysis as a cultivar which responded positively to AMF inoculation in the glasshouse, independent to performance under mock conditions (Chapter Four). *BONG SEN* is a traditional Vietnamese deep-water, so-called floating rice, which remains as the only floating rice variety still grown in Vinh Phuoc commune, Vietnam (Hoa, 2015; N. Lang et al., 2009). It has previously been highlighted for outstanding cold tolerance (Duc et al., 1987) but low yield compared to other varieties grown in the Mekong Delta, Vietnam (N. T. Lang et al., 2011), which could be due to traditional cultivation as a floating rice. Analysis of diverse germplasms including wild and traditional cultivars is therefore highlighted again as a valuable tool for understanding the genetic basis of AM colonisation and response. In addition, future

analysis of *BONG SEN* should confirm robust beneficial response to AM symbiosis such that the cultivar could subsequently be used as an exemplar rice cultivar with positive MGR.

Notably, the field experiment compared the broad effect of presence of AMF inoculum on growth and yield traits and variation in plant performance was confirmed between native AMF and native + AMF inoculum conditions. Further study should include quantification of root AM colonisation in the diverse cultivars in the field to additionally assess whether percentage root colonisation differed between the cultivars and how this was affected by AMF inoculum. Root and shoot material from the field experiment has been harvested for root colonisation and blumenol abundance measurements but this was beyond the timeframe of this project. In addition, it would be interesting to assess the diversity and species identity of AMF in the native and inoculated plots. It has previously been found that commercial and indigenous AMF inoculum have different effects on plant host response (Hart et al., 2018; Pellegrino et al., 2011, 2015; Rúa et al., 2016) and thus future studies should include additional commercial and indigenous inoculums in order to assess community composition and resultant plant host response.

Importantly, a template for experimental design experiments interrogating AMF in the field was recently recommended by Ryan & Graham, and includes determining key practices such as treatments required to manipulate colonisation levels (i.e. watering regime, fertiliser rate and crop species), and treatments to avoid yield losses (i.e. weeds, disease, soil structure and nutrients) (Ryan & Graham, 2018). The design was carefully considered using this template and the field experiment has been valuable in defining field conditions at IRRI for future assessments.

I conclude that impact of AMF-inoculum on host response has been observed in a dry-DSR systems with native AMF and added AMF-inoculum. In addition, I confirm that there is natural variation in response to AMF inoculation in *Indica* cultivars grown both in the glasshouse and field and this further advocates for a genetic screen of AM colonisation and MGR in *Indica* cultivars in the field. Such work would complement my glasshouse data, which facilitates identification of genetic factors

independent of unspecified environmental factors, to improve understanding of key genetic and environmental drivers of plant host response to AM symbiosis.

5.3 Conclusions

This analysis used a broad, field-experiment driven approach to assess the potential for AMF fertilisation of field-grown rice. First, the potential for application in direct-seeded rice grown in low input, aerobic regimes was assessed. AM colonisation was observed from native AMF in non-flooded fields at IRRI, Philippines. In addition, the first account, to current knowledge, of AM colonization in *NSIC Rc222 (IRRI 154),* one of the most popular varieties of rice grown in the Philippines, is reported. To fully understand the potential of AMF in such systems, further studies are required to identify beneficial cultivars and to ensure that yield and ecosystem function are maintained.

Assessment of diverse *Indica* lines with contrasting AM colonisation level and mycorrhizal growth response confirmed natural variation and cultivar-dependent response to AMF-inoculation in terms of plant height, biomass and grain yield in the field. This confirms that there is genetic variation in plant performance response to AMF-inoculation in rice, as identified in the glasshouse in Chapter Four. In addition, the study lays the groundwork for further field experiments assessing AM colonisation and MGR in the field at IRRI.

The results here describe small field experiments conducted during the wet season in the Philippines. Field experiments should be repeated over multiple seasons in different environments to assess the impact of environmental factors on AM outcome. Overall, the analyses provided broad assessment of the potential for AMF in future sustainable agroecosystems of rice production. The findings advocate for the potential of AMF in aerobic systems such as dry DSR but further analyses are required to determine the effect of AMF on plant growth and yield. In addition, further experiments such as a genetic screen in field conditions are recommended to complement glasshouse results and further resolve plant host genetic determinants of AM colonisation and response in field grown rice.

Acknowledgments

The work throughout this chapter was done in collaboration with Dr Amelia Henry and the Drought Physiology Group at International Research Institute, IRRI, Philippines. Field trial planning, planting, maintenance, harvest and analysis was completed by myself, Dr Amelia Henry and the Drought Physiology Group using facilities at International Research Institute, IRRI, Philippines.

The DSR experiment was conducted in collaboration with Dr Shalabh Dixit, Dr Amelia Henry and their respective groups at International Research Institute, IRRI, Philippines. The plants were sampled from ongoing DSR breeding trials owned by Dr Shalabh Dixit and DSR Breeding Trials Team at IRRI, Philippines. Harvest and analysis of AM colonisation was completed by myself, Dr Amelia Henry and the Drought Physiology Group using facilities at International Research Institute, IRRI, Philippines.

6 Chapter Six– General Discussion

AMF have long been recognised to form an integral link between plants and mineral nutrients in the soil (Bago et al., 2000; I. Jakobsen & Rosendahl, 1990; S. E. Smith & Read, 2008) and this has led to increasing interest in their potential as natural biofertilizers in sustainable agroecosystems (Berruti et al., 2015). Despite this, the potential is currently limited by the variable nature of plant host response to the interaction (B. A. D. Hetrick et al., 1992; Lehnert et al., 2018; Taylor et al., 2015; Thirkell et al., 2022b; Xavier & Germida, 1998). This PhD focused on understanding of genetic determinants of AM colonisation and response in rice, which is not only an important staple food crop for more than half of the world's population (Childs & LeBeau, 2023) but has a large amount of genetic material available for interrogation that has not yet been captured (Eizenga et al., 2014; Z. Li et al., 2014; Norton et al., 2018; W. Wang et al., 2018). The present study had two broad aims: first, to evaluate the use of blumenol as a high throughput (HTP) marker of AM colonisation in rice and second, to conduct a broad-scale analysis of genetic variation in AM colonisation and host response in glasshouse and field conditions.

6.1 Blumenol is recommended as a high throughput marker of AM colonisation in rice

In Chapter Three, in collaboration with Prof Ian Baldwin, Dr. Rayko Halitschke and Catarina Rocha at the Max Planck Institute for Chemical Ecology, Jena, the use of blumenols as a marker of AM colonisation in rice was interrogated. Apocarotenoids such as blumenols and the yellow-pigmented mycorradicin are known to be found to accumulate in the roots of mycorrhizal plants (Fester et al., 2002, 1999; Klingner et al., 1995; Maier et al., 1997; Schliemann, Ammer, et al., 2008; Schliemann, Kolbe, et al., 2008). More recently, Wang et al. identified that AMF-indicative blumenols accumulate in shoot material, likely through systemic transport from root biosynthesis, proving a reliable foliar marker of colonisation for high throughput analyses in multiple crop and model species (Mindt et al., 2019; M. Wang et al., 2018). Rice had not been interrogated at the time of publication, and thus this study aimed to determine the suitability of use of blumenols as foliar markers in rice. In addition, since Wang et al. noted the potential for use of the method in interrogating

AM colonisation in a genetically diverse panel of *N. attenuata,* the success of the marker was further assessed in diverse genetic material of rice to drive a decision whether to use this for screens of natural variation in AM phenotypes in diverse rice panels.

This analysis used a combination of targeted metabolomics and classic microscopy and AM marker gene expression techniques to confirm that blumenol C glycosides are accurate foliar markers of AM colonisation in rice, accumulating in correlation to percentage intraradical colonisation. Since it was previously reported that the blumenol derivative best correlating to AM colonisation differ by species (M. Wang et al., 2018), the blumenol C glycosides accumulating during AM symbiosis were newly determined in rice. A comparative analysis found both 11-carboxyblumenol C-Glc and 11-hydroxyblumenol C-Glc correlated to root colonisation, but the accumulation of 11-hydroxyblumenol C-Glc was less strictly in AMF-inoculated plants. 11-carboxyblumenol C-Glc was therefore recommended for use as a robust foliar marker of AM colonisation in rice.

Upon interrogation of diverse rice cultivars (Z. Li et al., 2014), I found that the correlation was maintained in ~90% of lines and provided an easy, HTP method for assessment of AM colonisation in large populations, beyond that which is currently possible with current methods. Despite this, the study importantly highlighted that there is natural variation in the correlation in diverse cultivars and thus screens using blumenol to probe AM colonisation should also consider that phenotypes observed could be due to variation in blumenol biosynthesis or accumulation. It is suggested that AM phenotypes in interesting lines should be complemented with visual and molecular diagnoses of root colonisation. Overall, blumenol is recommended as a high throughput marker of AM colonisation in rice.

6.2 A model for blumenol accumulation during AM symbiosis in rice; independent to phosphate and D14L/SMAX1 mediated signalling

Although it was known that blumenol accumulates in mycorrhizal roots (Fester et al., 2002, 1999; Maier et al., 1997; Schliemann, Ammer, et al., 2008; Schliemann, Kolbe, et al., 2008), particularly in correlation to intraradical AMF structures (Fester et al., 2002; M. Wang et al., 2018), little was known of the function and role of blumenol accumulation during AM symbiosis. In Chapter Three, I describe a novel assessment of the requirement of associated signalling pathways and canonical AMF structures in blumenol accumulation through interrogation of a suite of AM mutants that are available in rice. I newly report that colonisation of the root surface and outer root cell layers are not sufficient for blumenol accumulation during symbiosis and identified that accumulation instead relies either on formation of intraradical colonisation structures and/or associated gene signalling pathways initiated by the formation of arbuscules specifically, the expression of which are lost in rice *ccamk* and *pollux* mutants (C. Gutjahr et al., 2008; Pimprikar et al., 2016). Interestingly, analysis in *str1-2* fatty acid transporter mutants found that the arbuscule structure did not need to be properly unfolded or formed for blumenol to still accumulate during symbiosis.

In addition, I provide the first report of investigation of regulation of blumenol accumulation during AM symbiosis. I found that blumenol accumulates independently to SL signalling, the P_i-starvation response network and downstream *D14L/SMAX1* signalling. This contrasts regulation in other AM-associated apocarotenoids such as SLs and zaxinone (Ablazov et al., 2022; Das et al., 2022; X.-R. Li et al., 2022; Votta et al., 2022). I suggest that this points towards a functional, AM-specific role of blumenol in intraradical colonisation rather than pre-symbiotic signalling or additional plant growth and development responses.

Notably, CCD7 (D17) (Vogel et al., 2010) and CCD1 (Floss et al., 2008) had previously been implicated in blumenol biosynthesis and, due to isomeric substrate specificity (Bruno et al., 2014; Vogel et al., 2008), an additional isomerisation step was recognised. Based on gene expression analysis, D27 had previously been

suggested as an isomerase for such a step (M. Wang et al., 2018), but blumenol accumulation had not yet been assessed in *d27* mutants. Considering this, I interrogated blumenol biosynthesis in mutants of SL biosynthesis genes *D27, D17* and *D10* available in rice. I found that both *D27* and *D17* were required for blumenol biosynthesis, providing evidence that the proposed pathway (Fiorilli et al., 2019; M. Wang et al., 2018) is indeed implicated in rice: Zeaxanthin (C_{40}) is likely isomerised by D27 to 9-*cis*-C_{40}, which is cleaved into a C_{27} intermediate by CCD7. The all-trans-Apo-10'-zeaxanthinal product is cleaved to blumenol (C_{13}) and mycorradicin (C_{14}) products by CCD1. Subsequent enzymes such as cytochrome P450s likely form AMF-specific blumenol C glycosides from the C_{13} cyclohexanone, but these remain unknown. Further analysis of accumulation of these intermediates in the mutants, and of blumenol phenotypes of other CCDs, including CCD4, are additionally required to better elucidate further blumenol biosynthesis pathways in rice.

6.3 (Re)defining the requirement for SLs and apocarotenoids during AM symbiosis in rice

Over the last few years, the requirement of AM-associated apocarotenoids for AM symbiosis had been further elucidated in rice. A novel apocarotenoid, zaxinone, was identified and implicated in growth, architecture, strigolactone regulation and AM symbiosis in rice (Ablazov et al., 2022; Votta et al., 2022). In addition, although strigolactones had been known to be required for efficient pre-symbiotic signalling, and colonisation reduced in biosynthesis mutants in rice (C Gutjahr et al., 2012), the requirement for SLs during symbiosis progression was undetermined. In 2018, Kobae et al. provided further temporal resolution of the requirement at different stages of symbiosis and suggested that biosynthesis genes were required for punctual entry of AMF into host roots. Importantly, although initially reduced, colonisation could reach wild type levels in both mutants. In addition, a difference in severity of phenotype was reported between mutants of *D17* and *D10* (Kobae et al., 2018) and *D27* had not yet been assessed.

In this study, I found that AM colonisation phenotypes in *d17-1* and *d10-1* SL biosynthesis genes of rice are more plastic than previously appreciated and newly

report an AM phenotype for *d27-1.* Delayed colonisation is evident in all mutants under some experimental conditions and is consistently most severe in *d17-1*. Importantly, I also highlighted that wild type or wild type-like colonisation can be achieved in all mutants, particularly in *d10-1* and *d27-1*. This suggests that the AM colonisation delay observed in the mutants previously (C Gutjahr et al., 2012; Kobae et al., 2018) is likely a more plastic phenotype than had been anticipated. The requirement for SLs during colonisation is clearly important, particularly in initial internalisation, but not required for efficient symbiosis establishment and progression.

In collaboration with Prof. Paul Fraser and Dr Laura Perez at Royal Holloway University, London I further used a metabolomics approach to identify that apocarotenoid signatures of SL biosynthesis mutants. I found the signatures corroborated SL-independent roles of *D27* and *D17/CCD7*. In addition, the results invite for further analysis of AM-associated apocarotenoids and their function in AM symbiosis, which could elucidate the reasoning for greater requirement of D17/CCD7.

The novel finding of the requirement of both *D27* and *D17* in SL and blumenol biosynthesis in rice, coupled with a new appreciation of a plasticity of AM phenotypes in the mutants, facilitates greater understanding of the roles of AM-associated apocarotenoids in AM symbiosis. Since blumenol establishment is abolished in *d17-1* and colonisation still progresses in the mutant, blumenol is not essential for AM symbiosis in rice. Similarly, canonical SL 2′-epi-5-deoxystrigol is undetectable in the biosynthesis mutants (H. Lin et al., 2009; Umehara et al., 2008) and, as I found AM colonisation can still progress in the mutants, the derivative is likely required but not essential for symbiosis establishment. Ito et al. recently similarly found that canonical SLs 4-deoxyorobanchol, orobanchol and non-canonical isomer *MeO-5-DS is1* are abolished in *Os900-KO* mutants, which can still establish delayed but progressive root colonisation, suggesting SL derivatives are not essential for symbiosis (Ito et al., 2022). The requirement for other canonical and non-canonical SL derivatives remains to be elucidated by further analysis of derivatives present in SL and apocarotenoid biosynthesis mutants. In addition, although zaxinone is required for efficient colonisation, which is delayed in mutants

with reduced production, assessment of essentiality requires analysis of AM colonisation in mutants in which zaxinone is fully abolished. Overall, although apocarotenoids are clearly required for efficient establishment of symbiosis, they are currently not found to be essential for colonisation, as mutants can maintain intraradical colonisation and recover to wild type levels over time. Further study of the role of apocarotenoids in AM symbiosis, and associated apocarotenoid signatures of mutants unable to form effective colonisation, will facilitate greater understanding of the requirement for SLs and apocarotenoids during AM symbiosis in rice.

6.4 Natural variation in AM colonisation and responsiveness in diverse rice cultivars

In Chapter Four, a broad-scale analysis of genetic variation in AM colonisation and host response was conducted in a glasshouse experiment assessing ~2000 plants. Although natural variation in AM colonisation and mycorrhizal growth response (MGR) had previously been reported in the Rice Diversity Panel 1 (Davidson et al., 2019), this was the only large scale analysis described in rice, and variation had not yet been explored in the 3K-RG panel that includes global, genetic and functional diversity represented by 3,024 rice accessions (Z. Li et al., 2014; W. Wang et al., 2018). In addition, natural variation specifically in the *Indica* ecotype, which has previously been implicated for potential in improved breeding of upland rice cultivars (Saito et al., 2018), had not yet been studied with all available diversity (W. Wang et al., 2018).

Working in collaboration with the International Rice Research Institute (IRRI), I selected over 200 cultivars from the *Indica* ecotype that were representative of diversity present in the 3K-RG panel, whilst maintaining reduced population structure to be efficient in mapping studies. The panel is presented as a valuable addition to the available genetic diversity panels of rice (Eizenga et al., 2014; A. Kumar et al., 2020; Z. Li et al., 2014; Norton et al., 2018) and represents the first ecotype specific panel of the 3K-RG. Using physiological, metabolomic and ionomic analyses, I identified significant natural variation in growth traits in the panel when grown in P

deficiency, particularly in response to AMF inoculation. This data lends support for further analyses interrogating genetic factors determining plant growth and metabolic response in rice grown in P deplete conditions.

In addition, after confirmation of blumenols as HTP foliar markers of intraradical colonisation in Chapter Three, I report the first use of blumenol for a screen of AM phenotypes in a diverse rice panel. There was significant variation in AMF-indicative blumenol abundance in the *Indica* ecotype, independent to subpopulation. This concurs previous identification of significant variation in hyphal root colonisation in RDP1, (Davidson et al., 2019) and additionally suggests that there is great natural genetic diversity in root colonisation across *Indica* cultivars of the 3K-RG.

As found previously (Davidson et al., 2019), natural variation MGR was evident in the diverse panel. I report that host plant response was only partially driven by extent of colonisation and is likely determined by additional genetic factors, as has been reported previously in wheat and maize (Sawers et al., 2017; Thirkell et al., 2022). Notably, unlike in maize (Sawers et al., 2017), shoot biomass responses to AMF were independent to shoot P content and likely dependent on additional factors that remain to be elucidated. Beneficial responses in biomass and foliar P were observed in superior lines such as *BONG SEN,* and this was highlighted as a target cultivar for future analysis.

6.5 Genetic mapping of AM colonisation in rice

In recent years, use of genetic association studies in multiple plant species has been applied for identification of quantitative trait loci (QTLs) associated to AM colonisation (Davidson et al., 2019; De Vita et al., 2018; Lehnert et al., 2018; Pawlowski et al., 2020; Thirkell et al., 2022). Despite this, only one study has currently mapped genetic drivers of AM colonisation in rice. Using a genome wide association study (GWAS) with the RDP1, Davidson et al. reported 23 putative QTLs mapping to hyphal colonisation rates and candidate genes included a calcium/calmodulin serine/threonine protein kinase and two ammonium transporters (Davidson et al., 2019).

In Chapter Four, in collaboration with Dr. Dmytro Chebotarov at the International Rice Research Institute (IRRI), I conducted a GWAS interrogating natural variation in blumenol abundance and AM colonisation. Using the panel of ~200 diverse *Indica* cultivars from the 3K-RG, I report QTLs associated to natural variation in blumenol abundance and identified an exciting list of candidate genes. These include transcription factors regulated by AM symbiosis and genes involved in lipid biosynthesis, root development and plant defence. In addition, haplotype analysis identified strong candidate genes for further validation. A putative cytochrome monooxygenase P450 (CYP) was found to be associated to 11-hydroxyblumenol C-Glc abundance. CYPs have previously been implicated in biosynthesis of AM-associated apocarotenoids such as SLs (Abe et al., 2014; Fiorilli et al., 2019; Ito et al., 2022; Yoneyama et al., 2018; Y. Zhang et al., 2014), and the gene could have potential function in biosynthesis of additional apocarotenoids including blumenols during AM symbiosis. In addition, a PPDK enzyme was highlighted as being associated to 11-carboxyblumenol C-Glc. PPDKs have previously been implicated in control of carbon resources (H. Wang et al., 2020) and, PPDKA has been noted to be required for inducible metabolic response to abiotic stress (Moons et al., 1998). Since the gene has additionally been found to be upregulated upon inoculation of rice with *R. irregularis* AMF (S. Wang et al., 2020), *PPDKA* is a strong candidate for further analysis of a potential role in regulation of carbon allocation during AM symbiosis. Functional experimentation including analysis of root length colonisation and blumenol abundance in knock out mutants of candidate genes is recommended to identify roles specifically in either AM symbiosis and/or blumenol accumulation during AM symbiosis.

Since I additionally found natural variation in AM response in terms of biomass and foliar ion composition, the PhD has created a large amount of data that can be further analysed. A collaboration with Prof. Ruairidh Sawers and Dr Meng Li at Penn State College of Agricultural Sciences has been established and will focus on future use of the data in mapping of genetic regions associated to the growth and nutrient responses. This will use a previously described method that identified QTLs associated to beneficial host response to AMF in maize (Li et al., 2022; Ramírez-Flores et al., 2020). Such analyses will be used to identify QTLs and candidate

genes associated to blumenol abundance (root colonisation) and beneficial host response in terms of the growth and nutrient uptake in rice.

6.6 The potential for AMF in sustainable rice agroecosystems

The potential for use of AM symbiosis in sustainable rice production requires understanding of the yielding capacity and ecosystem function of AMF in different agroecosystems of rice. Most studies assessing the impact of AMF in the rice field have focused on lowland, paddy rice cultivated in flooded conditions where AMF are less abundant and root colonisation is low (Bernaola, et al., 2018; M. Vallino et al., 2009; Y. Wang et al., 2021). Recently, AMF inoculation was reported to mitigate negative effects of phosphate deficiency on agronomic traits in rice grown in pots with previous paddy field soil (Das et al., 2022). In addition, the potential in sustainable, alternate wetting and drying irrigation (AWD) systems has been considered. Vallino et al. noted a plastic adaption of functional symbiosis establishment in wet- or dry conditions in fields in Italy and found that colonisation and AMF abundance could recover once flooding has subsided. This suggests that there is potential for AM symbiosis in AWD rice cultivation. In contrast, little work has assessed the potential for AMF in sustainable, direct-seeded rice (DSR) systems in the field.

In Chapter Five, in collaboration with Dr. Amelia Henry and Dr. Shalabh Dixit at IRRI, I described a first-look, broad assessment of the presence of AMF in DSR breeding trial plots at IRRI, Philippines. The study provided a primary account, to current knowledge, of AM colonization in the elite rice cultivar *NSIC Rc222 (IRRI 154)* and confirmed presence of native AMF at the IRRI farm. In addition, I report that, although AMF were present in flooded soils of lowland, paddy rice or wet DSR, root colonisation was entirely abolished. This concurs previous reports of the impact of flooding on AM colonisation capacity (Bernaola, et al., 2018; M. Vallino et al., 2009; Y. Wang et al., 2021). In contrast, I report the presence of AM colonisation rice grown in the field in aerobic, dry-direct seeded systems that were non-flooded, either by irrigated or rainfed regimes. This promotes the potential for AMF in dry DSR

systems, although further work is required to determine yield capacity in regimes with optimal cultivar, fertilisation, and inoculation selection.

Next, I assessed the response of diverse *Indica* cultivars to AMF inoculum compared to native AMF in the field. In vegetative traits, AMF inoculation increased total crown root number and decreased shoot dry weight. Post-harvest, natural variation in plant performance in terms of biomass and yield response to AMF-inoculation was observed across the cultivars. This corroborates glasshouse data of natural variation in response to AMF in diverse cultivars of *Indica* rice. In addition, the study provided indication for future studies measuring genetic determinants of variation in host responsiveness directly in the field. Such work would complement glasshouse results and further resolve plant host genetic determinants of AM response in the field. This will be integral to the success of future studies assessing the potential for AMF in sustainable agroecosystems of rice.

6.7 Final Conclusions

This collaborative project has provided evidence for successful use of a novel, HTP foliar marker of AM colonisation in rice, which is an exciting tool that will facilitate ease of future large-scale studies. Such is integral in an era in which we recognise great genetic diversity in plant genotypes and begin to understand the impact of this on AM colonisation and host response. Overall, the project provides the groundwork for understanding of blumenol accumulation during AM symbiosis and use of the marker in assessing AM colonisation and host response in diverse rice lines; describes strong candidates for further analysis of their role in AM symbiosis; and produced data that can be further mined and built upon to understand the potential for AMF in future, sustainable, rice production.

7 References

Abbai, R., Singh, V. K., Nachimuthu, V. V., Sinha, P., Selvaraj, R., Vipparla, A. K., Singh, A. K., Singh, U. M., Varshney, R. K., & Kumar, A. (2019). Haplotype analysis of key genes governing grain yield and quality traits across 3K RG panel reveals scope for the development of tailor-made rice with enhanced genetic gains. *Plant Biotechnology Journal*, *17*(8), 1612–1622. https://onlinelibrary.wiley.com/doi/full/10.1111/pbi.13087

Abe, S., Sado, A., Tanaka, K., Kisugi, T., Asami, K., Ota, S., Il Kim, H., Yoneyama, K., Xie, X., Ohnishi, T., Seto, Y., Yamaguchi, S., Akiyama, K., Yoneyama, K., & Nomura, T. (2014). Carlactone is converted to carlactonoic acid by MAX1 in Arabidopsis and its methyl ester can directly interact with AtD14 in vitro. *Proceedings of the National Academy of Sciences of the United States of America*, *111*(50), 18084–18089. https://doi.org/10.1073/pnas.1410801111

Ablazov, A., Mi, J., Jamil, M., Jia, K. P., Wang, J. Y., Feng, Q., & Al-Babili, S. (2020). The Apocarotenoid Zaxinone Is a Positive Regulator of Strigolactone and Abscisic Acid Biosynthesis in Arabidopsis Roots. *Frontiers in Plant Science*, *11*. https://doi.org/10.3389/fpls.2020.00578

Ablazov, A., Votta, C., Fiorilli, V., & Wang, J. Y. (2022). ZAXINONE SYNTHASE 2 regulates growth and arbuscular mycorrhizal symbiosis in rice. *Plant Physiology*. https://doi.org/10.1093/PLPHYS/KIAC472

Abuauf, H., Haider, I., Jia, K. P., Ablazov, A., Mi, J., Blilou, I., & Al-Babili, S. (2018). The Arabidopsis DWARF27 gene encodes an all-trans-/9-cis-β-carotene isomerase and is induced by auxin, abscisic acid and phosphate deficiency. *Plant Science*, *277*, 33–42. https://doi.org/10.1016/j.plantsci.2018.06.024

Akiyama, K., Matsuzaki, K. I., & Hayashi, H. (2005). Plant sesquiterpenes induce hyphal branching in arbuscular mycorrhizal fungi. *Nature*, *435*(7043), 824–827. https://doi.org/10.1038/nature03608

Al-Babili, S., & Bouwmeester, H. J. (2015). Strigolactones, a Novel Carotenoid-Derived Plant Hormone. *Annual Review of Plant Biology*, *66*(1), 161–186. https://doi.org/10.1146/annurev-arplant-043014-114759

Al-Karaki, G. N., & Hammad, R. (2001). Mycorrhizal influence on fruit yield and mineral content of tomato grown under salt stress. *Journal of Plant Nutrition*, *24*(8), 1311–1323. https://doi.org/10.1081/PLN-100106983

Alder, A., Holdermann, I., Beyer, P., & Al-Babili, S. (2008). Carotenoid oxygenases involved in plant branching catalyse a highly specific conserved apocarotenoid cleavage reaction. *Biochemical Journal*, *416*(2), 289–296. https://doi.org/10.1042/BJ20080568

Alder, A., Jamil, M., Marzorati, M., Bruno, M., Vermathen, M., Bigler, P., Ghisla, S., Bouwmeester, H., Beyer, P., & Al-Babili, S. (2012). The path from β-carotene to

carlactone, a strigolactone-like plant hormone. *Science (New York, N.Y.)*, *335*(6074), 1348–1351. https://doi.org/10.1126/science.1218094

Alexander, T., Toth, R., Meier, R., & Weber, H. C. (1989). Dynamics of arbuscule development and degeneration in onion, bean, and tomato with reference to vesicular–arbuscular mycorrhizae in grasses. *Canadian Journal of Botany*, *67*(8), 2505–2513. https://doi.org/10.1139/b89-320

Alexandrov, N., Tai, S., Wang, W., Mansueto, L., Palis, K., Fuentes, R. R., Ulat, V. J., Chebotarov, D., Zhang, G., Li, Z., Mauleon, R., Hamilton, R. S., & McNally, K. L. (2015). SNP-Seek database of SNPs derived from 3000 rice genomes. *Nucleic Acids Research*, *43*(D1), D1023–D1027. https://doi.org/10.1093/nar/gku1039

Alvarez, J. M., Moyano, T. C., Zhang, T., Gras, D. E., Herrera, F. J., Araus, V., O'Brien, J. A., Carrillo, L., Medina, J., Vicente-Carbajosa, J., Jiang, J., & Gutiérrez, R. A. (2019). Local Changes in Chromatin Accessibility and Transcriptional Networks Underlying the Nitrate Response in Arabidopsis Roots. *Molecular Plant*, *12*(12), 1545–1560. https://doi.org/10.1016/J.MOLP.2019.09.002

An, G. H., Kobayashi, S., Enoki, H., Sonobe, K., Muraki, M., Karasawa, T., & Ezawa, T. (2010). How does arbuscular mycorrhizal colonization vary with host plant genotype? An example based on maize (Zea mays) germplasms. *Plant and Soil*, *327*(1), 441–453. https://doi.org/10.1007/s11104-009-0073-3

An, J., Sun, M., Van Velzen, R., Ji, C., Zheng, Z., Limpens, E., Bisseling, T., Deng, X., Xiao, S., & Pan, Z. (2018). Comparative transcriptome analysis of Poncirus trifoliata identifies a core set of genes involved in arbuscular mycorrhizal symbiosis. *Journal of Experimental Botany*, *69*(21), 5255–5264. https://doi.org/10.1093/jxb/ery283

Anneberg, T. J., & Segraves, K. A. (2019). Intraspecific polyploidy correlates with colonization by arbuscular mycorrhizal fungi in Heuchera cylindrica. *American Journal of Botany*, *106*(6), 894–900. https://doi.org/10.1002/ajb2.1294

Antolín-Llovera, M., Petutsching, E. K., Ried, M. K., Lipka, V., Nürnberger, T., Robatzek, S., & Parniske, M. (2014). Knowing your friends and foes - plant receptor-like kinases as initiators of symbiosis or defence. *New Phytologist*, *204*(4), 791–802. https://doi.org/10.1111/nph.13117

Arite, T., Iwata, H., Ohshima, K., Maekawa, M., Nakajima, M., Kojima, M., Sakakibara, H., & Kyozuka, J. (2007). DWARF10, an RMS1/MAX4/DAD1 ortholog, controls lateral bud outgrowth in rice. *Plant Journal*, *51*(6), 1019–1029. https://doi.org/10.1111/j.1365-313X.2007.03210.x

Arite, T., Umehara, M., Ishikawa, S., Hanada, A., Maekawa, M., Yamaguchi, S., & Kyozuka, J. (2009). d14, a Strigolactone-Insensitive Mutant of Rice, Shows an Accelerated Outgrowth of Tillers. *Plant and Cell Physiology*, *50*(8), 1416–1424. https://doi.org/10.1093/pcp/pcp091

Augé, R. M. (2001). Water relations, drought and vesicular-arbuscular mycorrhizal symbiosis. In *Mycorrhiza* (Vol. 11, Issue 1, pp. 3–42). https://doi.org/10.1007/s005720100097

Aung, K., Lin, S. I., Wu, C. C., Huang, Y. T., Su, C. L., & Chiou, T. J. (2006). pho2, a phosphate overaccumulator, is caused by a nonsense mutation in a microRNA399 target gene. *Plant Physiology*, *141*(3), 1000–1011. https://doi.org/10.1104/pp.106.078063

Avio, L., Pellegrino, E., Bonari, E., & Giovannetti, M. (2006). Functional diversity of arbuscular mycorrhizal fungal isolates in relation to extraradical mycelial networks. *New Phytologist*, *172*(2), 347–357. https://doi.org/10.1111/j.1469-8137.2006.01839.x

Bago, B., Pfeffer, P. E., & Shachar-Hill, Y. (2000). Carbon metabolism and transport in arbuscular mycorrhizas. In *Plant Physiology* (Vol. 124, Issue 3, pp. 949–957). American Society of Plant Biologists. https://doi.org/10.1104/pp.124.3.949

Balestrini, R., Berta, G., & Bonfante, P. (1992). The plant nucleus in mycorrhizal roots: positional and structural modifications. *Biology of the Cell*, *75*(1), 235–243. https://doi.org/10.1016/0248-4900(92)90145-Q

Balzergue, C., Chabaud, M., Barker, D. G., Bécard, G., & Rochange, S. F. (2013). High phosphate reduces host ability to develop arbuscular mycorrhizal symbiosis without affecting root calcium spiking responses to the fungus. *Frontiers in Plant Science*, *4*, 426. https://doi.org/10.3389/fpls.2013.00426

Banasiak, J., Borghi, L., Stec, N., Martinoia, E., & Jasiński, M. (2020). The Full-Size ABCG Transporter of Medicago truncatula Is Involved in Strigolactone Secretion, Affecting Arbuscular Mycorrhiza. *Frontiers in Plant Science*, *11*, 18. https://doi.org/10.3389/fpls.2020.00018

Banba, M., Gutjahr, C., Miyao, A., Hirochika, H., Paszkowski, U., Kouchi, H., & Imaizumi-Anraku, H. (2008). Divergence of Evolutionary Ways Among Common sym Genes: CASTOR and CCaMK Show Functional Conservation Between Two Symbiosis Systems and Constitute the Root of a Common Signaling Pathway. *Plant and Cell Physiology*, *49*(11), 1659–1671. https://doi.org/10.1093/pcp/pcn153

Bartoli, C., & Roux, F. (2017). Genome-wide association studies in plant pathosystems: Toward an ecological genomics approach. In *Frontiers in Plant Science* (Vol. 8, p. 763). Frontiers Media S.A. https://doi.org/10.3389/fpls.2017.00763

Bazghaleh, N., Hamel, C., Gan, Y., Tar'an, B., & Knight, J. D. (2018). Genotypic variation in the response of chickpea to arbuscular mycorrhizal fungi and non-mycorrhizal fungal endophytes. *Canadian Journal of Microbiology*, *64*(4), 265–275. https://doi.org/10.1139/cjm-2017-0521

Bécard, G., & Fortin, J. A. (1988). Early events of vesicular–arbuscular mycorrhiza

formation on Ri T-DNA transformed roots. *New Phytologist*, *108*(2), 211–218. https://doi.org/10.1111/j.1469-8137.1988.tb03698.x

Becard, G., Taylor, L. P., Douds, D. D., Pfeffer, P. E., & Doner, L. W. (1995). Flavonoids are not necessary plant signal compounds in arbuscular mycorrhizal symbioses. *Molecular Plant-Microbe Interactions*, *8*(2), 252–258. https://doi.org/10.1094/MPMI-8-0252

Benedetto, A., Magurno, F., Bonfante, P., & Lanfranco, L. (2005). Expression profiles of a phosphate transporter gene (GmosPT) from the endomycorrhizal fungus Glomus mosseae. *Mycorrhiza*, *15*(8), 620–627. https://doi.org/10.1007/s00572-005-0006-9

Bernaola, L., Cange, G., Way, M. O., Gore, J., Hardke, J., & Stout, M. (2018). Natural Colonization of Rice by Arbuscular Mycorrhizal Fungi in Different Production Areas. *Rice Science*, *25*(3), 169–174. https://doi.org/10.1016/J.RSCI.2018.02.006

Bernaola, L., Cosme, M., Schneider, R. W., & Stout, M. (2018). Belowground inoculation with arbuscular mycorrhizal fungi increases local and systemic susceptibility of rice plants to different pest organisms. *Frontiers in Plant Science*, *9*, 747. https://doi.org/10.3389/FPLS.2018.00747/BIBTEX

Berruti, A., Lumini, E., Balestrini, R., & Bianciotto, V. (2015). Arbuscular Mycorrhizal Fungi as Natural Biofertilizers: Let's Benefit from Past Successes. *Frontiers in Microbiology*, *6*, 1559. https://doi.org/10.3389/fmicb.2015.01559

Besserer, A., Bécard, G., Jauneau, A., Roux, C., & Séjalon-Delmas, N. (2008). GR24, a Synthetic Analog of Strigolactones, Stimulates the Mitosis and Growth of the Arbuscular Mycorrhizal Fungus Gigaspora rosea by Boosting Its Energy Metabolism. *Plant Physiology*, *148*(1), 402–413. https://doi.org/10.1104/pp.108.121400

Besserer, A., Puech-Pagès, V., Kiefer, P., Gomez-Roldan, V., Jauneau, A., Roy, S., Portais, J. C., Roux, C., Bécard, G., & Séjalon-Delmas, N. (2006). Strigolactones stimulate arbuscular mycorrhizal fungi by activating mitochondria. *PLoS Biology*, *4*(7), 1239–1247. https://doi.org/10.1371/journal.pbio.0040226

Bever, J. D. (2002). Negative feedback within a mutualism: Host-specific growth of mycorrhizal fungi reduces plant benefit. *Proceedings of the Royal Society B: Biological Sciences*, *269*(1509), 2595–2601. https://doi.org/10.1098/rspb.2002.2162

Bever, J. D., Platt, T. G., & Morton, E. R. (2012). Microbial Population and Community Dynamics on Plant Roots and Their Feedbacks on Plant Communities. *Annual Review of Microbiology*, *66*(1), 265–283. https://doi.org/10.1146/annurev-micro-092611-150107

Bidartondo, M. I., Redecker, D., Hijri, I., Wiemken, A., Bruns, T. D., Domínguez, L., Sérsic, A., Leake, J. R., & Read, D. J. (2002). Epiparasitic plants specialized on

arbuscular mycorrhizal fungi. *Nature*, *419*(6905), 389–392. https://doi.org/10.1038/nature01054

Bitterlich, M., Krügel, U., Boldt-Burisch, K., Franken, P., & Kühn, C. (2014). The sucrose transporter SlSUT2 from tomato interacts with brassinosteroid functioning and affects arbuscular mycorrhiza formation. *The Plant Journal*, *78*(5), 877–889. https://doi.org/10.1111/TPJ.12515

Bradbury, P. J., Zhang, Z., Kroon, D. E., Casstevens, T. M., Ramdoss, Y., & Buckler, E. S. (2007). TASSEL: software for association mapping of complex traits in diverse samples. *Bioinformatics*, *23*(19), 2633–2635. https://doi.org/10.1093/BIOINFORMATICS/BTM308

Bravo, A., Brands, M., Wewer, V., Dörmann, P., & Harrison, M. J. (2017). Arbuscular mycorrhiza-specific enzymes FatM and RAM2 fine-tune lipid biosynthesis to promote development of arbuscular mycorrhiza. *New Phytologist*, *214*(4), 1631–1645. https://doi.org/10.1111/nph.14533

Bravo, A., York, T., Pumplin, N., Mueller, L. A., & Harrison, M. J. (2016). Genes conserved for arbuscular mycorrhizal symbiosis identified through phylogenomics. *Nature Plants*, *2*(2), 15208. https://doi.org/10.1038/NPLANTS.2015.208

Breuillin-Sessoms, F., Floss, D. S., Karen Gomez, S., Pumplin, N., Ding, Y., Levesque-Tremblay, V., Noar, R. D., Daniels, D. A., Bravo, A., Eaglesham, J. B., Benedito, V. A., Udvardi, M. K., & Harrison, M. J. (2015). Suppression of arbuscule degeneration in Medicago truncatula phosphate transporter4 mutants is dependent on the ammonium transporter 2 family protein AMT2;3. *Plant Cell*, *27*(4), 1352–1366. https://doi.org/10.1105/tpc.114.131144

Breuillin, F., Schramm, J., Hajirezaei, M., Ahkami, A., Favre, P., Druege, U., Hause, B., Bucher, M., Kretzschmar, T., Bossolini, E., Kuhlemeier, C., Martinoia, E., Franken, P., Scholz, U., & Reinhardt, D. (2010). Phosphate systemically inhibits development of arbuscular mycorrhiza in Petunia hybrida and represses genes involved in mycorrhizal functioning. *Plant Journal*, *64*(6), 1002–1017. https://doi.org/10.1111/j.1365-313X.2010.04385.x

Brundrett, M. C., Piché, Y, and Peterson, R. L. 2011. A new method for observing the morphology of vesicular–arbuscular mycorrhizae. *Canadian Journal of Botany*. 62(10): 2128-2134. https://doi.org/10.1139/b84-290

Bruno, M., & Al-Babili, S. (2016). On the substrate specificity of the rice strigolactone biosynthesis enzyme DWARF27. *Planta*, *243*(6), 1429–1440. https://doi.org/10.1007/s00425-016-2487-5

Bruno, M., Beyer, P., & Al-Babili, S. (2015). The potato carotenoid cleavage dioxygenase 4 catalyzes a single cleavage of β-ionone ring-containing carotenes and non-epoxidated xanthophylls. *Archives of Biochemistry and Biophysics*, *572*, 126–133. https://doi.org/10.1016/j.abb.2015.02.011

Bruno, M., Hofmann, M., Vermathen, M., Alder, A., Beyer, P., & Al-Babili, S. (2014). On the substrate- and stereospecificity of the plant carotenoid cleavage dioxygenase 7. *FEBS Letters*, *588*(9), 1802–1807. https://doi.org/10.1016/j.febslet.2014.03.041

Bruno, M., Koschmieder, J., Wuest, F., Schaub, P., Fehling-Kaschek, M., Timmer, J., Beyer, P., & Al-Babili, S. (2016). Enzymatic study on AtCCD4 and AtCCD7 and their potential to form acyclic regulatory metabolites. *Journal of Experimental Botany*, *67*(21), 5993–6005. https://doi.org/10.1093/jxb/erw356

Bruno, M., Vermathen, M., Alder, A., Wüst, F., Schaub, P., van der Steen, R., Beyer, P., Ghisla, S., & Al-Babili, S. (2017). Insights into the formation of carlactone from in-depth analysis of the CCD8-catalyzed reactions. *FEBS Letters*, *591*(5), 792–800. https://doi.org/10.1002/1873-3468.12593

Bryla, D. R., & Koide, R. T. (1990). Regulation of reproduction in wild and cultivated Lycopersicon esculentum Mill. by vesicular-arbuscular mycorrhizal infection. *Oecologia*, *84*(1), 74–81. https://doi.org/10.1007/BF00665598/METRICS

Bucher, M. (2007). Functional biology of plant phosphate uptake at root and mycorrhiza interfaces. *New Phytologist*, *173*(1), 11–26. https://doi.org/10.1111/j.1469-8137.2006.01935.x

Butler, L. G. (1994). *Chemical Communication Between the Parasitic Weed Striga and Its Crop Host* (pp. 158–168). https://doi.org/10.1021/bk-1995-0582.ch012

Bythell-Douglas, R., Rothfels, C. J., Stevenson, D. W. D., Graham, S. W., Wong, G. K. S., Nelson, D. C., & Bennett, T. (2017). Evolution of strigolactone receptors by gradual neo-functionalization of KAI2 paralogues. *BMC Biology*, *15*(1). https://doi.org/10.1186/S12915-017-0397-Z

C. E, C., Leona P, W., Beverly, T., Monroe E, W., & Grant H, E. (1966). Germination of Witchweed (Striga lutea Lour.): Isolation and Properties of a Potent Stimulant. *Science*, *154*(3753), 1189–1190. https://science.sciencemag.org/content/154/3753/1189.short

Cabusora, C. C., Buluran, R. D., & Desamero, N. V. (2022). NSIC Rc222-derived Mutants Characterized for Field Performance Identifying Putative Complete Submergence Tolerant Lines. *Philippine Journal of Science*, *151*(3), 985–1001. https://doi.org/10.56899/151.03.17

Cameron, D. D., Neal, A. L., van Wees, S. C. M., & Ton, J. (2013). Mycorrhiza-induced resistance: more than the sum of its parts? *Trends in Plant Science*, *18*(10), 539. https://doi.org/10.1016/J.TPLANTS.2013.06.004

Campo, S., Martín-Cardoso, H., Olivé, M., Pla, E., Catala-Forner, M., Martínez-Eixarch, M., & San Segundo, B. (2020). Effect of Root Colonization by Arbuscular Mycorrhizal Fungi on Growth, Productivity and Blast Resistance in Rice. *Rice*, *13*(1), 1–14. https://pubmed.ncbi.nlm.nih.gov/32572623/

Carotenuto, G., Chabaud, M., Miyata, K., Capozzi, M., Takeda, N., Kaku, H., Shibuya, N., Nakagawa, T., Barker, D. G., & Genre, A. (2017). The rice LysM receptor-like kinase Os CERK1 is required for the perception of short-chain chitin oligomers in arbuscular mycorrhizal signaling. *New Phytologist*, *214*(4), 1440–1446. https://doi.org/10.1111/nph.14539

Charpentier, M., Sun, J., Martins, T. V., Radhakrishnan, G. V., Findlay, K., Soumpourou, E., Thouin, J., Véry, A. A., Sanders, D., Morris, R. J., & Oldroyd, G. E. D. (2016). Nuclear-localized cyclic nucleotide-gated channels mediate symbiotic calcium oscillations. *Science*, *352*(6289), 1102–1105. https://doi.org/10.1126/science.aae0109

Charpentier, M., Sun, J., Wen, J., Mysore, K. S., & Oldroyd, G. E. D. (2014). Abscisic acid promotion of arbuscular mycorrhizal colonization requires a component of the PROTEIN PHOSPHATASE 2A complex. *Plant Physiology*, *166*(4), 2077–2090. https://doi.org/10.1104/pp.114.246371

Childs, N., & LeBeau, B. (2023). Rice Outlook: January 2023. *U.S. Department of Agriculture, Economic Research Service*, *RCS-23A*.

Chin, J. H., Gamuyao, R., Dalid, C., Bustamam, M., Prasetiyono, J., Moeljopawiro, S., Wissuwa, M., & Heuer, S. (2011). Developing Rice with High Yield under Phosphorus Deficiency: Pup1 Sequence to Application. *Plant Physiology*, *156*(3), 1202–1216. https://doi.org/10.1104/PP.111.175471

Chiou, T. J., Aung, K., Lin, S. I., Wu, C. C., Chiang, S. F., & Su, C. L. (2006). Regulation of phosphate homeostasis by MicroRNA in Arabidopsis. *Plant Cell*, *18*(2), 412–421. https://doi.org/10.1105/tpc.105.038943

Chirinda, N., Arenas, L., Katto, M., Loaiza, S., Correa, F., Isthitani, M., Loboguerrero, A. M., Martínez-Barón, D., Graterol, E., Jaramillo, S., Torres, C. F., Arango, M., Guzmán, M., Avila, I., Hube, S., Kurtz, D. B., Zorrilla, G., Terra, J., Irisarri, P., … Bayer, C. (2018). Sustainable and Low Greenhouse Gas Emitting Rice Production in Latin America and the Caribbean: A Review on the Transition from Ideality to Reality. *Sustainability 2018, Vol. 10, Page 671*, *10*(3), 671. https://doi.org/10.3390/SU10030671

Chiu, C. H., Choi, J., & Paszkowski, U. (2018). Independent signalling cues underpin arbuscular mycorrhizal symbiosis and large lateral root induction in rice. *New Phytologist*, *217*(2), 552–557. https://doi.org/10.1111/nph.14936

Chiu, C. H., & Paszkowski, U. (2020). Receptor-like kinases sustain symbiotic scrutiny. *Plant Physiology*, *182*(4), pp.01341.2019. https://doi.org/10.1104/pp.19.01341

Choi, J., Lee, T., Cho, J., Servante, E., Pucker, B., Summers, W., Bowden, S., Rahimi, M., An, K., An, G., Bouwmeester, H., Wallington, E., Oldroyd, G., & Paszkowski, U. (2020). The negative regulator SMAX1 controls mycorrhizal symbiosis and strigolactone biosynthesis in rice. *Nature Communications*, *11*(1), 2114. https://doi.org/10.1038/s41467-020-16021-1

Choi, J., Summers, W., & Paszkowski, U. (2018). Mechanisms Underlying Establishment of Arbuscular Mycorrhizal Symbioses. *Annual Review of Phytopathology*, *56*(1), 135–160. https://doi.org/10.1146/annurev-phyto-080516-035521

Cingolani, P., Platts, A., Wang, L. L., Coon, M., Nguyen, T., Wang, L., Land, S. J., Lu, X., & Ruden, D. M. (2012). A program for annotating and predicting the effects of single nucleotide polymorphisms, SnpEff: SNPs in the genome of Drosophila melanogaster strain w1118; iso-2; iso-3. *Fly*, *6*(2), 80. https://doi.org/10.4161/FLY.19695

Cobb, J. N., Chen, C., Shi, Y., Maron, L. G., Liu, D., Rutzke, M., Greenberg, A., Craft, E., Shaff, J., Paul, E., Akther, K., Wang, S., Kochian, L. V., Zhang, D., Zhang, M., & McCouch, S. R. (2021). Genetic architecture of root and shoot ionomes in rice (Oryza sativa L.). *TAG. Theoretical and Applied Genetics. Theoretische Und Angewandte Genetik*, *134*(8), 2613. https://doi.org/10.1007/S00122-021-03848-5

Conway, G. (1997). The doubly Green Revolution: food for all in the twenty-first century. *The Doubly Green Revolution: Food for All in the Twenty-First Century.*

Cordell, D., Drangert, J. O., & White, S. (2009). The story of phosphorus: Global food security and food for thought. *Global Environmental Change*, *19*(2), 292–305. https://doi.org/10.1016/j.gloenvcha.2008.10.009

Cordier, C., Pozo, M. J., Barea, J. M., Gianinazzi, S., & Gianinazzi-Pearson, V. (1998). Cell Defense Responses Associated with Localized and Systemic Resistance to *Phytophthora parasitica* Induced in Tomato by an Arbuscular Mycorrhizal Fungus. *Molecular Plant-Microbe Interactions*, *11*(10), 1017–1028. https://doi.org/10.1094/MPMI.1998.11.10.1017

Cosme, M., Fernández, I., Van der Heijden, M. G. A., & Pieterse, C. M. J. (2018). Non-Mycorrhizal Plants: The Exceptions that Prove the Rule. *Trends in Plant Science*, *23*(7), 577–587. https://doi.org/10.1016/j.tplants.2018.04.004

Cruz, C., Egsgaard, H., Trujillo, C., Ambus, P., Requena, N., Martins-Loução, M. A., & Jakobsen, I. (2007). Enzymatic evidence for the key role of arginine in nitrogen translocation by arbuscular mycorrhizal fungi. *Plant Physiology*, *144*(2), 782–792. https://doi.org/10.1104/pp.106.090522

Cullis, B. R., Smith, A. B., & Coombes, N. E. (2006). On the design of early generation variety trials with correlated data. *Journal of Agricultural, Biological, and Environmental Statistics*, *11*(4), 381–393. https://doi.org/10.1198/108571106X154443/METRICS

Danneberg, G., Latus, C., Zimmer, W., Hundeshagen, B., Schneider-Poetsch, H., & Bothe, H. (1993). Influence of vesicular-arbuscular mycorrhiza on phytohormone balances in maize (Zea mays L.). *Journal of Plant Physiology*, *141*(1), 33–39. https://doi.org/10.1016/S0176-1617(11)80848-5

Das, D., Paries, M., Hobecker, K., Gigl, M., Dawid, C., Lam, H. M., Zhang, J., Chen, M., & Gutjahr, C. (2022). PHOSPHATE STARVATION RESPONSE transcription factors enable arbuscular mycorrhiza symbiosis. *Nature Communications*, *13*(1). https://doi.org/10.1038/s41467-022-27976-8

Davidson, H., Shrestha, R., Cornulier, T., Douglas, A., Travis, T., Johnson, D., & Price, A. H. (2019). Spatial effects and GWA mapping of root colonization assessed in the interaction between the rice diversity panel 1 and an arbuscular mycorrhizal fungus. *Frontiers in Plant Science*, *10*. https://doi.org/10.3389/fpls.2019.00633

de Leeuw, C. A., Mooij, J. M., Heskes, T., & Posthuma, D. (2015). MAGMA: Generalized Gene-Set Analysis of GWAS Data. *PLOS Computational Biology*, *11*(4), e1004219. https://doi.org/10.1371/JOURNAL.PCBI.1004219

De Vita, P., Avio, L., Sbrana, C., Laidò, G., Marone, D., Mastrangelo, A. M., Cattivelli, L., & Giovannetti, M. (2018). Genetic markers associated to arbuscular mycorrhizal colonization in durum wheat. *Scientific Reports*, *8*(1), 1–12. https://doi.org/10.1038/s41598-018-29020-6

Decker, E. L., Alder, A., Hunn, S., Ferguson, J., Lehtonen, M. T., Scheler, B., Kerres, K. L., Wiedemann, G., Safavi-Rizi, V., Nordzieke, S., Balakrishna, A., Baz, L., Avalos, J., Valkonen, J. P. T., Reski, R., & Al-Babili, S. (2017). Strigolactone biosynthesis is evolutionarily conserved, regulated by phosphate starvation and contributes to resistance against phytopathogenic fungi in a moss, Physcomitrella patens. *New Phytologist*, *216*(2), 455–468. https://doi.org/10.1111/nph.14506

Delaux, P. M., Varala, K., Edger, P. P., Coruzzi, G. M., Pires, J. C., & Ané, J. M. (2014). Comparative Phylogenomics Uncovers the Impact of Symbiotic Associations on Host Genome Evolution. *PLoS Genetics*, *10*(7), e1004487. https://doi.org/10.1371/journal.pgen.1004487

Delaux, P. M., Xie, X., Timme, R. E., Puech-Pages, V., Dunand, C., Lecompte, E., Delwiche, C. F., Yoneyama, K., Bécard, G., & Séjalon-Delmas, N. (2012). Origin of strigolactones in the green lineage. *New Phytologist*, *195*(4), 857–871. https://doi.org/10.1111/j.1469-8137.2012.04209.x

Dhillion, S. S. (1992). Host-endophyte specificity of vesicular-arbuscular mycorrhizal colonization of Oryza sativa l. at the pre-transplant stage in low or high phosphorus soil. *Soil Biology and Biochemistry*, *24*(5), 405–411. https://doi.org/10.1016/0038-0717(92)90202-9

Diedhiou, A. G., Mbaye, F. K., Mbodj, D., Faye, M. N., Pignoly, S., Ndoye, I., Djaman, K., Gaye, S., Kane, A., Laplaze, L., Manneh, B., & Champion, A. (2016). Field trials reveal ecotype-specific responses to mycorrhizal inoculation in rice. *PLoS ONE*, *11*(12), e0167014. https://doi.org/10.1371/journal.pone.0167014

Dodd, I. C. (2013). Abscisic acid and stomatal closure: A hydraulic conductance conundrum? In *New Phytologist* (Vol. 197, Issue 1, pp. 6–8). https://doi.org/10.1111/nph.12052

Dreher, D., Yadav, H., Zander, S., & Hause, B. (2017). Is there genetic variation in mycorrhization of Medicago truncatula? *PeerJ*, *2017*(9), e3713. https://doi.org/10.7717/peerj.3713

Duc, D., Thanhtri, V. D., Visperas, R. ., & Vergara, B. S. (1987). *Low temperature tolerance of traditional Vietnamese varieties*. AGRIS FAO. https://agris.fao.org/agris-search/search.do?recordID=PH8811108

Eizenga, G. C., Ali, M. L., Bryant, R. J., Yeater, K. M., McClung, A. M., & McCouch, S. R. (2014). Registration of the Rice Diversity Panel 1 for Genomewide Association Studies. *Journal of Plant Registrations*, *8*(1), 109–116. https://doi.org/10.3198/JPR2013.03.0013CRMP

Endelman, J. B., Jannink, J.-L., & Holley, R. W. (2012). *Shrinkage Estimation of the Realized Relationship Matrix*. https://doi.org/10.1534/g3.112.004259

Evangelisti, E., Turner, C., McDowell, A., Shenhav, L., Yunusov, T., Gavrin, A., Servante, E. K., Quan, C., & Schornack, S. (2021). Artificial intelligence enables the identification and quantification of arbuscular mycorrhizal fungi in plant roots. *BioRxiv*, 2021.03.05.434067. https://doi.org/10.1101/2021.03.05.434067

Ezawa, T., Cavagnaro, T. R., Smith, S. E., Smith, F. A., & Ohtomo, R. (2004). Rapid accumulation of polyphosphate in extraradical hyphae of an arbuscular mycorrhizal fungus as revealed by histochemistry and a polyphosphate kinase/luciferase system. *New Phytologist*, *161*(2), 387–392. https://doi.org/10.1046/j.1469-8137.2003.00966.x

Fabiańska, I., Gerlach, N., Almario, J., & Bucher, M. (2019). Plant-mediated effects of soil phosphorus on the root-associated fungal microbiota in Arabidopsis thaliana. *New Phytologist*, *221*(4), 2123–2137. https://doi.org/10.1111/nph.15538

Fageria, N. K., Wright, R. J., & Baligar, V. C. (1988). Rice cultivar evaluation for phosphorus use efficiency. *Plant and Soil*, *111*(1), 105–109. https://doi.org/10.1007/BF02182043/METRICS

Fageria, Nand Kumar. (2016). The Use of Nutrients in Crop Plants. *The Use of Nutrients in Crop Plants*. https://doi.org/10.1201/9781420075113

Feng, F., Sun, J., Radhakrishnan, G. V., Lee, T., Bozsóki, Z., Fort, S., Gavrin, A., Gysel, K., Thygesen, M. B., Andersen, K. R., Radutoiu, S., Stougaard, J., & Oldroyd, G. E. D. (2019). A combination of chitooligosaccharide and lipochitooligosaccharide recognition promotes arbuscular mycorrhizal associations in Medicago truncatula. *Nature Communications*, *10*(1), 1–12. https://doi.org/10.1038/s41467-019-12999-5

Fester, T., Fetzer, I., Buchert, S., Lucas, R., Rillig, M. C., & Härtig, C. (2011). Towards a systemic metabolic signature of the arbuscular mycorrhizal interaction. *Oecologia*, *167*(4), 913–924. https://doi.org/10.1007/s00442-011-2037-6

Fester, T., Hause, B., Schmidt, D., Halfmann, K., Schmidt, J., Wray, V., Hause, G., & Strack, D. (2002). Occurrence and Localization of Apocarotenoids in Arbuscular Mycorrhizal Plant Roots. *Plant and Cell Physiology*, *43*(3), 256–265. https://doi.org/10.1093/pcp/pcf029

Fester, T., Maier, W., & Strack, D. (1999). Accumulation of secondary compounds in barley and wheat roots in response to inoculation with an arbuscular mycorrhizal fungus and co-inoculation with rhizosphere bacteria. *Mycorrhiza*, *8*(5), 241–246. https://doi.org/10.1007/s005720050240

Field, K. J., Rimington, W. R., Bidartondo, M. I., Allinson, K. E., Beerling, D. J., Cameron, D. D., Duckett, J. G., Leake, J. R., & Pressel, S. (2015). First evidence of mutualism between ancient plant lineages (Haplomitriopsida liverworts) and Mucoromycotina fungi and its response to simulated Palaeozoic changes in atmospheric CO2. *New Phytologist*, *205*(2), 743–756. https://doi.org/10.1111/nph.13024

Fiorilli, V., Wang, J. Y., Bonfante, P., Lanfranco, L., & Al-Babili, S. (2019). Apocarotenoids: Old and New Mediators of the Arbuscular Mycorrhizal Symbiosis. In *Frontiers in Plant Science* (Vol. 10, p. 1186). Frontiers Media S.A. https://doi.org/10.3389/fpls.2019.01186

Flematti, G. R., Ghisalberti, E. L., Dixon, K. W., & Trengove, R. D. (2004). A compound from smoke that promotes seed germination. *Science (New York, N.Y.)*, *305*(5686), 977. https://doi.org/10.1126/SCIENCE.1099944

Floková, K., Shimels, M., Andreo Jimenez, B., Bardaro, N., Strnad, M., Novák, O., & Bouwmeester, H. J. (2020). An improved strategy to analyse strigolactones in complex sample matrices using UHPLC-MS/MS. *Plant Methods*, *16*(1), 1–17. https://doi.org/10.1186/s13007-020-00669-3

Floss, D. S., Gomez, S. K., Park, H. J., MacLean, A. M., Müller, L. M., Bhattarai, K. K., Lévesque-Tremblay, V., Maldonado-Mendoza, I. E., & Harrison, M. J. (2017). A Transcriptional Program for Arbuscule Degeneration during AM Symbiosis Is Regulated by MYB1. *Current Biology*, *27*(8), 1206–1212. https://doi.org/10.1016/j.cub.2017.03.003

Floß, D. S., Hause, B., Lange, P. R., Küster, H., Strack, D., & Walter, M. H. (2008). Knock-down of the MEP pathway isogene 1-deoxy-d-xylulose 5-phosphate synthase 2 inhibits formation of arbuscular mycorrhiza-induced apocarotenoids, and abolishes normal expression of mycorrhiza-specific plant marker genes. *Plant Journal*, *56*(1), 86–100. https://doi.org/10.1111/j.1365-313X.2008.03575.x

Floss, D. S., Schliemann, W., Schmidt, J., Strack, D., & Walter, M. H. (2008). RNA Interference-Mediated Repression of *MtCCD1* in Mycorrhizal Roots of *Medicago*

truncatula Causes Accumulation of C $_{27}$ Apocarotenoids, Shedding Light on the Functional Role of CCD1. *Plant Physiology*, *148*(3), 1267–1282. https://doi.org/10.1104/pp.108.125062

Fyson, A., & Oaks, A. (1992). Rapid methods for quantifying VAM fungal infections in maize roots. *Plant and Soil*, *147*(2), 317–319. https://doi.org/10.1007/BF00029083/METRICS

Galván, G. A., Kuyper, T. W., Burger, K., Keizer, L. C. P., Hoekstra, R. F., Kik, C., & Scholten, O. E. (2011). Genetic analysis of the interaction between Allium species and arbuscular mycorrhizal fungi. *Theoretical and Applied Genetics*, *122*(5), 947–960. https://doi.org/10.1007/s00122-010-1501-8

Ganugi, P., Masoni, A., Sbrana, C., Dell'Acqua, M., Pietramellara, G., Benedettelli, S., & Avio, L. (2021). Genetic variability assessment of 127 Triticum turgidum L. accessions for mycorrhizal susceptibility-related traits detection. *Scientific Reports*, *11*(1), 13426. https://doi.org/10.1038/S41598-021-92837-1

Gao, X., Kuyper, T. W., Zou, C., Zhang, F., & Hoffland, E. (2007). Mycorrhizal responsiveness of aerobic rice genotypes is negatively correlated with their zinc uptake when nonmycorrhizal. *Plant and Soil*, *290*(1–2), 283–291. https://doi.org/10.1007/s11104-006-9160-x

Garris, A. J., Tai, T. H., Coburn, J., Kresovich, S., & McCouch, S. (2005). Genetic Structure and Diversity in Oryza sativa L. *Genetics*, *169*(3), 1631–1638. https://doi.org/10.1534/GENETICS.104.035642

Gaur, A., Gaur, A., & Adholeya, A. (2000). Growth and flowering in Petunia hybrida, Callistephus chinensis and Impatiens balsamina inoculated with mixed AM inocula or chemical fertilizers in a soil of low P fertility. *Scientia Horticulturae*, *84*(1–2), 151–162. https://doi.org/10.1016/S0304-4238(99)00105-3

Gavito, M. E., Olsson, P. A., Rouhier, H., Medina-Peñafiel, A., Jakobsen, I., Bago, A., & Azcón-Aguilar, C. (2005). Temperature constraints on the growth and functioning of root organ cultures with arbuscular mycorrhizal fungi. *The New Phytologist*, *168*(1), 179–188. https://doi.org/10.1111/J.1469-8137.2005.01481.X

Genre, A., Chabaud, M., Balzergue, C., Puech-Pagès, V., Novero, M., Rey, T., Fournier, J., Rochange, S., Bécard, G., Bonfante, P., & Barker, D. G. (2013). Short-chain chitin oligomers from arbuscular mycorrhizal fungi trigger nuclear Ca2+ spiking in Medicago truncatula roots and their production is enhanced by strigolactone. *New Phytologist*, *198*(1), 190–202. https://doi.org/10.1111/nph.12146

Genre, A., Chabaud, M., Faccio, A., Barker, D. G., & Bonfante, P. (2008). Prepenetration apparatus assembly precedes and predicts the colonization patterns of arbuscular mycorrhizal fungi within the root cortex of both Medicago truncatula and Daucus carota. *Plant Cell*, *20*(5), 1407–1420. https://doi.org/10.1105/tpc.108.059014

Genre, A., Chabaud, M., Timmers, T., Bonfante, P., & Barker, D. G. (2005). Arbuscular mycorrhizal fungi elicit a novel intracellular apparatus in Medicago truncatula root epidermal cells before infection. *Plant Cell*, *17*(12), 3489–3499. https://doi.org/10.1105/tpc.105.035410

Genre, A., & Russo, G. (2016). Does a Common Pathway Transduce Symbiotic Signals in Plant-Microbe Interactions? *Frontiers in Plant Science*, *7*, 96. https://doi.org/10.3389/fpls.2016.00096

Gewaily, S. (2019). Influence of Arbuscular Mycorrhizal (AMF) Inoculation on the Performance of Sakha 107 Rice Cultivar under Different Irrigation Intervals. *Environment, Biodiversity and Soil Security*, *3*(2019), 119–129. https://doi.org/10.21608/JENVBS.2019.15637.1068

Gianinazzi-Pearson, V., Arnould, C., Oufattole, M., Arango, M., & Gianinazzi, S. (2000). Differential activation of H+-ATPase genes by an arbuscular mycorrhizal fungus in root cells of transgenic tobacco. *Planta*, *211*(5), 609–613. https://doi.org/10.1007/s004250000323

Gibelin-Viala, C., Amblard, E., Puech-Pages, V., Bonhomme, M., Garcia, M., Bascaules-Bedin, A., Fliegmann, J., Wen, J., Mysore, K. S., le Signor, C., Jacquet, C., & Gough, C. (2019). The Medicago truncatula LysM receptor-like kinase LYK9 plays a dual role in immunity and the arbuscular mycorrhizal symbiosis. *New Phytologist*, *223*(3), 1516–1529. https://doi.org/10.1111/nph.15891

Giovannetti, M., & Mosse, B. (1980). An Evaluation Of Techniques For Measuring Vesicular Arbuscular Mycorrhizal Infection In Roots. *New Phytologist*, *84*(3), 489–500. https://doi.org/10.1111/j.1469-8137.1980.tb04556.x

Girardin, A., Wang, T., Ding, Y., Keller, J., Buendia, L., Gaston, M., Ribeyre, C., Gasciolli, V., Auriac, M. C., Vernié, T., Bendahmane, A., Ried, M. K., Parniske, M., Morel, P., Vandenbussche, M., Schorderet, M., Reinhardt, D., Delaux, P. M., Bono, J. J., & Lefebvre, B. (2019). LCO Receptors Involved in Arbuscular Mycorrhiza Are Functional for Rhizobia Perception in Legumes. *Current Biology*, *29*(24), 4249-4259.e5. https://doi.org/10.1016/j.cub.2019.11.038

Glaszmann, J. C. (1987). Isozymes and classification of Asian rice varieties. *Theoretical and Applied Genetics*, *74*(1), 21–30. https://link.springer.com/article/10.1007/BF00290078

Goff, S. A., Ricke, D., Lan, T. H., Presting, G., Wang, R., Dunn, M., Glazebrook, J., Sessions, A., Oeller, P., Varma, H., Hadley, D., Hutchison, D., Martin, C., Katagiri, F., Lange, B. M., Moughamer, T., Xia, Y., Budworth, P., Zhong, J., … Briggs, S. (2002). A draft sequence of the rice genome (Oryza sativa L. ssp. japonica). *Science (New York, N.Y.)*, *296*(5565), 92–100. https://doi.org/10.1126/SCIENCE.1068275

Goldmann, K., Boeddinghaus, R. S., Klemmer, S., Regan, K. M., Heintz-Buschart, A., Fischer, M., Prati, D., Piepho, H. P., Berner, D., Marhan, S., Kandeler, E.,

Buscot, F., & Wubet, T. (2020). Unraveling spatiotemporal variability of arbuscular mycorrhizal fungi in a temperate grassland plot. *Environmental Microbiology*, *22*(3), 873–888. https://doi.org/10.1111/1462-2920.14653

Gomez, S. K., Javot, H., Deewatthanawong, P., Torres-Jerez, I., Tang, Y., Blancaflor, E. B., Udvardi, M. K., & Harrison, M. J. (2009). Medicago truncatula and Glomus intraradices gene expression in cortical cells harboring arbuscules in the arbuscular mycorrhizal symbiosis. *BMC Plant Biology*, *9*, 10. https://doi.org/10.1186/1471-2229-9-10

Govindarajulu, M., Pfeffer, P. E., Jin, H., Abubaker, J., Douds, D. D., Allen, J. W., Bücking, H., Lammers, P. J., & Shachar-Hill, Y. (2005). Nitrogen transfer in the arbuscular mycorrhizal symbiosis. *Nature*, *435*(7043), 819–823. https://doi.org/10.1038/nature03610

Graham, J. H., & Abbott, L. K. (2000). Wheat responses to aggressive and non-aggressive arbuscular mycorrhizal fungi. *Plant and Soil*, *220*(1–2), 207–218. https://doi.org/10.1023/A:1004709209009

Groth, M., Takeda, N., Perry, J., Uchid, H., Dräxl, S., Brachmann, A., Sato, S., Tabata, S., Kawaguchi, M., Wang, T. L., & Parniskea, M. (2010). NENA, a Lotus japonicus homolog of Sec13, is required for rhizodermal infection by arbuscular mycorrhiza fungi and rhizobia but dispensable for cortical endosymbiotic development. *Plant Cell*, *22*(7), 2509–2526. https://doi.org/10.1105/tpc.109.069807

Gu, X., Gao, S., Li, J., Song, P., Zhang, Q., Guo, J., Wang, X., Han, X., Wang, X., Zhu, Y., & Zhu, Z. (2021). The bHLH transcription factor regulated gene OsWIH2 is a positive regulator of drought tolerance in rice. *Plant Physiology and Biochemistry*, *169*, 269–279. https://doi.org/10.1016/J.PLAPHY.2021.11.031

Guether, M., Neuhäuser, B., Balestrini, R., Dynowski, M., Ludewig, U., & Bonfante, P. (2009). A mycorrhizal-specific ammonium transporter from lotus japonicus acquires nitrogen released by Arbuscular Mycorrhizal Fungi. *Plant Physiology*, *150*(1), 73–83. https://doi.org/10.1104/pp.109.136390

Guimil, S., Chang, H.-S., Zhu, T., Sesma, A., Osbourn, A., Roux, C., Ioannidis, V., Oakeley, E. J., Docquier, M., Descombes, P., Briggs, S. P., & Paszkowski, U. (2005). Comparative transcriptomics of rice reveals an ancient pattern of response to microbial colonization. *Proceedings of the National Academy of Sciences*, *102*(22), 8066–8070. https://doi.org/10.1073/pnas.0502999102

Gutjahr, C., Banba, M., Croset, V., An, K., Miyao, A., An, G., Hirochika, H., Imaizumi-Anraku, H., & Paszkowski, U. (2008). Arbuscular Mycorrhiza-Specific Signaling in Rice Transcends the Common Symbiosis Signaling Pathway. *THE PLANT CELL ONLINE*, *20*(11), 2989–3005. https://doi.org/10.1105/tpc.108.062414

Gutjahr, C, Radovanovic, D., Geoffroy, J., Zhang, Q., Siegler, H., Chiapello, M., Casieri, L., An, K., An, G., Guiderdoni, E., Kumar, C. S., Sundaresan, V., Harrison, M. J., & Paszkowski, U. (2012). The half-size ABC transporters STR1

and STR2 are indispensable for mycorrhizal arbuscule formation in rice. *Plant Journal*, *69*(5), 906–920. https://doi.org/10.1111/j.1365-313X.2011.04842.x

Gutjahr, Caroline, Casieri, L., & Paszkowski, U. (2009). Glomus intraradices induces changes in root system architecture of rice independently of common symbiosis signaling. *New Phytologist*, *182*(4), 829–837. http://www.ncbi.nlm.nih.gov/pubmed/19383099

Gutjahr, Caroline, Gobbato, E., Choi, J., Riemann, M., Johnston, M. G., Summers, W., Carbonnel, S., Mansfield, C., Yang, S.-Y., Nadal, M., Acosta, I., Takano, M., Jiao, W.-B., Schneeberger, K., Kelly, K. A., & Paszkowski, U. (2015). Rice perception of symbiotic arbuscular mycorrhizal fungi requires the karrikin receptor complex. *Science*, *350*(6267), 1521–1524. https://doi.org/10.1126/SCIENCE.AAC9715

Gutjahr, Caroline, & Parniske, M. (2013). Cell and Developmental Biology of Arbuscular Mycorrhiza Symbiosis. *Https://Doi.Org/10.1146/Annurev-Cellbio-101512-122413*, *29*, 593–617. https://doi.org/10.1146/ANNUREV-CELLBIO-101512-122413

Haefele, S. M., Nelson, A., & Hijmans, R. J. (2014). Soil quality and constraints in global rice production. *Geoderma*, *235–236*, 250–259. https://doi.org/10.1016/J.GEODERMA.2014.07.019

Haefele, S. M., Siopongco, J. D. L. C., Boling, A. A., Bouman, B. A. M., & Tuong, T. P. (2009). Transpiration efficiency of rice (Oryza sativa L.). *Field Crops Research*, *111*(1–2), 1–10. https://doi.org/10.1016/J.FCR.2008.09.008

Hamiaux, C., Drummond, R. S. M., Janssen, B. J., Ledger, S. E., Cooney, J. M., Newcomb, R. D., & Snowden, K. C. (2012). DAD2 is an α/β hydrolase likely to be involved in the perception of the plant branching hormone, strigolactone. *Current Biology*, *22*(21), 2032–2036. https://doi.org/10.1016/j.cub.2012.08.007

Hao, L., Renxiao, W., Qian, Q., Meixian, Y., Xiangbing, M., Zhiming, F., Cunyu, Y., Biao, J., Zhen, S., Jiayang, L., & Yonghong, W. (2009). DWARF27,an iron-containing protein required for the biosynthesis of strigolactones,regulates rice tiller bud outgrowth. *Plant Cell*, *21*(5), 1512–1525. https://doi.org/10.1105/tpc.109.065987

Harrison, M. J., Dewbre, G. R., & Liu, J. (2002). A phosphate transporter from Medicago truncatula involved in the acquisition of phosphate released by arbuscular mycorrhizal fungi. *Plant Cell*, *14*(10), 2413–2429. https://doi.org/10.1105/tpc.004861

Harrison, M. J., & Van Buuren, M. L. (1995). A phosphate transporter from the mycorrhizal fungus Glomus versiforme. *Nature*, *378*(6557), 626–629. https://doi.org/10.1038/378626a0

Hart, M. M., Antunes, P. M., Chaudhary, V. B., & Abbott, L. K. (2018). Fungal inoculants in the field: Is the reward greater than the risk? *Functional Ecology*, *32*(1), 126–135. https://doi.org/10.1111/1365-2435.12976/SUPPINFO

Heck, C., Kuhn, H., Heidt, S., Walter, S., Rieger, N., & Requena, N. (2016). Symbiotic Fungi Control Plant Root Cortex Development through the Novel GRAS Transcription Factor MIG1. *Current Biology*, *26*(20), 2770–2778. https://doi.org/10.1016/j.cub.2016.07.059

Hedley, M. J., Kirk, G. J. R., & Santos, M. B. (1994). Phosphorus efficiency and the forms of soil phosphorus utilized by upland rice cultivars. *Plant and Soil*, *158*(1), 53–62. https://doi.org/10.1007/BF00007917/METRICS

Helber, N., Wippel, K., Sauer, N., Schaarschmidt, S., Hause, B., & Requena, N. (2011). A versatile monosaccharide transporter that operates in the arbuscular mycorrhizal fungus Glomus sp is crucial for the symbiotic relationship with plants. *Plant Cell*, *23*(10), 3812–3823. https://doi.org/10.1105/tpc.111.089813

Henry, S., Dievart, A., Divol, F., Pauluzzi, G., Meynard, D., Swarup, R., Wu, S., Gallagher, K. L., & Périn, C. (2017). SHR overexpression induces the formation of supernumerary cell layers with cortex cell identity in rice. *Developmental Biology*, *425*(1), 1–7. https://doi.org/10.1016/J.YDBIO.2017.03.001

Herrera-Medina, M. J., Steinkellner, S., Vierheilig, H., Ocampo Bote, J. A., & García Garrido, J. M. (2007). Abscisic acid determines arbuscule development and functionality in the tomato arbuscular mycorrhiza. *New Phytologist*, *175*(3), 554–564. https://doi.org/10.1111/j.1469-8137.2007.02107.x

Hetrick, B. A. D., Wilson, G. W. T., & Cox, T. S. (1992). Mycorrhizal dependence of modern wheat varieties, landraces, and ancestors. *Canadian Journal of Botany*, *70*(10), 2032–2040. https://doi.org/10.1139/b92-253

Hetrick, B. A. D., Wilson, G. W. T., & Todd, T. C. (1996). Mycorrhizal response in wheat cultivars: Relationship to phosphorus. *Canadian Journal of Botany*, *74*(1), 19–25. https://doi.org/10.1139/b96-003

Hetrick, B. A., Wilson, G. W., Gill, B. S., & Cox, T. S. (1995). Chromosome location of mycorrhizal responsive genes in wheat. *Canadian Journal of Botany*, *73*(6), 891–897. https://doi.org/10.1139/b95-097

Hill, E. M., Robinson, L. A., Abdul-Sada, A., Vanbergen, A. J., Hodge, A., & Hartley, S. E. (2018). Arbuscular Mycorrhizal Fungi and Plant Chemical Defence: Effects of Colonisation on Aboveground and Belowground Metabolomes. *Journal of Chemical Ecology*, *44*(2), 198–208. https://doi.org/10.1007/s10886-017-0921-1

Hiruma, K., Gerlach, N., Sacristán, S., Nakano, R. T., Hacquard, S., Kracher, B., Neumann, U., Ramírez, D., Bucher, M., O'Connell, R. J., & Schulze-Lefert, P. (2016). Root Endophyte Colletotrichum tofieldiae Confers Plant Fitness Benefits that Are Phosphate Status Dependent. *Cell*, *165*(2), 464–474. https://doi.org/10.1016/j.cell.2016.02.028

Hoa, D. T. M. (2015). Conservation of the deep water rice-upland vegetables system in Viet Nam. *Tropical Agriculture Association*, *25*(Agriculture for Development).

http://www.intl-pag.org/19/abstracts/W68_PAGXIX_433.html]
Hong, J. J., Park, Y. S., Bravo, A., Bhattarai, K. K., Daniels, D. A., & Harrison, M. J. (2012). Diversity of morphology and function in arbuscular mycorrhizal symbioses in Brachypodium distachyon. *Planta*, *236*(3), 851–865. https://doi.org/10.1007/s00425-012-1677-z

Hou, X. L., Wu, P., Jiao, F. C., Jia, Q. J., Chen, H. M., Yu, J., Song, X. W., & Yi, K. K. (2005). Regulation of the expression of OsIPS1 and OsIPS2 in rice via systemic and local Pi signalling and hormones. *Plant, Cell and Environment*, *28*(3), 353–364. https://doi.org/10.1111/j.1365-3040.2005.01272.x

Hou, X., Rivers, J., León, P., McQuinn, R. P., & Pogson, B. J. (2016). Synthesis and Function of Apocarotenoid Signals in Plants. In *Trends in Plant Science* (Vol. 21, Issue 9, pp. 792–803). Elsevier Ltd. https://doi.org/10.1016/j.tplants.2016.06.001

Howlin, P., & Yates, P. (1999). The potential effectiveness of social skills groups for adults with autism. In *Autism* (Vol. 3, Issue 3, pp. 299–307). Food and Agriculture Organization of the United Nations. https://doi.org/10.1177/1362361399003003007

Hsieh, L. C., Lin, S. I., Shih, A. C. C., Chen, J. W., Lin, W. Y., Tseng, C. Y., Li, W. H., & Chiou, T. J. (2009). Uncovering small RNA-mediated responses to phosphate deficiency in Arabidopsis by deep sequencing. *Plant Physiology*, *151*(4), 2120–2132. https://doi.org/10.1104/pp.109.147280

Huang, R., Li, Z., Mao, C., Zhang, H., Sun, Z., Li, H., Huang, C., Feng, Y., Shen, X., Bucher, M., Zhang, Z., Lin, Y., Cao, Y., & Duanmu, D. (2020). Natural variation at OsCERK1 regulates arbuscular mycorrhizal symbiosis in rice. *New Phytologist*, *225*(4), 1762–1776. https://doi.org/10.1111/nph.16158

Huang, X. Y., Liu, H., Zhu, Y. F., Pinson, S. R. M., Lin, H. X., Guerinot, M. Lou, Zhao, F. J., & Salt, D. E. (2019). Natural variation in a molybdate transporter controls grain molybdenum concentration in rice. *New Phytologist*, *221*(4), 1983–1997. https://doi.org/10.1111/nph.15546

Hühn, M. (1990). Comments on the Calculation of Mean Harvest Indices. *Journal of Agronomy and Crop Science*, *165*(2–3), 86–93. https://doi.org/10.1111/j.1439-037X.1990.tb00838.x

Hull, R., Choi, J., & Paszkowski, U. (2021). Conditioning plants for arbuscular mycorrhizal symbiosis through DWARF14-LIKE signalling. In *Current opinion in plant biology* (Vol. 62, p. 102071). Elsevier. https://doi.org/10.1016/j.pbi.2021.102071

Ilag, L. L., Rosales, A. M., Elazegui, F. A., & Mew, T. W. (1987). Changes in the population of infective endomycorrhizal fungi in a rice-based cropping system. *Plant and Soil*, *103*(1), 67–73. https://doi.org/10.1007/BF02370669

Ilg, A., Bruno, M., Beyer, P., & Al-Babili, S. (2014). Tomato carotenoid cleavage dioxygenases 1A and 1B: Relaxed double bond specificity leads to a plenitude

of dialdehydes, mono-apocarotenoids and isoprenoid volatiles. *FEBS Open Bio*, *4*, 584–593. https://doi.org/10.1016/j.fob.2014.06.005

Ishikawa, S., Maekawa, M., Arite, T., Onishi, K., Takamure, I., & Kyozuka, J. (2005). Suppression of Tiller Bud Activity in Tillering Dwarf Mutants of Rice. *Plant and Cell Physiology*, *46*(1), 79–86. https://doi.org/10.1093/pcp/pci022

Ito, S., Braguy, J., Wang, J. Y., Yoda, A., Fiorilli, V., Takahashi, I., Jamil, M., Felemban, A., Miyazaki, S., Mazzarella, T., Shinozawa, A., Balakrishna, A., Berqdar, L., Rajan, C., Ali, S., Haider, I., Sasaki, Y., Yajima, S., Akiyama, K., … Al-Babili, S. (2022). Canonical Strigolactones Are Not the Tillering-Inhibitory Hormone but Rhizospheric Signals in Rice. *BioRxiv*, *8*(44), 2022.04.05.487102. https://doi.org/10.1126/SCIADV.ADD1278

Jabaji-Hare, S. (1988). Lipid and Fatty Acid Profiles of Some Vesicular-Arbuscular Mycorrhizal Fungi: Contribution to Taxonomy. *Mycologia*, *80*(5), 622. https://doi.org/10.2307/3807710

Jabaji-Hare, S., Deschene, A., & Kendrick, B. (1984). Lipid Content and Composition of Vesicles of a Vesicular-Arbuscular Mycorrhizal Fungus. *Mycologia*, *76*(6), 1024. https://doi.org/10.2307/3793017

Jakobsen, I., & Rosendahl, L. (1990). Carbon flow into soil and external hyphae from roots of mycorrhizal cucumber plants. *New Phytologist*, *115*(1), 77–83. https://doi.org/10.1111/j.1469-8137.1990.tb00924.x

Jakobsen, Iver, & Hammer, E. C. (2015). *Nutrient Dynamics in Arbuscular Mycorrhizal Networks* (pp. 91–131). Springer, Dordrecht. https://doi.org/10.1007/978-94-017-7395-9_4

Janos, D. P. (2007). Plant responsiveness to mycorrhizas differs from dependence upon mycorrhizas. *Mycorrhiza*, *17*(2), 75–91. https://pubmed.ncbi.nlm.nih.gov/17216499/

Javot, H., Penmetsa, R. V., Breuillin, F., Bhattarai, K. K., Noar, R. D., Gomez, S. K., Zhang, Q., Cook, D. R., & Harrison, M. J. (2011). Medicago truncatula mtpt4 mutants reveal a role for nitrogen in the regulation of arbuscule degeneration in arbuscular mycorrhizal symbiosis. *Plant Journal*, *68*(6), 954–965. https://doi.org/10.1111/j.1365-313X.2011.04746.x

Javot, H., Penmetsa, R. V., Terzaghi, N., Cook, D. R., & Harrison, M. J. (2007). A Medicago truncatula phosphate transporter indispensable for the arbuscular mycorrhizal symbiosis. *Proceedings of the National Academy of Sciences of the United States of America*, *104*(5), 1720–1725. https://doi.org/10.1073/pnas.0608136104

Jeong, K., Chin, J. H., Heuer, S., Paszkowski, U., Mattes, N., & Catausan, S. (2015). Genetic diversity for mycorrhizal symbiosis and phosphate transporters in rice. *Journal of Integrative Plant Biology*, *57*(11), 969–979. https://doi.org/10.1111/jipb.12435

Jia, K. P., Baz, L., & Al-Babili, S. (2018). From carotenoids to strigolactones. In *Journal of Experimental Botany* (Vol. 69, Issue 9, pp. 2189–2204). https://doi.org/10.1093/jxb/erx476

Jiang, Y., Wang, W., Xie, Q., Liu, N., Liu, L., Wang, D., Zhang, X., Yang, C., Chen, X., Tang, D., & Wang, E. (2017). Plants transfer lipids to sustain colonization by mutualistic mycorrhizal and parasitic fungi. *Science*, *356*(6343), 1172–1173. https://doi.org/10.1126/science.aam9970

Johnson, N. C., Graham, J. H., & Smith, F. A. (1997). Functioning of mycorrhizal associations along the mutualism–parasitism continuum. *The New Phytologist*, *135*(4), 575–585. https://doi.org/10.1046/J.1469-8137.1997.00729.X

Jones, F. R. (1924). *A mycorrhizal fungus in the roots of legumes and some other plants*.

Kaeppler, S. M., Parke, J. L., Mueller, S. M., Senior, L., Stuber, C., & Tracy, W. F. (2000). Variation among Maize Inbred Lines and Detection of Quantitative Trait Loci for Growth at Low Phosphorus and Responsiveness to Arbuscular Mycorrhizal Fungi. *Crop Science*, *40*(2), 358. https://doi.org/10.2135/cropsci2000.402358x

Kameoka, H., Tsutsui, I., Saito, K., Kikuchi, Y., Handa, Y., Ezawa, T., Hayashi, H., Kawaguchi, M., & Akiyama, K. (2019). Stimulation of asymbiotic sporulation in arbuscular mycorrhizal fungi by fatty acids. In *Nature Microbiology* (Vol. 4, Issue 10, pp. 1654–1660). Nat Microbiol. https://doi.org/10.1038/s41564-019-0485-7

Karandashov, V., Nagy, R., Wegmüller, S., Amrhein, N., & Bucher, M. (2004). Evolutionary conservation of a phosphate transporter in the arbuscular mycorrhizal symbiosis. *Proceedings of the National Academy of Sciences of the United States of America*, *101*(16), 6285–6290. https://doi.org/10.1073/pnas.0306074101

Karlo, M., Boschiero, C., Landerslev, K. G., Blanco, G. S., Wen, J., Mysore, K. S., Dai, X., Zhao, P. X., De Bang, T. C., & Christian De Bang, T. (2020). The CLE53-SUNN genetic pathway negatively regulates arbuscular mycorrhiza root colonization in Medicago truncatula. *Journal of Experimental Botany*. https://doi.org/10.1093/jxb/eraa193/5822653

Kato, S., Kosaka, H., & Hara, S. (1928). On the affinity of rice varieties as shown by the fertility of rice plants. *Central Agricultural Institute of Kyushu Imperial University*, *2*(1), 241–276. https://doi.org/doi/10.15055/00003385

Keymer, A., Pimprikar, P., Wewer, V., Huber, C., Brands, M., Bucerius, S. L., Delaux, P. M., Klingl, V., von Röpenack-Lahaye, E., Wang, T. L., Eisenreich, W., Dörmann, P., Parniske, M., & Gutjahr, C. (2017). Lipid transfer from plants to arbuscular mycorrhiza fungi. *ELife*, *6*. https://doi.org/10.7554/eLife.29107

Kiers, E. T., Duhamel, M., Beesetty, Y., Mensah, J. A., Franken, O., Verbruggen, E.,

Fellbaum, C. R., Kowalchuk, G. A., Hart, M. M., Bago, A., Palmer, T. M., West, S. A., Vandenkoornhuyse, P., Jansa, J., & Bücking, H. (2011). Reciprocal rewards stabilize cooperation in the mycorrhizal symbiosis. *Science*, *333*(6044), 880–882. https://doi.org/10.1126/science.1208473

Kim, H. Il, Kisugi, T., Khetkam, P., Xie, X., Yoneyema, K., Uchida, K., Yokota, T., Nomura, T., McErlean, C. S. P., & Yoneyama, K. (2014). Avenaol, a germination stimulant for root parasitic plants from Avena strigosa. *Phytochemistry*, *103*, 85–88. https://doi.org/10.1016/j.phytochem.2014.03.030

Kim, S., Zeng, W., Bernard, S., Liao, J., Venkateshwaran, M., Ane, J. M., & Jiang, Y. (2019). Ca2+-regulated Ca2+ channels with an RCK gating ring control plant symbiotic associations. *Nature Communications*, *10*(1). https://doi.org/10.1038/s41467-019-11698-5

Klingner, A., Bothe, H., Wray, V., & Marner, F. J. (1995). Identification of a yellow pigment formed in maize roots upon mycorrhizal colonization. *Phytochemistry*, *38*(1), 53–55. https://doi.org/10.1016/0031-9422(94)00538-5

Kobae, Y., Gutjahr, C., Paszkowski, U., Kojima, T., Fujiwara, T., & Hata, S. (2014). Lipid droplets of arbuscular mycorrhizal fungi emerge in concert with arbuscule collapse. *Plant and Cell Physiology*, *55*(11), 1945–1953. https://doi.org/10.1093/pcp/pcu123

Kobae, Y., & Hata, S. (2010). Dynamics of Periarbuscular Membranes Visualized with a Fluorescent Phosphate Transporter in Arbuscular Mycorrhizal Roots of Rice. *Plant and Cell Physiology*, *51*(3), 341–353. https://doi.org/10.1093/pcp/pcq013

Kobae, Y., Kameoka, H., Sugimura, Y., Saito, K., Ohtomo, R., Fujiwara, T., & Kyozuka, J. (2018). Strigolactone Biosynthesis Genes of Rice are Required for the Punctual Entry of Arbuscular Mycorrhizal Fungi into the Roots. *Plant and Cell Physiology*, *59*(3), 544–553. https://doi.org/10.1093/pcp/pcy001

Kobae, Y., Ohmori, Y., Saito, C., Yano, K., Ohtomo, R., & Fujiwara, T. (2016). Phosphate Treatment Strongly Inhibits New Arbuscule Development But Not the Maintenance of Arbuscule in Mycorrhizal Rice Roots. *Plant Physiology*, *171*(1), 566–579. https://doi.org/10.1104/pp.16.00127

Kobae, Y., Tamura, Y., Takai, S., Banba, M., & Hata, S. (2010). Localized expression of arbuscular mycorrhiza-inducible ammonium transporters in soybean. *Plant and Cell Physiology*, *51*(9), 1411–1415. https://doi.org/10.1093/pcp/pcq099

Koch, A. M., Antunes, P. M., Maherali, H., Hart, M. M., & Klironomos, J. N. (2017). Evolutionary asymmetry in the arbuscular mycorrhizal symbiosis: conservatism in fungal morphology does not predict host plant growth. *New Phytologist*, *214*(3), 1330–1337. https://doi.org/10.1111/NPH.14465

Kodama, K., Rich, M. K., Yoda, A., Shimazaki, S., Xie, X., Akiyama, K., Mizuno, Y.,

Komatsu, A., Luo, Y., Suzuki, H., Kameoka, H., Libourel, C., Keller, J., Sakakibara, K., Nishiyama, T., Nakagawa, T., Mashiguchi, K., Uchida, K., Yoneyama, K., … Kyozuka, J. (2022). An ancestral function of strigolactones as symbiotic rhizosphere signals. *Nature Communications*, *13*(1). https://doi.org/10.1038/s41467-022-31708-3

Koegel, S., Ait Lahmidi, N., Arnould, C., Chatagnier, O., Walder, F., Ineichen, K., Boller, T., Wipf, D., Wiemken, A., & Courty, P. E. (2013). The family of ammonium transporters (AMT) in Sorghum bicolor: Two AMT members are induced locally, but not systemically in roots colonized by arbuscular mycorrhizal fungi. *New Phytologist*, *198*(3), 853–865. https://doi.org/10.1111/nph.12199

Koizumi, T., Hubertus, S., & Furuhashi, G. (2021). Reviewing Indica and Japonica rice market developments. *OECD Publishing*, *April*. https://www.oecd.org/publications/reviewing-indica-and-japonica-rice-market-developments-0c500e05-en.htm

Kokkoris, V., Pogiatzis, A., & Hart, M. M. (2019). Contrasting common measures of arbuscular mycorrhizal fungal root colonization. *Journal of Microbiological Methods*, *167*, 105727. https://doi.org/10.1016/J.MIMET.2019.105727

Krajinski, F., Hause, B., Gianinazzi-Pearson, V., & Franken, P. (2002). Mtha1, a plasma membrane H+-ATPase gene from Medicago truncatula, shows arbuscule-specific induced expression in mycorrhizal tissue. *Plant Biology*, *4*(6), 754–761. https://doi.org/10.1055/s-2002-37407

Krajinski, Franziska, Courty, P. E., Sieh, D., Franken, P., Zhang, H., Bucher, M., Gerlach, N., Kryvoruchko, I., Zoeller, D., Udvardi, M., & Hause, B. (2014). The H+-ATPase HA1 of Medicago truncatula is essential for phosphate transport and plant growth during arbuscular mycorrhizal symbiosis. *Plant Cell*, *26*(4), 1808–1817. https://doi.org/10.1105/tpc.113.120436

Kretzschmar, T., Kohlen, W., Sasse, J., Borghi, L., Schlegel, M., Bachelier, J. B., Reinhardt, D., Bours, R., Bouwmeester, H. J., & Martinoia, E. (2012). A petunia ABC protein controls strigolactone-dependent symbiotic signalling and branching. *Nature*, *483*(7389), 341–344. https://doi.org/10.1038/nature10873

Kumar, A., Kumar, S., Prasad, M., & Thakur, J. K. (2019). Designing of a mini-core that effectively represents 3004 diverse accessions of rice. *BioRxiv*, 762070. https://doi.org/10.1101/762070

Kumar, A., Kumar, S., Singh, K. B. M., Prasad, M., & Thakur, J. K. (2020). Designing a Mini-Core Collection Effectively Representing 3004 Diverse Rice Accessions. *Plant Communications*, *1*(5), 100049. https://doi.org/10.1016/J.XPLC.2020.100049

Kumar, V., & Ladha, J. K. (2011). Direct Seeding of Rice. Recent Developments and Future Research Needs. In *Advances in Agronomy* (Vol. 111). Academic Press. https://doi.org/10.1016/B978-0-12-387689-8.00001-1

Lander, E. S., & Schork, N. J. (1994). Genetic dissection of complex traits. *Science*, *265*(5181), 2037–2048. https://doi.org/10.1126/science.8091226

Lang, N. T., Buu, B. C., & Tho, C. (2011). Rice Genetic Resource Conservation and Utilization in the Mekong Delta. *Omonrice*, *33*, 22–33.

Lang, N., Tu, B., Thanh, N. C., Buu, B. C., & Ismail, A. (2009). Genetic diversity of salt tolerance rice landraces in Vietnam. *Journal of Plant Breeding and Crop Science*, *1*(5), 230–243. http://www.academicjournals.org/jpbcs

Larose, G., Chênevert, R., Moutoglis, P., Gagné, S., Piché, Y., & Vierheilig, H. (2002). Flavonoid levels in roots of Medicago sativa are modulated by the developmental stage of the symbiosis and the root colonizing arbuscular mycorrhizal fungus. *Journal of Plant Physiology*, *159*(12), 1329–1339. https://doi.org/10.1078/0176-1617-00896

Leff, J. W., Jones, S. E., Prober, S. M., Barberán, A., Borer, E. T., Firn, J. L., Harpole, W. S., Hobbie, S. E., Hofmockel, K. S., Knops, J. M. H., McCulley, R. L., La Pierre, K., Risch, A. C., Seabloom, E. W., Schütz, M., Steenbock, C., Stevens, C. J., & Fierer, N. (2015). Consistent responses of soil microbial communities to elevated nutrient inputs in grasslands across the globe. *Proceedings of the National Academy of Sciences of the United States of America*, *112*(35), 10967–10972. https://doi.org/10.1073/pnas.1508382112

Lehmann, A., Barto, E. K., Powell, J. R., & Rillig, M. C. (2012). Mycorrhizal responsiveness trends in annual crop plants and their wild relatives-a meta-analysis on studies from 1981 to 2010. *Plant and Soil*, *355*(1–2), 231–250. https://doi.org/10.1007/s11104-011-1095-1

Lehnert, H., Serfling, A., Enders, M., Friedt, W., & Ordon, F. (2017). Genetics of mycorrhizal symbiosis in winter wheat (Triticum aestivum). *New Phytologist*, *215*(2), 779–791. https://doi.org/10.1111/nph.14595

Lehnert, H., Serfling, A., Friedt, W., & Ordon, F. (2018). Genome-wide association studies reveal genomic regions associated with the response of wheat (triticum aestivum l.) to mycorrhizae under drought stress conditions. *Frontiers in Plant Science*, *871*, 1728. https://doi.org/10.3389/fpls.2018.01728

Leifheit, E. F., Veresoglou, S. D., Lehmann, A., Morris, E. K., & Rillig, M. C. (2014). Multiple factors influence the role of arbuscular mycorrhizal fungi in soil aggregation-a meta-analysis. *Plant and Soil*, *374*(1–2), 523–537. https://doi.org/10.1007/S11104-013-1899-2/TABLES/1

Leigh, J., Hodge, A., & Fitter, A. H. (2009). Arbuscular mycorrhizal fungi can transfer substantial amounts of nitrogen to their host plant from organic material. *New Phytologist*, *181*(1), 199–207. https://doi.org/10.1111/j.1469-8137.2008.02630.x

Leiser, W. L., Olatoye, M. O., Rattunde, H. F. W., Neumann, G., Weltzien, E., & Haussmann, B. I. G. (2016). No need to breed for enhanced colonization by arbuscular mycorrhizal fungi to improve low-P adaptation of West African

sorghums. *Plant and Soil*, *401*(1–2), 51–64. http://link.springer.com/10.1007/s11104-015-2437-1

Leppyanen, I. V., Shakhnazarova, V. Y., Shtark, O. Y., Vishnevskaya, N. A., Tikhonovich, I. A., & Dolgikh, E. A. (2018). Receptor-like kinase LYK9 in Pisum sativum L. Is the CERK1-like receptor that controls both plant immunity and AM symbiosis development. *International Journal of Molecular Sciences*, *19*(1), 8. https://doi.org/10.3390/ijms19010008

Levy, J., Bres, C., Geurts, R., Chalhoub, B., Kulikova, O., Duc, G., Journet, E.-P., Ané, J.-M., Lauber, E., Bisseling, T., Dénarié, J., Rosenberg, C., & Debellé, F. (2004). A Putative Ca2+ and Calmodulin-Dependent Protein Kinase Required for Bacterial and Fungal Symbioses. *Science*, *303*(5662), 1361–1364. https://doi.org/10.1126/science.1093038

Li, H., Chen, X. W., & Wong, M. H. (2016). Arbuscular mycorrhizal fungi reduced the ratios of inorganic/organic arsenic in rice grains. *Chemosphere*, *145*, 224–230. https://doi.org/10.1016/j.chemosphere.2015.10.067

Li, H. Y., Zhu, Y. G., Marschner, P., Smith, F. A., & Smith, S. E. (2005). Wheat responses to arbuscular mycorrhizal fungi in a highly calcareous soil differ from those of clover, and change with plant development and P supply. *Plant and Soil*, *277*(1–2), 221–232. https://doi.org/10.1007/s11104-005-7082-7

Li, J. Y., Wang, J., & Zeigler, R. S. (2014). The 3,000 rice genomes project: New opportunities and challenges for future rice research. In *GigaScience* (Vol. 3, Issue 1, p. 8). BioMed Central. https://doi.org/10.1186/2047-217X-3-8

Li, M., Perez-Limón, S., Ramírez-Flores, M. R., Barrales-Gamez, B., Meraz-Mercado, M. A., Ziegler, G., Baxter, I., Olalde-Portugal, V., & Sawers, R. J. H. (2022). Mycorrhizal status impacts the genetic architecture of mineral accumulation in field grown maize (Zea mays ssp. mays L.). *BioRxiv*, 2022.12.12.520122. https://doi.org/10.1101/2022.12.12.520122

Li, X.-R., Sun, J., Albinsky, D., Zarrabian, D., Hull, R., Lee, T., Jarratt-Barnham, E., Jacobsen, A., Soumpourou, E., Kohlen, W., Luginbeuhl, L., Guillotin, B., Lawrensen, T., Lin, H., Murray, J., Wallington, E., Harwood, W., Choi, J., Paszkowski, U., & Oldroyd, G. E. D. (2022). *Nutrient regulation of lipochitooligosaccharide recognition in plants via Nodulation signaling pathway (NSP)1 and NSP2*. https://doi.org/10.1038/s41467-022-33908-3

Li, Z., Fu, B. Y., Gao, Y. M., Wang, W. S., Xu, J. L. J., Zhang, F., Zhao, X. Q., Zheng, T. Q., Zhou, Y. L., Zhang, G., Tai, S., Xu, J. L. J., Hu, W., Yang, M., Niu, Y., Wang, M., Li, Y., Bian, L., Han, X., … Leung, H. (2014). The 3,000 rice genomes project. *GigaScience*, *3*(1), 17. https://doi.org/10.1186/2047-217X-3-7

Liang, Z., Zhang, Q., Ji, C., Hu, G., Zhang, P., Wang, Y., Yang, L., & Gu, X. (2021). Reorganization of the 3D chromatin architecture of rice genomes during heat stress. *BMC Biology*, *19*(1). https://doi.org/10.1186/S12915-021-00996-4

Liao, D., Sun, X., Wang, N., Song, F., & Liang, Y. (2018). Tomato LysM Receptor-Like Kinase SlLYK12 Is Involved in Arbuscular Mycorrhizal Symbiosis. *Frontiers in Plant Science*, *9*, 1004. https://doi.org/10.3389/fpls.2018.01004

Lin, H., Wang, R., Qian, Q., Yan, M., Meng, X., Fu, Z., Yan, C., Jiang, B., Su, Z., Li, J., & Wang, Y. (2009). DWARF27, an Iron-Containing Protein Required for the Biosynthesis of Strigolactones, Regulates Rice Tiller Bud Outgrowth. *The Plant Cell*, *21*(5), 1512–1525. https://doi.org/10.1105/tpc.109.065987

Lin, Y. L., Wu, D. H., Wu, C. C., & Huang, Y. F. (2021). Explore the genetics of weedy traits using rice 3K database. *Botanical Studies*, *62*(1), 1–16. https://doi.org/10.1186/s40529-020-00309-y

Lipka, A. E., Tian, F., Wang, Q., Peiffer, J., Li, M., Bradbury, P. J., Gore, M. A., Buckler, E. S., & Zhang, Z. (2012). GAPIT: genome association and prediction integrated tool. *Bioinformatics*, *28*(18), 2397–2399. https://doi.org/10.1093/BIOINFORMATICS/BTS444

Liu, G., Stirnemann, M., Gübeli, C., Egloff, S., Courty, P. E., Aubry, S., Vandenbussche, M., Morel, P., Reinhardt, D., Martinoia, E., & Borghi, L. (2019). Strigolactones Play an Important Role in Shaping Exodermal Morphology via a KAI2-Dependent Pathway. *IScience*, *17*, 144–154. https://doi.org/10.1016/j.isci.2019.06.024

Liu, W., Kohlen, W., Lillo, A., den Camp, R. O., Ivanov, S., Hartog, M., Limpens, E., Jamil, M., Smaczniak, C., Kaufmann, K., Yang, W. C., Hooiveld, G. J. E. J., Charnikhova, T., Bouwmeester, H. J., Bisseling, T., & Geurts, R. (2011). Strigolactone biosynthesis in Medicago truncatula and rice requires the symbiotic GRAS-type transcription factors NSP1 and NSP2. *Plant Cell*, *23*(10), 3853–3865. https://doi.org/10.1105/tpc.111.089771

Liu, W., Kohlen, W., Lillo, A., Op den Camp, R., Ivanov, S., Hartog, M., Limpens, E., Jamil, M., Smaczniak, C., Kaufmann, K., Yang, W.-C., Hooiveld, G. J. E. J., Charnikhova, T., Bouwmeester, H. J., Bisseling, T., & Geurts, R. (2011). Strigolactone biosynthesis in Medicago truncatula and rice requires the symbiotic GRAS-type transcription factors NSP1 and NSP2. *The Plant Cell*, *23*(10), 3853–3865. https://doi.org/10.1105/tpc.111.089771

Liu, W., Zhang, Y., Jiang, S., Deng, Y., Christie, P., Murray, P. J., Li, X., & Zhang, J. (2016). Arbuscular mycorrhizal fungi in soil and roots respond differently to phosphorus inputs in an intensively managed calcareous agricultural soil. *Scientific Reports*, *6*. https://doi.org/10.1038/srep24902

López-Ráez, Juan A., Fernández, I., García, J. M., Berrio, E., Bonfante, P., Walter, M. H., & Pozo, M. J. (2015). Differential spatio-temporal expression of carotenoid cleavage dioxygenases regulates apocarotenoid fluxes during AM symbiosis. *Plant Science*, *230*, 59–69. https://doi.org/10.1016/j.plantsci.2014.10.010

López-Ráez, Juan A., Kohlen, W., Charnikhova, T., Mulder, P., Undas, A. K.,

Sergeant, M. J., Verstappen, F., Bugg, T. D. H., Thompson, A. J., Ruyter-Spira, C., & Bouwmeester, H. (2010). Does abscisic acid affect strigolactone biosynthesis? *New Phytologist*, *187*(2), 343–354. https://doi.org/10.1111/j.1469-8137.2010.03291.x

López-Ráez, Juan Antonio, Charnikhova, T., Gómez-Roldán, V., Matusova, R., Kohlen, W., De Vos, R., Verstappen, F., Puech-Pages, V., Bécard, G., Mulder, P., & Bouwmeester, H. (2008). Tomato strigolactones are derived from carotenoids and their biosynthesis is promoted by phosphate starvation. *New Phytologist*, *178*(4), 863–874. https://doi.org/10.1111/j.1469-8137.2008.02406.x

Lu, X., & Koide, R. T. (1994). The effects of mycorrhizal infection on components of plant growth and reproduction. *New Phytologist*, *128*(2), 211–218. https://doi.org/10.1111/j.1469-8137.1994.tb04004.x

Ludwig-Müller, J. (2010). Hormonal responses in host plants triggered by arbuscular mycorrhizal fungi. In *Arbuscular Mycorrhizas: Physiology and Function* (pp. 169–190). Springer Netherlands. https://doi.org/10.1007/978-90-481-9489-6_8

Luginbuehl, L. H., Menard, G. N., Kurup, S., Van Erp, H., Radhakrishnan, G. V, Breakspear, A., Oldroyd, G. E. D., & Eastmond, P. J. (2017). Fatty acids in arbuscular mycorrhizal fungi are synthesized by the host plant. *Science*, *356*(6343), 1175–1178. https://doi.org/10.1126/science.aan0081

Luginbuehl, L. H., & Oldroyd, G. E. D. (2017). Understanding the Arbuscule at the Heart of Endomycorrhizal Symbioses in Plants. *Current Biology*, *27*(17), R952–R963. https://doi.org/10.1016/j.cub.2017.06.042

Lumini, E., Vallino, M., Alguacil, M. M., Romani, M., & Bianciotto, V. (2011). Different farming and water regimes in Italian rice fields affect arbuscular mycorrhizal fungal soil communities. *Ecological Applications*, *21*(5), 1696–1707. https://doi.org/10.1890/10-1542.1

Ma, X., Luo, W., Li, J., & Wu, F. (2019). Arbuscular mycorrhizal fungi increase both concentrations and bioavilability of Zn in wheat (Triticum aestivum L) grain on Zn-spiked soils. *Applied Soil Ecology*, *135*, 91–97. https://doi.org/10.1016/J.APSOIL.2018.11.007

Maclean, A. M., Bravo, A., & Harrison, M. J. (2017). Plant Signaling and Metabolic Pathways Enabling Arbuscular MycorrhizalSymbiosis. *The Plant Cell*, *29*(10), 2319. https://doi.org/10.1105/TPC.17.00555

Maclean, J. L., Dawe, D. C., & Hettel, G. P. (2002). Rice Almanac: source book for the most important economic activity on earth. In *Rice Almanac: source book for the most important economic activity on earth*. CABI Pub. https://doi.org/10.1079/9780851996363.0000

Maier, W., Peipp, H., Schmidt, J., Wray, V., & Strack, D. (1995). Levels of a terpenoid glycoside (Blumenin) and cell wall-bound phenolics in some cereal mycorrhizas. *Plant Physiology*, *109*(2), 465–470.

https://doi.org/10.1104/pp.109.2.465

Maier, Walter, Hammer, K., Dammann, U., Schulz, B., & Strack, D. (1997). Accumulation of sesquiterpenoid cyclohexenone derivatives induced by an arbuscular mycorrhizal fungus in members of the Poaceae. *Planta*, *202*(1), 36–42. https://doi.org/10.1007/s004250050100

Maier, Walter, Schneider, B., & Strack, D. (1998). Biosynthesis of sesquiterpenoid cyclohexenone derivatives in mycorrhizal barley roots proceeds via the glyceraldehyde 3-phosphate/pyruvate pathway. *Tetrahedron Letters*, *39*(7), 521–524. https://doi.org/10.1016/S0040-4039(97)10673-6

Maillet, F., Poinsot, V., André, O., Puech-Pagés, V., Haouy, A., Gueunier, M., Cromer, L., Giraudet, D., Formey, D., Niebel, A., Martinez, E. A., Driguez, H., Bécard, G., & Dénarié, J. (2011). Fungal lipochitooligosaccharide symbiotic signals in arbuscular mycorrhiza. *Nature*, *469*(7328), 58–64. https://doi.org/10.1038/nature09622

Maiti, D., Singh, R. K., & Variar, M. (2012). Rice-based crop rotation for enhancing native arbuscular mycorrhizal (AM) activity to improve phosphorus nutrition of upland rice (Oryza sativa L.). *Biology and Fertility of Soils*, *48*(1), 67–73. https://doi.org/10.1007/s00374-011-0609-6

Maldonado-Mendoza, I. E., Dewbre, G. R., & Harrison, M. J. (2001). A phosphate transporter gene from the extra-radical mycelium of an arbuscular mycorrhizal fungus glomus intraradices is regulated in response to phosphate in the environment. *Molecular Plant-Microbe Interactions*, *14*(10), 1140–1148. https://doi.org/10.1094/MPMI.2001.14.10.1140

Manley, B. F., Lotharukpong, J. S., Berrera-Redondo, J., Llewellyn, T., Yildirir, G., Sperschneider, J., Corradi, N., Paszowksi, U., Miska, E. A., Dallaire, A. (2023). A highly contiguous genome assembly reveals sources of genomic novelty in the symbiotic fungus Rhizophagus irregularis, G3 Genes|Genomes|Genetics, Volume 13, Issue 6, June 2023, jkad077, https://doi.org/10.1093/g3journal/jkad077

Marcos, R., Izquierdo, Y., Vellosillo, T., Kulasekaran, S., Cascón, T., Hamberg, M., & Castresana, C. (2015). 9-Lipoxygenase-Derived Oxylipins Activate Brassinosteroid Signaling to Promote Cell Wall-Based Defense and Limit Pathogen Infection. *Plant Physiology*, *169*(3), 2324. https://doi.org/10.1104/PP.15.00992

Marla, S. S., & Singh, V. K. (2012). LOX genes in blast fungus (Magnaporthe grisea) resistance in rice. *Functional & Integrative Genomics*, *12*(2), 265–275. https://doi.org/10.1007/S10142-012-0268-1

Marleau, J., Dalpé, Y., St-Arnaud, M., & Hijri, M. (2011). Spore development and nuclear inheritance in arbuscular mycorrhizal fungi. *BMC Evolutionary Biology*, *11*(1), 51. https://doi.org/10.1186/1471-2148-11-51

Martín-Rodríguez, J. A., Huertas, R., Ho-Plágaro, T., Ocampo, J. A., Čková, V. T., Tarkowská, D., Ludwig-Müller, J., & García-Garrido, J. M. (2016). Gibberellin-abscisic acid balances during arbuscular mycorrhiza formation in tomato. *Frontiers in Plant Science*, *7*(AUG2016), 1273. https://doi.org/10.3389/fpls.2016.01273

Martín-Rodríguez, J. Á., León-Morcillo, R., Vierheilig, H., Ocampo, J. A., Ludwig-Müller, J., & García-Garrido, J. M. (2011). Ethylene-dependent/ethylene-independent ABA regulation of tomato plants colonized by arbuscular mycorrhiza fungi. *New Phytologist*, *190*(1), 193–205. https://doi.org/10.1111/j.1469-8137.2010.03610.x

Matsumoto, T., Wu, J., Kanamori, H., Katayose, Y., Fujisawa, M., Namiki, N., Mizuno, H., Yamamoto, K., Antonio, B. A., Baba, T., Sakata, K., Nagamura, Y., Aoki, H., Arikawa, K., Arita, K., Bito, T., Chiden, Y., Fujitsuka, N., Fukunaka, R., … Burr, B. (2005). The map-based sequence of the rice genome. *Nature*, *436*(7052), 793–800. https://doi.org/10.1038/NATURE03895

Maya, M. A., & Matsubara, Y. ichi. (2013). Influence of arbuscular mycorrhiza on the growth and antioxidative activity in cyclamen under heat stress. *Mycorrhiza*, *23*(5), 381–390. https://doi.org/10.1007/S00572-013-0477-Z

McCouch, S. R., Wright, M. H., Tung, C. W., Maron, L. G., McNally, K. L., Fitzgerald, M., Singh, N., DeClerck, G., Agosto-Perez, F., Korniliev, P., Greenberg, A. J., Naredo, M. E. B., Mercado, S. M. Q., Harrington, S. E., Shi, Y., Branchini, D. A., Kuser-Falcão, P. R., Leung, H., Ebana, K., … Mezey, J. (2016). Open access resources for genome-wide association mapping in rice. *Nature Communications 2016 7:1*, *7*(1), 1–14. https://doi.org/10.1038/ncomms10532

McNally, K. L., Childs, K. L., Bohnert, R., Davidson, R. M., Zhao, K., Ulat, V. J., Zeller, G., Clark, R. M., Hoen, D. R., Bureau, T. E., Stokowski, R., Ballinger, D. G., Frazer, K. A., Cox, D. R., Padhukasahasram, B., Bustamante, C. D., Weigel, D., Mackill, D. J., Bruskiewich, R. M., … Leach, J. E. (2009). Genomewide SNP variation reveals relationships among landraces and modern varieties of rice. *Proceedings of the National Academy of Sciences of the United States of America*, *106*(30), 12273–12278. https://doi.org/10.1073/PNAS.0900992106/SUPPL_FILE/0900992106SI.PDF

Meixner, C., Ludwig-Müller, J., Miersch, O., Gresshoff, P., Staehelin, C., & Vierheilig, H. (2005). Lack of mycorrhizal autoregulation and phytohormonal changes in the supernodulating soybean mutant nts1007. *Planta*, *222*(4), 709–715. https://doi.org/10.1007/S00425-005-0003-4/FIGURES/4

Menard, G., Sandhu, N., Anderson, D., Catolos, M., Hassall, K. L., Eastmond, P. J., Kumar, A., & Kurup, S. (2021). Laboratory phenomics predicts field performance and identifies superior indica haplotypes for early seedling vigour in dry direct-seeded rice. *Genomics*, *113*(6), 4227–4236. https://doi.org/10.1016/j.ygeno.2021.11.006

Mensah, J. A., Koch, A. M., Antunes, P. M., Kiers, E. T., Hart, M., & Bücking, H. (2015). High functional diversity within species of arbuscular mycorrhizal fungi is associated with differences in phosphate and nitrogen uptake and fungal phosphate metabolism. *Mycorrhiza*, *25*(7), 533–546. https://doi.org/10.1007/S00572-015-0631-X

Merilo, E., Jalakas, P., Laanemets, K., Mohammadi, O., Hõrak, H., Kollist, H., & Brosché, M. (2015). Abscisic acid transport and homeostasis in the context of stomatal regulation. In *Molecular Plant* (Vol. 8, Issue 9, pp. 1321–1333). Cell Press. https://doi.org/10.1016/j.molp.2015.06.006

Mindt, E., Wang, M., Schäfer, M., Halitschke, R., & Baldwin, I. (2019). Quantification of Blumenol Derivatives as Leaf Biomarkers for Plant-AMF Association. *BIO-PROTOCOL*, *9*(14). https://doi.org/10.21769/bioprotoc.3301

Miyao, A., Tanaka, K., Murata, K., Sawaki, H., Takeda, S., Abe, K., Shinozuka, Y., Onosato, K., & Hirochika, H. (2003). Target site specificity of the Tos17 retrotransposon shows a preference for insertion within genes and against insertion in retrotransposon-rich regions of the genome. *Plant Cell*, *15*(8), 1771–1780. https://doi.org/10.1105/tpc.012559

Miyata, K., Kozaki, T., Kouzai, Y., Ozawa, K., Ishii, K., Asamizu, E., Okabe, Y., Umehara, Y., Miyamoto, A., Kobae, Y., Akiyama, K., Kaku, H., Nishizawa, Y., Shibuya, N., & Nakagawa, T. (2014). The Bifunctional Plant Receptor, OsCERK1, Regulates Both Chitin-Triggered Immunity and Arbuscular Mycorrhizal Symbiosis in Rice. *Plant and Cell Physiology*, *55*(11), 1864–1872. https://doi.org/10.1093/pcp/pcu129

Montero, H., Choi, J., & Paszkowski, U. (2018). Arbuscular mycorrhizal phenotyping: the dos and don’ts. *New Phytologist*, *221*(3), 1182–1186. https://doi.org/10.1111/nph.15489

Montgomery, D. C. (1984). *Design and Analysis of Experiments*. https://books.google.co.uk/books?hl=en&lr=&id=Py7bDgAAQBAJ&oi=fnd&pg=PA1&dq=design+and+analysis+of+experiments+montgomery&ots=X7w_o_OM23&sig=eNMtzbirmpLORIDjURD1cvMk39k&redir_esc=y#v=onepage&q=design and analysis of experiments montgomery&f=false

Moons, A., Valcke, R., & Van Montagu, M. (1998). Low-oxygen stress and water deficit induce cytosolic pyruvate orthophosphate dikinase (PPDK) expression in roots of rice, a C3 plant. *The Plant Journal : For Cell and Molecular Biology*, *15*(1), 89–98. https://doi.org/10.1046/J.1365-313X.1998.00185.X

Mori, N., Nishiuma, K., Sugiyama, T., Hayashi, H., & Akiyama, K. (2016). Carlactone-type strigolactones and their synthetic analogues as inducers of hyphal branching in arbuscular mycorrhizal fungi. *Phytochemistry*, *130*, 90–98. https://doi.org/10.1016/j.phytochem.2016.05.012

Mosse, B. (1973). Plant growth reponses to vesicular-arbuscular mycorrhiza. *New Phytologist*, *72*(1), 127–136. https://doi.org/10.1111/j.1469-8137.1973.tb02017.x

Müller, L. M., Flokova, K., Schnabel, E., Sun, X., Fei, Z., Frugoli, J., Bouwmeester, H. J., & Harrison, M. J. (2019). A CLE–SUNN module regulates strigolactone content and fungal colonization in arbuscular mycorrhiza. *Nature Plants*, *5*(9), 933–939. https://doi.org/10.1038/s41477-019-0501-1

Müller, L. M., & Harrison, M. J. (2019). Phytohormones, miRNAs, and peptide signals integrate plant phosphorus status with arbuscular mycorrhizal symbiosis. *Current Opinion in Plant Biology*, *50*, 132–139. https://doi.org/10.1016/J.PBI.2019.05.004

Nadal, M., Sawers, R., Naseem, S., Bassin, B., Kulicke, C., Sharman, A., An, G., An, K., Ahern, K. R., Romag, A., Brutnell, T. P., Gutjahr, C., Geldner, N., Roux, C., Martinoia, E., Konopka, J. B., & Paszkowski, U. (2017). An N-acetylglucosamine transporter required for arbuscular mycorrhizal symbioses in rice and maize. *Nature Plants*, *3*, 17073. https://doi.org/10.1038/nplants.2017.73

Nagahashi, G., & Douds, D. D. (1997). Appressorium formation by AM fungi on isolated cell walls of carrot roots. *New Phytologist*, *136*(2), 299–304. https://doi.org/10.1046/j.1469-8137.1997.00739.x

Nagy, R., Karandashov, V., Chague, V., Kalinkevich, K., Tamasloukht, M., Xu, G., Jakobsen, I., Levy, A. A., Amrhein, N., & Bucher, M. (2005). The characterization of novel mycorrhiza-specific phosphate transporters from Lycopersicon esculentum and Solanum tuberosum uncovers functional redundancy in symbiotic phosphate transport in solanaceous species. *Plant Journal*, *42*(2), 236–250. https://doi.org/10.1111/j.1365-313X.2005.02364.x

Norton, G. J., Travis, A. J., Douglas, A., Fairley, S., Alves, E. D. P., Ruang-areerate, P., Naredo, M. E. B., McNally, K. L., Hossain, M., Islam, M. R., & Price, A. H. (2018). Genome Wide Association Mapping of Grain and Straw Biomass Traits in the Rice Bengal and Assam Aus Panel (BAAP) Grown Under Alternate Wetting and Drying and Permanently Flooded Irrigation. *Frontiers in Plant Science*, *9*. https://doi.org/10.3389/FPLS.2018.01223

Nouri, E., Breuillin-Sessoms, F., Feller, U., & Reinhardt, D. (2014). Phosphorus and Nitrogen Regulate Arbuscular Mycorrhizal Symbiosis in Petunia hybrida. *PLOS ONE*, *9*(3), e90841. https://doi.org/10.1371/JOURNAL.PONE.0090841

Oláh, B., Brière, C., Bécard, G., Dénarié, J., & Gough, C. (2005). Nod factors and a diffusible factor from arbuscular mycorrhizal fungi stimulate lateral root formation in Medicago truncatula via the DMI1/DMI2 signalling pathway. *Plant Journal*, *44*(2), 195–207. https://doi.org/10.1111/J.1365-313X.2005.02522.X

Ortas, I. (2012). The effect of mycorrhizal fungal inoculation on plant yield, nutrient uptake and inoculation effectiveness under long-term field conditions. *Field Crops Research*, *125*, 35–48. https://doi.org/10.1016/j.fcr.2011.08.005

Ortiz-Berrocal, M., Lozano, L., Sanchez-Flores, A., Nava, N., Hernández, G., & Reddy, P. M. (2017). Expression in rice of an autoactive variant of Medicago

truncatula DMI3, the Ca+2/calmodulin-dependent protein kinase from the common symbiotic pathway modifies root transcriptome and improves mycorrhizal colonization. *Plant Biotechnology Reports*, *11*(5), 271–287. https://doi.org/10.1007/s11816-017-0449-4

Panda, S., Majhi, P. K., Anandan, A., Mahender, A., Veludandi, S., Bastia, D., Guttala, S. B., Singh, S. K., Saha, S., & Ali, J. (2021). Proofing direct-seeded rice with better root plasticity and architecture. *International Journal of Molecular Sciences*, *22*(11), 6058. https://doi.org/10.3390/IJMS22116058/S1

Paszkowski, U., Jakovleva, L., & Boller, T. (2006). Maize mutants affected at distinct stages of the arbuscular mycorrhizal symbiosis. *The Plant Journal*, *47*(2), 165–173. https://doi.org/10.1111/J.1365-313X.2006.02785.X

Paszkowski, U., Kroken, S., Roux, C., & Briggs, S. P. (2002). Rice phosphate transporters include an evolutionarily divergent gene specifically activated in arbuscular mycorrhizal symbiosis. *Proceedings of the National Academy of Sciences*, *99*(20), 13324–13329. https://doi.org/10.1073/pnas.202474599

Pawlowski, M. L., Vuong, T. D., Valliyodan, B., Nguyen, H. T., & Hartman, G. L. (2020). Whole-genome resequencing identifies quantitative trait loci associated with mycorrhizal colonization of soybean. *Theoretical and Applied Genetics*, *133*(2), 409–417. https://doi.org/10.1007/s00122-019-03471-5

Pellegrino, E., Bedini, S., Avio, L., Bonari, E., & Giovannetti, M. (2011). Field inoculation effectiveness of native and exotic arbuscular mycorrhizal fungi in a Mediterranean agricultural soil. *Soil Biology and Biochemistry*, *43*(2), 367–376. https://doi.org/10.1016/J.SOILBIO.2010.11.002

Pellegrino, E., Öpik, M., Bonari, E., & Ercoli, L. (2015). Responses of wheat to arbuscular mycorrhizal fungi: A meta-analysis of field studies from 1975 to 2013. *Soil Biology and Biochemistry*, *84*, 210–217. https://doi.org/10.1016/J.SOILBIO.2015.02.020

Pérez-Tienda, J., Corrêa, A., Azcón-Aguilar, C., & Ferrol, N. (2014). Transcriptional regulation of host NH4+ transporters and GS/GOGAT pathway in arbuscular mycorrhizal rice roots. *Plant Physiology and Biochemistry*, *75*, 1–8. https://doi.org/10.1016/j.plaphy.2013.11.029

Phillips, J. M., & Hayman, D. S. (1970). Improved procedures for clearing roots and staining parasitic and vesicular-arbuscular mycorrhizal fungi for rapid assessment of infection. *Transactions of the British Mycological Society*, *55*(1), 158-IN18. https://doi.org/10.1016/s0007-1536(70)80110-3

Pimprikar, P., Carbonnel, S., Paries, M., Katzer, K., Klingl, V., Bohmer, M. J., Karl, L., Floss, D. S., Harrison, M. J., Parniske, M., & Gutjahr, C. (2016). A CCaMK-CYCLOPS-DELLA complex activates transcription of RAM1 to regulate arbuscule branching. *Current Biology*, *26*(8), 987–998. https://doi.org/10.1016/j.cub.2016.01.069

Plouznikoff, K., Asins, M. J., de Boulois, H. D., Carbonell, E. A., & Declerck, S. (2019). Genetic analysis of tomato root colonization by arbuscular mycorrhizal fungi. *Annals of Botany*, *124*(6), 933–946. https://doi.org/10.1093/AOB/MCY240

Power, A. G. (1999). Linking Ecological Sustainability and World Food Needs. *Environment, Development and Sustainability 1999 1:3*, *1*(3), 185–196. https://doi.org/10.1023/A:1010074805303

Pumplin, N., & Harrison, M. J. (2009). Live-cell imaging reveals periarbuscular membrane domains and organelle location in Medicago truncatula roots during arbuscular mycorrhizal symbiosis. *Plant Physiology*, *151*(2), 809–819. https://doi.org/10.1104/pp.109.141879

Pumplin, N., Zhang, X., Noar, R. D., & Harrison, M. J. (2012). Polar localization of a symbiosis-specific phosphate transporter is mediated by a transient reorientation of secretion. *Proceedings of the National Academy of Sciences of the United States of America*, *109*(11), E665-72. https://doi.org/10.1073/pnas.1110215109

Qin, M., Li, L., Miranda, J. P., Tang, Y., Song, B., Oosthuizen, M. K., & Wei, W. (2022). Experimental duration determines the effect of arbuscular mycorrhizal fungi on plant biomass in pot experiments: A meta-analysis. *Frontiers in Plant Science*, *13*, 4451. https://doi.org/10.3389/FPLS.2022.1024874/BIBTEX

Radhakrishnan, G. V., Keller, J., Rich, M. K., Vernié, T., Mbadinga Mbadinga, D. L., Vigneron, N., Cottret, L., Clemente, H. S., Libourel, C., Cheema, J., Linde, A. M., Eklund, D. M., Cheng, S., Wong, G. K. S., Lagercrantz, U., Li, F. W., Oldroyd, G. E. D., & Delaux, P. M. (2020). An ancestral signalling pathway is conserved in intracellular symbioses-forming plant lineages. *Nature Plants*, *6*(3), 280–289. https://doi.org/10.1038/s41477-020-0613-7

Rahman, M. (2019). Potential Benefits of Dry Direct Seeded Rice : A Review. *Fundamental and Applied Agriculture*, *0*, 1. https://doi.org/10.5455/faa.16534

Ramírez-Flores, M. R., Perez-Limon, S., Li, M., Barrales-Gamez, B., Albinsky, D., Paszkowski, U., Olalde-Portugal, V., & Sawers, R. J. H. (2020). The genetic architecture of host response reveals the importance of arbuscular mycorrhizae to maize cultivation. *ELife*, *9*, 1–18. https://doi.org/10.7554/eLife.61701

Raun, W. R., & Johnson, G. V. (1999). Improving nitrogen use efficiency for cereal production. In *Agronomy Journal* (Vol. 91, Issue 3, pp. 357–363). American Society of Agronomy. https://doi.org/10.2134/agronj1999.00021962009100030001x

Remy, W., Taylor, T. N., Hass, H., & Kerp, H. (1994). Four hundred-million-year-old vesicular arbuscular mycorrhizae. *Proceedings of the National Academy of Sciences of the United States of America*, *91*(25), 11841–11843. https://doi.org/10.1073/pnas.91.25.11841

Ried, M. K., Antolín-Llovera, M., & Parniske, M. (2014). Spontaneous symbiotic reprogramming of plant roots triggered by receptor-like kinases. *ELife*, *3*(November), 1–17. https://doi.org/10.7554/eLife.03891

Rillig, M. C., Aguilar-Trigueros, C. A., Bergmann, J., Verbruggen, E., Veresoglou, S. D., & Lehmann, A. (2015). Plant root and mycorrhizal fungal traits for understanding soil aggregation. *New Phytologist*, *205*(4), 1385–1388. https://doi.org/10.1111/NPH.13045

Rillig, M. C., & Mummey, D. L. (2006). Mycorrhizas and soil structure. *New Phytologist*, *171*(1), 41–53. https://doi.org/10.1111/J.1469-8137.2006.01750.X

Rose, T. J., Rose, M. T., Pariasca-Tanaka, J., Heuer, S., & Wissuwa, M. (2011). The frustration with utilization: Why have improvements in internal phosphorus utilization efficiency in crops remained so elusive? *Frontiers in Plant Science*, *2*(NOV), 73. https://doi.org/10.3389/FPLS.2011.00073/BIBTEX

Roth, R., Chiapello, M., Montero, H., Gehrig, P., Grossmann, J., O'Holleran, K., Hartken, D., Walters, F., Yang, S. Y., Hillmer, S., Schumacher, K., Bowden, S., Craze, M., Wallington, E. J., Miyao, A., Sawers, R., Martinoia, E., & Paszkowski, U. (2018). *A rice Serine/Threonine receptor-like kinase regulates arbuscular mycorrhizal symbiosis at the peri-arbuscular membrane*. *9*(1). https://doi.org/10.1038/s41467-018-06865-z

Roth, R., Hillmer, S., Funaya, C., Chiapello, M., Schumacher, K., Lo Presti, L., Kahmann, R., & Paszkowski, U. (2019). Arbuscular cell invasion coincides with extracellular vesicles and membrane tubules. *Nature Plants*, *5*(2), 204–211. https://doi.org/10.1038/s41477-019-0365-4

Rúa, M. A., Antoninka, A., Antunes, P. M., Chaudhary, V. B., Gehring, C., Lamit, L. J., Piculell, B. J., Bever, J. D., Zabinski, C., Meadow, J. F., Lajeunesse, M. J., Milligan, B. G., Karst, J., & Hoeksema, J. D. (2016). Home-field advantage? evidence of local adaptation among plants, soil, and arbuscular mycorrhizal fungi through meta-analysis. *BMC Evolutionary Biology*, *16*(1). https://doi.org/10.1186/S12862-016-0698-9

Ruiz-Lozano, J. M., Collados, C., Barea, J. M., & Azcón, R. (2001). Arbuscular mycorrhizal symbiosis can alleviate drought-induced nodule senescence in soybean plants. *New Phytologist*, *151*(2), 493–502. https://doi.org/10.1046/j.0028-646X.2001.00196.x

Ruiz-Lozano, J. M., Porcel, R., Bárzana, G., Azcón, R., & Aroca, R. (2012). Contribution of arbuscular mycorrhizal symbiosis to plant drought tolerance: State of the art. In *Plant Responses to Drought Stress: From Morphological to Molecular Features* (Vol. 9783642326, pp. 335–362). Springer-Verlag Berlin Heidelberg. https://doi.org/10.1007/978-3-642-32653-0_13

Ruiz-Sánchez, M., Aroca, R., Muñoz, Y., Polón, R., & Ruiz-Lozano, J. M. (2010). The arbuscular mycorrhizal symbiosis enhances the photosynthetic efficiency and the antioxidative response of rice plants subjected to drought stress.

Journal of Plant Physiology, *167*(11), 862–869. https://doi.org/10.1016/j.jplph.2010.01.018

Runcie, D. E., & Crawford, L. (2019). Fast and flexible linear mixed models for genome-wide genetics. *PLoS Genetics*, *15*(2). https://doi.org/10.1371/JOURNAL.PGEN.1007978

Ruyter-Spira, C., & Bouwmeester, H. (2012). Strigolactones affect development in primitive plants. The missing link between plants and arbuscular mycorrhizal fungi? In *New Phytologist* (Vol. 195, Issue 4, pp. 730–733). John Wiley & Sons, Ltd. https://doi.org/10.1111/j.1469-8137.2012.04261.x

Ryan, M.H., & Angus, J. F. (2003). Arbuscular mycorrhizae in wheat and field pea crops on a low P soil: increased Zn-uptake but no increase in P-uptake or yield. *Plant and Soil*, *250*(2), 225–239. https://doi.org/10.1023/A:1022839930134

Ryan, Megan H., & Graham, J. H. (2018). Little evidence that farmers should consider abundance or diversity of arbuscular mycorrhizal fungi when managing crops. *New Phytologist*, *220*(4), 1092–1107. https://doi.org/10.1111/NPH.15308

Saito, K., Asai, H., Zhao, D., Laborte, A. G., & Grenier, C. (2018). Progress in varietal improvement for increasing upland rice productivity in the tropics. In *Plant Production Science* (Vol. 21, Issue 3, pp. 145–158). https://doi.org/10.1080/1343943X.2018.1459751

Saleque, M. A., Abedin, M. J., Panaullah, G. M., & Bhuiyan, N. I. (2008). Yield and phosphorus efficiency of some lowland rice varieties at different levels of soil-available phosphorus. *Http://Dx.Doi.Org/10.1080/00103629809370164*, *29*(19–20), 2905–2916. https://doi.org/10.1080/00103629809370164

Sallaud, C., Gay, C., Larmande, P., Bès, M., Piffanelli, P., Piégu, B., Droc, G., Regad, F., Bourgeois, E., Meynard, D., Périn, C., Sabau, X., Ghesquière, A., Glaszmann, J. C., Delseny, M., & Guiderdoni, E. (2004). High throughput T-DNA insertion mutagenesis in rice: A first step towards in silico reverse genetics. In *Plant Journal* (Vol. 39, Issue 3, pp. 450–464). https://doi.org/10.1111/j.1365-313X.2004.02145.x

Sanders, I. R., & Rodriguez, A. (2016). Aligning molecular studies of mycorrhizal fungal diversity with ecologically important levels of diversity in ecosystems. *The ISME Journal 2016 10:12*, *10*(12), 2780–2786. https://doi.org/10.1038/ismej.2016.73

Sandhu, N.; Yadav, S.; Kumar Singh, V.; Kumar, A. Effective Crop Management and Modern Breeding Strategies to Ensure Higher Crop Productivity under Direct Seeded Rice Cultivation System: A Review. Agronomy 2021, 11, 1264. https://doi.org/10.3390/agronomy11071264

Savary, R., Dupuis, C., Masclaux, F. G., Mateus, I. D., Rojas, E. C., & Sanders, I. R. (2020). Genetic variation and evolutionary history of a mycorrhizal fungus regulate the currency of exchange in symbiosis with the food security crop

cassava. *ISME Journal*, 1–12. https://doi.org/10.1038/s41396-020-0606-6

Sawers, R. J. H., Gebreselassie, M. N., Janos, D. P., & Paszkowski, U. (2010). Characterizing variation in mycorrhiza effect among diverse plant varieties. *Theoretical and Applied Genetics*, *120*(5), 1029–1039. https://doi.org/10.1007/s00122-009-1231-y

Sawers, R. J. H., Gutjahr, C., & Paszkowski, U. (2008). Cereal mycorrhiza: an ancient symbiosis in modern agriculture. In *Trends in Plant Science* (Vol. 13, Issue 2, pp. 93–97). https://doi.org/10.1016/j.tplants.2007.11.006

Sawers, R. J. H., Svane, S. F., Quan, C., Grønlund, M., Wozniak, B., Gebreselassie, M. N., González-Muñoz, E., Chávez Montes, R. A., Baxter, I., Goudet, J., Jakobsen, I., & Paszkowski, U. (2017). Phosphorus acquisition efficiency in arbuscular mycorrhizal maize is correlated with the abundance of root-external hyphae and the accumulation of transcripts encoding PHT1 phosphate transporters. *New Phytologist*, *214*(2), 632–643. https://doi.org/10.1111/nph.14403

Schliemann, W., Ammer, C., & Strack, D. (2008). Metabolite profiling of mycorrhizal roots of Medicago truncatula. *Phytochemistry*, *69*(1), 112–146. https://doi.org/10.1016/j.phytochem.2007.06.032

Schliemann, W., Kolbe, B., Schmidt, J., Nimtz, M., & Wray, V. (2008). Accumulation of apocarotenoids in mycorrhizal roots of leek (Allium porrum). *Phytochemistry*, *69*(8), 1680–1688. https://doi.org/10.1016/j.phytochem.2008.02.015

Schüßler, A., Martin, H., Cohen, D., Fitz, M., & Wipf, D. (2006). Characterization of a carbohydrate transporter from symbiotic glomeromycotan fungi. *Nature*, *444*(7121), 933–936. https://doi.org/10.1038/nature05364

Secilia, J., & Bagyaraj, D. J. (1994). Evaluation and first-year field testing of efficient vesicular arbuscular mycorrhizal fungi for inoculation of wetland rice seedlings. *World Journal of Microbiology & Biotechnology*, *10*(4), 381–384. https://doi.org/10.1007/BF00144455

Shachar-Hill, Y., Pfeffer, P. E., Douds, D., Osman, S. F., Doner, L. W., & Ratcliffe, R. G. (1995). Partitioning of intermediary carbon metabolism in vesicular-arbuscular mycorrhizal leek. *Plant Physiology*, *108*(1), 7–15. https://doi.org/10.1104/pp.108.1.7

Shenton, M., Iwamoto, C., Kurata, N., & Ikeo, K. (2016). Effect of Wild and Cultivated Rice Genotypes on Rhizosphere Bacterial Community Composition. *Rice*, *9*(1). https://doi.org/10.1186/s12284-016-0111-8

Shi, J., Zhao, B., Zheng, S., Zhang, X., Wang, X., Dong, W., Xie, Q., Wang, G., Xiao, Y., Chen, F., Yu, N., & Wang, E. (2021). A phosphate starvation response-centered network regulates mycorrhizal symbiosis. *Cell*, *184*(22), 5527-5540.e18. https://doi.org/10.1016/J.CELL.2021.09.030

Shimoda, Y., Han, L., Yamazaki, T., Suzuki, R., Hayashi, M., & Imaizumi-Anraku, H. (2012). Rhizobial and Fungal Symbioses Show Different Requirements for Calmodulin Binding to Calcium Calmodulin-Dependent Protein Kinase in Lotus japonicus. *The Plant Cell*, *24*(1), 304–321. https://doi.org/10.1105/tpc.111.092197

Shindo, M., Shimomura, K., Yamaguchi, S., & Umehara, M. (2018). Upregulation of DWARF27 is associated with increased strigolactone levels under sulfur deficiency in rice. *Plant Direct*, *2*(4), e00050. https://doi.org/10.1002/pld3.50

Singla, P., & Garg, N. (2017). Plant flavonoids: Key players in signaling, establishment, and regulation of rhizobial and mycorrhizal endosymbioses. In *Mycorrhiza - Function, Diversity, State of the Art: Fourth Edition* (pp. 133–176). Springer International Publishing. https://doi.org/10.1007/978-3-319-53064-2_8

Sisaphaithong, T., Hanai, S., Tomioka, R., Kobae, Y., Tanaka, A., Yano, K., Takenaka, C., & Hata, S. (2017). Varietal differences in the growth responses of rice to an arbuscular mycorrhizal fungus under natural upland conditions. *Plant Signaling and Behavior*, *12*(1), e1274483. https://doi.org/10.1080/15592324.2016.1274483

Šmilauer, P., Košnar, J., Kotilínek, M., & Šmilauerová, M. (2020). Contrasting effects of host identity, plant community, and local species pool on the composition and colonization levels of arbuscular mycorrhizal fungal community in a temperate grassland. *New Phytologist*, *225*(1), 461–473. https://doi.org/10.1111/nph.16112

Smith, S. E. (2003). Mycorrhizal Fungi Can Dominate Phosphate Supply to Plants Irrespective of Growth Responses. *PLANT PHYSIOLOGY*, *133*(1), 16–20. https://doi.org/10.1104/pp.103.024380

Smith, S. E., & Read, D. J. (David J. . (2008). *Mycorrhizal symbiosis*. Academic Press.

Smith, Sally E., Smith, F. A., & Jakobsen, I. (2004). Functional diversity in arbuscular mycorrhizal (AM) symbioses: the contribution of the mycorrhizal P uptake pathway is not correlated with mycorrhizal responses in growth or total P uptake. *New Phytologist*, *162*(2), 511–524. https://doi.org/10.1111/j.1469-8137.2004.01039.x

Solaiman, M. Z., & Hirata, H. (1997). Effect of arbuscular mycorrhizal fungi inoculation of rice seedlings at the nursery stage upon performance in the paddy field and greenhouse. *Plant and Soil*, *191*(1), 1–12. https://doi.org/10.1023/A:1004238028617

Soudzilovskaia, N. A., Vaessen, S., Barcelo, M., He, J., Rahimlou, S., Abarenkov, K., Brundrett, M. C., Gomes, S. I. F., Merckx, V., & Tedersoo, L. (2020). FungalRoot: global online database of plant mycorrhizal associations. *New Phytologist*, *227*(3), 955–966. https://doi.org/10.1111/NPH.16569

Soundappan, I., Bennett, T., Morffy, N., Liang, Y., Stanga, J. P., Abbas, A., Leyser, O., & Nelsona, D. C. (2015). SMAX1-LIKE/D53 family members enable distinct MAX2-dependent responses to strigolactones and karrikins in arabidopsis. *Plant Cell*, *27*(11), 3143–3159. https://doi.org/10.1105/tpc.15.00562

Staddon, P. L., Ramsey, C. B., Ostle, N., Ineson, P., & Fitter, A. H. (2003). Rapid turnover of hyphae of mycorrhizal fungi determined by AMS microanalysis of 14C. *Science*, *300*(5622), 1138–1140. https://doi.org/10.1126/science.1084269

Stahlhut, K. N., Dowell, J. A., Temme, A. A., Burke, J. M., Goolsby, E. W., & Mason, C. M. (2021). Genetic control of arbuscular mycorrhizal colonization by Rhizophagus intraradices in Helianthus annuus (L.). *Mycorrhiza*, *31*(6), 723–734. https://doi.org/10.1007/S00572-021-01050-5/TABLES/2

Stauder, R., Welsch, R., Camagna, M., Kohlen, W., Balcke, G. U., Tissier, A., & Walter, M. H. (2018). Strigolactone levels in dicot roots are determined by an ancestral symbiosis-regulated clade of the PHYTOENE SYNTHASE gene family. *Frontiers in Plant Science*, *9*, 255. https://doi.org/10.3389/fpls.2018.00255

Stirnberg, P., Furner, I. J., & Ottoline Leyser, H. M. (2007). MAX2 participates in an SCF complex which acts locally at the node to suppress shoot branching. *The Plant Journal*, *50*(1), 80–94. https://doi.org/10.1111/J.1365-313X.2007.03032.X

Stoian, V., Vidican, R., Crişan, I., Puia, C., Şandor, M., Stoian, V. A., Păcurar, F., & Vaida, I. (2019). Sensitive approach and future perspectives in microscopic patterns of mycorrhizal roots. *Scientific Reports 2019 9:1*, *9*(1), 1–8. https://doi.org/10.1038/s41598-019-46743-2

Strack, D., & Fester, T. (2006). Isoprenoid metabolism and plastid reorganization in arbuscular mycorrhizal roots. In *New Phytologist* (Vol. 172, Issue 1, pp. 22–34). https://doi.org/10.1111/j.1469-8137.2006.01837.x

Styger, E. (2014). *Rice production diagnostic for Chinsali (Chinsali District, Northern Province) and Mfuwe (Mwambe District, Eastern Province), Zambia*. http://sri.cals.cornell.edu/,

Sun, H., Tao, J., Liu, S., Huang, S., Chen, S., Xie, X., Yoneyama, K., Zhang, Y., & Xu, G. (2014). Strigolactones are involved in phosphate- and nitrate-deficiency-induced root development and auxin transport in rice. *Journal of Experimental Botany*, *65*(22), 6735–6746. https://doi.org/10.1093/jxb/eru029

Sun, J., He, N., Niu, L., Huang, Y., Shen, W., Zhang, Y., Li, L., & Hou, C. (2019). Global Quantitative Mapping of Enhancers in Rice by STARR-seq. *Genomics, Proteomics and Bioinformatics*, *17*(2), 140–153. https://doi.org/10.1016/J.GPB.2018.11.003

Sun, X. D., & Ni, M. (2011). HYPOSENSITIVE TO LIGHT, an alpha/beta fold protein, acts downstream of ELONGATED HYPOCOTYL 5 to regulate seedling de-etiolation. *Molecular Plant*, *4*(1), 116–126. https://doi.org/10.1093/MP/SSQ055

Sun, Z., Hans, J., Walter, M. H., Matusova, R., Beekwilder, J., Verstappen, F. W. A., Ming, Z., Van Echtelt, E., Strack, D., Bisseling, T., & Bouwmeester, H. J. (2008). Cloning and characterisation of a maize carotenoid cleavage dioxygenase (ZmCCD1) and its involvement in the biosynthesis of apocarotenoids with various roles in mutualistic and parasitic interactions. *Planta*, *228*(5), 789–801. https://doi.org/10.1007/s00425-008-0781-6

Suzuki, S., Kobae, Y., Sisaphaithong, T., Tomioka, R., Takenaka, C., & Hata, S. (2015). Differential Growth Responses of Rice Cultivars to an Arbuscular Mycorrhizal Fungus, Funneliformis mosseae. *Journal of Horticulture*, *2*(3), 1–4. https://doi.org/10.4172/2376-0354.1000142

Sze, H., Li, X., & Palmgren, M. G. (1999). Energization of plant cell membranes by H+-pumping ATPases: Regulation and biosynthesis. *Plant Cell*, *11*(4), 677–689. https://doi.org/10.1105/tpc.11.4.677

Takeda, N., Maekawa, T., & Hayashi, M. (2012). Nuclear-localized and deregulated calcium- and calmodulin-dependent protein kinase activates rhizobial and mycorrhizal responses in Lotus japonicus. *Plant Cell*, *24*(2), 810–822. https://doi.org/10.1105/tpc.111.091827

Tal, L., Palayam, M., Ron, M., Young, A., Britt, A., & Shabek, N. (2022). A conformational switch in the SCF-D3/MAX2 ubiquitin ligase facilitates strigolactone signalling. *Nature Plants 2022 8:5*, *8*(5), 561–573. https://doi.org/10.1038/s41477-022-01145-7

Tanaka, Y., & Yano, K. (2005). Nitrogen delivery to maize via mycorrhizal hyphae depends on the form of N supplied. *Plant, Cell and Environment*, *28*(10), 1247–1254. https://doi.org/10.1111/j.1365-3040.2005.01360.x

Taulera, Q., Lauressergues, D., Martin, K., Cadoret, M., Servajean, V., Boyer, F.-D., & Rochange, S. (2020). Initiation of arbuscular mycorrhizal symbiosis involves a novel pathway independent from hyphal branching. *Mycorrhiza*, 1–11. https://doi.org/10.1007/s00572-020-00965-9

Taylor, A., Pereira, N., Thomas, B., Pink, D. A. C., Jones, J. E., & Bending, G. D. (2015). Growth and nutritional responses to arbuscular mycorrhizal fungi are dependent on onion genotype and fungal species. *Biology and Fertility of Soils*, *51*(7), 801–813. https://doi.org/10.1007/s00374-015-1027-y

Thirkell, T. J., Grimmer, M., James, L., Pastok, D., Allary, T., Elliott, A., Paveley, N., Daniell, T., & Field, K. J. (2022). Variation in mycorrhizal growth response among a spring wheat mapping population shows potential to breed for symbiotic benefit. *Food and Energy Security*, *11*(2), e370. https://doi.org/10.1002/FES3.370

Thonar, C., Schnepf, A., Frossard, E., Roose, T., & Jansa, J. (2011). Traits related to differences in function among three arbuscular mycorrhizal fungi. *Plant and Soil*, *339*(1), 231–245. https://doi.org/10.1007/s11104-010-0571-3

Tibbs Cortes, L., Zhang, Z., & Yu, J. (2021). Status and prospects of genome-wide association studies in plants. *The Plant Genome*, *14*(1), e20077. https://doi.org/10.1002/TPG2.20077

Tilman, D., Fargione, J., Wolff, B., D'Antonio, C., Dobson, A., Howarth, R., Schindler, D., Schlesinger, W. H., Simberloff, D., & Swackhamer, D. (2001). Forecasting agriculturally driven global environmental change. *Science*, *292*(5515), 281–284. https://doi.org/10.1126/SCIENCE.1057544/ASSET/F38116C6-6331-49C7-9B73-433B3496A402/ASSETS/GRAPHIC/SE1419341001.JPEG

Tilman, David, Cassman, K. G., Matson, P. A., Naylor, R., & Polasky, S. (2002). Agricultural sustainability and intensive production practices. *Nature 2002 418:6898*, *418*(6898), 671–677. https://doi.org/10.1038/nature01014

Timoneda, A., Yunusov, T., Quan, C., Gavrin, A., Brockington, S. F., & Schornack, S. (2021). MycoRed: Betalain pigments enable in vivo real-time visualisation of arbuscular mycorrhizal colonisation. *PLOS Biology*, *19*(7), e3001326. https://doi.org/10.1371/JOURNAL.PBIO.3001326

Tisserant, E., Malbreil, M., Kuo, A., Kohler, A., Symeonidi, A., Balestrini, R., Charron, P., Duensing, N., Frei Dit Frey, N., Gianinazzi-Pearson, V., Gilbert, L. B., Handa, Y., Herr, J. R., Hijri, M., Koul, R., Kawaguchi, M., Krajinski, F., Lammers, P. J., Masclaux, F. G., … Martin, F. (2013). Genome of an arbuscular mycorrhizal fungus provides insight into the oldest plant symbiosis. *Proceedings of the National Academy of Sciences of the United States of America*, *110*(50), 20117–20122. https://doi.org/10.1073/pnas.1313452110

Tnani, H., Chebotarov, D., Thapa, R., Ignacio, J. C. I., Israel, W. K., Quilloy, F. A., Dixit, S., Septiningsih, E. M., & Kretzschmar, T. (2021). Enriched-gwas and transcriptome analysis to refine and characterize a major qtl for anaerobic germination tolerance in rice. *International Journal of Molecular Sciences*, *22*(9). https://doi.org/10.3390/ijms22094445

Toth, R., & Miller, R. M. (1984). Dynamics of arbuscule development and degeneration in a Zea mays mycorrhiza. *American Journal of Botany*, *71*(4), 449–460. https://doi.org/10.1002/j.1537-2197.1984.tb12530.x

Tromas, A., Parizot, B., Diagne, N., Champion, A., Hocher, V., Cissoko, M., Crabos, A., Prodjinoto, H., Lahouze, B., Bogusz, D., Laplaze, L., & Svistoonoff, S. (2012). Heart of Endosymbioses: Transcriptomics Reveals a Conserved Genetic Program among Arbuscular Mycorrhizal, Actinorhizal and Legume-Rhizobial Symbioses. *PLoS ONE*, *7*(9), e44742. https://doi.org/10.1371/journal.pone.0044742

Tsuzuki, S., Handa, Y., Takeda, N., & Kawaguchi, M. (2016). Strigolactone-induced putative secreted protein 1 is required for the establishment of symbiosis by the arbuscular mycorrhizal fungus Rhizophagus irregularis. *Molecular Plant-Microbe Interactions*, *29*(4), 277–286. https://doi.org/10.1094/MPMI-10-15-0234-R

Tuan, P. A., Kumar, R., Rehal, P. K., Toora, P. K., & Ayele, B. T. (2018). Molecular mechanisms underlying abscisic acid/gibberellin balance in the control of seed dormancy and germination in cereals. In *Frontiers in Plant Science* (Vol. 9). Frontiers Media S.A. https://doi.org/10.3389/fpls.2018.00668

Ueno, K., Furumoto, T., Umeda, S., Mizutani, M., Takikawa, H., Batchvarova, R., & Sugimoto, Y. (2014). Heliolactone, a non-sesquiterpene lactone germination stimulant for root parasitic weeds from sunflower. *Phytochemistry*, *108*, 122–128. https://doi.org/10.1016/j.phytochem.2014.09.018

Umehara, M., Hanada, A., Yoshida, S., Akiyama, K., Arite, T., Takeda-Kamiya, N., Magome, H., Kamiya, Y., Shirasu, K., Yoneyama, K., Kyozuka, J., & Yamaguchi, S. (2008). Inhibition of shoot branching by new terpenoid plant hormones. *Nature*, *455*(7210), 195–200. https://doi.org/10.1038/nature07272

USDA. (2021). *USDA ERS - Rice Sector at a Glance* (Issue table 1, pp. 1–11). https://www.ers.usda.gov/topics/crops/rice/rice-sector-at-a-glance/

Vaingankar, J. D., & Rodrigues, B. F. (2015). Effect of Arbuscular Mycorrhizal (AM) Inoculation on Growth and Flowering in Crossandra infundibuliformis (L.) Nees. *Http://Dx.Doi.Org/10.1080/01904167.2014.957398*, *38*(10), 1478–1488. https://doi.org/10.1080/01904167.2014.957398

Vallino, M., Greppi, D., Novero, M., Bonfante, P., & Lupotto, E. (2009). Rice root colonisation by mycorrhizal and endophytic fungi in aerobic soil. *Annals of Applied Biology*, *154*(2), 195–204. https://doi.org/10.1111/j.1744-7348.2008.00286.x

Vallino, Marta, Fiorilli, V., & Bonfante, P. (2014). Rice flooding negatively impacts root branching and arbuscular mycorrhizal colonization, but not fungal viability. *Plant, Cell and Environment*, *37*(3), 557–572. https://doi.org/10.1111/PCE.12177/SUPPINFO

Van Der Heijden, M. G. A., Klironomos, J. N., Ursic, M., Moutoglis, P., Streitwolf-Engel, R., Boller, T., Wiemken, A., & Sanders, I. R. (1998). *Mycorrhizal fungal diversity determines plant biodiversity, ecosystem variability and productivity*. *396*(6706), 69–72. https://doi.org/10.1038/23932

Van Rhijn, P., Fang, Y., Galili, S., Shaul, O., Atzmon, N., Wininger, S., Eshed, Y., Lum, M., Li, Y., To, V., Fujishige, N., Kapulnik, Y., & Hirsch, A. M. (1997). Expression of early nodulin genes in alfalfa mycorrhizae indicates that signal transduction pathways used in forming arbuscular mycorrhizae and Rhizobium-induced nodules may be conserved. *Proceedings of the National Academy of Sciences*, *94*(10), 5467–5472. https://doi.org/10.1073/PNAS.94.10.5467

van Zeijl, A., Liu, W., Xiao, T. T., Kohlen, W., Yang, W. C., Bisseling, T., & Geurts, R. (2015). The strigolactone biosynthesis gene DWARF27 is co-opted in rhizobium symbiosis. *BMC Plant Biology*, *15*(1), 1–15. https://doi.org/10.1186/S12870-015-0651-X/FIGURES/9

Verbruggen, E., & Kiers, T. E. (2010). Evolutionary ecology of mycorrhizal functional diversity in agricultural systems. *Evolutionary Applications*, *3*(5–6), 547–560. https://doi.org/10.1111/J.1752-4571.2010.00145.X

Vierheilig, H., Coughlan, A. P., Wyss, U., & Piché, Y. (1998). Ink and vinegar, a simple staining technique for arbuscular-mycorrhizal fungi. *Applied and Environmental Microbiology*, *64*(12), 5004–5007. https://doi.org/10.1128/aem.64.12.5004-5007.1998

Vitousek, P. M., Mooney, H. A., Lubchenco, J., & Melillo, J. M. (1997). Human domination of Earth's ecosystems. *Science*, *277*(5325), 494–499. https://doi.org/10.1126/SCIENCE.277.5325.494/ASSET/865F55CF-AB01-4FAE-8408-9C87CFEDC964/ASSETS/GRAPHIC/SE3075509004.JPEG

Vogel, J. T., Tan, B. C., McCarty, D. R., & Klee, H. J. (2008). The carotenoid cleavage dioxygenase 1 enzyme has broad substrate specificity, cleaving multiple carotenoids at two different bond positions. *Journal of Biological Chemistry*, *283*(17), 11364–11373. https://doi.org/10.1074/jbc.M710106200

Vogel, J. T., Walter, M. H., Giavalisco, P., Lytovchenko, A., Kohlen, W., Charnikhova, T., Simkin, A. J., Goulet, C., Strack, D., Bouwmeester, H. J., Fernie, A. R., & Klee, H. J. (2010). SlCCD7 controls strigolactone biosynthesis, shoot branching and mycorrhiza-induced apocarotenoid formation in tomato. *Plant Journal*, *61*(2), 300–311. https://doi.org/10.1111/j.1365-313X.2009.04056.x

Votta, C., Fiorilli, V., Haider, I., Wang, J. Y., Balestrini, R., Petřík, I., Tarkowská, D., Novák, O., Serikbayeva, A., Bonfante, P., Al-Babili, S., & Lanfranco, L. (2022). Zaxinone synthase controls arbuscular mycorrhizal colonization level in rice. *Plant Journal*, *111*(6), 1688–1700. https://doi.org/10.1111/tpj.15917

W.N., B., & J.W., G. (1977). Colorimetric quantification of vesicular-arbuscular mycorrhizal infection in onion. *New Phytologist*. https://doi.org/10.3/JQUERY-UI.JS

Walder, F., Niemann, H., Natarajan, M., Lehmann, M. F., Boller, T., & Wiemken, A. (2012). Mycorrhizal Networks: Common Goods of Plants Shared under Unequal Terms of Trade. *PLANT PHYSIOLOGY*, *159*(2), 789–797. https://doi.org/10.1104/pp.112.195727

Walker, C. H., Siu-Ting, K., Taylor, A., O'Connell, M. J., & Bennett, T. (2019). Strigolactone synthesis is ancestral in land plants, but canonical strigolactone signalling is a flowering plant innovation. *BMC Biology*, *17*(1), 70. https://doi.org/10.1186/s12915-019-0689-6

Walter, M H, Fester, T., & Strack, D. (2000). Arbuscular mycorrhizal fungi induce the non-mevalonate methylerythritol phosphate pathway of isoprenoid biosynthesis correlated with accumulation of the "yellow pigment" and other apocarotenoids. *The Plant Journal : For Cell and Molecular Biology*, *21*(6), 571–578. http://www.ncbi.nlm.nih.gov/pubmed/10758508

Walter, Michael H., Floß, D. S., Hans, J., Fester, T., & Strack, D. (2007). Apocarotenoid biosynthesis in arbuscular mycorrhizal roots: Contributions from methylerythritol phosphate pathway isogenes and tools for its manipulation. In *Phytochemistry* (Vol. 68, Issue 1, pp. 130–138). https://doi.org/10.1016/j.phytochem.2006.09.032

Walter, Michael H., & Strack, D. (2011). Carotenoids and their cleavage products: Biosynthesis and functions. In *Natural Product Reports* (Vol. 28, Issue 4, pp. 663–692). https://doi.org/10.1039/c0np00036a

Wang, B., & Qiu, Y. L. (2006). Phylogenetic distribution and evolution of mycorrhizas in land plants. *Mycorrhiza*, *16*(5), 299–363. https://doi.org/10.1007/S00572-005-0033-6/FIGURES/1

Wang, C., Ying, S., Huang, H., Li, K., Wu, P., & Shou, H. (2009). Involvement of OsSPX1 in phosphate homeostasis in rice. *Plant Journal*, *57*(5), 895–904. https://doi.org/10.1111/j.1365-313X.2008.03734.x

Wang, E., Yu, N., Bano, S. A., Liu, C., Miller, A. J., Cousins, D., Zhang, X., Ratet, P., Tadege, M., Mysore, K. S., Downie, J. A., Murray, J. D., Oldroyd, G. E. D., & Schultze, M. (2014). A H+-ATPase that energizes nutrient uptake during mycorrhizal symbioses in rice and Medicago truncatula. *Plant Cell*, *26*(4), 1818–1830. https://doi.org/10.1105/tpc.113.120527

Wang, H., Ham, T. H., Im, D. E., Lar, S. M., Jang, S. G., Lee, J., Mo, Y., Jeung, J. U., Kim, S. T., & Kwon, S. W. (2020). A New SNP in Rice Gene Encoding Pyruvate Phosphate Dikinase (PPDK) Associated with Floury Endosperm. *Genes*, *11*(4). https://doi.org/10.3390/GENES11040465

Wang, J. Y., Alseekh, S., Xiao, T., Ablazov, A., Perez de Souza, L., Fiorilli, V., Anggarani, M., Lin, P. Y., Votta, C., Novero, M., Jamil, M., Lanfranco, L., Hsing, Y. I. C., Blilou, I., Fernie, A. R., & Al-Babili, S. (2021). Multi-omics approaches explain the growth-promoting effect of the apocarotenoid growth regulator zaxinone in rice. *Communications Biology*, *4*(1), 1–11. https://doi.org/10.1038/s42003-021-02740-8

Wang, J. Y., Chen, G. T. E., Jamil, M., Braguy, J., Sioud, S., Liew, K. X., Balakrishna, A., & Al-Babili, S. (2022). Protocol for characterizing strigolactones released by plant roots. *STAR Protocols*, *3*(2). https://doi.org/10.1016/j.xpro.2022.101352

Wang, J. Y., Haider, I., Jamil, M., Fiorilli, V., Saito, Y., Mi, J., Baz, L., Kountche, B. A., Jia, K. P., Guo, X., Balakrishna, A., Ntui, V. O., Reinke, B., Volpe, V., Gojobori, T., Blilou, I., Lanfranco, L., Bonfante, P., & Al-Babili, S. (2019). The apocarotenoid metabolite zaxinone regulates growth and strigolactone biosynthesis in rice. *Nature Communications*, *10*(1), 810. https://doi.org/10.1038/s41467-019-08461-1

Wang, L., Wang, B., Jiang, L., Liu, X., Li, X., Lu, Z., Meng, X., Wang, Y., Smith, S. M., & Lia, J. (2015). Strigolactone signaling in Arabidopsis regulates shoot development by targeting D53-like SMXL repressor proteins for ubiquitination and degradation. *Plant Cell*, *27*(11), 3128–3142. https://doi.org/10.1105/tpc.15.00605

Wang, M., Schäfer, M., Li, D., Halitschke, R., Dong, C., McGale, E., Paetz, C., Song, Y., Li, S., Dong, J., Heiling, S., Groten, K., Franken, P., Bitterlich, M., Harrison, M., Paszkowski, U., & Baldwin, I. T. (2018). Blumenols as shoot markers of root symbiosis with arbuscular mycorrhizal fungi. *ELife*, *7*. https://doi.org/10.7554/eLife.37093

Wang, S., Chen, A., Xie, K., Yang, X., Luo, Z., Chen, J., Zeng, D., Ren, Y., Yang, C., Wang, L., Feng, H., López-Arredondo, D. L., Herrera-Estrella, L. R., & Xu, G. (2020). Functional analysis of the OsNPF4.5 nitrate transporter reveals a conserved mycorrhizal pathway of nitrogen acquisition in plants. *Proceedings of the National Academy of Sciences*, 202000926. https://doi.org/10.1073/pnas.2000926117

Wang, Wanxiao, Shi, J., Xie, Q., Jiang, Y., Yu, N., Wang, E., & Yu nyu, N. (2017). Nutrient Exchange and Regulation in Arbuscular Mycorrhizal Symbiosis. *Molecular Plant*, *10*, 1147–1158. https://doi.org/10.1016/j.molp.2017.07.012

Wang, Wensheng, Mauleon, R., Hu, Z., Chebotarov, D., Tai, S., Wu, Z., Li, M., Zheng, T., Fuentes, R. R., Zhang, F., Mansueto, L., Copetti, D., Sanciangco, M., Palis, K. C., Xu, J. J., Sun, C., Fu, B., Zhang, H., Gao, Y., … Leung, H. (2018). *Genomic variation in 3,010 diverse accessions of Asian cultivated rice*. *557*(7703), 43–49. https://doi.org/10.1038/s41586-018-0063-9

Wang, Yuexing, Shang, L., Yu, H., Zeng, L., Hu, J., Ni, S., Rao, Y., Li, S., Chu, J., Meng, X., Wang, L., Hu, P., Yan, J., Kang, S., Qu, M., Lin, H., Wang, T., Wang, Q., Hu, X., … Qian, Q. (2020). A Strigolactone Biosynthesis Gene Contributed to the Green Revolution in Rice. *Molecular Plant*, *13*(6), 923–932. https://doi.org/10.1016/J.MOLP.2020.03.009

Wang, Yutao, Bao, X., & Li, S. (2021). Effects of Arbuscular Mycorrhizal Fungi on Rice Growth Under Different Flooding and Shading Regimes. *Frontiers in Microbiology*, *12*, 3276. https://doi.org/10.3389/FMICB.2021.756752/BIBTEX

Wang, Yutao, Li, T., Li, Y., Björn, L. O., Rosendahl, S., Olsson, P. A., Li, S., & Fu, X. (2015). Community dynamics of arbuscular mycorrhizal fungi in high-input and intensively irrigated rice cultivation systems. *Applied and Environmental Microbiology*, *81*(8), 2958–2965. https://doi.org/10.1128/AEM.03769-14/SUPPL_FILE/ZAM999116198SO1.PDF

Wang, Z., Ruan, W., Shi, J., Zhang, L., Xiang, D., Yang, C., Li, C., Wu, Z., Liu, Y., Yu, Y., Shou, H., Mo, X., Mao, C., & Wu, P. (2014). Rice SPX1 and SPX2 inhibit phosphate starvation responses through interacting with PHR2 in a phosphate-dependent manner. *Proceedings of the National Academy of Sciences of the United States of America*, *111*(41), 14953–14958.

https://doi.org/10.1073/pnas.1404680111

Watanarojanaporn, N., Boonkerd, N., Tittabutr, P., Longtonglang, A., Young, J. P. W., Teaumroong, N., Peter, J., Young, W., & Teaumroong, N. (2013). *Effect of Rice Cultivation Systems on Indigenous Arbuscular Mycorrhizal Fungal Community Structure*. *3*, 316. https://www.jstage.jst.go.jp/browse/jsme2

Waters, M. T., Nelson, D. C., Scaffidi, A., Flematti, G. R., Sun, Y. K., Dixon, K. W., & Smith, S. M. (2012). Specialisation within the DWARF14 protein family confers distinct responses to karrikins and strigolactones in Arabidopsis. *Development (Cambridge, England)*, *139*(7), 1285–1295. https://doi.org/10.1242/DEV.074567

Waters, M. T., & Smith, S. M. (2013). KAI2- and MAX2-Mediated Responses to Karrikins and Strigolactones Are Largely Independent of HY5 in Arabidopsis Seedlings. *Molecular Plant*, *6*(1), 63–75. https://doi.org/10.1093/MP/SSS127

Watts-Williams, S. J., Emmett, B. D., Levesque-Tremblay, V., MacLean, A. M., Sun, X., Satterlee, J. W., Fei, Z., & Harrison, M. J. (2019). Diverse Sorghum bicolor accessions show marked variation in growth and transcriptional responses to arbuscular mycorrhizal fungi. *Plant Cell and Environment*, *42*(5), 1758–1774. https://doi.org/10.1111/pce.13509

Wegel, E., Schauser, L., Sandal, N., Stougaard, J., & Parniske, M. (1998). Mycorrhiza mutants of Lotus japonicus define genetically independent steps during symbiotic infection. *Molecular Plant-Microbe Interactions*, *11*(9), 933–936. https://doi.org/10.1094/MPMI.1998.11.9.933

Wissuwa, M., Ae, N., & Jones, S. S. (2001). Genotypic variation for tolerance to phosphorus deficiency in rice and the potential for its exploitation in rice improvement. *Plant Breeding*, *120*(1), 43–48. https://doi.org/10.1046/J.1439-0523.2001.00561.X

Wissuwa, Matthias, Kondo, K., Fukuda, T., Mori, A., Rose, M. T., Pariasca-Tanaka, J., Kretzschmar, T., Haefele, S. M., & Rose, T. J. (2015). Unmasking Novel Loci for Internal Phosphorus Utilization Efficiency in Rice Germplasm through Genome-Wide Association Analysis. *PLOS ONE*, *10*(4), e0124215. https://doi.org/10.1371/journal.pone.0124215

Wong, J. E. M. M., Nadzieja, M., Madsen, L. H., Bücherl, C. A., Dam, S., Sandal, N. N., Couto, D., Derbyshire, P., Uldum-Berentsen, M., Schroeder, S., Schwämmle, V., Nogueira, F. C. S., Asmussen, M. H., Thirup, S., Radutoiu, S., Blaise, M., Andersen, K. R., Menke, F. L. H., Zipfel, C., & Stougaard, J. (2019). A Lotus japonicus cytoplasmic kinase connects Nod factor perception by the NFR5 LysM receptor to nodulation. *Proceedings of the National Academy of Sciences of the United States of America*, *116*(28), 14339–14348. https://doi.org/10.1073/PNAS.1815425116/-/DCSUPPLEMENTAL

Xavier, L. J. C., & Germida, J. J. (1998). Response of spring wheat cultivars to Glomus clarum NT4 in a P-deficient soil containing arbuscular mycorrhizal fungi. *Canadian Journal of Soil Science*, *78*(3), 481–484. https://doi.org/10.4141/S97

Xie, X. (2016). Structural diversity of strigolactones and their distribution in the plant kingdom. *Journal of Pesticide Science*, *41*(4), 175–180. https://doi.org/10.1584/jpestics.J16-02

Xie, X., Mori, N., Yoneyama, K., Nomura, T., Uchida, K., Yoneyama, K., & Akiyama, K. (2019). Lotuslactone, a non-canonical strigolactone from Lotus japonicus. *Phytochemistry*, *157*, 200–205. https://doi.org/10.1016/j.phytochem.2018.10.034

Yang, S.-Y., Grønlund, M., Jakobsen, I., Grotemeyer, M. S., Rentsch, D., Miyao, A., Hirochika, H., Kumar, C. S., Sundaresan, V., Salamin, N., Catausan, S., Mattes, N., Heuer, S., & Paszkowski, U. (2012). Nonredundant Regulation of Rice Arbuscular Mycorrhizal Symbiosis by Two Members of the PHOSPHATE TRANSPORTER1 Gene Family. *The Plant Cell*, *24*(10), 4236–4251. https://doi.org/10.1105/tpc.112.104901

Yano, K., Yoshida, S., Muller, J., Singh, S., Banba, M., Vickers, K., Markmann, K., White, C., Schuller, B., Sato, S., Asamizu, E., Tabata, S., Murooka, Y., Perry, J., Wang, T. L., Kawaguchi, M., Imaizumi-Anraku, H., Hayashi, M., & Parniske, M. (2008). CYCLOPS, a mediator of symbiotic intracellular accommodation. *Proceedings of the National Academy of Sciences*, *105*(51), 20540–20545. https://doi.org/10.1073/pnas.0806858105

Yoneyama, K. K., Mori, N., Sato, T., Yoda, A., Xie, X., Okamoto, M., Iwanaga, M., Ohnishi, T., Nishiwaki, H., Asami, T., Yokota, T., Akiyama, K., Yoneyama, K. K., & Nomura, T. (2018). Conversion of carlactone to carlactonoic acid is a conserved function of MAX1 homologs in strigolactone biosynthesis. *New Phytologist*, *218*(4), 1522–1533. https://doi.org/10.1111/nph.15055

Yoshida, S., Kameoka, H., Tempo, M., Akiyama, K., Umehara, M., Yamaguchi, S., Hayashi, H., Kyozuka, J., & Shirasu, K. (2012). The D3 F-box protein is a key component in host strigolactone responses essential for arbuscular mycorrhizal symbiosis. *New Phytologist*, *196*(4), 1208–1216. https://doi.org/10.1111/j.1469-8137.2012.04339.x

Youngdahl, L. J., Pacheco, R., Street, J. J., & Vlek, P. L. G. (1982). The kinetics of ammonium and nitrate uptake by young rice plants. *Plant and Soil*, *69*, 225–232.

Yu, J., Hu, S., Wang, J., Wong, G. K. S., Li, S., Liu, B., Deng, Y., Dai, L., Zhou, Y., Zhang, X., Cao, M., Liu, J., Sun, J., Tang, J., Chen, Y., Huang, X., Lin, W., Ye, C., Tong, W., … Yang, H. (2002). A draft sequence of the rice genome (Oryza sativa L. ssp. indica). *Science (New York, N.Y.)*, *296*(5565), 79–92. https://doi.org/10.1126/SCIENCE.1068037

Yu, Jianming, Pressoir, G., Briggs, W. H., Bi, I. V., Yamasaki, M., Doebley, J. F., McMullen, M. D., Gaut, B. S., Nielsen, D. M., Holland, J. B., Kresovich, S., & Buckler, E. S. (2006). A unified mixed-model method for association mapping that accounts for multiple levels of relatedness. *Nature Genetics*, *38*(2), 203–208. https://doi.org/10.1038/ng1702

Zhang, L., Yuan, L., Staehelin, C., Li, Y., Ruan, J., Liang, Z., Xie, Z., Wang, W., Xie, J., & Huang, S. (2019). The LYSIN MOTIF-CONTAINING RECEPTOR-LIKE KINASE 1 protein of banana is required for perception of pathogenic and symbiotic signals. *New Phytologist*, *223*(3), 1530–1546. https://doi.org/10.1111/nph.15888

Zhang, Q., Blaylock, L. A., & Harrison, M. J. (2010). Two Medicago truncatula half-ABC transporters are essential for arbuscule development in arbuscular mycorrhizal symbiosis. *Plant Cell*, *22*(5), 1483–1497. https://doi.org/10.1105/tpc.110.074955

Zhang, S., Wang, L., Ma, F., Bloomfield, K. J., Yang, J., Atkin, O. K., Zhang, S., Wang, L., Ma, F., Bloomfield, K. J., Yang, J., & Atkin, O. K. (2015). Is resource allocation and grain yield of rice altered by inoculation with arbuscular mycorrhizal fungi? *Journal of Plant Ecology*, *8*(4), 436. https://doi.org/10.1093/JPE/RTU025

Zhang, Xiaowei, Dong, W., Sun, J., Feng, F., Deng, Y., He, Z., Oldroyd, G. E. D., & Wang, E. (2015). *The receptor kinase CERK1 has dual functions in symbiosis and immunity signalling*. *81*(2), 258–267. https://doi.org/10.1111/tpj.12723

Zhang, Xinchun, Pumplin, N., Ivanov, S., & Harrison, M. J. (2015). EXO70I is required for development of a sub-domain of the periarbuscular membrane during arbuscular mycorrhizal symbiosis. *Current Biology*, *25*(16), 2189–2195. https://doi.org/10.1016/j.cub.2015.06.075

Zhang, Y., van Dijk, A. D. J., Scaffidi, A., Flematti, G. R., Hofmann, M., Charnikhova, T., Verstappen, F., Hepworth, J., van der Krol, S., Leyser, O., Smith, S. M., Zwanenburg, B., Al-Babili, S., Ruyter-Spira, C., & Bouwmeester, H. J. (2014). Rice cytochrome P450 MAX1 homologs catalyze distinct steps in strigolactone biosynthesis. *Nature Chemical Biology*, *10*(12), 1028–1033. https://doi.org/10.1038/nchembio.1660

Zhao, H., Li, J., Yang, L., Qin, G., Xia, C., Xu, X., Su, Y., Liu, Y., Ming, L., Chen, L. L., Xiong, L., & Xie, W. (2021). An inferred functional impact map of genetic variants in rice. *Molecular Plant*, *14*(9), 1584–1599. https://doi.org/10.1016/J.MOLP.2021.06.025

Zhao, H., Yao, W., Ouyang, Y., Yang, W., Wang, G., Lian, X., Xing, Y., Chen, L., & Xie, W. (2015). RiceVarMap: a comprehensive database of rice genomic variations. *Nucleic Acids Research*, *43*. https://doi.org/10.1093/NAR/GKU894

Zhao, K., Tung, C. W., Eizenga, G. C., Wright, M. H., Ali, M. L., Price, A. H., Norton, G. J., Islam, M. R., Reynolds, A., Mezey, J., McClung, A. M., Bustamante, C. D., & McCouch, S. R. (2011). Genome-wide association mapping reveals a rich genetic architecture of complex traits in Oryza sativa. *Nature Communications*, *2*(1), 1–10. https://doi.org/10.1038/ncomms1467

Zheng, X., Yang, Y., & Al-Babili, S. (2021). Exploring the Diversity and Regulation of Apocarotenoid Metabolic Pathways in Plants. *Frontiers in Plant Science*, *12*,

2894. https://doi.org/10.3389/FPLS.2021.787049/BIBTEX

Zhong, H., Liu, S., Zhao, G., Zhang, C., Peng, Z., Wang, Z., Yang, J., & Li, Y. (2021). Genetic Diversity Relationship Between Grain Quality and Appearance in Rice. *Frontiers in Plant Science*, *12*, 1490. https://doi.org/10.3389/FPLS.2021.708996/BIBTEX

Zhou, F., Lin, Q., Zhu, L., Ren, Y., Zhou, K., Shabek, N., Wu, F., Mao, H., Dong, W., Gan, L., Ma, W., Gao, H., Chen, J., Yang, C., Wang, D., Tan, J., Zhang, X., Guo, X., Wang, J., … Wan, J. (2013). D14-SCF(D3)-dependent degradation of D53 regulates strigolactone signalling. *Nature*, *504*(7480), 406–410. https://doi.org/10.1038/nature12878

Zhu, C., Gore, M., Buckler, E. S., & Yu, J. (2008). Status and Prospects of Association Mapping in Plants. *The Plant Genome*, *1*(1), 5–20. https://doi.org/10.3835/plantgenome2008.02.0089

Zhu, Y. G., Smith, S. E., Barritt, A. R., & Smith, F. A. (2001). Phosphorus (P) efficiencies and mycorrhizal responsiveness of old and modern wheat cultivars. *Plant and Soil*, *237*(2), 249–255. https://doi.org/10.1023/A:1013343811110